

Objective Detection by Signal Analysis  
of the  
Auditory Evoked Cortical EEG Potential

A thesis submitted for the degree of Doctor of Philosophy  
of the University of London

by

Almira Jane Ross

October 1978

Engineering in Medicine Laboratory  
Department of Electrical Engineering  
Imperial College  
London SW7

## ABSTRACT

The work reported in this thesis aims at the development of objective techniques for the clinical evaluation of auditory function. The auditory evoked potential (AEP), a convenient electrophysiological signal, has been examined in detail. Several statistically-based methods have been devised and assessed for its objective detection. Power measures have been studied, together with two pattern recognition techniques: phase distribution analysis, and template matching by cross-correlation.

The detection of the AEP is rendered particularly difficult by several factors: the variability of the AEP, its low signal-to-noise ratio, and its interaction with a nonstationary noise source. These features limit the efficacy of methods based on amplitude or power measures. Pattern features are therefore potentially more attractive and a phase spectral approach is convenient. Phase values, however, are inherently periodic, and this cannot help but complicate statistical analysis and interpretation. Nonetheless, by recourse to a data simulation, and to rotational statistical procedures, the sampling statistics of certain phase measures can be determined. Although a strong sample size bias has emerged very clearly from the analysis, the empirical phase statistics have been shown to be well-behaved and entirely reliable for objective use in indicating the presence of the AEP. The effectiveness of the phase techniques suggests that a pattern recognition approach is appropriate to the data, and this finding is further confirmed by the cross-correlation studies.

## ACKNOWLEDGEMENTS

A sincere and very special word of thanks is due to my supervisor, Professor B. McA. Sayers, for the guidance, criticism, and patience he has shown me throughout the course of my research.

That gratitude is extended to Mr. H. A. Beagley of the Department of Electrophysiology, Royal National Throat, Nose, and Ear Hospital, who has kindly allowed me the use of his facilities there, and patiently answered my many questions on auditory physiology.

I would also like to thank the members of the Engineering in Medicine Laboratory for the ideas and suggestions which have often flowed from our discussions. In particular, may I thank Dr. Maurice Thai Thien Nghia for his advice on assembler programming for the HP 2100, and Mr. William Cutler for his help on matters of practical electronics related to my project. I am also indebted to Dr. Donald Monro for the use of his ADC and FFT subroutines.

In addition, I would like to thank Mr. Michael Powell for the understanding, companionship, and help he has offered me in preparing the text of this thesis. A very special thank you to my mother, Marguerite Ross, for the support she has given me throughout the course of my studies.

This research was made possible by a grant from the Medical Research Council of Great Britain. Additional funds from the Government of Manitoba, University Grants Commission, are also appreciated.

## INDEX

Abstract .....	ii
Acknowledgements .....	iii
1. Introduction .....	1
2. Electric Response Audiometry	
2.1. Early Developments in ERA .....	4
2.2.i. Recording .....	6
2.2.ii. Electrodes .....	7
2.2.iii. Recording Apparatus .....	10
2.3.i. The Auditory Evoked Potential .....	10
2.3.ii. AEP Variability .....	12
2.3.iii. Nonstationarities .....	14
2.4.i. The Noise Sources .....	16
2.4.ii. The EEG .....	16
2.4.iii. Muscle Noise .....	19
2.5. Detection of the AEP .....	21
2.6.i. Amplitude Measures and the S/N .....	23
2.6.ii. Pattern Recognition Techniques .....	24
3. Power Measures and the S/N	
3.1.i. Introduction .....	26
3.1.ii. Theoretical Considerations .....	26
3.2.i. The Power Test .....	27
3.2.ii. The F-statistic .....	28
3.2.iii. The Power of the Test .....	30
3.3.i. Simulation .....	32
3.3.ii. Discussion .....	34
3.4. Distributions of Power .....	36
3.5. Spectral Analysis .....	40



3.6.	Concluding Remarks .....	44
3.7.	Tables 3-i to 3-x .....	46
4. Phase Distributional Analysis		
4.1.i	Introduction .....	58
4.1.ii.	Theoretical Background .....	58
4.1.iii.	The $\chi^2$ Test .....	63
4.2.i.	On-line Trials .....	64
4.2.ii.	Discussion .....	66
4.3.i.	The Behaviour of $\chi^2$ .....	70
4.3.ii.	Simulation .....	72
4.3.iii.	The Distribution of the Maximum .....	74
4.4.i.	Off-line analysis .....	79
4.4.ii.	Discussion .....	80
4.5.i.	The Mean Phase Vector .....	83
4.5.ii.	Theoretical Background .....	84
4.5.iii.	The Sampling Statistics of $\bar{Z}_i$ .....	86
4.6.i.	Data Analysis by the Phase Vector Method .....	92
4.6.ii.	Discussion .....	94
4.7.	Concluding Remarks .....	98
4.8.	Tables 4-i to 4-cxxviii .....	100
5. Template Matching by Cross-correlation		
5.1.i.	Introduction .....	234
5.1.ii.	Template Matching .....	234
5.1.iii.	Cross-correlation Coefficients: the Null Hypothesis .....	235
5.2.i.	An Exploratory Cross-correlation Study .....	238
5.2.ii.	Discussion .....	240
5.3.i.	An On-line Study .....	243

5.3.ii.	Discussion .....	244
5.4.	Concluding Remarks .....	246
5.5.	Tables 5-i to 5-xxxix .....	248
6.	Conclusion	
6.1.	Introduction .....	294
6.2.	Objective AEP Detection .....	294
6.3.	AEP Analysis .....	296
6.4.	Proposals for Future Study .....	297
	References .....	300

## CHAPTER ONE

### INTRODUCTION

Within the field of clinical audiometry, there has always been a need for some objective means of testing auditory function. Subjective tests, where the patient himself indicates 'heard' or 'not heard' in response to an acoustic stimulus, break down whenever his cooperation cannot be relied upon. Some physiological or electrophysiological variable, such as the electrocochleogram (ECoChG) or electroencephalogram (EEG), must then be used to indicate the presence or absence of a response to sound stimulation. These physiological responses can be assessed in one of two ways: either the tester scores them visually, a situation which retains an element of subjectivity insofar as his bias is involved; or they may be assessed by machine scoring. Here, the criteria for detecting the responses are in-built and statistically derived, making the test truly objective. The work reported in this thesis examines one of these responses, the late components of the auditory evoked potential (AEP) present in the EEG, and explores several new techniques for detecting it objectively, based largely on a pattern recognition approach.

Study of the auditory evoked potential is of considerable interest and importance. Although a diffuse and non-specific response, the AEP in some way reflects the integrity of the entire auditory pathway. As such, it provides us with a clinically useful

physiological response to acoustic stimulation. As an audiological test, its merits are limited only for want of some objective means of detecting the evoked potential. This, in itself, is a challenging problem in signal analysis. Whenever both signal, the AEP, and noise, primarily the EEG, occupy a similar frequency band, signal detection by some means of frequency selectivity, such as analog filtering or coherent averaging, is limited in scope and applicability. Differentiation on the basis of signal strength will only be effective where signal-to-noise (S/N) ratios are high, a situation seldom encountered with AEP data. Use of pattern recognition techniques assume a consistent signal will be found in stimulated records. Whatever methods of signal detection are employed, statistical measures must be relied upon to indicate significant or nonsignificant findings. The nonstationarities experienced in EEG records can and often do affect the statistics applied, and care must always be taken in interpreting the results of any analysis performed.

Once these problems are resolved, and some objective methods developed to detect the evoked potential consistently and reliably, many further developments are possible. The same, or similar, techniques can then be applied effectively to other electrophysiological responses with similar characteristics, such as the brain-stem evoked potentials (BSEP) or the ECoChG. This would greatly extend the use, and reduce the expense, of electric response audiometry (ERA) by eliminating the need for clinically trained personnel to assess these responses visually. Surveys could then be conducted in a much wider context than has been attempted to date for want of a simple, objective, and universally accepted means of audiometric testing.

The present study is primarily concerned with the detection of the AEP. A consistent means of detection would place this particular audiometric test on an objective and reliable footing, and possibly allow for similar developments in other areas of ERA. As will be seen, the techniques developed and outlined here have also allowed us to examine individual evoked potentials, a study that could not be considered before. Analysis of individual records may well enable us to gain some further insight into the physiology underlying the generation of the AEP and aid in any inferences we make as to the possible location of their generators.

## CHAPTER TWO

## ELECTRIC RESPONSE AUDIOMETRY

## 2.1. Early Developments in ERA

The auditory evoked potentials (AEP's) under study are present in, though frequently obscured by, the spontaneous electrical activity of the brain. The presence of electric potentials in the exposed cortex of animals was first observed by Caton in 1875. These, he suggested, were related to cortical function, and in some way influenced by sensory stimulation. It was not until fifty years later that similar potentials were observed from the human brain. Berger (1929) identified the alpha-rhythm in the electroencephalogram (EEG) as having a frequency centered on 10 Hz, and being associated with a resting or inattentive state. Alpha-activity, he found, was blocked by visual alertness and less frequently by sound. Later Adrian and Matthews (1934) confirmed his observations and noted that the Berger- or alpha-rhythm could be induced by photic stimulation.

Specific changes in the EEG in response to an acoustic stimulus were reported by P. Davis and by Davis, Davis, Loomis et al. in 1939. Presentation of tones was found to check the alpha-activity or beta-activity in some waking subjects. ( Davis, P., 1939 ) For others, a diphasic or triphasic wave accompanied the onset or cessation of the sound. These on- or off-effects were

not always discernible in the EEG and did vary greatly in amplitude. Because they were maximally recorded from the vertex, they have come to be known as the vertex- or V-potentials.

A similar response could also be evoked during sleep. The K-complex ( Davis, Davis, Loomis, et al., 1939 ) consisted of two components, both of which varied systematically with the different stages of sleep. A slow component, closely related to the waking on-effect, was often followed by bursts of faster activity which decreased in frequency and grew more regular as sleep became deeper. Both the K-complex and the V-potential could be evoked by visual and tactile stimuli, suggesting that they were diffuse, non-specific responses of the brain to any sensory input.

V-potentials, much smaller and more labile than the K-complex, were frequently obscured by spontaneous EEG of much greater amplitude than the responses themselves. Providing some reliable means of detecting them was a necessary first step in coming to a better understanding of their morphology and clinical usefulness. Superposition of as many as twenty responses ( Dawson, 1947 ) enabled workers to identify the evoked potential more readily. However, it was not until the introduction of averaging ( Dawson, 1951 ) and the development of the averaging computer ( Dawson, 1954, and Clark, 1958 ) that AEP's could be recognized with any degree of reliability.

With the advent of averaging, it was still uncertain, and by no means universally accepted, that the auditory evoked potential was indeed of cortical origin. Most of the controversy surrounded the early components ( first 30 ms ) of the response, which could

be due to muscle tone or eye movements. ( Borsanyi and Blanchard, 1964 ) Although movement artifacts do influence the evoked potential and can obscure its presence, the late components described by various authors ( Davis, 1964 a&b, inter alia ) are now thought of as originating in the cerebral cortex. Whether they are specific responses, originating from the primary projection areas of the cortex ( Vaughan and Ritter, 1970 ) or of a more diffuse origin ( Celesia and Puletti, 1969 ) remains unresolved. They do represent an electrophysiological response to acoustic stimulation, and as such, have been used clinically as an objective audiometric test.

Clinical applications, however, have been limited by several factors. Inter- and intra-subject variability of evoked potentials makes them difficult to assess visually. Each tester follows his own in-built criteria. ( Rose, Keating, et al., 1971 ) Children pose special problems. Their EEG's and AEP's are more labile than those of an adult, and muscle contaminants frequently obscure their averaged responses. With the use of signal detection techniques, it may be possible to improve the clinical situation by providing an objective and consistent means of detecting the evoked potential.

### 2.2.i. Recording

Auditory evoked potentials, the V-potentials of P. Davis, are recorded extra-cranially using scalp electrodes. The electrodes themselves are remote from the source of the AEP, separated from it by scalp, skull, and indifferent but not necessarily inactive cortex. Thus, these scalp electrodes will record volume-conducted



electrical events both related and unrelated to the evoked potential. Muscle contraction at or around any electrode will introduce further contaminants. In addition, far-field signals are substantially attenuated by the media through which they are conducted. Recordings made intra-cranially in both humans and animals are on average twenty times as large as those detected in the far-field. ( Celesia, 1968, Celesia and Puletti, 1969 ) What is picked up on the scalp, then, is a composite of electrical activity generated in, and conducted through, layers of cortex, and possibly contaminated by muscle contractions. The evoked potential is small and frequently engulfed by other volume conducted cortical potentials.

Faithful reproduction of EEG potentials can only be realized with an appropriate choice of both electrodes and recording apparatus. Special consideration will be given to each of these topics.

#### 2.2.ii. Electrodes

The relatively small potentials detected on the scalp are typically of the order of 100  $\mu$ V, demanding the use of reversible, rather than non-reversible, electrodes. This distinction is based on the behaviour of the electrical double layer, a phenomenon related to the existence of electrode potentials. When an electrode is immersed in a conducting solution, ions pass from the metal into the solution and vice versa, causing a potential difference, the electrode potential, to develop between the metal and the surrounding solution. If the outward flux of metal ions into solution exceeds the inward flow of ions from the solution,

an excess of charge builds up in the solution immediately surrounding the electrode, giving rise to an electric double layer. Once an equilibrium is established, a small change in voltage applied to the electrode will disturb the double layer. For a reversible electrode, a substantial, steady current will flow, indicating a low electrode resistance. Non-reversible electrodes, on the other hand, behave more like capacitors, passing very little current under these conditions.

The reversible electrode most commonly used for scalp recording of the EEG is the silver -- silver-chloride (  $Ag-AgCl$  ) disc electrode. When in contact with a solution or gel of sodium-chloride (  $NaCl$  ), its resistance and capacitance may both be large. However, if the input impedance of the amplifiers is high (  $> .5 M\Omega$  ), a.c. recordings will not be seriously affected. For d.c. recordings, impedances of order  $50 M\Omega$  are required.

Three electrodes are used for recording auditory evoked potentials. Because these are thought to be maximum over the vertex, a conventional placement of electrodes has evolved. An active electrode on the vertex is taken as a positive reference. Potential differences between it and an inactive electrode located on the mastoid are then detected. A third electrode on the forehead acts as body ground. This type of recording is often referred to as monopolar, because only the vertex electrode is assumed to be active. A bipolar recording results from determining the potential differences between active electrode pairs. Bipolar configurations are common in EEG recording and essential for any contour mapping of the evoked potential.

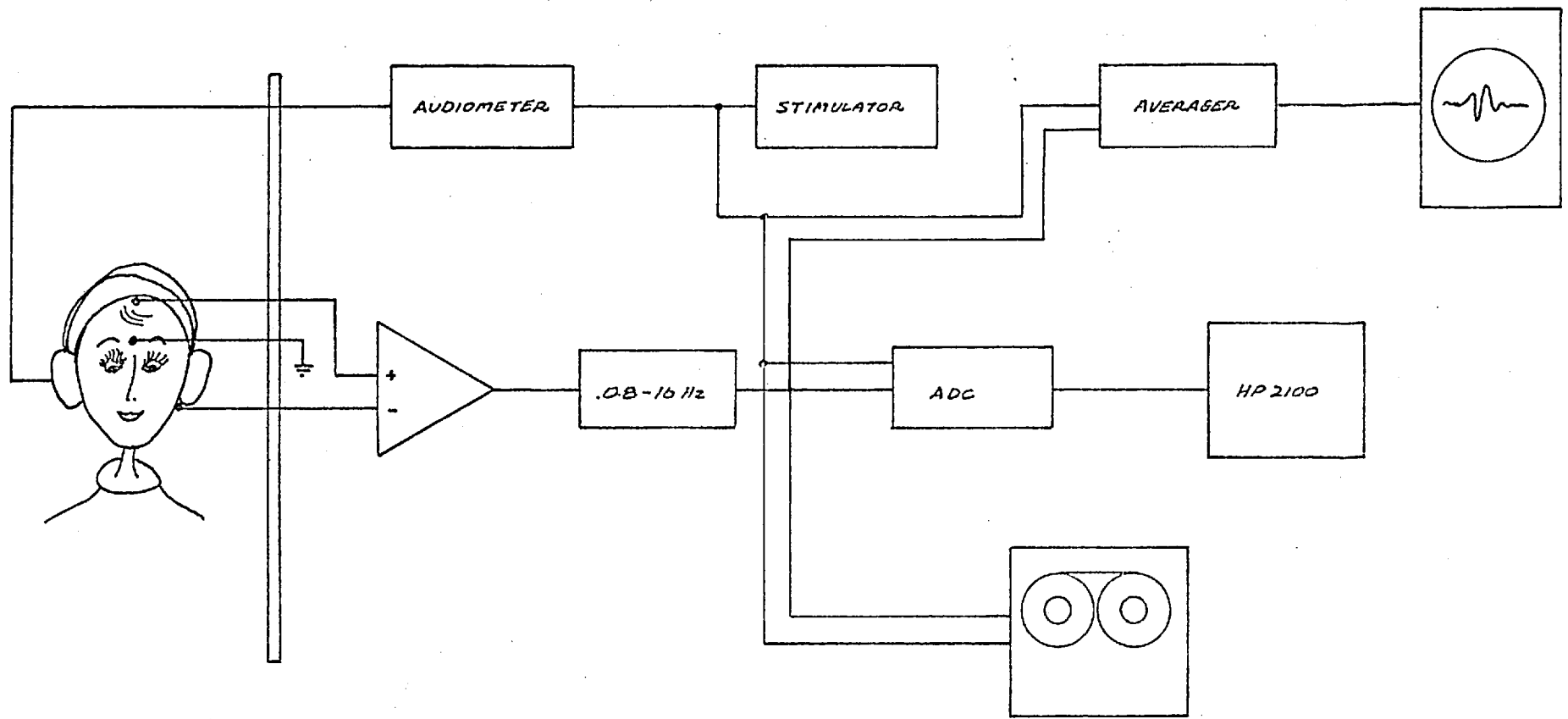


Fig. 2.1. The recording equipment.

### 2.2.iii. Recording Apparatus

A detailed schematic of all the recording apparatus used in this study is shown in Fig. 2.1. The signals picked up between vertex and mastoid electrodes were fed into a differential FET amplifier of approximately 10 M $\Omega$  input impedance. The output voltage passed through further stages of amplification for an overall gain of  $10^4$ . For most of the recordings taken, the filters were set at .08 Hz and 16 Hz. A digital averager computed the averaged response and displayed this on an oscilloscope. Timing of the averager was controlled by a stimulator, which in turn triggered an audiometer. Tone bursts were delivered through the audiometer at a rate set to one every two seconds. These had a rise and fall time of 10 ms and an overall duration of 100 ms.

For off-line analysis of these data, both the stimulus marker pulse and the signal output from Stage 2 were stored on analog tape and later digitized. In addition to this, on-line analysis of the data was also attempted. The same two signals were fed into an analog-to-digital convertor (ADC) and processed by a Hewlett-Packard 2100 computer.

### 2.3.i. The Auditory Evoked Potential

The characteristic features of the AEP described in the literature pertain to averaged rather than individual responses. If N sweeps are summed for each post-stimulus time, an average waveform can be derived. Events related to the stimulus, such as the evoked potential, will be enhanced by averaging many records. Any random or unrelated EEG activity, on the other hand, will be

diminished. Ensemble or coherent averaging can improve the signal-to-noise ratio ( $S/N$ ) by a factor of  $\sqrt{N}$ .

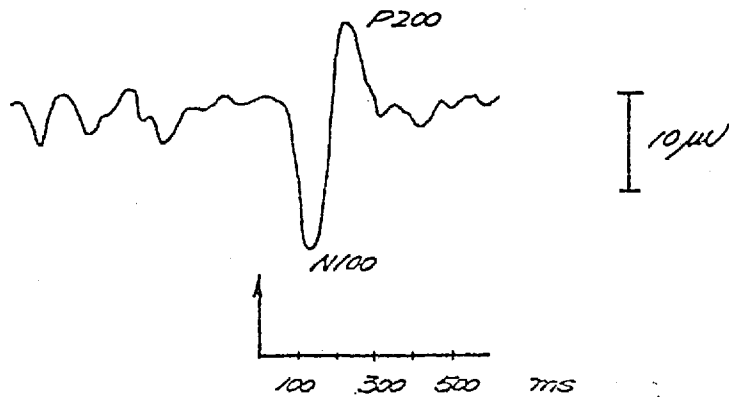


Fig. 2.2. Typical averaged auditory evoked potential.

The typical auditory evoked potential consists of several characteristic components. Of these, only those occurring more than 50 ms post-stimulus time have been considered. A small vertex positive peak may or may not be seen at 50 to 75 ms post-stimulus time. ( Fig. 2.2. ) A striking vertex negative trough between 100 ms and 150 ms and followed by a positive deflection anywhere between 175 and 200 ms is the most consistent feature of the response. A second low negative trough occurring at approximately 250 ms is often prominent in children but less common in adults. A further slow positive wave at about 300 ms may also be present. This latter component ( Sutton, Braren, et al., 1965 ) and the contingent negative variation ( Walter, Cooper, et al., 1964 ) are related to stimulus expectancy. Because the present study was not concerned with the secondary psychological aspects of perception, recordings were set up so as to minimize any effects due to conditioning or stimulus uncertainty. Thus, neither of these components is prominent in Fig. 2.2. Here, and throughout the text, vertex positive deflections are plotted upwards.

To date, no satisfactory terminology exists for the naming of the components outlined above. Throughout this text, the scheme suggested by Davis ( 1976 ) will apply. Vertex positive components are labelled with a P, vertex negative waves with an N. Both are followed by a subscript indicating the approximate post-stimulus time at which they occur. Thus, the components described in the preceding paragraph would be designated by: P<sub>50</sub>, N<sub>100</sub>, P<sub>200</sub>, N<sub>250</sub> and P<sub>300</sub>.

### 2.3.ii. AEP Variability

Although Fig. 2.2. attempts to illustrate a 'typical' evoked potential, the variability of waveform experienced both among subjects and within the same subject is considerable. Some aspects of this variability are reasonably systematic, like the changes in amplitude and latency as a function of stimulus intensity. Others do not appear to follow any specific pattern.

With changes in intensity level, the evoked potential decreases in magnitude and increases in latency until no observable response can be seen in the averaged record. ( Fig. 2.3. ) Changes in both parameters are gradual as the intensity is reduced to about 30 dB SL. Below this, latency shift of the N<sub>100</sub> and P<sub>200</sub> components is marked and may change by as much as 100 ms.

Any variations in psychological state may affect the nature of the evoked potential, often in ways which are difficult to define. Certain broad generalizations can often be made. A reduction in amplitude of the AEP with repetitive or boring stimuli, for example, is known to occur. The presentation of random or surprise stimuli frequently enhances the amplitude of the response. Sleep and drugs both affect the AEP in broadly similar ways. The background

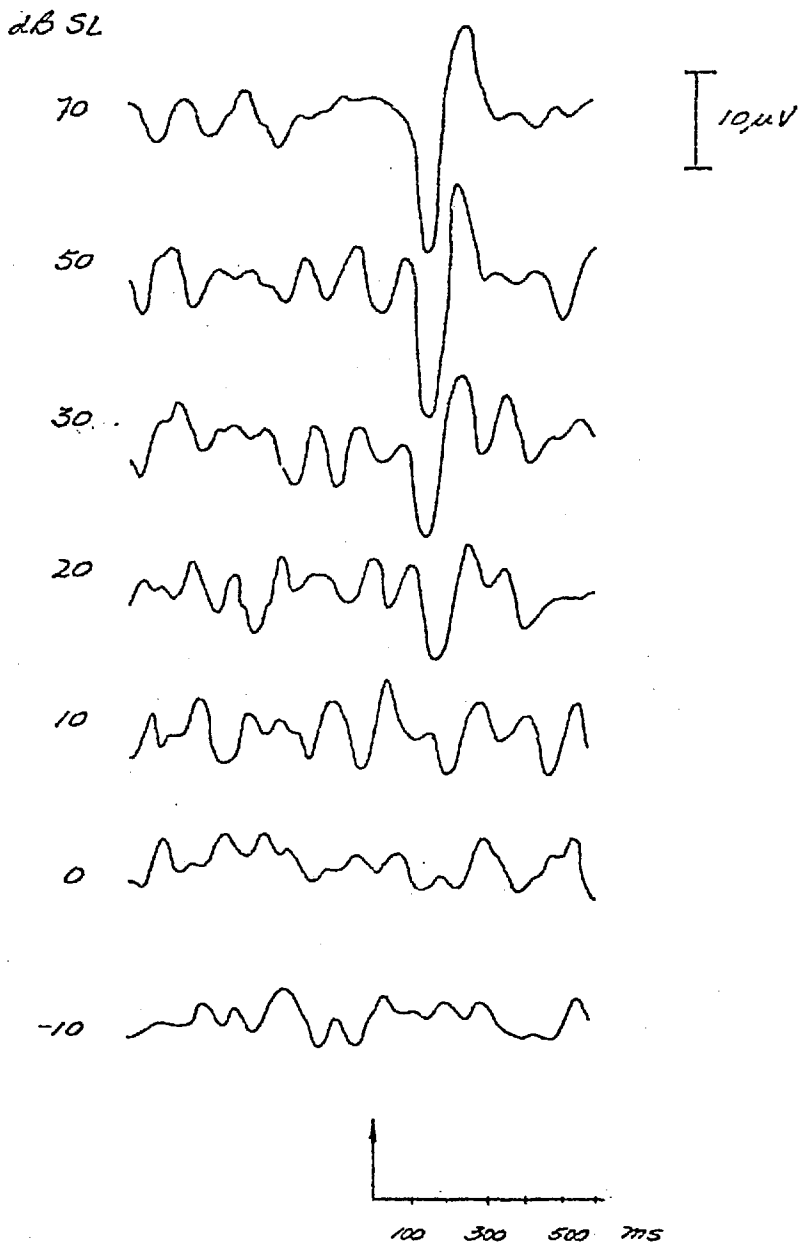


Fig. 2.2. Averaged auditory evoked potentials as a function of stimulus intensity. Subject JD, F., age 23, at 1 kHz.

EEG progresses through distinct stages during sleep, and the evoked potential becomes larger, broader and more prolonged. A fast rhythmic component often follows the response. In deep sleep or general anaesthesia, the AEP is rarely found.

The averaged waveforms in children are even more variable. In part, this is attributed to the immaturity of the central nervous system (CNS). As neural pathways develop, greater and greater consistency can be found in the evoked potential. Activity and restlessness may also account for the fluctuations experienced. The response is distinctly different in many features from the adult response, as illustrated in Fig. 2.4. In older children, it is possible to detect both adult and childlike waveforms.

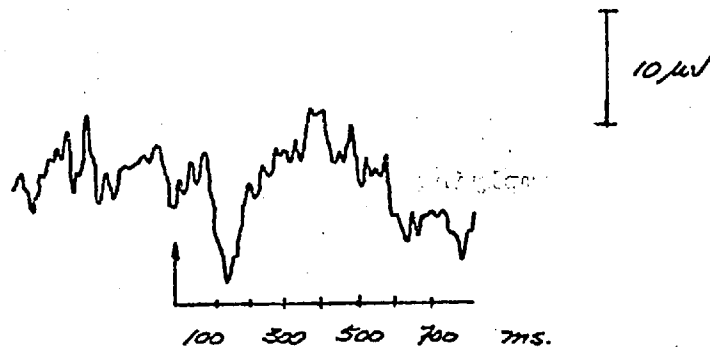


Fig. 2.4. The average response from a 3-year old child.

### 2.3.iii. Nonstationarities

Some of the variability mentioned above reflects the presence of nonstationarities in the data. Most physical or physiological data does exhibit time-varying statistical properties such as the mean, the second or higher moments of its distribution.



Nonstationarities may arise from transients in the system under study, or during long-range periods of time where the system gradually undergoes a change of state. This second condition is probably more descriptive of the nonstationarities present in the EEG, because it implies that a given input, such as an acoustic stimulus, will produce a variable output with the passage of time. The precise nature of the nonstationarities, though, has never been adequately examined. Time-varying means, variances and frequency structures may be found in EEG records. Chapter Three considers the problems of a nonstationary variance in detail, while Chapter Four suggests some means of examining the time-varying frequency structures present in some EEG data.

Very few satisfactory methods exist for the treatment of nonstationary data. Often an assumption of stationarity is made and a variety of statistical tests performed on the data. Distortions may result from assuming that the statistical properties of the sample do not change with the course of time. Tapering of a linear trend, for example, would introduce a false first harmonic in the frequency domain representation of the signal. Even coherent averaging can be affected by the presence of nonstationarities. Bursts of high amplitude EEG activity of variable frequency often swamp the average response.

If an assumption of stationarity is made with the EEG data, care must be taken in interpreting the results of any tests or processing applied. Certain features, such as trends, can be removed, if it can be shown that these are influencing the statistical test results, but not a characteristic feature of the system as a whole. Or, the effects of particular processing techniques, like the distortion of trends by Hanning or tapering, may

be ignored in interpreting specific tests involving the discrete Fourier transform. Some nonstationary methods are also available. These involve determining nonstationary probability density functions from unbiased estimates of time-varying means and variances. These are likely to be different for each subject tested, and probably for the same subject over the course of time. Nonstationary statistical procedures would only be warranted if careful and selective analysis accounting for the presence of certain nonstationarities proves to be inadequate.

#### 2.4.i. The Noise Sources

Two main sources of biological noise are present in AEP data: the spontaneous electrical activity of the brain; and myogenic artifacts, mostly due to the contraction of neck muscles. Each of these will be discussed under separate headings.

#### 2.4.ii. The EEG

The EEG is an extremely complex and inherently nonstationary signal; its amplitude and frequency vary considerably with the passage of time. Several reasonably regular waveforms, however, have been identified. These have come to be associated with various physiological states and with the maturation of the central nervous system (CNS). Even though certain rhythms may be more prominent at one time of life than another, or at one time of day than another, they wax and wane, giving way to different characteristic rhythms within the space of a few seconds or a few minutes. Several of these more characteristic waveforms will be considered

in this section.

EEG activity is more variable in children than in adults, a feature generally attributed to the growth and development of the CNS. Particular rhythms, usually of low frequency and high but irregular amplitude, are characteristic in the young child. Delta-activity ( $< 4$  Hz) is dominant and often asynchronous in the first few months of life. As the child develops, these highly variable waves are gradually replaced by more regular activity of higher frequency and lower amplitude. The generation of theta waves (4 to 8 Hz) and some alpha (8 to 13 Hz) can be observed after a year or so of birth. These rhythms gradually become more regular in appearance and more specific in origins as the child matures. By the time the child reaches puberty, the EEG closely resembles that of an adult, though irregular, high amplitude, low frequency rhythms may still be found in the recordings.

The EEG of an adult is characterized by the local generation of alpha-activity in the occipital regions of the brain. This consistent rhythm is usually most prominent when the subject is resting with eyes closed. This is the Berger effect. Higher frequency beta waves ( $> 13$  Hz) may also be seen intermingled with the lower frequency theta described earlier. Usually, for both children and adults, a composite of activity is to be found. One prominent rhythm gives way to a second, or several appear superimposed on one another.

Physiological changes of state, such as sleep or the administration of drugs, produce substantial changes in the character of EEG waveforms. During the various stages of sleep, for example, the alpha-activity of the resting state waxes and wanes until it is replaced by the emergence of theta and the occurrence of higher

frequency sleep spindles or sigma rhythms ( 14 Hz ). As sleep becomes more profound, delta waves develop. REM sleep marks a return of low amplitude, relatively high frequency waveforms. Drugs, too, affect the rhythms observed in the EEG. Anaesthetics generally reduce the frequency of prominent rhythms and increase their amplitude and variability. Thus, in the early stages of anaesthesia, alpha is quickly replaced by the widespread generation of theta and delta activity. In deep anaesthesia, little EEG activity can be seen.

Other patterns may also be seen in EEG tracings, though these are attributed to extra-cerebral sources and constitute biological artifacts. Eye blinks, for example, introduce localized triangular deflections in the frontal regions of the scalp, while eye movements show up as slow waves both frontally and temporally. Muscle contraction produces spindles, again highly localized. Sweating, too, introduces extremely slow delta waves, usually in frontal regions. Head or limb movement is reflected by variable waveforms in the EEG, a common occurrence with children.

All of the rhythms described above occur spontaneously. It is possible, however, to induce specific rhythms or to check their presence. Adrian and Matthews ( 1934 ) were able to induce alpha activity by the use of strobe flashes. Sounds, or the attention to problems of mental arithmetic, can block this activity, as can visual alertness. The discrimination of complex visual patterns seems to enhance the generation of beta. Reading, restlessness or boredom cause the EEG to change in as yet ill-defined ways, all contributing to the complex temporal pattern of the signal, and, of necessity, give rise to many of the nonstationary properties observed in the data.

### 2.4.iii. Muscle Noise

The second source of biological noise common to AEP recordings arises from muscle contraction. These muscle spindles are localized to the region immediately surrounding their generation, but can introduce artifacts of high amplitude should a recording electrode be placed in that vicinity. For AEP data, the main source of myogenic contamination is the mastoid. Head or neck movements may produce high amplitude spindles which can easily obscure the signal detected at the reference electrode. When recordings are taken, care must be exercised to ensure that the subject is relaxed, with head comfortably resting on a high backed chair or lying down. This relaxes the important neck muscles. When testing adults or older children, this can be accomplished without difficulty. Young children, hyperactive or disturbed subjects, or those suffering from lack of muscle coordination present substantial problems, as can epileptics.

### 2.5. Detection of the AEP

The variability of the evoked potential, its low S/N and its interaction with a nonstationary noise source of similar frequency range all compound the difficulties of signal detection and interpretation. Any method of analysis chosen will be effective only insofar as the data conforms to the assumptions inherent in that technique. In order to simplify statistical analyses, an assumption of stationarity is often made which may limit the resolution or reliability of the signal methods used in detecting the AEP. However, the usefulness of objective techniques for analysing ERA data cannot be overlooked. At present, no really reliable,

objective means of detecting the evoked potential is available. Although several machine scoring methods have been proposed, coherent averaging is still widely used in the clinical setting. As long as records are visually assessed, considerable variability will be experienced both on an inter-judge and intra-judge basis. ( Rose, Keating, Hedgecock, et al., 1971 ) Providing a method of detection based on statistical probabilities rather than variable, subjective criteria will put ERA on a more objective footing. In addition, it may come to be accepted as a standard procedure, allowing audiometric surveys to be carried out with full assurance that the data from regional centres could be compared unequivocally. Signal analysis methods may also provide the means for examining individual AEP sweeps in greater detail, thereby adding to existing knowledge and understanding of the evoked potential.

In the first instance, detection is of primary concern. Two general approaches to this problem exist. Each makes different assumptions as to how the AEP might be generated. If the evoked potential can be thought of as a signal superimposed on a noise source, then differences in amplitude, power, or signal strength could be found between stimulated and unstimulated records of EEG, suggesting that methods which improve the signal-to-noise ratio would be worth investigating. If, however, the AEP is thought to result from some synchronization or time-locking of existing EEG activity, pattern recognition techniques would be indicated.

### 2.6.i. Amplitude Measures and the S/N

Improving the signal-to-noise ratio of AEP data has been attempted with considerable success, suggesting that, to some extent at least, the evoked potential may indeed be a specific response superimposed on continuous EEG. Coherent averaging, for example, enhances the response at the expense of any random fluctuations in the background activity. Determining the characteristic amplitudes and frequencies of the EEG in pre-stimulus epochs, then removing these elements from post-stimulus records ( Salomon and Barford, 1977 ) reduces the effects of periodic, rather than random, aspects of the noise source.

Superimposing a signal on a noisy background has been assumed to produce an increase in the amplitude and power of the noise source alone. This working hypothesis ( Schimmel, Rapin and Cohen, 1974 ) has led to detection techniques which are as sensitive as the visual scoring of averaged waveforms. The assumption, however, can only be justified for relatively high signal-to-noise ratios; for those encountered in ERA data, other factors, such as the phase of both signal and noise, must be taken into account. A more detailed account and critique of these procedures may be found in Chapter Three.

Several other amplitude measures have been developed, each supposedly as sensitive as the subjective assessment of averaged records. ( Shimizu and Glackin, 1967, Saloman, 1970, 1974 ) Averaging, itself, is limited by the discrepancies between the assumed and actual behaviour of the data, viz., its variability and non-stationarity. In addition, subjective criteria introduce a further element of variability, making this choice of reference unsatisfactory

for establishing the effectiveness of any new signal detection technique. Sensation level (SL) is another possibility, but it, too, is subjective on the part of the listener, and discrepancies have been found to exist between SL and threshold detection by ERA averaging. ( Rapin, 1974, Rose, Keating, et al., 1972, inter alia ) Neither reference, then, is really adequate, yet it is only on the basis of one or the other that any comparisons can be made.

For this study, SL at the time of ERA testing has been arbitrarily chosen as a reference. Like averaging, sensation level still retains some elements of subjectivity, but makes no simplifying assumptions about the data which might influence test results.

The reasonably consistent results reported by authors using averaging, or some amplitude or power measures to detect the AEP does suggest there may be some merit in modelling the evoked potential by superposition. Such a description, however, does not conform to present-day understanding of how neurophysiological mechanisms are thought to function. Neurones fire spontaneously, and send off synchronous volleys of impulses whenever they are stimulated. No superposition of response on the background activity is observed, but rather, the spontaneous discharges are seen as synchronized to the stimulus. From the physiological point of view, it would be more reasonable to assume that similar mechanisms are at work at the cortical level. The evoked response can be strongly influenced by background EEG, being of similar amplitude and frequency in both the waking and sleeping states. To speak of the AEP as resulting from some synchronization of existing EEG activity allows us to consider pattern recognition techniques which may be of greater resolution than those which rely on a superposition



model.

## 2.6.ii. Pattern Recognition Techniques

If spontaneous EEG became synchronized in response to an acoustic stimulus, then some consistent pattern would be found in an ensemble of post-stimulus sweeps. The presence of a consistent pattern could then be detected in either the time or frequency domains.

In the time domain, both autocorrelation and cross-correlation with a response template could bring out the pattern in the data. The choice of template, however, must take certain known sources of response variability into account. Simulating one from the use of second order differential equations ( Derbyshire, Osenar, et al., 1971 ) will only be effective when inter-subject variability of responses is small. As this seldom happens, this template will only be successful when applied to those subjects whose response pattern closely resembles the template. Using each subject as his or her own reference, and possibly adapting the template to account for latency shifts at lower intensity levels may prove more effective.

In the frequency domain, synchronization of the EEG should be seen in the re-ordering or constraint of the phase spectral components. By comparing the distribution of phase values in both stimulated and unstimulated data, Sayers, Beagley, and Henshall ( 1974 ) have demonstrated the power of this signal detection technique. In addition, they have been able to synthesize an evoked potential pattern on continuous EEG and random noise ( Sayers, and Beagley, 1974 ) merely by constraining the phase values, suggesting that the AEP may indeed result from synchronization of that activity.

Beyond the advantages of improving response detection, modelling the AEP in this way may lead to a greater understanding of how the response is generated. Individual evoked potentials could then be examined in greater detail than at present. This, in turn, could allow us to make new inferences about the physiological mechanisms which give rise to the observed behaviour and characteristics of the AEP.

## 2.7. Conspectus

The AEP, then, provides us with challenging problems of signal detection and analysis. Both general approaches outlined above, based on the superposition and synchronization models, will be examined in detail in the next three chapters. Chapter Three deals exclusively with the superposition model and with the merits and problems of detection techniques based on signal-to-noise considerations. Chapters Four and Five, on the other hand, are devoted to two pattern recognition techniques which assume a synchronization model for AEP generation. The phase distributional analysis of Chapter Four considers the problem of pattern detection in frequency domain terms. With the phase approach, any consistent pattern other than noise is sought out from ensembles of post-stimulus EEG records. The template matching techniques of Chapter Five, on the other hand, make use of the known features of the AEP by attempting to match a high level response with individual members of ensembles for post-stimulus epochs. The problems and effectiveness of each of these methods will be considered in detail.

## CHAPTER THREE

## POWER MEASURES AND THE S/N

## 3.1.i. Introduction

Traditionally, the electroencephalogram has been analysed in terms of its power content. The power spectrum, in particular, serves as a means of identifying the rhythms present in the EEG record, and providing some quantitative measure of their relative signal strengths. Similar methods may provide a useful means of detecting the auditory evoked potential. This chapter examines a few of them in detail.

## 3.1.ii. Theoretical Considerations

A simple, but widely accepted, model of AEP generation suggests that a consistent and characteristic signal is superimposed on the EEG in response to acoustic stimulation. The background EEG is thought of as bandlimited random noise, both Gaussian and stationary in order to facilitate statistical analysis. Admittedly, a model of this kind fails to account for either the known variability of the AEP or the nonstationarities inherent in the EEG. It may, however, be viewed as an acceptable set of working hypotheses broadly descriptive of ERA data.

On this basis, the premise of superposition suggests a

variety of signal detection techniques based on magnitude and power measures that could be applied to the evoked potential. Firstly, the power of a signal superimposed on uncorrelated noise should exceed that of the noise source alone. This effect should be even more pronounced when the signal is enhanced by coherent averaging. Secondly, examination of the power spectra of signal and noise may reveal differences in the distribution of power among the available frequency components. The effectiveness of these, or similar, methods rests largely on the extent to which the hypotheses made apply to the data under study.

### 3.2.1. The Power Test

Relying on these assumptions, Schimmel, Rapin and Cohen ( 1974 ) have implemented several different amplitude and power measures for detecting the AEP. Because of the successes they reported, it seemed reasonable to accept the basic tenets of their model and to consider one procedure, initially, as a means of verifying their claims. A simple a.c. power comparison between averaged pre- and post-stimulus waveforms was chosen for this purpose.

A single trial consisted of 54 sweeps, each composed of 640 ms of pre-stimulus and 640 ms of continuous post-stimulus EEG. A total of 88 trials were chosen in the first instance. These consisted of the ERA data from five normal young adults, each tested under a maximum of 18 different stimulating conditions from supra-threshold to sub-threshold intensity levels. Four of the 18 trials were drawn from unstimulated EEG to serve as a control for the analysis.

The coherent average for each trial was then determined and the variance of pre- and post-stimulus intervals compared on the assumption that no significant difference would be seen if the AEP were not present in the post-stimulus record. A Fisher-test formed the basis of the comparison. When applying an F-test to the data under these conditions, certain considerations must be taken into account. These involve the notion of degrees of freedom and how they pertain to the definition of the F-statistic.

### 3.2.ii. The F-Statistic

For a normally distributed variable,  $x_i$ , with sample mean,  $\bar{x}$ , and population variance,  $\sigma_1^2$ , the following quantity can be defined:

$$u = \sum_{i=1}^n \left[ \frac{x_i - \bar{x}}{\sigma_1} \right]^2$$

The parameter  $u$  is distributed as  $\chi^2$  with  $(n-1)$  degrees of freedom where  $n$  is the number of independent samples making up the ensemble. For a second variable,  $y_i$ , with mean,  $\bar{y}$ , variance,  $\sigma_2^2$ , and ensemble length,  $m$ ,

$$v = \sum_{i=1}^m \left[ \frac{y_i - \bar{y}}{\sigma_2} \right]^2$$

The F-statistic is then defined as the ratio of these two quantities divided by their respective degrees of freedom.

$$F = \frac{\frac{u}{n-1}}{\frac{v}{m-1}}$$

As can be readily seen, the use of the F-test requires a knowledge of the number of degrees of freedom of the data. Because each sample in the ensemble average cannot be thought of as independent of the next, the equivalent number of degrees of freedom,  $df_e$ , must be estimated from the Blackman-Tukey relations.  $df_e$  is given by the following equation:

$$df_e = 2 B_e T - 1$$

where  $T$  is the period or data length in seconds, and  $B_e$  is the equivalent bandwidth of the data determined by comparing its smoothed power spectrum,  $P_i$ , to that of white noise of the same power variability.

$$B_e = \frac{\left[ \sum_{i=1}^{N/2} P_i(f) \frac{1}{N\Delta T} \right]^2}{\sum_{i=1}^{N/2} P_i^2(f) \frac{1}{N\Delta T}}$$

Here,  $N$  is the number of samples per sweep, and  $\Delta T$  is the interval, in seconds, between neighbouring samples.

Under the null hypothesis,  $\sigma_1^2$  and  $\sigma_2^2$  are assumed equal. Any significance in the value of  $F$  will force us to reject  $H_0$  in favour of the alternative hypothesis:  $\sigma_1^2 > \sigma_2^2$ . The subscript 1 denotes the post-stimulus record, thought to contain the evoked potential and therefore be of greater variance or power than the pre-stimulus EEG. For these conditions,  $F$  reduces to the following

relation, where  $x$  and  $y$  represent the post- and pre-stimulus sweeps respectively:

$$F = \frac{\sum_{i=1}^N (x_i - \bar{x})^2}{\sum_{i=1}^N (y_i - \bar{y})^2} \cdot \frac{df_2}{df_1}$$

This, rather than the conventional formula for  $F$ , was applied to all 88 pre- and post-stimulus averaged waveforms and tested for  $F(df_1, df_2)$  at 5%. The results of the study are found in Tables 3-i to 3-v. Every table is divided into two sections. Each section pertains to one of the two tone burst frequencies under which the subjects were tested. For every intensity level, quoted in dB SL, the averaged waveform for both pre- and post-stimulus epochs is depicted. The degrees of freedom for the post-stimulus record,  $df_1$ , and those for the pre-stimulus interval,  $df_2$ , are tabulated alongside.  $F$ -values are given, as are the probability levels of the test. Any nonsignificant finding is denoted by a dashed line. The presence of an asterisk (\*) to the right of an  $F$ -value indicates that greater variability is seen in the pre- rather than post-stimulus waveform.

### 3.2.iii. The Power of the Test

With reference to sensation level, 62 of these 88 trials can be identified as supra-threshold, and 26 as either sub-threshold or control EEG. To within the confidence limits set up for testing  $H_0$ , we would expect the supra-threshold records to show significance

and sub-threshold records or runs of spontaneous EEG to show little or none.

Very broadly speaking, a pattern of this kind can be found in the data of Tables 3-i to 3-v. It would be unwise, however, to press the matter much further. Inconsistencies do arise, as a comparison of the results from subjects CH at 500 Hz ( Table 3-i ) and JS at 2 kHz ( Table 3-iii ) will illustrate. In the first case, supra-threshold records correspond with significant, threshold and control runs with nonsignificant, values of  $F$  as expected under  $H_0$ . The second example reveals exactly the opposite. The data from all other subjects lie somewhere between these two extremes, showing only a general tendency towards significance at supra-threshold intensity levels ( 34 in 62 ) and nonsignificance elsewhere ( 17 in 26 ).

Taken overall, then, only 56% of the trials indicate response/no response conditions reliably. Of the remaining 42%, false negatives account for approximately 32% and false positives for 10%. These percentages are based on sensation level, which is often considered to be somewhat more sensitive than threshold estimation by ERA testing. Disparities between the two estimates may help to explain some of the insensitivity seen in Tables 3-i to 3-v at or near threshold. It does not, however, account for the considerable amount of nonsignificance found at higher intensity levels.

These inconsistencies do force us to consider more critically the set of hypotheses which gave rise to the test procedure itself. Failure to recognize or account for nonstationarities in the data, for example, may be introducing distortions into the analysis. It could be that the variance itself is a nonstationary statistic in the EEG. As such, it might well be overshadowing any



significant increase in the power of supra-threshold records; but even the expectation of such an increase in power may not be valid when applied to ERA data.

The outcome of single test, however, is insufficient as a basis for investigating any of these possibilities. Nor does it serve as an adequate critique of amplitude and power measures as a means of detecting the evoked potential. Further examination of the power is therefore necessary. Indeed, its statistical properties, distributions under stimulated and unstimulated conditions, and its frequency domain characteristics may give us some valuable insights into the nature and behaviour of ERA data. A comparison between actual data and data simulated to match our assumptions of a signal superimposed on a stationary noise source may therefore help to clarify the validity of that set of working hypotheses in relation to the data itself.

### 3.3.i. Simulation

ERA data was synthesized from normally distributed broadband noise in the following manner. The noise was filtered digitally so that its amplitude spectrum closely resembled the amplitude spectrum of spontaneous EEG. Filtering was performed on blocks of 128 samples by a frequency domain multiplication of the Fourier coefficients of the noise with the amplitude spectrum shown in Fig. 3.1. This was chosen arbitrarily from the GF 1 kHz file because little difference could be detected in the amplitude spectra for any of the control runs. A characteristic signal, the averaged response shown in Fig. 3.2., was then superimposed by addition on the second half of the 128 sample sweep at various

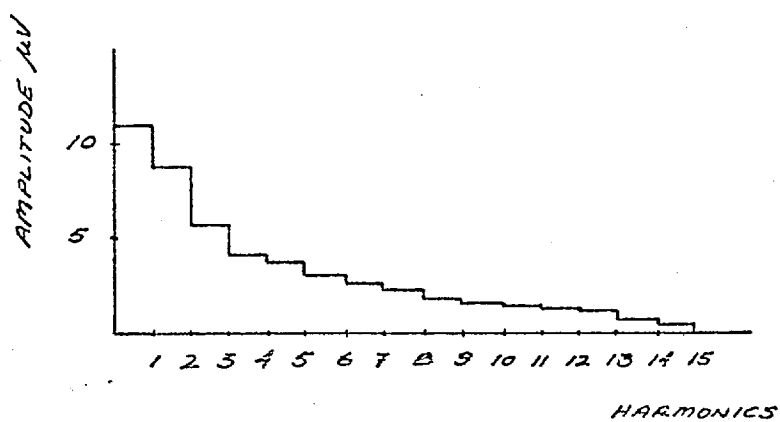


Fig. 3.1. The amplitude spectrum used as the filter characteristic for the simulation. GF, M, age 26, at 1 kHz.

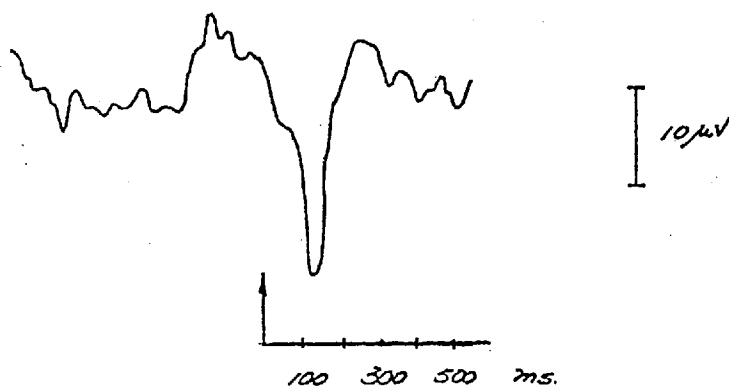


Fig. 3.2. Averaged response to high level acoustic stimulation used as the characteristic signal superimposed on bandlimited random noise.

signal-to-noise ratios.

Signal-to-noise ratio ( $S/N$ ) is defined here as the rms level of the signal divided by that of the noise. For this simulation, the unbiased standard deviation served as the estimate of rms values for both the averaged response and the filtered noise.  $S/N$  was considered at four approximate levels thought to be fairly typical of ERA data, 0.5, 0.25, 0.1, and 0.05.

Once simulated, the data was organized into 72 'supra-threshold' trials, each consisting of 54 sweeps of pre- and post-stimulus record 640 ms long. A further 18 trials of bandlimited random noise served as a control. The F-test was then performed on the coherent averages of each of these 54 sweep ensembles. The results of the test are tabulated in Tables 3-vi to 3-x. Every table is divided into two sections, each consisting of nine separate trials for a given signal-to-noise ratio. For each trial, the coherent average is depicted. To the right can be found the degrees of freedom for the 'post-stimulus' interval,  $df_1$ , and that for the 'pre-stimulus' period,  $df_2$ . F-values and their probabilities at 5% are tabulated alongside. An asterisk (\*) denotes any F-value which indicates a higher variance in the pre- rather than post-stimulus interval.

### 3.3.ii. Discussion

Not unexpectedly, signal-to-noise ratio appears to be the crucial factor in deciding the outcome of the F-test. Throughout this discussion, the signal-to-noise ratio is referred to individual sweeps of simulated data. Ensemble averaging improves this by as much as  $\sqrt{N}$ , or approximately 7.5 for the sample size

chosen.

For  $S/N$  equal to or greater than 0.25, highly significant values of  $F$  occur consistently. Most are considerably greater in magnitude than those found in the application of the  $F$ -statistic to the actual ERA data in Tables 3-i to 3-v. In addition, they often correspond to substantially more pronounced coherent averages, suggesting that, all other things being equal,  $S/N$  for ERA data is typically 0.25 or less. Compare the coherent averages for  $S/N$  of 0.5 ( Table 3-vi ) with that of the actual template ( Fig. 3.2. ).

Below a signal-to-noise ratio of 0.25, less consistency is to be seen. A value of 0.1, for example, reveals slightly better than half the records as significant. At 0.05, this figure is reduced again by approximately two. Typical ensemble averages at each of these  $S/N$  are found in Tables 3-viii and 3-ix. Note that, although a characteristic signal is known to be present in each post-stimulus sweep making up these averages, its rms level at a signal-to-noise ratio of 0.05 is too low for a pattern to emerge in the averaged waveforms. Those for  $S/N$  of 0.1, however, are comparable to supra-threshold records in the range from 10 to about 30 dB SL.

A comparison of this kind brings to light one very important matter: the signal-to-noise ratio of ERA data is often too low for a power measure of this kind to be any more than modestly effective in detecting the evoked potential. This conclusion, of course, assumes that our other hypotheses concerning the signal and noise sources are applicable to the data. Superposition and normality here are probably not as critical as the assumption of statistical stationarity. An investigation of the power distributions for both simulated and actual data may help to elucidate this matter.

### 3.4. Distributions of Power

Using the same ERA and simulated data, a second statistical parameter, the power or variance of each 64 sample sweep, was examined for both pre- and post-stimulus ensembles. A distribution was then formed from a total of 9 by 54, or 486, estimates of variance in each instance.

For broadband Gaussian random noise, this distribution should be  $\chi^2$  distributed with  $(n-1)$  degrees of freedom, where  $n$  is the number of independent samples making up each power estimate. Bandlimiting reduces the number of degrees of freedom to about 9 on average as estimated by the Blackman-Tukey equations. The simulated 'pre-stimulus' and 'unstimulated' data should behave in this manner and serve as a control. Any statistically significant differences between the control distributions and those for the simulated 'post-stimulus' ensembles may suggest some means of using the power per sweep measure in detecting the presence of the signal. Any disparities found between the control and the actual data may reveal the nature and extent of irregularities present in the EEG.

Fig. 3.3. illustrates the type of power distribution typical of 'unstimulated' data for the simulation. As expected, it is  $\chi^2$  distributed with an estimated 8.42 degrees of freedom. This estimate was taken from the relationship known to hold for  $\chi^2$  variables, namely:

$$df_{cv} = \frac{2}{CV_p^2}$$

where  $CV_p$  is the coefficient of variation of the power, defined

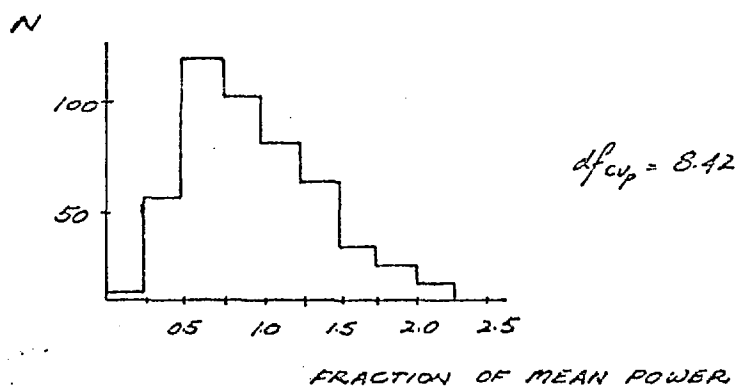


Fig. 3.3. Distribution of power per sweep for bandlimited Gaussian random noise.  $N = 486$ .

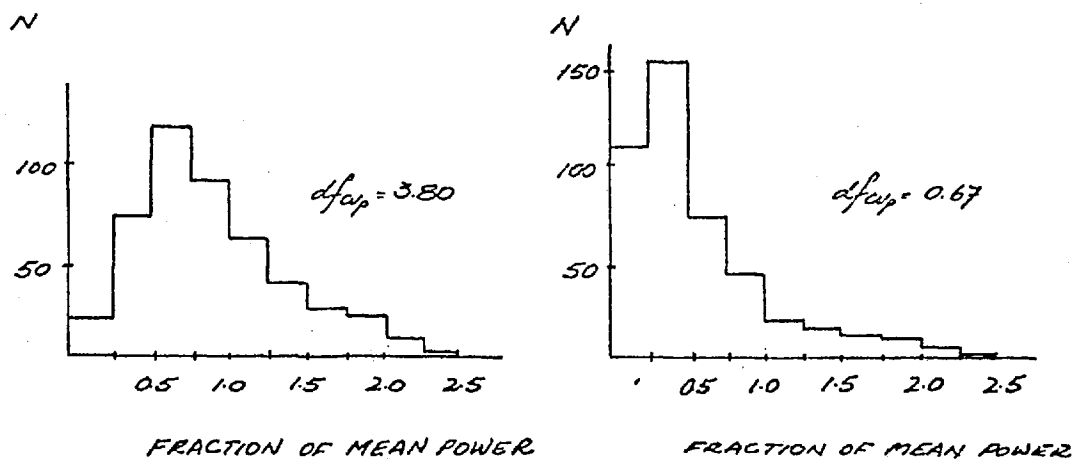


Fig. 3.4. Distributions of power per sweep for the 640 ms pre-stimulus interval. Subjects FN and CR. Note the decrease in  $df$ .

as:

$$CV_p = \frac{sd(\text{power})}{\text{mean}(\text{power})}$$

For large enough df, the sampling statistics of  $CV_p$  can be assumed reasonably normal. Estimates of degrees of freedom by this means are likely to vary by approximately  $\pm 3$  for the 5% confidence interval, being somewhat smaller on average than those estimated by the Blackman-Tukey equations. These equations pertain to the smoothed power spectrum. Smoothing tends to reduce the original power variability, thereby increasing the number of degrees of freedom. As no such filtering operation is used in deriving the coefficient of variation, the greater variability here will introduce a slightly lower estimate of df on average. In addition, a wider spread to these estimates would be expected and this can be determined from the following relation, from which the range of df quoted above is derived.

$$sd_{CV_p} = \sqrt{\frac{CV_p^2}{2df} (1 + CV_p^2)}$$

For all unstimulated control distributions, i.e., for simulated data, no significant difference could be detected between and among them as determined by a Kolmogorov-Smirnov two-sample test on their respective cumulative frequency distributions at 5%. Neither could any statistical significance be found between the controls and any of the simulated 'supra-threshold' distributions on the same basis. Such a finding is not surprising in the light of the F-test performed on the averaged waveforms. The signal-to-

noise ratio of individual sweeps is too low for a power or amplitude measure to reveal any significance on a sweep-to-sweep basis.

Comparison of the control distributions with those derived from the five ERA test subjects, however, reveals striking and highly significant results, suggesting that on the basis of their respective power, the simulated and actual data are drawn from two very different underlying populations. In addition, cross-comparisons of the power distributions between subjects are often significant. Only within a given subject does significance fail to arise. Fig. 3.4. gives some indication of the kinds of power distributions experienced with ERA data.

Although significantly different from the control and from one another, the power distributions of Fig. 3.4. are still  $\chi^2$  distributed. The number of degrees of freedom of these distributions, however, is severely reduced, suggesting a much greater power variability present in the data than would be expected on our assumptions of normality and stationarity. The disparity between the two estimates of df are well outside the 5% confidence interval of  $9 \pm 3$  mentioned above. The Blackman-Tukey estimates for all subjects are comparable to those determined for the synthesized data. Df as derived from the coefficient of variation of the power distribution lie well below this in the range from 0.67 to 4.95.

Unusual and consistently high variability is one characteristic of a nonstationary source. Nonstationarity implies that the estimates of any statistical parameter, here the second moment or variance, vary with the course of time. This will undoubtedly lead to irregularities of one kind or another in the distribution of that statistic. A nonstationary mean, for example, may turn



out to be bimodally distributed where a normally distributed variable is expected on the assumption of stationarity. The second moment, the power chosen for this study, remains essentially  $\chi^2$  distributed. The existence in the EEG of a significantly large number of sweeps either of much higher or much lower power content than synthesized data tends to reduce the degrees of freedom of that  $\chi^2$  variable, often by a factor of four or five.

Any attempts to use the power as a response indicator would be unwise on two counts. The signal-to-noise ratio is often too low to afford reliable results. Even if this were not so, the nonstationarities experienced with the power distributions would require the use of involved nonstationary statistical procedures. Each subject would then have to be considered in and of himself, as the possibilities of pooling power distributions on an inter-subject basis are virtually negligible.

### 3.5. Spectral Analysis

In the time domain, an examination of the a. c. power has failed to offer any consistent means of detecting the evoked potential. It has, however, afforded us some very valuable insights into the behaviour of ERA data. Frequency domain analysis may reveal other signal and noise features related to specific harmonic components which may not be readily recognizable in the time domain. To explore this possibility, the averaged amplitude spectra have been determined for all stimulated and unstimulated trials mentioned before. The synthesized data once again serve as a reference.

The amplitude spectra were derived from the real and

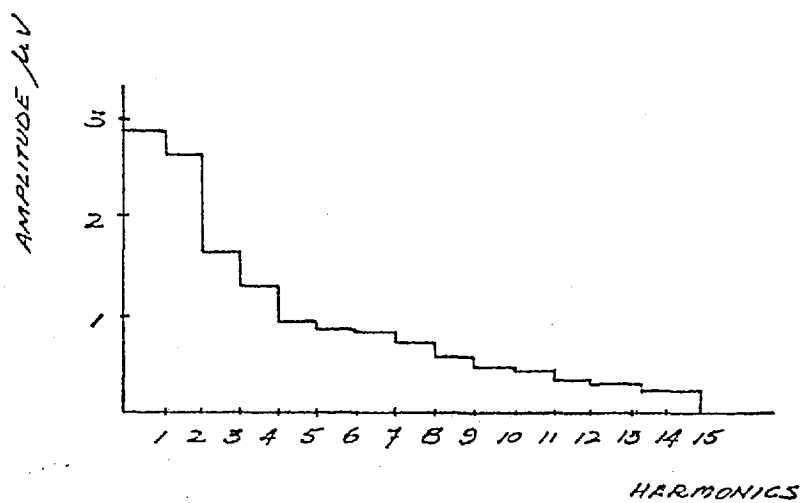


Fig. 3.5. A typical amplitude spectrum for bandlimited random noise.

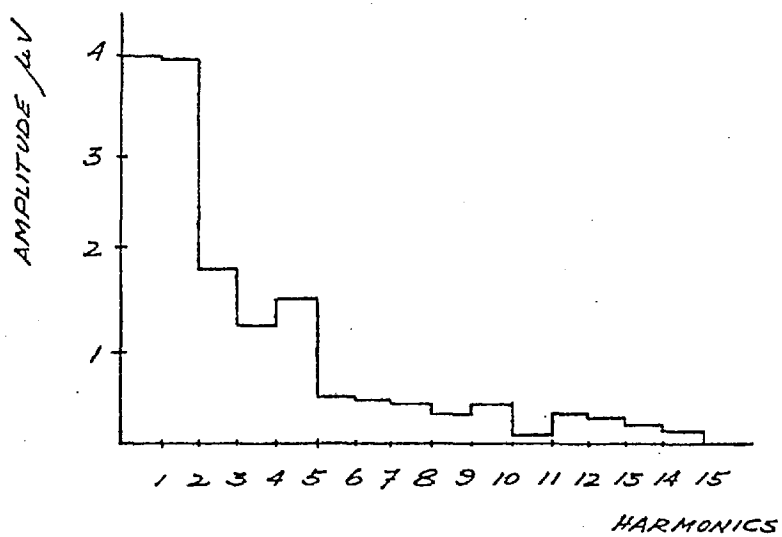


Fig. 3.6. The amplitude spectrum for the template used in the simulation.

imaginary components of the discrete Fourier transform performed on each 64 sample sweep of data. These were then averaged over blocks 54 sweeps long. Fig. 3.5. shows a typical amplitude spectrum for a trial of 'unstimulated' synthesized data. Compare this with the amplitude spectrum of Fig. 3.6., that of the characteristic signal used for the superposition. Both are of the same general character, but with a few important differences. Harmonics 1, 2, and 5 of the template are accentuated, suggesting the possibility of differentiating signal from noise on the basis of their spectral magnitude or power.

When one considers the amplitude spectra of synthesized data for S/N typical of ERA data, i.e., 0.25 or 0.1, the contrast fails to be as marked. See Fig. 3.7. There is often some slight and detectable increase in the signal strength of harmonics 1 and 2 over unstimulated trials, but this is not statistically significant at 5%, nor is it always present, as Fig. 3.7.b. illustrates.

The averaged amplitude spectra of the actual data are fairly similar in character to that of either the 'unstimulated' or 'stimulated' data from the simulation. The presence of non-stationarities is evident at times, as Fig. 3.8. illustrates. These are the amplitude spectra taken from the pre-stimulus EEG of the same subject for two consecutive 54 sweep intervals, a total in ERA testing time of approximately four minutes. Note the very dramatic increase in signal strength of the first few harmonics for the first two minute interval.

These illustrations and comments refer, of course, to an amplitude spectrum derived from a time domain signal 64 samples ( 640 ms ) long. A different choice of record length would either

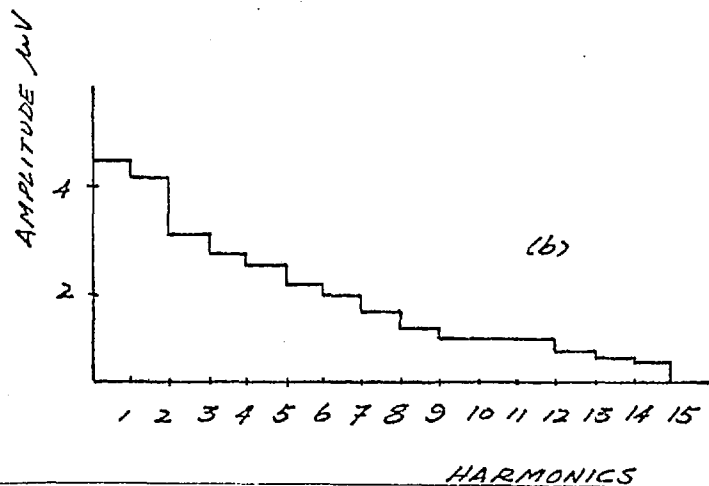
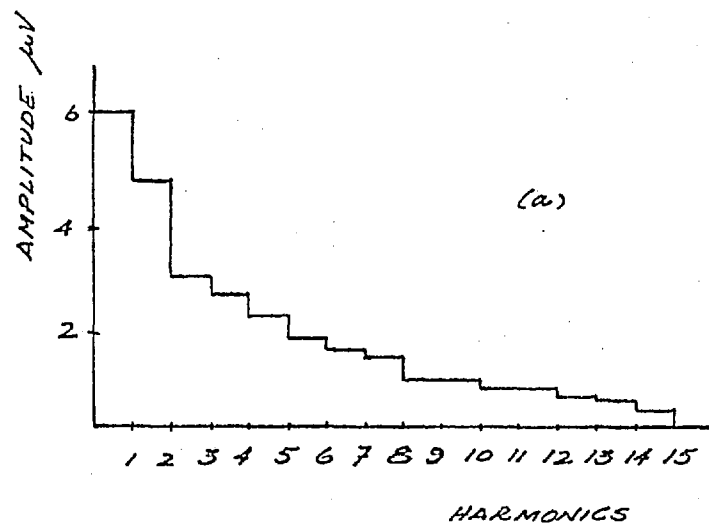


Fig. 3.7. Amplitude spectra for simulated data at  
 a) S/N of 0.25 and  
 b) S/N of 0.1.

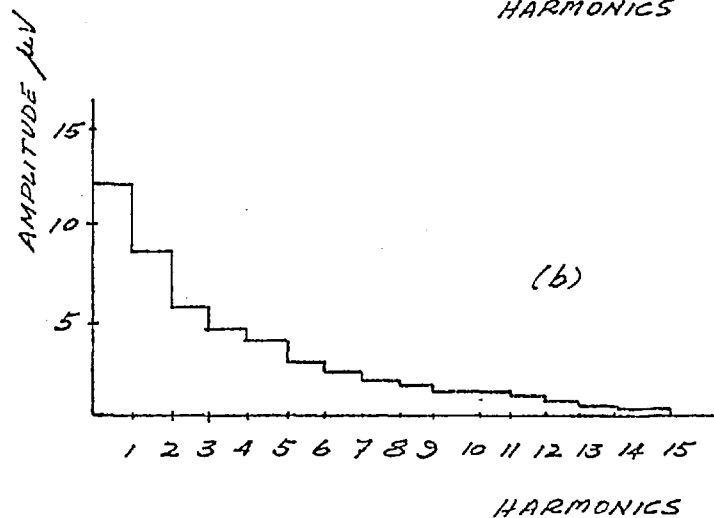
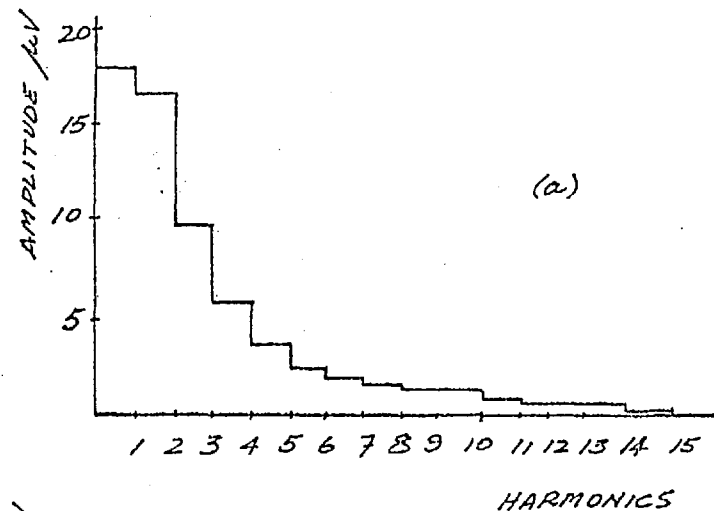


Fig. 3.8. Amplitude spectra from the JS 2 kHz file.  
 a) pre-stimulus trial for 10 dB SL  
 b) trial at 0 dB SL recorded approximately two minutes later.

improve or reduce the resolution among the frequency components of the discrete Fourier transform. Generally speaking, the longer the time interval chosen, the greater the frequency resolution. Ideally, then, for differentiation of signal and noise sources on the basis of their respective spectral components, the longer the interval chosen, the better. Nonstationarities in the EEG and the time duration of the evoked potential make the 640 ms period considered here a reasonable compromise. For this interval, little difference can be seen in the spectral components of signal and signal plus noise conditions.

### 3.6. Concluding Remarks

In the light of the studies discussed in this chapter, several conclusions can be made. The signal-to-noise ratio of ERA data is often too low for amplitude or power measures to be effective in differentiating between response and no response conditions. Even when the S/N is improved by coherent averaging, inconsistent results are prevalent, confirming this conclusion. More importantly, the variance or power is nonstationary for EEG records. Without recourse to nonstationary statistical procedures, variance cannot be used as the basis of a statistical test for significance.

Amplitude and power spectra do little more than provide us with a general description of a signal, in terms of the relative magnitudes of its frequency components. The general character of both the EEG and the evoked potential are remarkably similar. Both occupy essentially the same frequency range, the signal strength of one not often significantly different from the other.

Yet, differences do exist between them. These are of a far more subtle nature, in that the evoked potential may be recognized as having a particular characteristic shape or pattern. The information as to the relative timing of the various frequency components can also be seen in the Fourier transform. The phase spectrum, often regarded as problematic because of a condition known as wrap-around, is nonetheless available for analysis. Because phases reflect all the timing information of the harmonics, they hold more promise as a means of detecting a signal such as the AEP. The next chapter deals exclusively with the phase characteristics of both the EEG and the evoked potential.

Tables 3-i to 3-x

F-test Results on AEP and Simulated Data

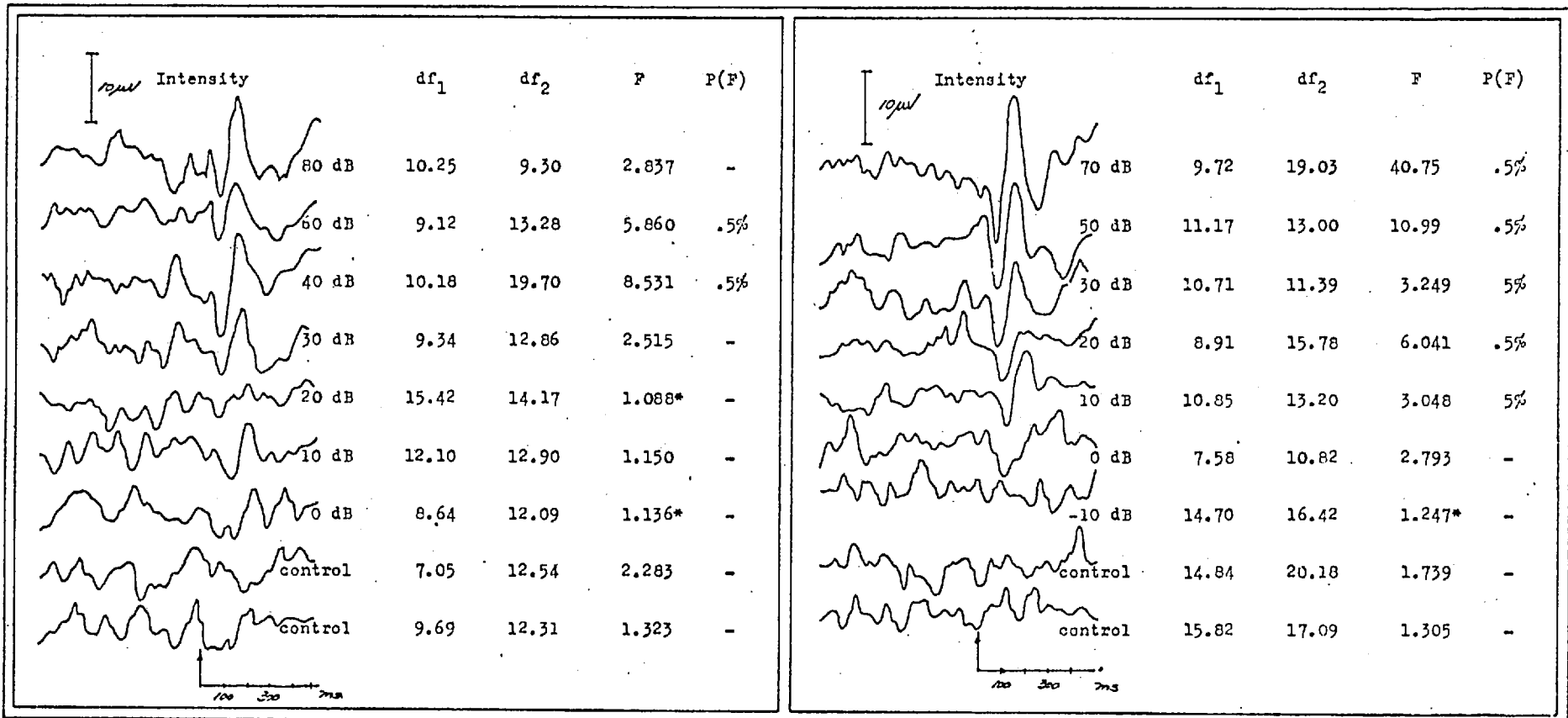


Table 3-1. Subject CH, F, age 23, at 2 kHz and 500 Hz.



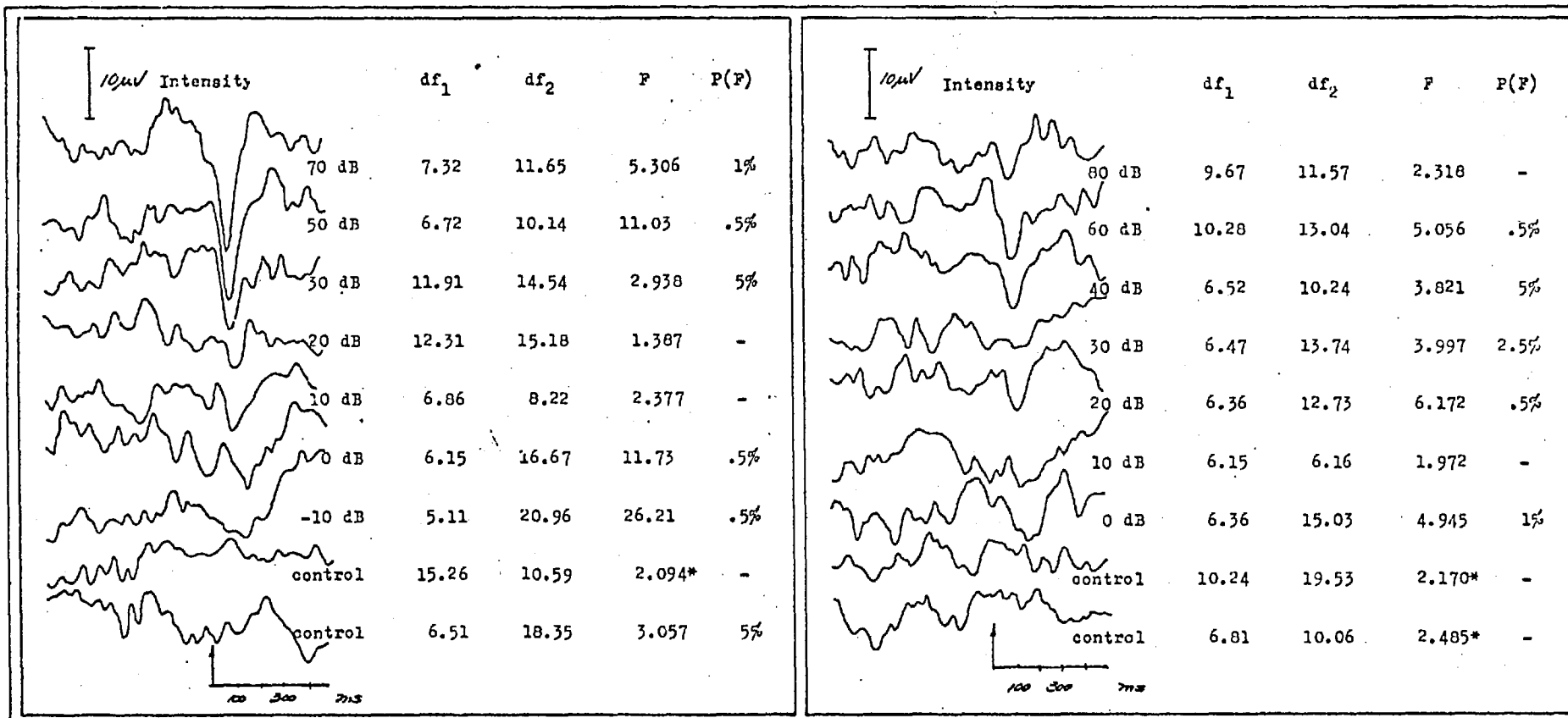


Table 3-ii. Subject GF, M, age 28, at 1 kHz and 4 kHz.

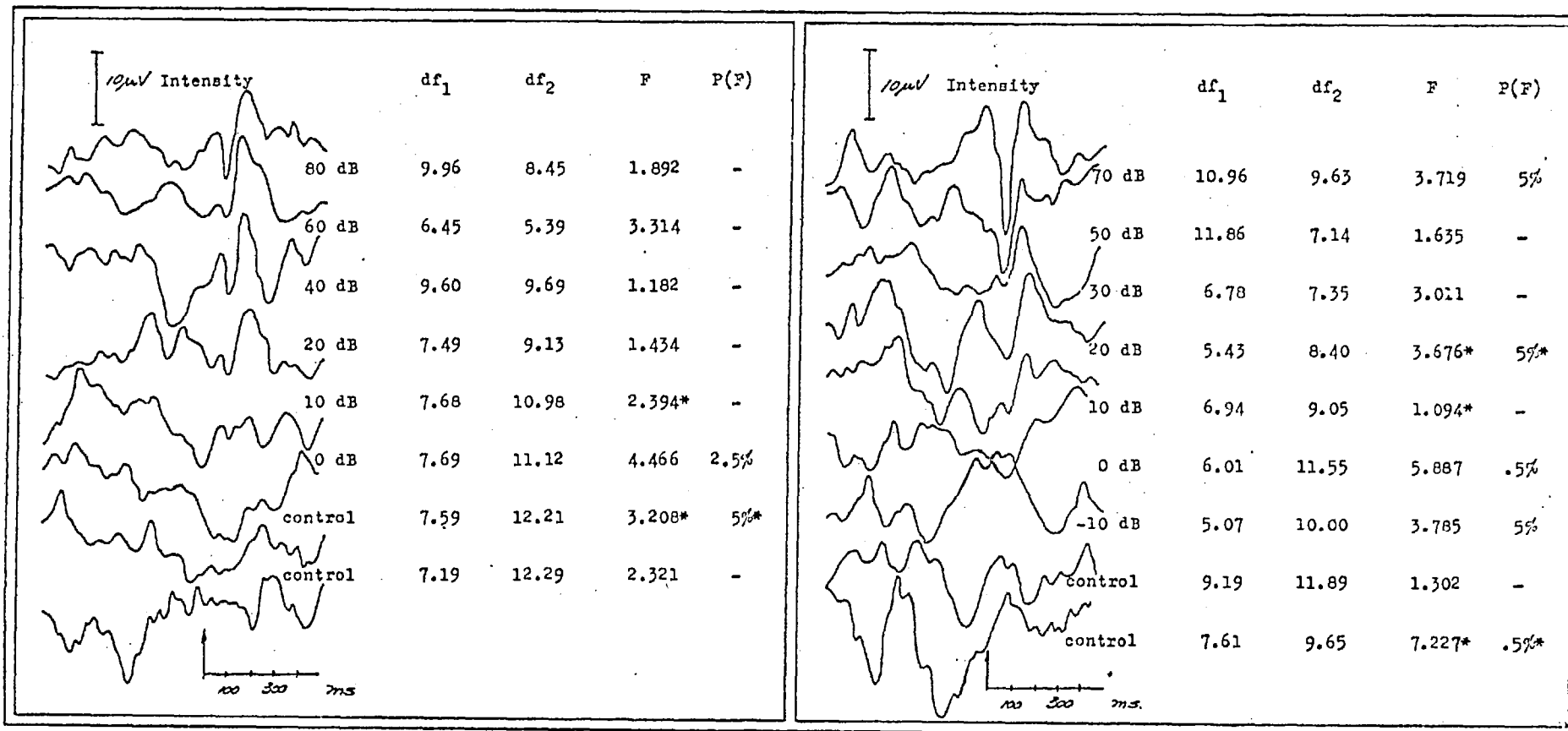


Table 3-111. Subject JS, F, age 23, at 2 kHz and 500 Hz.

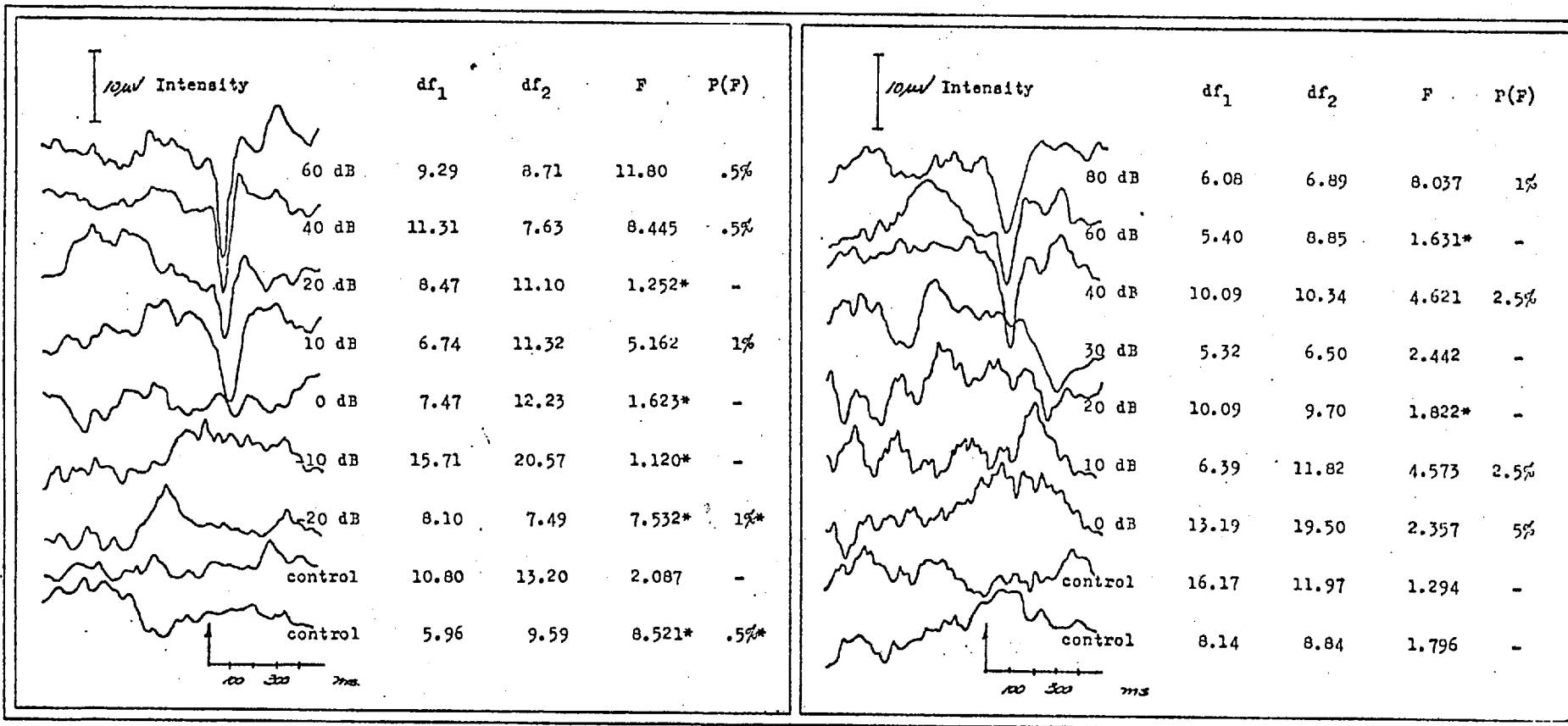


Table 3-iv. Subject CR, F, age 31, at 1 kHz and 4 kHz.

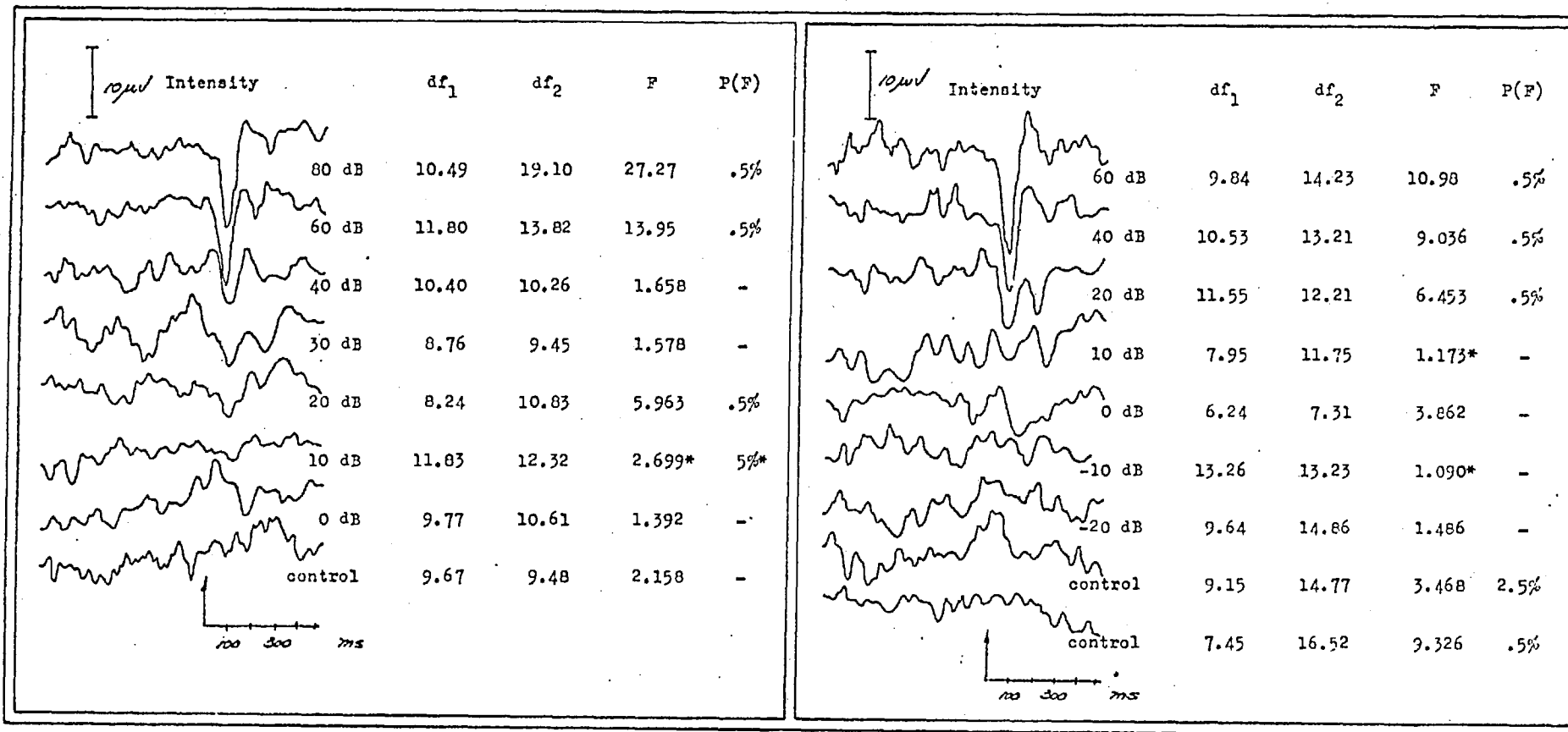


Table 3-v. Subject FN, M, age 28, at 2 kHz and 500 Hz.

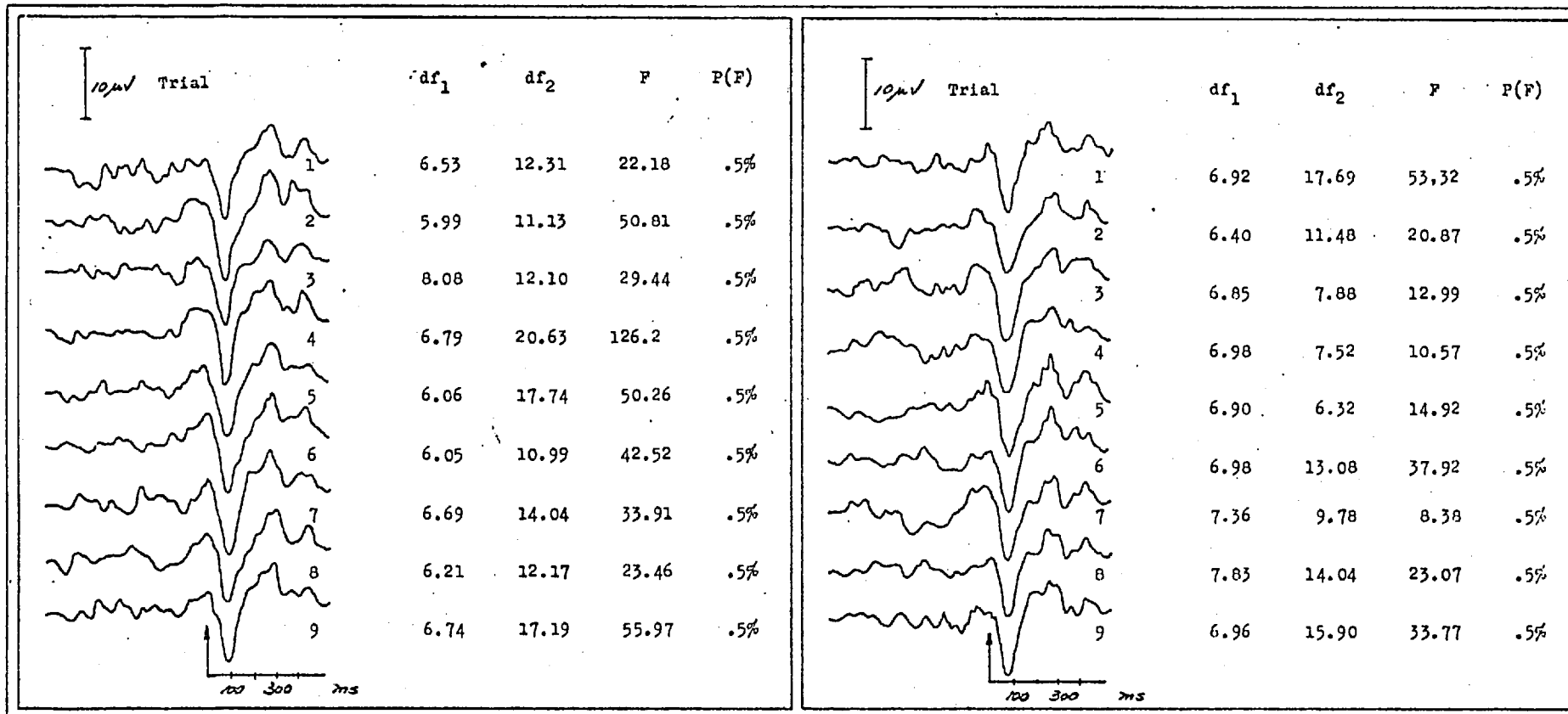


Table 3-vi. Bandlimited Gaussian random noise for S/N of 0.5.

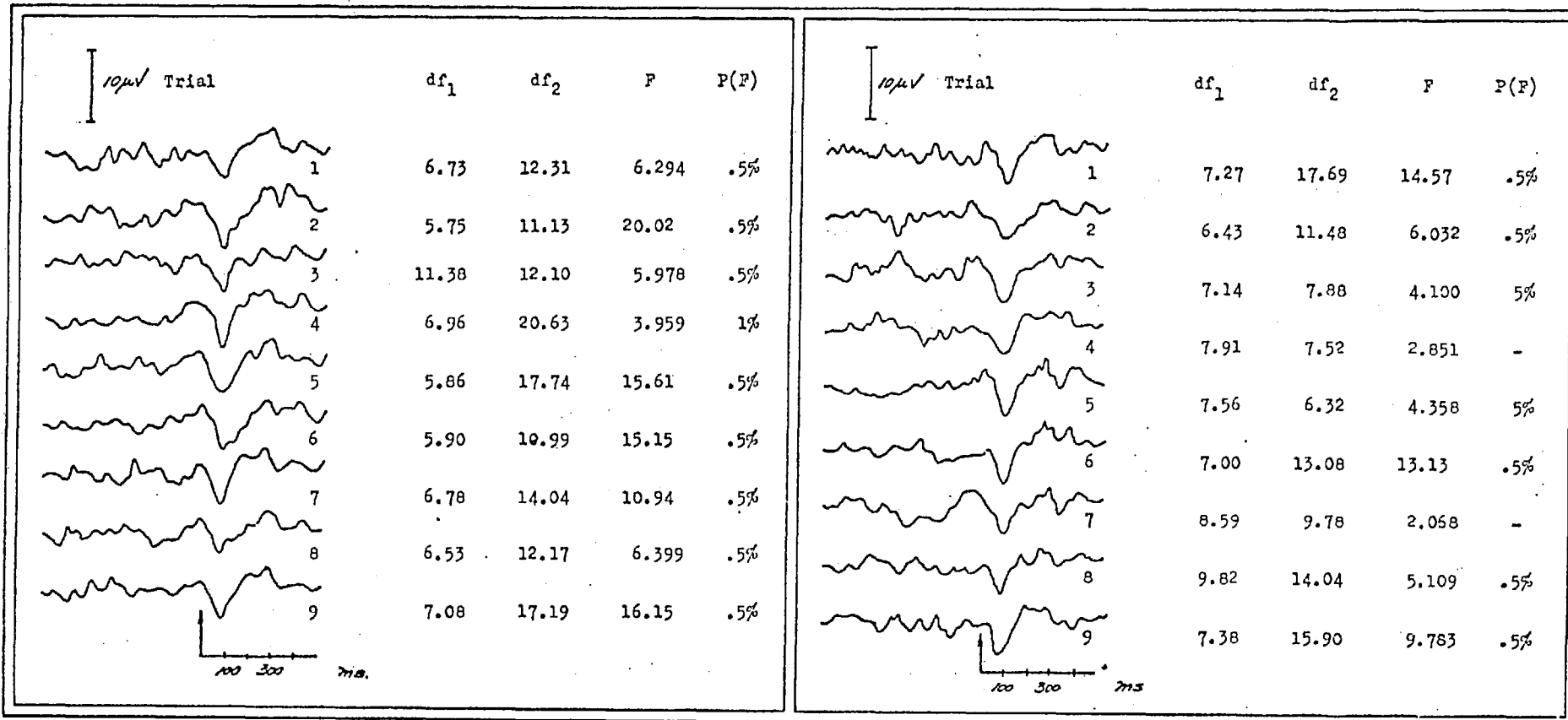


Table 3-vii. Bandlimited Gaussian random noise for S/N of 0.25.

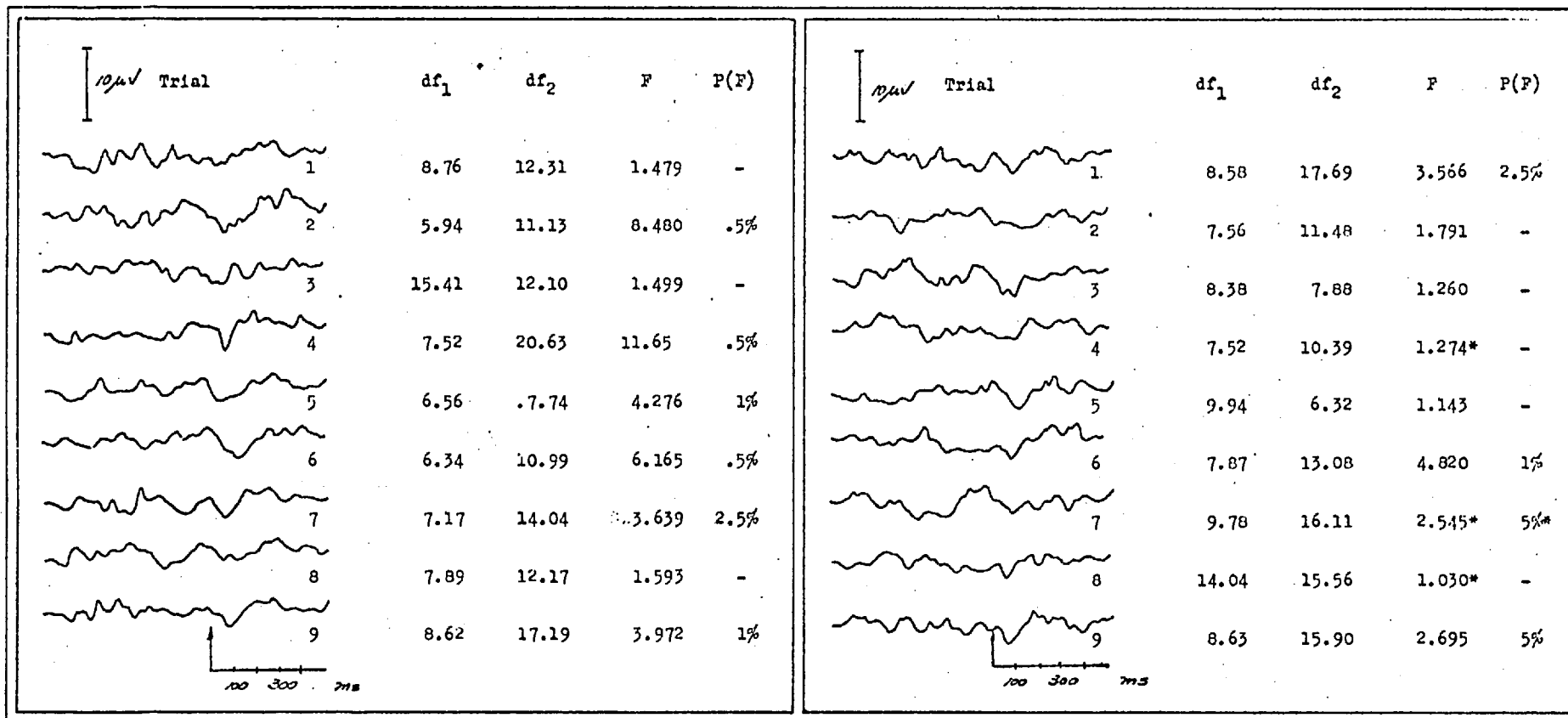


Table 3-viii. Bandlimited Gaussian random noise for S/N of 0.1.

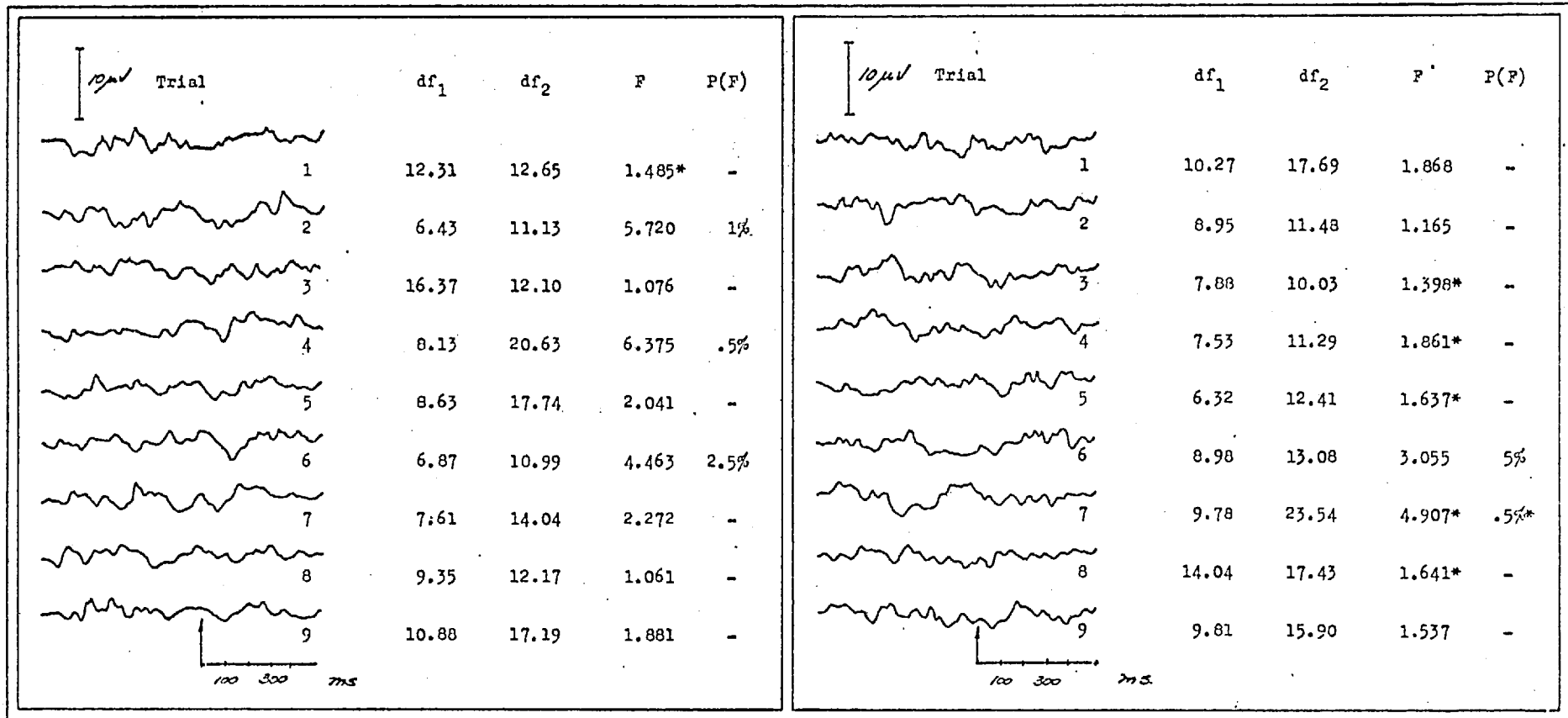


Table 3-ix. Bandlimited Gaussian random noise for S/N of 0.05.



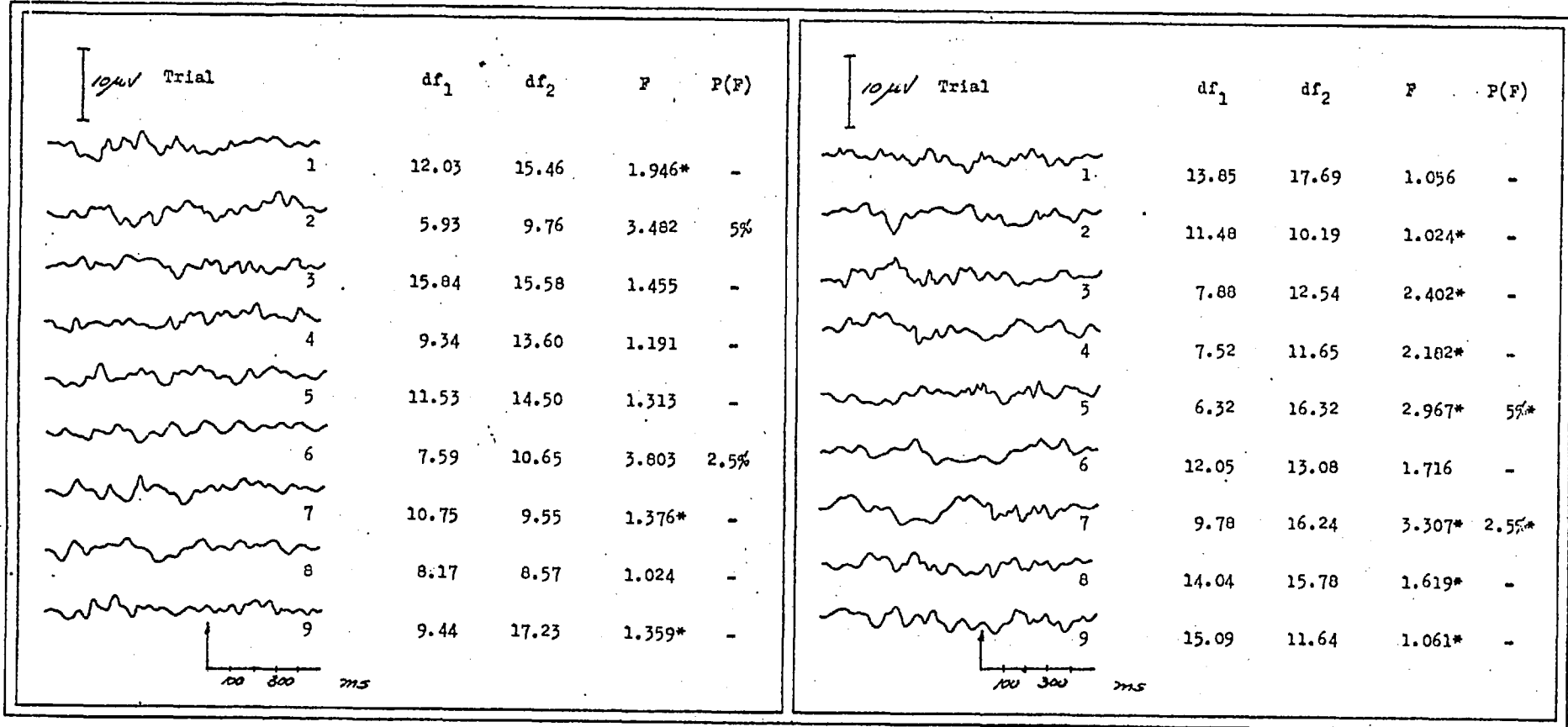


Table 3-x. Bandlimited Gaussian random noise.

## CHAPTER FOUR

## PHASE DISTRIBUTIONAL ANALYSIS

## 4.1.i. Introduction

Although too small to be detected reliably in terms of its signal strength, the evoked potential is nonetheless a signal of characteristic shape. Exploiting this property through various pattern recognition techniques may provide some more effective means of detecting the AEP, and possibly further our understanding of the behaviour of both signal and noise sources. Two general approaches are possible. Some methods assume prior knowledge of the pattern to be detected, such as the template matching techniques dealt with in Chapter Five. Others make no such assumption, but merely reveal the presence of any consistent pattern other than noise. The phase distribution analysis discussed here is of this second kind.

## 4.1.ii. Theoretical Background

Any signal or length of noise can be described by a series of sine and cosine components known as its Fourier coefficients. These complex numbers provide a frequency domain representation of the signal in terms of the magnitude and phase of its fundamental and higher order harmonics. Often, it is both

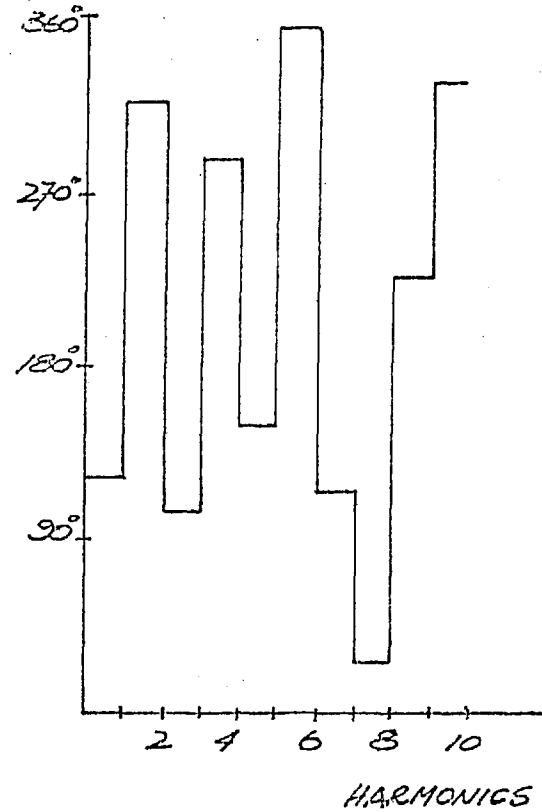
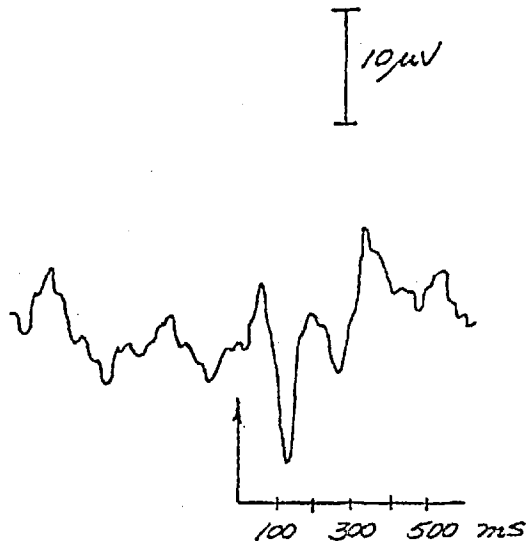


Fig. 4.1.a. A high level evoked potential.

Fig. 4.1.b. The phase spectrum of Fig. 4.1.a. taken over the first ten harmonics.

convenient and illuminating to analyse a signal in the frequency domain.

In the past, attention has centered on the amplitude or power spectra. This particular approach, we concluded, is not sufficiently sensitive to the subtle differences in pattern observed between the AEP and EEG. A recurring pattern implies some synchronization of activity in the time domain, and this information is reflected as a constraint in the harmonics of the phase spectrum.

Phase spectra, however, are more difficult to analyse. In this context, any phase value arises out of the conversion from Cartesian to polar coordinates of its complex Fourier coefficients. Because this conversion relies on the use of the arc-tangent function, phases are restricted to a  $180^\circ$  range. By the use of further information, specifically the sign of the real part of the complex number, this range can be extended to  $360^\circ$ . From here, by inference at least, the range of phase values can be extended even further.

Consider the signal of distinctive shape shown in Fig. 4.1.a. Its phase spectrum ( Fig. 4.1.b. ) can be thought of as consisting of two superimposed functions of frequency. One reflects the shape of the signal, the other, its time delay from a point of maximum symmetry. Neither of these two components can be distinguished readily from the phase spectrum shown in Fig. 4.1.b. However, by making use of this information, the phases can be unwrapped, thereby extending the range of phase values, and revealing the presence of a linear trend proportional to frequency. See Fig. 4.2.a. Removal of this trend results

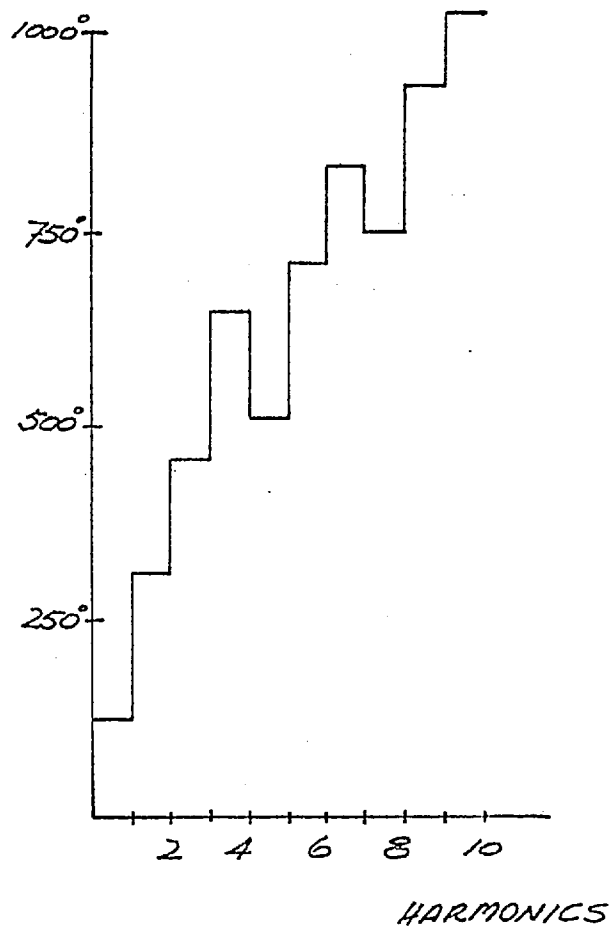


Fig. 4.2.a. The phase spectrum of Fig. 4.1.b. after unwrapping.

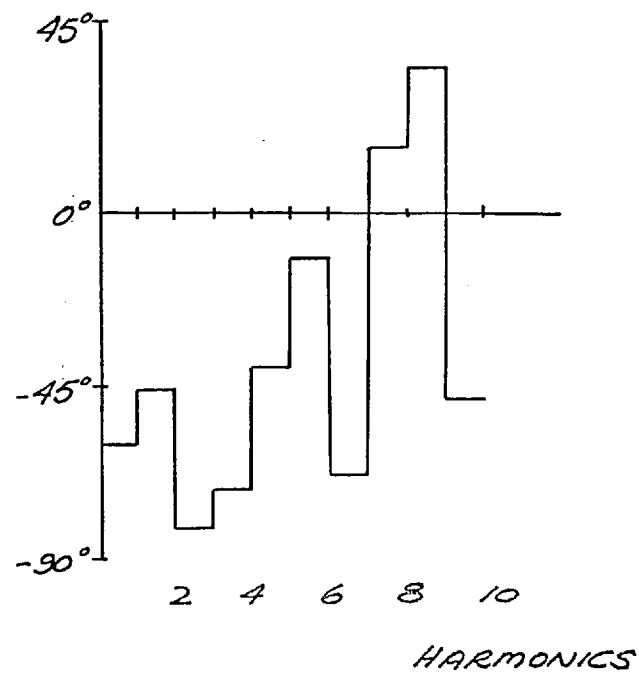


Fig. 4.2.b. The same phase spectrum after removal of the linear trend.

in a phase spectrum solely reflecting the pattern of the AEP taken from its point of maximum symmetry. ( Fig. 4.2.b. )

Once the phase spectrum has been determined for each sweep of an ensemble, the distribution of phase values for each harmonic of interest can be set up, and some means devised for testing its significance. If no recurring pattern is present in the record, as is the case for spontaneous EEG, we would expect the phase distribution to be uniform. This constitutes the null hypothesis,  $H_0$ . The presence of a signal such as the AEP in successive sweeps of the ensemble, however, implies some synchronization of the continuous EEG. This should be reflected as a significantly non-uniform distribution of the phases for the particular harmonics involved in producing that pattern. ( Sayers, Beagley, and Henshall, 1974 )

The uniform distribution postulated under  $H_0$  is in fact a cylindrical one. In the first instance, it may be possible to ignore this inherent periodicity without introducing too much distortion to either the outcome or the interpretation of test results. This could be implemented very simply, by considering the phase distributions to be rectangular and then applying a  $\chi^2$  or perhaps Kolmogorov-Smirnov goodness of fit test for significance. Should this lead to anomalies or inconsistencies, then rotational statistical procedures would have to be introduced to account for the periodic nature of the phase distributions. These might involve a modification to the  $\chi^2$  test, where the rectangular distribution is rotated in discrete steps from  $0^\circ$  to  $360^\circ$ , or an examination of the mean phase vector, which under  $H_0$ , would tend to zero magnitude.

4.1.iii. The  $\chi^2$  Test

To explore the possibilities of using this approach to detect the AEP, a one-sample  $\chi^2$  goodness of fit test was chosen in the first instance. ( Riha, J., 1975 ) From an ensemble of 64 records of either stimulated or unstimulated EEG, each 640 ms sweep was Hanned and the phase spectrum of harmonics one to five determined. These were found to contribute most to the characteristic pattern of the AEP. The ensemble phase distributions for each of these harmonics were then formed into histograms of four, six and twelve bins and comparisons made with the rectangular distribution expected under  $H_0$  by means of the following relation:

$$\chi^2_{k-1} = \sum_{i=1}^k \frac{(O_i - E_i)^2}{E_i}$$

Here,  $O_i$  is the observed, and  $E_i$ , the expected, number of phase values in a given bin, while  $k$  is the number of categories or bins for the test. The variable  $\chi^2_{k-1}$  is distributed as  $\chi^2$  with  $k-1$  degrees of freedom.

This statistic was applied to a sample of data taken from nine normal young adults under a total of 65 stimulus conditions. In most instances, significance in the  $\chi^2$  statistic was seen to coincide with a visually scored positive response. Unstimulated records failed to reveal any significance other than what was expected under  $H_0$ .

Certain factors, such as the bin size or the arbitrary choice of reference for the phase histograms, were found to

influence  $\chi^2$  test results. This, coupled with its apparent effectiveness in differentiating between response and no response conditions, justified further investigation. In order to validate the technique, an on-line clinical trial was proposed. The data collected would then allow us to explore the behaviour of the  $\chi^2$  statistic, particularly in relation to the essentially periodic nature of the phase distributions.

#### 4.2.i. The On-Line Trials

16 normal hearing young adults aged 20 to 31 took part in a clinical on-line trial designed to test the effectiveness of the phase technique in a real-time situation. In addition, the data was stored on analog tape for subsequent analysis off-line. A detailed description of the experimental set-up may be found in Chapter Two.

Each subject was tested at two different tone burst frequencies, approximately one-half of the group at 500 Hz and 2 kHz, the rest at 1 kHz and 4 kHz. A frequency trial consisted of seven runs of 64 stimulus presentations ranging in intensity from 80 dB to 0 dB HL. A no stimulus control run was performed at the beginning and end of each trial. This, it was hoped, would give us some indication of the effects on the test results of any long-term changes in the character of the EEG.

Because of both core and timing limitations of the computer used for this study, certain compromises had to be made. Only 40 of the 64 sweeps could be digitized and analysed on-line. Once the Fourier transform was taken and the phase spectra for



harmonics 2 to 6 derived, a single  $\chi^2$  test was all that could be accommodated. For this, four bins were chosen with the phase histograms referenced to  $0^\circ$ . Although a small statistical sample and an arbitrary choice of goodness of fit test for  $H_0$ , it was thought to be adequate for a preliminary trial of the phase technique.

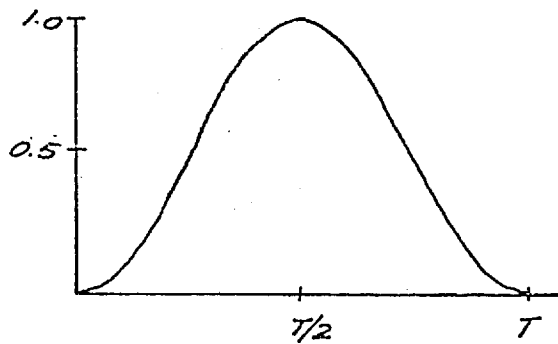


Fig. 4.3. The full Hanning window.

The stimulus marker pulse was set up in such a way that it triggered the ADC to begin data collection 150 ms prior to the presentation of the stimulus. This was introduced in order to reduce the effects of Hanning on the individual evoked potentials. A sampled, aperiodic signal such as the EEG is often multiplied by some gating function before Fourier analysis is undertaken. The discrete Fourier transform which results from this procedure is then interpreted as an isolated statistical sample from the convolution of the spectra of these two signals. To assure continuity at the beginning and end of each sweep, the full Hanning

window is often chosen as the gating function. This is the bell-shaped curve shown in Fig. 4.3. As can be readily seen, the first and last 10% to 15% of any sweep multiplied by this curve will be seriously attenuated. So as not to distort the evoked potential, a 150 ms time delay to the presentation of the stimulus was implemented.

For the results of this on-line study, consult Tables 4-i to 4-xvi. Every table is divided into two sections, one pertaining to each of the two tone burst frequencies used in testing a given subject. Within each section, the nine stimulus trials are stated in terms of dB sensation level (SL) for the test, and accompanied by their respective averaged responses over the interval chosen for analysis. Here, the analysis window is 640 ms long and begins 150 ms prior to stimulus presentation. The vertical arrow on the time base at the foot of each section indicates the time of stimulus presentation. Unless otherwise stated, a calibration of 12  $\mu\text{V}/\text{cm}$  applies throughout. Probability levels for  $\chi^2_3$  performed on the phase distributions of harmonics 2 through 6 are tabulated alongside; dashed lines refer to nonsignificant findings.

#### 4.2.ii. Discussion

At high intensity levels, the average evoked potential is usually a large and sharply defined signal. As the intensity is reduced, however, the averaged response becomes smaller and less distinctive in shape. Such behaviour may be interpreted in several ways. Either the number of individual evoked potentials in the ensemble, their shape and amplitude, or both, diminishes

with diminishing intensity. In the light of the assumptions made concerning the phase distributions, we would expect different findings for each of these possibilities.

If numbers alone are involved in creating the difference in averaged waveforms, essentially the same frequency components should exhibit a phase constraint at all supra-threshold levels. This constraint would then become less and less pronounced as the intensity is reduced. If, however, the shape of individual evoked potentials is responsible, we would expect the phase constraint to engage first higher, then lower, order harmonics with reductions in intensity level. A change of shape might equally likely reflect some altered relative latencies in the components making up the response and this would reveal a shift in the relative phases of several harmonics. Should both mechanisms be at work, some combination of these two findings will no doubt emerge.

With reference to Tables 4-i to 4-xvi, both the degree of phase constraint and the harmonics involved are seen to change with intensity level for most of the subjects tested. Generally speaking, high intensities coincide with a significant amount of phase constraint in several, if not all, the harmonics considered. As the intensity is reduced, the degree of constraint reflected in the probability level of  $\chi^2$  test results diminishes accordingly and usually involves fewer harmonics, although not necessarily the lower order ones.

Consider Subject SA at 500 Hz. ( Table 4-xiv ) Significance is seen mostly at .1% for intensities of 50 dB SL or greater and all harmonics are engaged. For records taken at 30 dB SL or less, the level of significance drops to either 2% or 5% and only two or three frequencies are constrained. On the

basis of our assumptions, these findings suggest that a reasonably consistent response is evoked at all supra-threshold levels. At reduced intensities, however, fewer frequencies in the EEG are synchronized to the stimulus on fewer occasions.

There is, of course, evidence of more erratic behaviour as the files for Subject GF at 4 kHz ( Table 4-ii ) will illustrate. Sporadic patches of significance can be seen in most records down to 0 dB SL, but in all instances only one harmonic per record is engaged, and seldom the same one. Less consistency is to be found in the averaged waveforms here than is the case for Subject SA. This suggests that a smaller number of individual sweeps contribute to the average, and that the time-locking mechanism we postulate affects different EEG rhythms over the course of time. This second inference may well reflect a non-stationary frequency structure in the EEG.

Viewed overall, our expectations are confirmed by the results of this on-line study. The phase distributions of supra-threshold records do exhibit a significant degree of nonuniformity, indicating that some reasonably consistent feature other than noise is present in these records. There is, however, a larger percentage ( 20% ) of false negatives than the number anticipated on the basis of preliminary off-line investigations. Most of these occur within 20 dB or so of threshold, suggesting that this particular test is insensitive to the presence of the evoked potential at lower intensity levels. Even more striking are a few cases, for example, Subjects DF at 2 kHz ( Table 4-xv ) and LS at 4 kHz ( Table 4-xvi ), where most of the supra-threshold records are nonsignificant, yet the coherent average indicates a definite response.

The sample size chosen for this study may go some way towards explaining the anomalies. Certainly, at lower intensity levels where the AEP exhibits less phase constraint, a small statistical sample might not be sensitive enough to detect it. The phase histograms of these records, however, frequently reveal a considerable degree of nonuniformity which the  $\chi^2$  test has failed to detect as significant. See Fig. 4.4. Both the bin size and the choice of zero reference for the use of  $\chi^2$  are known to affect the test results. These findings suggest that, in certain cases at least, some account must be taken of the periodicity of the phase distributions. The next section is devoted exclusively to the  $\chi^2$  statistic, its behaviour and application to synthesized data of an inherently cyclic nature.

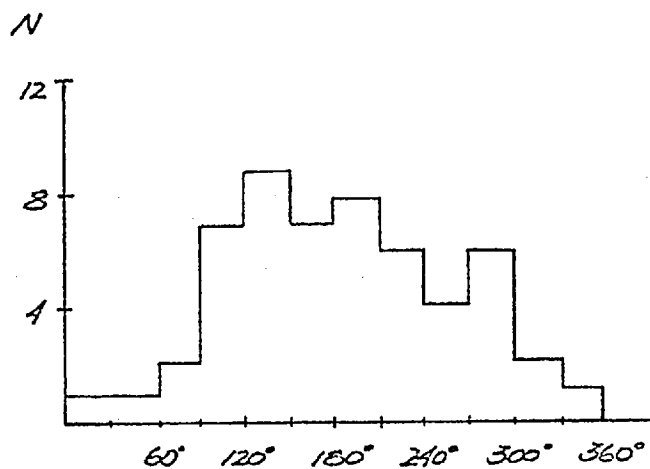


Fig. 4.4. A 12 bin phase histogram revealing a constraint undetected by the  $\chi^2$  test.

#### 4.3.i. The Behaviour of $\chi^2$

When applied to phase distributions, the  $\chi^2$  variable is influenced by two factors. One is the choice of bin size, or number of categories, for the test. The other is the arbitrary choice of reference for the comparison made between the actual, periodic, histograms, and the rectangular distribution expected under  $H_0$ .

For a  $\chi^2$  variable, the greater the number of degrees of freedom, or categories, the lower its variability. Increasing the number of bins, then, should improve the consistency and sensitivity of the test. This is limited by one factor only: the expected number of values in any one category must not drop below five or inconsistencies will arise. ( Cochran, 1952 )

On the whole, phase distributions tend to be only broadly constrained about some value  $\theta$ , especially at lower intensity levels. ( Fig. 4.4. ) Dividing the histograms into as many bins as possible would break up this constraint and tend to reduce, rather than improve, the chances of detecting this feature. Although theoretically less sensitive, a smaller number of bins, two in this instance, was chosen so as to accentuate the broad constraint often seen in the phase histograms.

The uniform distribution postulated under  $H_0$  is now taken to be cylindrical. Initially, a zero degree reference is chosen and a two bin  $\chi^2$  goodness of fit test performed on it. Then, for the same histogram, the reference is incremented in discrete  $10^\circ$  steps as illustrated in Fig. 4.5. Each  $10^\circ$  rotation of the histogram produces a  $\chi^2$  value, which can then be considered

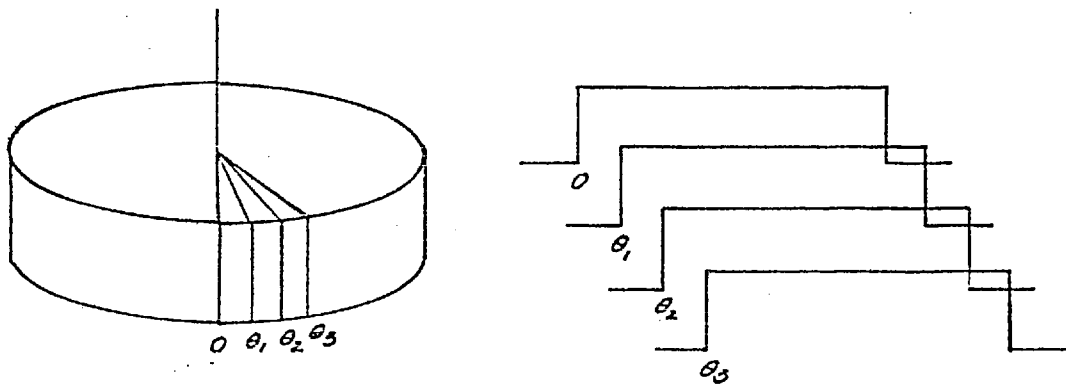


Fig. 4.5. The cylindrical distribution now postulated under  $H_0$ . Slicing the cylinder at  $\theta_1$ ,  $\theta_2$ , etc., produces the rectangular distributions shown on the right.

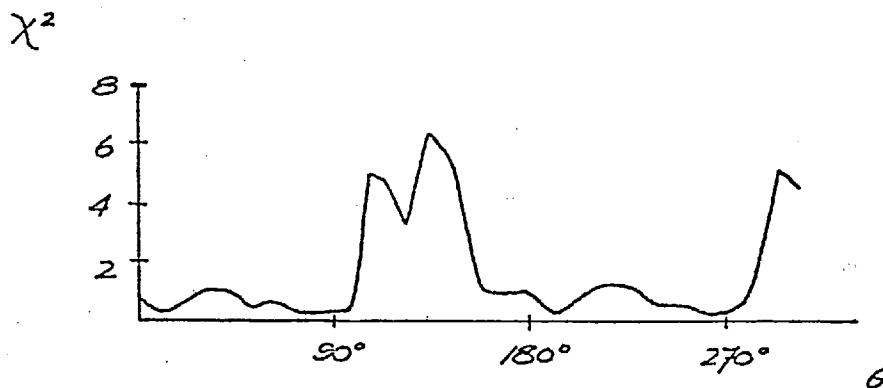


Fig. 4.6. The  $\chi^2_1(\theta)$  function, periodic over  $180^\circ$ .

as a function of rotation,  $\theta$ . The step-wise rotation is implemented through  $180^\circ$ , at which point the  $\chi^2_1(\theta)$  function becomes periodic. See Fig. 4.6.

As can be seen from this figure, the values of  $\chi^2_1$  fluctuate considerably as a function of  $\theta$ . There will always be a theoretical minimum of zero, when an equal number of phases are found in each bin. The maximum will occur corresponding to the angle  $\theta_m$  where the greatest deviation from the uniform distribution is seen. Choosing the maximum value, denoted by  $\chi^2_1(\theta_m)$ , should optimize the procedure, affording far greater sensitivity to the test itself.

#### 4.3.ii. Simulation

Both uniformly distributed, and broadband Gaussian random noise were generated in order to study the sampling statistics of the rotational  $\chi^2$  variable. Uniformly distributed data, periodic over  $360^\circ$ , served as a control on the use of  $\chi^2$  as a test of the null hypothesis. From the Gaussian random data, the effects of signal processing on the phase distributions could be investigated. Hanning, in particular, affects the phase spectrum, introducing dependence among the harmonics. This is, of course, a sequential interdependence; the distribution of all second, third, or  $n$ th harmonics should not, at least theoretically, be seriously affected. Because of the anomalies experienced in some of the on-line data, the effects of signal processing were still thought to be worth verifying empirically.

To this end, uniformly distributed data was generated



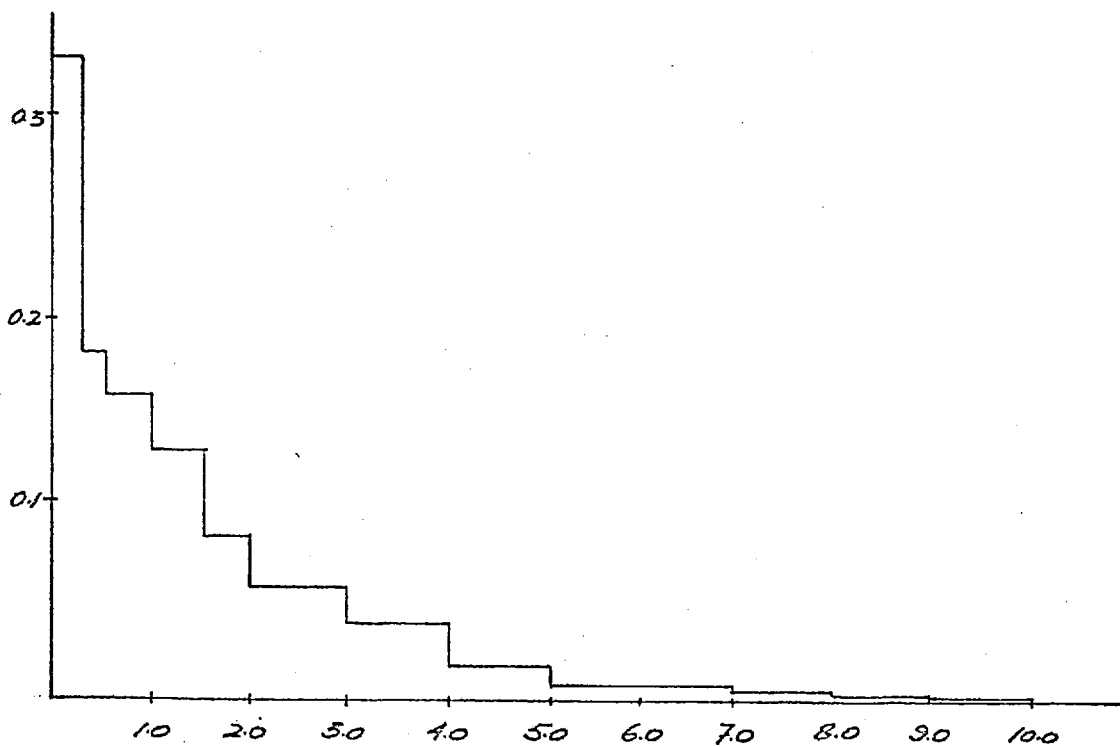


Fig. 4.7.a. Probability density function for  $\chi^2_1(0^\circ)$  derived empirically from uniformly distributed data.

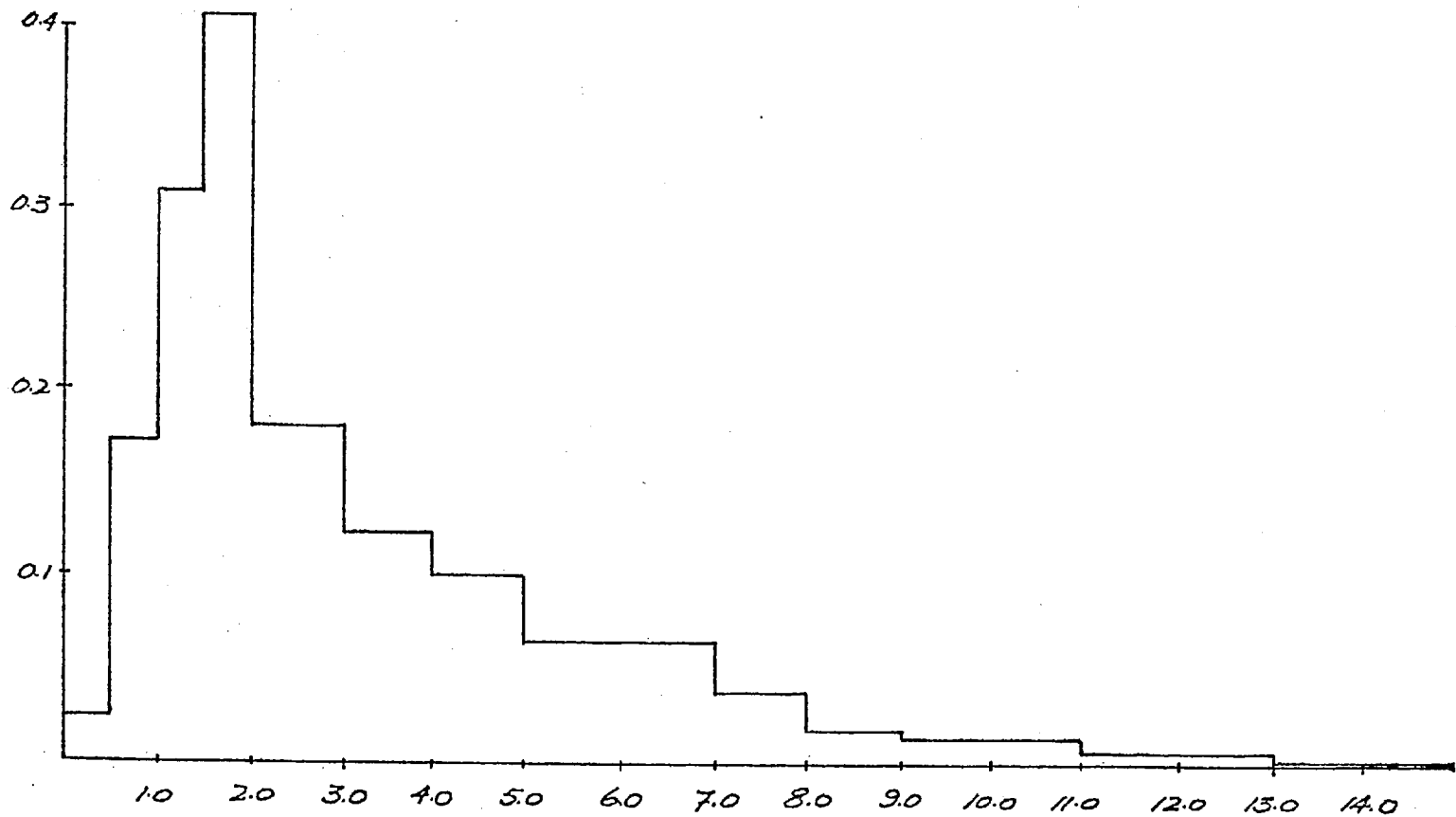


Fig. 4.7.b. Probability density function for the maximum of the  $\chi^2_1(\theta)$  function derived empirically from uniformly distributed data.

in blocks 54 samples long and then arranged into trials consisting of 1080 blocks. Gaussian random noise was generated as described in Chapter Three, where 64 samples made up a sweep, 54 sweeps a block, and 108 blocks in a trial. Phase distributions for the first ten harmonics were considered, and pooled to form an overall sample size of 1080 for  $\chi^2$  analysis.

The number 54 was chosen so as to coincide with the data taken from the on-line study. Of the 64 sweeps recorded on analog tape, only 54 were selected as free from saturation or other recording artifacts.

Once generated, both types of data were subjected to an exploratory  $\chi^2$  survey. In the case of normally distributed data, each sweep was first Hanned and then the phase spectrum determined. From blocks of 54 sweeps, phase histograms for the first ten harmonics were set up and  $\chi^2_1(\theta)$  results pooled over these harmonics. In both instances, 1080  $\chi^2_1(\theta)$  functions were determined and two values, the maximum denoted by  $\chi^2_1(\theta_m)$ , and that corresponding to a zero degree reference,  $\chi^2_1(0^\circ)$ , were selected. The probability density functions for each of these variables may be found in Fig. 4.7.

#### 4.3.iii. The Distribution of the Maximum

Both uniformly distributed data and the phase histograms formed from broadband Gaussian random noise behaved in a very similar manner, ruling out any possibilities of distortions due to signal processing. For simplicity, this discussion will only make reference to uniformly distributed data.

From Fig. 4.7., a striking difference may be seen in the probability density functions for the two  $\chi^2$  variables under study. As expected,  $\chi^2_1(\theta^0)$  is distributed as  $\chi^2$  with a single degree of freedom. Both the mean and standard deviation of the distribution of the maximum  $\chi^2$ , however, indicate that this particular variable is distributed with three degrees of freedom. A one-sample Kolmogorov-Smirnov test on its cumulative frequency distribution confirms this finding, revealing no significant difference, at 5%, from a  $\chi^2_3$  distribution.

To some extent, the increase in degrees of freedom is to be expected. Choosing the maximum cannot help but introduce a bias in the distribution towards a greater percentage of higher  $\chi^2$  values. This, in turn, increases the sensitivity of the test, by reducing the variability of the  $\chi^2$  statistic. Because the bin size remains constant throughout, the position of the maximum must in some way influence this variability. Elementary probability theory affords us some insight on how this influence may be effected.

For this, we postulate that each  $\chi^2_1(\theta)$  function can be thought of as having  $n$  degrees of freedom. From this function the maximum only is chosen, and we may describe this choice as the probability that  $\chi^2_1(\theta)$  is greater than some specified level denoted by:

$$P(\chi^2_1 > x) = g(x)$$

Determining the probability that the maximum has a value at least  $x$  is related to the probability that, assuming independent  $\chi^2_1$ ,

all  $\chi^2_1$  are less than  $x$ , or:

$$P(\chi^2_1(\theta_m) > x) = 1 - P(\chi^2_1(\theta_1) < x \cup \chi^2_1(\theta_2) < x \cup \dots \\ \dots \cup \chi^2_n(\theta_n) < x)$$

If  $f(x)$  is the cumulative frequency distribution for a  $\chi^2_1$  variable, the above expression reduces to:

$$P(\chi^2_1(\theta_m) > x) = 1 - f(x).f(x)\dots f(x)$$

n times

or:

$$P(\chi^2_1(\theta_m) > x) = 1 - f^n(x)$$

This is the probability for the maximum. Its cumulative frequency distribution is what concerns us, and this is given by:

$$F(x) = P(\chi^2_1(\theta_m) < x) \\ = 1 - (1 - f^n(x)) \\ = f^n(x)$$

The cumulative frequency distribution of the maximum, then, can be predicted by taking the cumulative frequency distribution of  $\chi^2_1$  and raising it to the power  $n$ , where  $n$  represents the number of degrees of freedom, on average, in  $\chi^2_1(\theta)$  records. For this particular function, degrees of freedom may

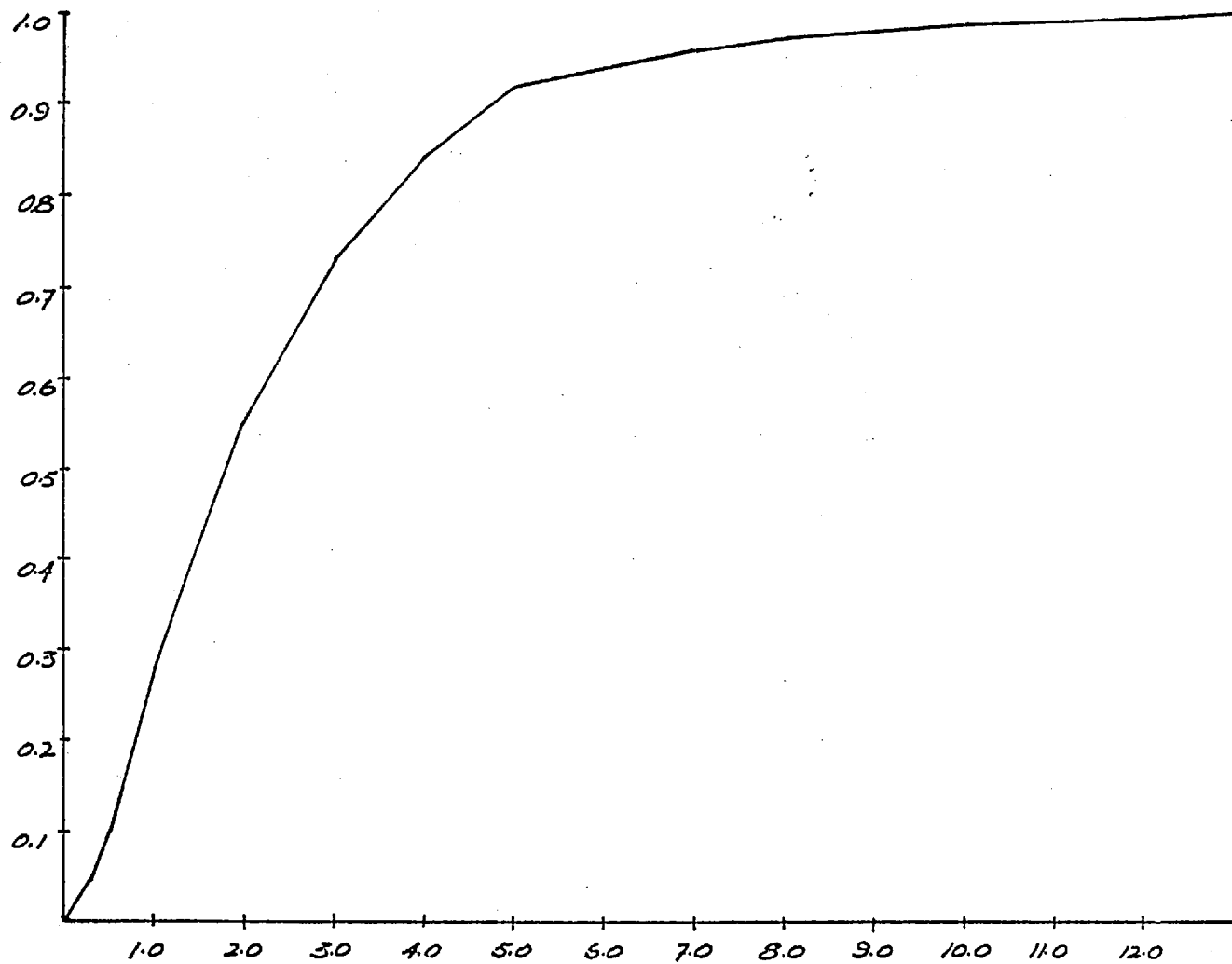


Fig. 4.8. Cumulative frequency distribution predicted from  $f^n(x)$  for  $n = 3$ .

be estimated from the following relation between the standard error and standard deviation of the ensemble:

$$df = \left[ \frac{sd}{se} \right]^2$$

From this equation, the  $\chi^2_1$  function is found to have three independent samples, or degrees of freedom. Substituting  $n = 3$  into the formula  $F(x) = f^n(x)$  derived earlier results in the predicted cumulative frequency distribution illustrated in Fig. 4.8.

Comparing this cumulative frequency distribution with that for a  $\chi^2$  variable with three degrees of freedom reveals that the predicted curve of Fig. 4.8. is significantly different at 1%. Significance is also seen when comparisons are drawn between the predicted cumulative frequency distribution and that for a variable distributed as  $\chi^2_2$ . The Kolmogorov-Smirnov one-sample test used for these comparisons indicates that the significance seen results from the predicted curve being smaller than  $\chi^2_3$ , in the first case, and larger than  $\chi^2_2$ , in the second. Such a finding suggests that the estimated cumulative frequency distribution of Fig. 4.8. has between two and three degrees of freedom, slightly less than that determined empirically.

The use of elementary probability theory, then, has given us some quantitative basis on which to explain the increased degrees of freedom observed in the distribution of the maximum of each  $\chi^2_1(\theta)$  function. The disparities seen in the degrees of freedom, approximately 2.5 predicted to 3 observed empirically, are not substantial, and may well reflect some statistical sampling effects. This inference, however, has not been investigated

any further.

Knowing the distribution of  $\chi^2_1(\theta_m)$ , it is now possible to apply the rotational  $\chi^2$  procedure to data in an off-line situation, testing the maximum against the confidence intervals established empirically.

#### 4.4.i. Off-Line Data Analysis

Three different  $\chi^2$  goodness of fit tests were performed on the data collected from the on-line study discussed in Section 4-2. An additional 22 files taken from another study have also been examined. To confirm the results of the on-line study, a four bin  $\chi^2$  test against the rectangular distribution was examined. In addition, the rotational  $\chi^2$  test was applied in order to determine the effectiveness of this procedure in detecting the presence of the evoked potential. Two  $\chi^2_1$  values were selected: the maximum, and that corresponding to a zero degree shift.

Each ensemble analysed consisted of 54 sweeps of either stimulated or unstimulated EEG. From these, the phase distributions of the first ten harmonics were formed, and the two  $\chi^2$  tests applied.

Results of this investigation on the data from the on-line phase study may be found in Tables 4-xvii to 4-1, where every table consists of the nine trials from a given subject at one tone burst frequency. The additional 22 files analysed are presented in Tables 4-li to 4-lxxii. Here, only eight trials per subject are available, all taken under stimulated conditions.

For both sets of tables, intensities are quoted in dB SL and accompanied by their respective averaged responses for the 640 ms interval analysed. The vertical arrow on the time base serves as an indication of the time of stimulus presentation. Three entries may be found under each intensity heading. The first of these, M, refers to the outcome of the rotational  $\chi^2$  test for which the maximum value of the  $\chi^2_1(\theta)$  function has been chosen. The second entry, denoted by 1, refers to the outcome of the two bin  $\chi^2$  test with the phase histograms referenced to  $0^\circ$ . The third, 3, represents the results of a four bin  $\chi^2$  test, again with a  $0^\circ$  reference for the phase histograms. The  $\chi^2$  test results for the first ten harmonics considered are tabulated alongside the relevant entry. Dashed lines refer to any finding which fails to return significance at 5%.

#### 4.4.ii. Discussion

Examination of these tables allows us to draw comparisons between the various  $\chi^2$  measures chosen, and assess the merits of each in turn. With reference to the on-line phase study discussed in Section 4-2 ( Tables 4-i through 4-xvi ), yet further comparisons can be made.

Consider the four bin test chosen to confirm the initial on-line investigation. ( Tables 4-i to 4-xvi and 4-xvii to 4-l ) For almost all subjects tested, the off-line verification marks an improvement in the sensitivity and consistency of the  $\chi^2$  test results. Subject LS at 4 kHz ( Tables 4-xvi and 4-xlix ) serves as an illustration. In the on-line trial, only two of the seven



supra-threshold records, those at 80 dB and 60 dB, show any significance, yet a consistent response is present in the average for each of these intensities. Compare this with the results of the confirming off-line study, Table 4-xlix, where a greater number, six of the seven records, reveal significance in at least two harmonics. For the off-line verification, often the degree of phase aggregation as determined by  $\chi^2_3(0^\circ)$  is at higher probability levels and seen to affect a greater number of frequency components as is the case with the on-line study.

Such differences may well be due to the size of the statistical sample analysed. Where an ensemble size of 40 produced a 20% false negative score in the on-line study, this is now reduced to approximately 12% for the four bin  $\chi^2$  test performed off-line on a sample of 54. Most often, the false negatives are seen in the region of subjective threshold. Here, even the coherent average often fails to detect a response. The four bin  $\chi^2$  test with phase histograms referenced to  $0^\circ$ , then, may be regarded as a reasonable indicator of response and no response conditions, provided a large enough sample is analysed.

The rotational  $\chi^2$  results are remarkably similar to those found for the off-line four bin  $\chi^2$  study in almost all respects. Occasionally, the four bin test is more sensitive in the region of subjective threshold. ( Subject FN at 2 kHz, Table 4-xxv ) At other times, the rotational statistic provides a better indication. ( Subject JS at 500 Hz, Table 4-xxii ) When viewed overall, though, very few differences are to be found between these two tests and this is not surprising. The rotational statistic is known to be distributed as  $\chi^2$  with three degrees of freedom. But,

because a cylindrical, rather than rectangular, distribution is postulated under  $H_0$ , a greater confidence can be placed in the rotational  $\chi^2$  test results. The phase constraint observed in the histograms may fall at or near the boundary of the bins chosen for  $\chi^2$  analysis. The resulting  $\chi^2$  value, then, might reflect a lack of phase aggregation even though a significant nonuniformity exists in the histogram. The step-wise rotation introduced to the two bin  $\chi^2$  test eliminates these boundary problems, thus assuring us that the choice of reference for the phase histograms cannot influence the test results. Comparing the rotational statistic to the four bin off-line investigation reveals a false negative rating of 14%, only slightly higher than the 12% quoted earlier in this discussion. In both instances, the false positive score is the expected 5%.

As is to be expected, the two bin off-line test showed the greatest inconsistency. Most of the nonsignificant findings are within 20 dB or so of threshold, suggesting the procedure is insensitive to the broader phase constraint present at these levels. Anomalies do exist, such as the GF 4 kHz file. ( Table 4-xx ) This particular file showed similar inconsistencies for the on-line study, and it may well be that some nonstationary frequency structure in the EEG is responsible. Even the more sensitive four bin test and the rotational  $\chi^2$  statistics reveal similar, though less striking, inconsistencies. When viewed overall, false negatives account for about 16% of the two bin  $\chi^2$  records, and false positives, the 5% expected under  $H_0$ .

Accounting for the periodicity of the phase distributions, then, has certainly improved the sensitivity and reliability of the

test results. This improvement is most striking when comparisons are made between the rotational  $\chi^2$  statistic and the two bin test from which it is derived. When comparisons are drawn between the rotational statistic and the four bin  $\chi^2$  test to which it is related by virtue of its sampling statistics, fewer differences are to be seen. There is, however, the important assurance that the arbitrary choice of reference for the phase histograms does not influence the rotational test results. The step-wise rotation inherent in this procedure reduces the boundary effects mentioned earlier, thereby optimizing the search for phase constraint. This cannot be said of the four bin test, or any other procedure which postulates a rectangular distribution of phases. Without accounting for the cyclic nature of the phase histograms, a nonsignificant finding might well reflect only a poor choice of reference.

#### 4.5.i. The Mean Phase Vector

The rotational  $\chi^2$  statistic is only one of a number of procedures which can be devised and applied to data of an inherently periodic nature. In its application, we merely approximate the cylindrical distribution postulated under  $H_0$  by rotating the phase histograms through discrete  $10^\circ$  steps. Other statistics, such as the mean phase vector, its magnitude or standard deviation, assume a continuous, rather than discrete, distribution of phases. Because no approximations are made in the application of a technique of this kind, the phase vector method may prove more reliable than the rotational  $\chi^2$  statistic. By taking a slightly different approach to the detection of phase constraint, it may well offer further insights

not obvious from the use of the  $\chi^2$  statistic.

#### 4.5.ii. Theoretical Background

Instead of viewing each ensemble of phase values as drawn from a cylindrical distribution, we picture them as lying on the circumference of a circle of unit radius. See Fig. 4.9. An arrow drawn from the center of the circle to each phase value defines the phase vector,  $\vec{\psi}_i$ . In vector notation, this is given by:

$$\vec{\psi}_i = |\vec{\psi}_i| \angle \theta_i$$

where  $|\vec{\psi}_i|$  denotes the magnitude, and  $\angle \theta_i$ , the direction of the vector  $\vec{\psi}_i$ .

From the vector sum of all members of the ensemble, the mean phase vector,  $\vec{\psi}_m$ , its absolute value,  $|\vec{\psi}_m|$ , and standard deviation, sd, can be derived. In the absence of any phase constraint, the magnitude of  $\vec{\psi}_m$  will tend to zero, while its sd will approach an expected value given by  $\sigma_{\psi_i}$ . Should there be some aggregation of phase values, however, the magnitude will be significantly greater than zero, and the standard deviation significantly less than  $\sigma_{\psi_i}$ . If phase ensembles taken from spontaneous EEG records are chosen as a reference, the cumulative frequency distributions for each of these statistics can be derived. From these, the confidence intervals for a statistical test of phase constraint are readily available.

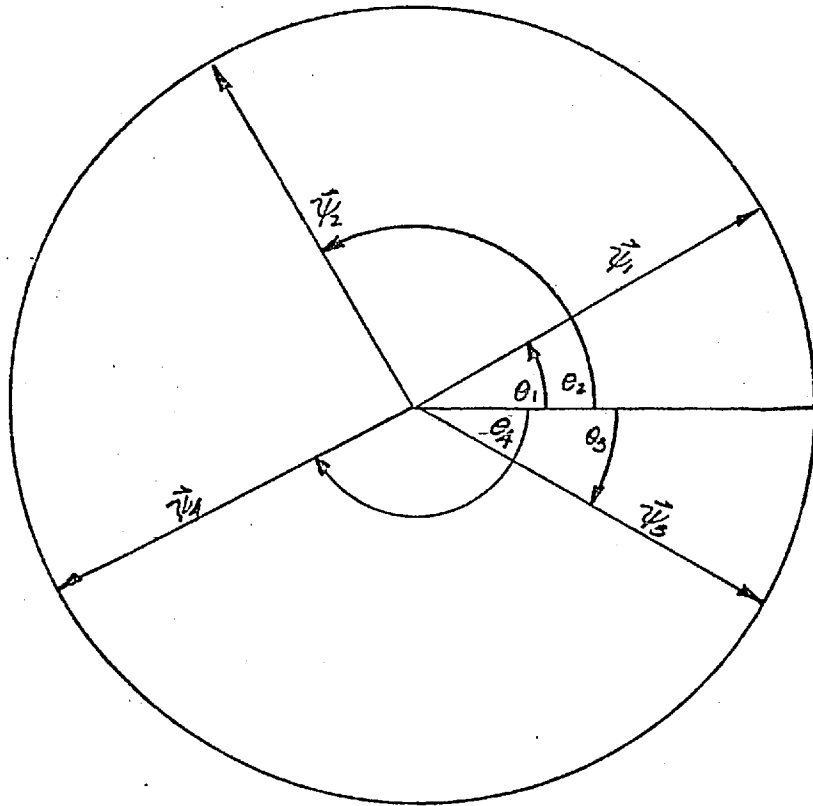


Fig. 4.9. An ensemble of phase vectors.

#### 4.5.iii. The Sampling Statistics of $\vec{\psi}_i$

Unstimulated EEG records taken from the on-line phase study served as a reference on the behaviour of the mean phase vector. From each 54 sweep ensemble, the phases of harmonics one to ten were derived and the mean phase vector, its magnitude and standard deviation calculated. A total of 680 estimates of each statistic were then available for establishing the cumulative frequency distributions shown in Figs. 4.10 and 4.11.

The sampling statistics of the two parameters which concern us, the absolute value of the phase vector and its standard deviation for a 54 sample ensemble, can be derived from the two distributions of Figs. 4.10 and 4.11. The absolute value is seen to be distributed about a mean value of 0.125, while the standard deviation is centered on  $96.5^\circ$ . The means of both these distributions are different, possibly significantly different, from the expected values of  $|\vec{\psi}_{in}| = 0$  and  $sd = 104^\circ$  determined theoretically for uniformly distributed data.

These two expected values have been derived from the following relation by assuming a continuous and uniform distribution of phases between  $-180^\circ$  and  $+180^\circ$ .

$$x = \int_{-180^\circ}^{+180^\circ} x p(x) dx$$

Here,  $x$  is the statistic of interest, and  $p(x)$  the probability density function. For a continuous, uniformly distributed variable,  $p(x)$  is a constant and equal to  $1/360^\circ$ .

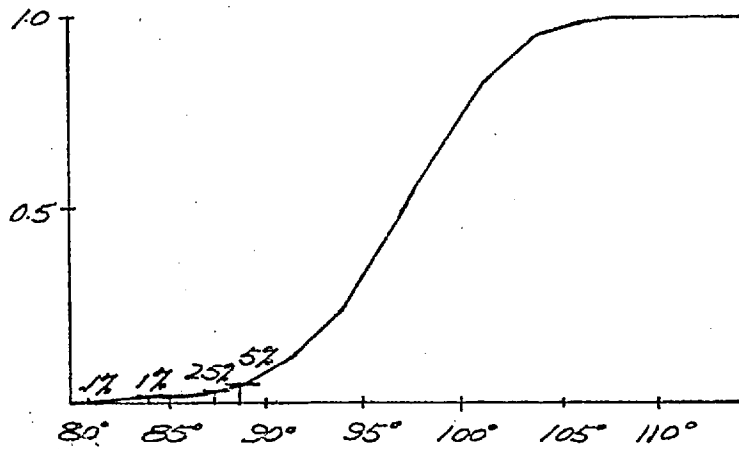


Fig. 4.10. Cumulative frequency distribution of  $\text{sd } \vec{\psi}_i$ , derived from the phase ensembles of spontaneous EEG.

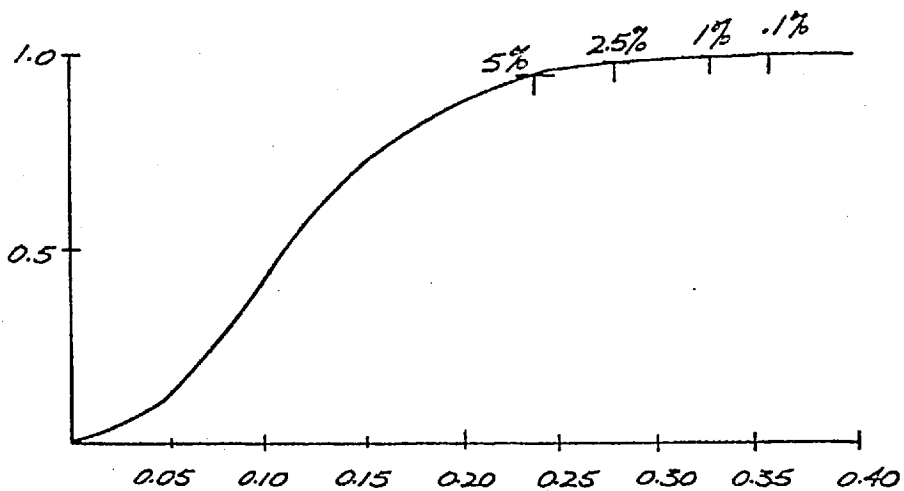


Fig. 4.11. Cumulative frequency distribution of  $|\vec{\psi}_m|$ , derived from the phase ensembles of spontaneous EEG.

The disparities seen between observed and expected values, then, may well reflect either some nonuniformity in the phase distributions of spontaneous EEG or the effects of drawing a limited sample from a continuous distribution. In order to examine these possibilities in greater detail, distributions of the standard deviation were set up for data known to be drawn from a uniform distribution and compared with those determined for spontaneous EEG. Because of the possibility that certain rhythms in the EEG may be introducing a phase constraint, and hence a bias in the distribution of the sd, each individual harmonic was considered separately.

If EEG rhythms are contributing to the difference between the observed and expected mean of the distribution, we would expect this contribution to be most marked in the first few harmonics, where slow waves predominate, or in harmonics six through eight, the range of  $\alpha$ -activity. An examination of the records for individual subjects occasionally confirms this hypothesis. When distributions are formed for each harmonic, however, there is little evidence of any synchronous background activity for any frequency to approximately 10 Hz. Those histograms for harmonics seven and eight do reveal some evidence of a bimodal distribution, as Fig. 4.12 illustrates. A preponderance of  $\alpha$ -activity in some, but not all, subjects, then, may be introducing a slight bias into the overall cumulative frequency distributions of Fig. 4.11. But, because the means of the distributions for all harmonics are not significantly different from the overall mean of  $96.5^\circ$ , synchronous activity in the EEG cannot be responsible for the disparities observed between the expected and empirically derived distributions.

Both uniformly distributed data, and the phase distributions



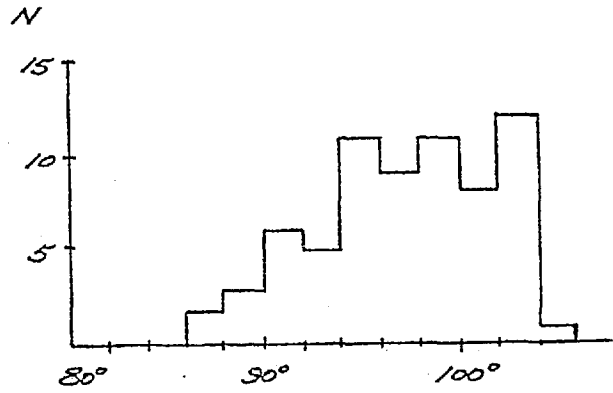
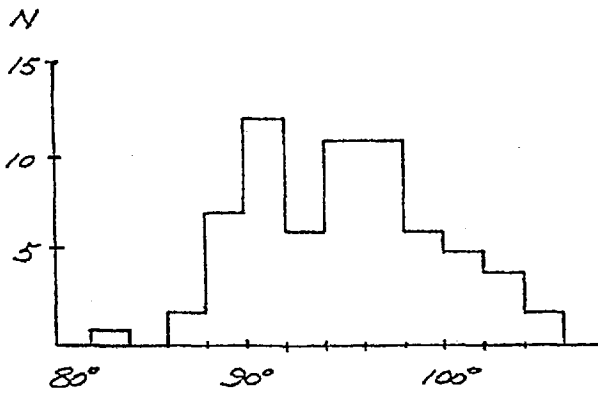


Fig. 4.12. Histograms of the sd for Harmonics 7 ( 10.5 Hz ) and 8 ( 12 Hz ).

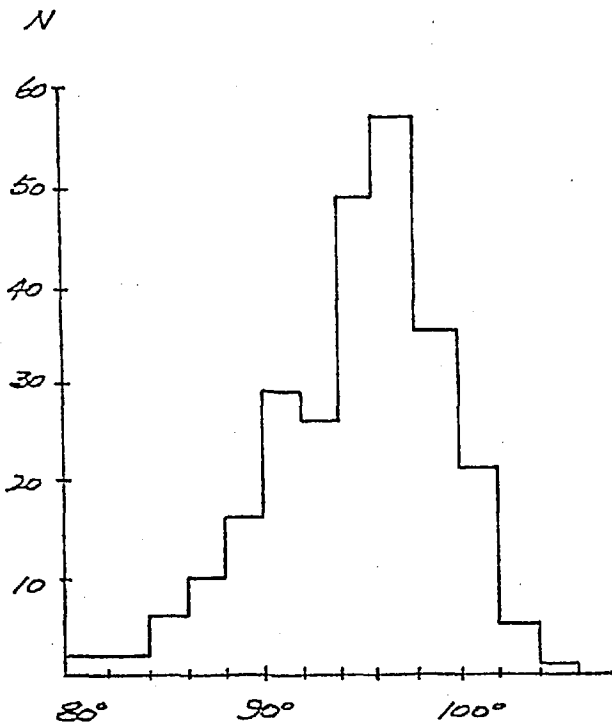


Fig. 4.13.

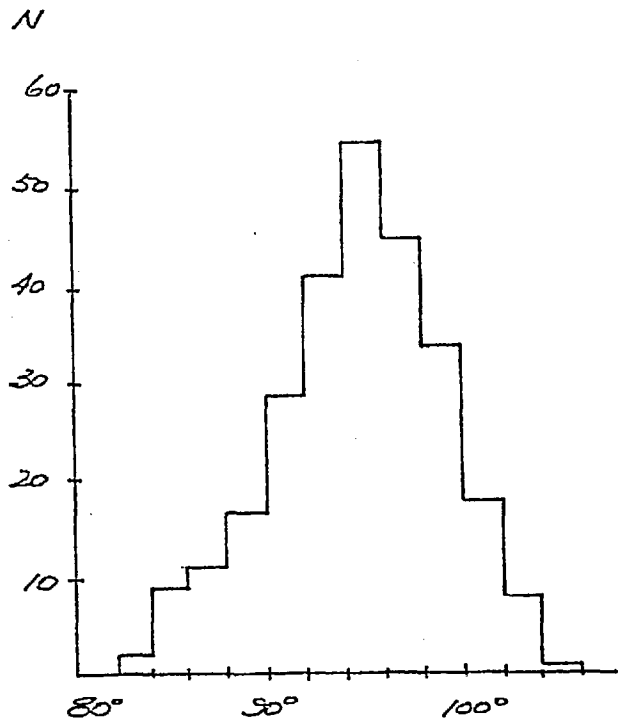


Fig. 4.14.

Distributions of sd  $\vec{\psi}_i$  derived from the phase ensembles of bandlimited Gaussian random noise ( Fig. 4.13. ) and from uniformly distributed data. In both cases, each estimate of the sd is derived from a sample of 54.

of bandlimited Gaussian random noise were generated in order to clarify the behaviour of the sd. 54 sweeps of bandlimited noise made up each ensemble, from which the phase distributions of the first ten harmonics were derived. A total of 270 estimates of sd were then determined, and formed into the histogram shown in Fig. 4.13. Initially, uniformly distributed data was generated in blocks 54 long, and from these, the distribution of Fig. 4.14 was derived.

These two distributions are remarkably similar to one another, and this observation is confirmed when a two sample Kolmogorov-Smirnov test is applied to their respective cumulative frequency distributions. No significant difference is to be seen between them at 5%. In addition, comparing either of these distributions with that derived from the phase distributions of spontaneous EEG ( Fig. 4.11 ), reveals that none of these distributions are significantly different from one another. From this, we may conclude that an assumption of uniformly distributed data is certainly a reasonable one to make as regards the phases of continuous EEG.

The sample size, then, may be responsible for the disparities we observe between the expected and actual values of the standard deviation. In order to investigate this matter, uniformly distributed data were generated in blocks 200 long. Its probability density function for the sd is shown in Fig. 4.15.a. Note the shift in mean value from approximately  $96^{\circ}$  to  $100^{\circ}$ , and the way in which the distribution has narrowed to a range between  $92^{\circ}$  and  $106^{\circ}$ . When 1000 uniformly distributed variables make up each estimate of sd, the distribution shifts even further to the right so that it is centered on  $102^{\circ}$ , and limited to the range from  $100^{\circ}$  to  $106^{\circ}$ . See Fig. 4.15.b.

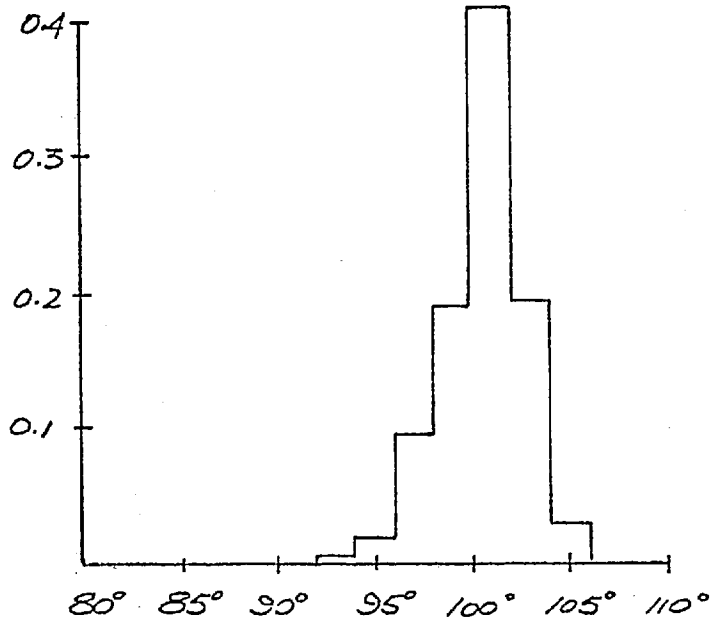


Fig. 4.15.a. Probability density function for  $\text{sd } \vec{\psi}_i$  taken from uniformly distributed data. Each of the 270 estimates is formed from 200 variables.

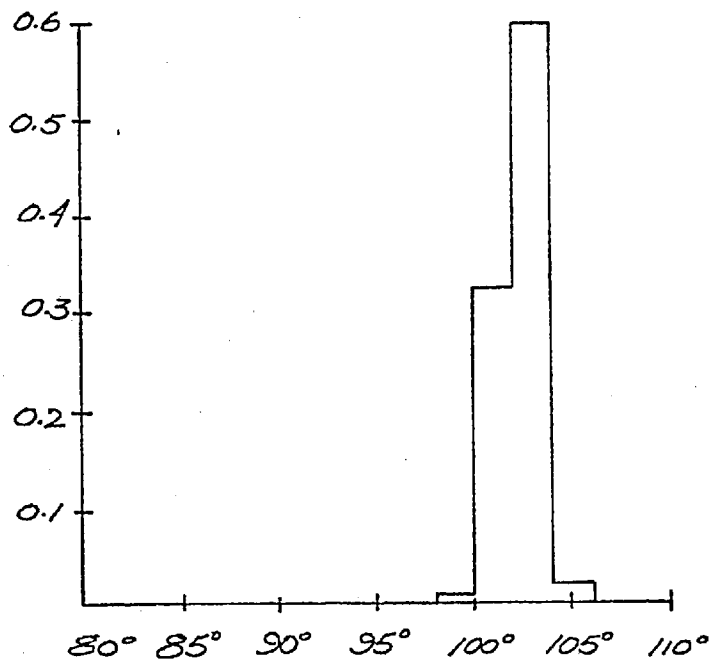


Fig. 4.15.b. Probability density function for  $\text{sd } \vec{\psi}_i$  where each estimate of  $\text{sd}$  is derived from 1000 variables.

The standard deviation of the mean phase vector, then, is a biased estimator, which approaches its theoretical, expected value as the sample size increases. The nature of this bias is a non-linear one, as Fig. 4.16 illustrates. Here, the mean of each empirically derived distribution of sd is plotted against sample size. The vertical bars indicate  $\pm 1$  standard deviations on each estimate. Note how the mean increases in value, while its spread decreases, with increased sample size.

Confidence intervals for a biased estimator such as the sd, and, by inference, the absolute value, of the mean phase vector, then, must be determined empirically for a given sample size. For the 54 sample ensemble we have been investigating, these are given by:

	$P( \vec{Z}_m  > \vec{Z})$	$P(sd < s)$
5%	0.24	86.5°
2%	0.28	87.5°
1%	0.33	84.0°
.1%	0.36	81.0°

For other sample sizes, consult the table on page 99.

#### 4.6.i. Data Analysis by the Phase Vector Method

All stimulated records can now be assessed in the light of these findings. The same 34 files from the on-line phase study, and the additional 22 files discussed in Section 4.4 were subjected to phase vector analysis.

The results of this study are to be found in Tables 4-lxxiii

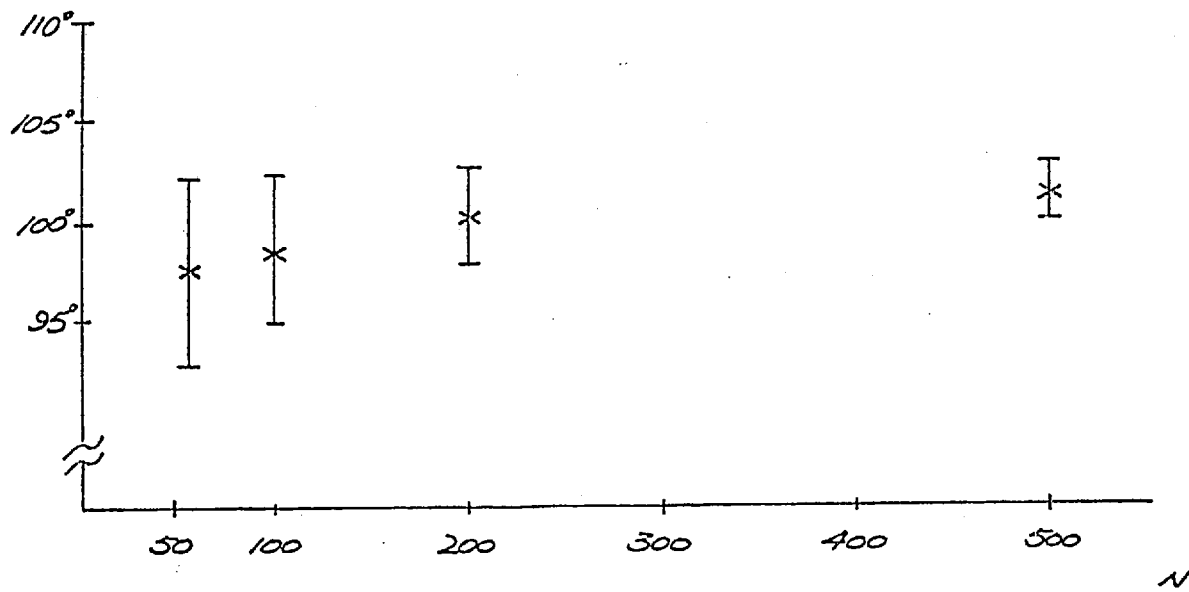


Fig. 4.16.  $Sd \bar{\psi}_i$  as a function of sample size  $N$ .

to 4-cxxviii. The format here is similar to that of the other tables in this chapter. Each intensity is quoted in dB SL and accompanied by its averaged response. Three separate headings are to be found alongside each intensity level. The first of these,  $\theta_m$ , refers to the angle of incidence of the mean phase vector,  $\vec{\psi}_m$ . To the right are tabulated the relevant values of  $\theta_m$  for each of the ten harmonics analysed. The second heading,  $\vec{\psi}_m$ , refers to the absolute value of the mean phase vector, while the third, sd, refers to its standard deviation. To the right of the second and third headings may be found the respective probability levels for these statistics. Dashed lines refer to any value which fails to reveal significance at 5%.

#### 4.6.ii. Discussion

The results of Tables 4-lxxiii to 4-cxxviii reveal findings remarkably similar to the off-line  $\chi^2$  results ( Tables 4-xvii to 4-lxxii ) discussed in Section 4.4.ii. For the most part, high intensities of acoustic stimulation illustrate a striking phase constraint in several, if not all, the harmonics considered. The degree of constraint, as indicated by the probability levels of both the absolute value and standard deviation statistics, diminishes substantially below intensities of 20 dB or 30 dB SL, almost always engaging fewer harmonics.

In addition, these two statistics afford us some insights into the nature and behaviour of any phase aggregation seen in the records. Consider Subject B0 at 2 kHz. ( Table 4-lxxxvi ) For all records from 70 dB to 10 dB SL, the second to fifth harmonics

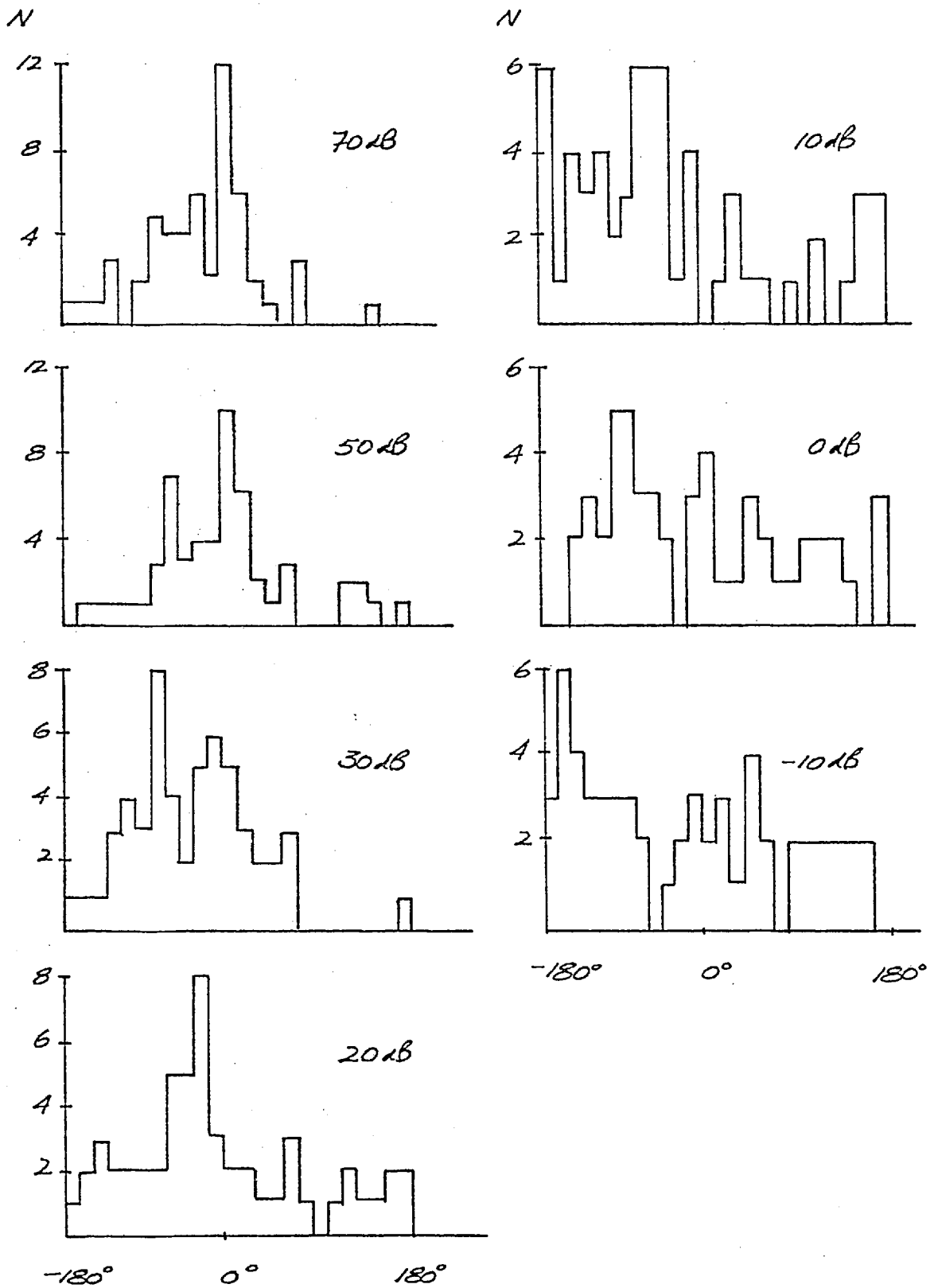


Fig. 4.17. Phase histograms for the third harmonic taken from the records of Subject B0, M, age 31, at 2 kHz.

are significant with only a few exceptions. For intensities of 30 dB SL or greater, these harmonics are very tightly constrained. Although not noted in the tables, the standard deviation is about  $65^\circ$  on average, significantly smaller than the mean of  $96.5^\circ$  derived from spontaneous EEG files. Such a finding suggests that the majority of phases lie very close to the mean value,  $\phi_m$ , and this is confirmed by the phase histograms shown in Fig. 4.17. In almost all cases above 30 dB SL, the mean phase value,  $\phi_m$  does not change substantially as a function of intensity level, pointing to a consistency in both the shape and latency, and the number of individual evoked potentials in the records.

Below 30 dB SL, both the extent of phase constraint and the number of harmonics involved is progressively reduced until little or no significance is to be seen. Once again, the standard deviation provides us with a quantitative measure of the spread of phases about the mean phase value,  $\phi_m$ . On average, the sd has increased to  $82^\circ$ , still significant, but substantially higher than the figure of  $65^\circ$  quoted above. The phases of a given harmonic, then, are much more broadly constrained about the mean phase value. The mean itself is seen to shift. This could reflect either a shift in the latency of individual evoked potentials in the records or a reduction in their numbers, or possibly both.

Comparing the mean phase vector angle,  $\phi_m$ , with the median of each of the phase distributions depicted in Fig. 4.17 allows us to investigate this matter further. For the third harmonic,  $\phi_m$  ( Table 4-lxxxvi ) is found to be  $-17^\circ$  and  $-10^\circ$  at 70 dB and 50 dB SL respectively. As the intensity is reduced, this shifts to values of  $-37^\circ$  at 30 dB,  $-46^\circ$  at 20 dB and finally



to  $-81^\circ$  at 10 dB before significance is lost. The median of the phase histograms ( Fig. 4.17 ) at intensities above 30 dB SL corresponds favourably with the mean phase angle,  $\theta_m$ . At reduced intensities, however, it, too, shifts, but usually not as substantially as  $\theta_m$ . Consider the 10 dB record. The median of the distribution is seen to lie at approximately  $-60^\circ$ , while the mean phase vector is found to be  $-81^\circ$ .

This finding suggests that the latency of the third harmonic does indeed shift as a function of intensity level. The time-locking mechanism we postulate has become less effective on two counts. Fewer sweeps are synchronized to the time of stimulus, and those sweeps which are synchronized are locked less sharply to the stimulus.

When considered overall, the phase vector method is somewhat more sensitive and consistent than the  $\chi^2$  tests discussed in Section 4.4. Its false negative rating is 11%, as opposed to either 12% or 14% experienced with  $\chi^2$ . False positives are within the expected 5% interval.

Because the phase vector approach assumes a uniform and continuous distribution of phases, it is the statistical procedure best suited to data of an inherently periodic kind. When compared to a procedure which only approximates the periodicity of phases, the rotational  $\chi^2$  statistic, the phase vector method is only marginally more sensitive. <sup>Its</sup> being a simpler and faster algorithm is the greatest advantage of phase vector analysis. Computing time, for example, is reduced by at least a factor of three, an important consideration if real-time clinical trials are to be carried out in future.

#### 4.7. Concluding Remarks

Postulating that the AEP results from some synchronization of existing EEG activity has led us to search for the presence of a consistent and recurring pattern in an ensemble of post-stimulus sweeps. This recurring pattern can be seen as a constraint in the phases of the individual harmonics which constitute it. Phase analysis, however, is complicated by the inherent periodicity of the phases themselves, and demands the use of rotational statistical procedures. A data simulation has allowed us to explore the behaviour of several phase measures and establish their sampling statistics empirically. Despite the sample size bias observed, the empirical phase statistics are seen to be well-behaved and capable of detecting the AEP to within +10 dB of subjective threshold on average. Thus, either the rotational  $\chi^2$  procedure, or the standard deviation of the vector angle could be used for the clinical assessment of auditory thresholds, achieving one of the objectives of this research. In addition, their effectiveness as response indicators suggests that a pattern recognition approach is appropriate to AEP data. The simple template-matching procedure discussed in Chapter Five is considered in order to establish the use of pattern recognition techniques for AEP detection.

The standard deviation,  $sd \bar{z}_1$ , as a function of sample size  $N$ . A total of 500 estimates formed the empirical cumulative frequency distributions from which the following confidence intervals were derived.

$N$	5%	2.5%	1%	0.5%
8	60.7°	53.9°	48.0°	45.3°
12	71.0°	67.2°	61.9°	55.8°
16	75.0°	71.6°	65.0°	58.7°
20	77.3°	73.4°	69.4°	68.0°
24	76.7°	73.6°	69.4°	68.2°
28	83.0°	80.5°	76.5°	66.5°
32	83.0°	80.9°	78.4°	73.8°
36	84.7°	82.8°	80.7°	78.2°
40	86.3°	83.5°	80.7°	78.7°
44	86.5°	83.5°	81.5°	79.3°
48	87.8°	85.5°	83.1°	80.5°
54	88.5°	87.5°	84.0°	81.8°
60	90.1°	87.5°	84.6°	82.7°
70	91.0°	88.8°	87.7°	86.2°
80	91.5°	90.3°	88.2°	86.4°
90	92.5°	90.6°	89.0°	87.7°
100	93.5°	91.8°	90.4°	89.3°

Tables 4-i to 4-xvi

The On-line  $\chi^2_3$  Study

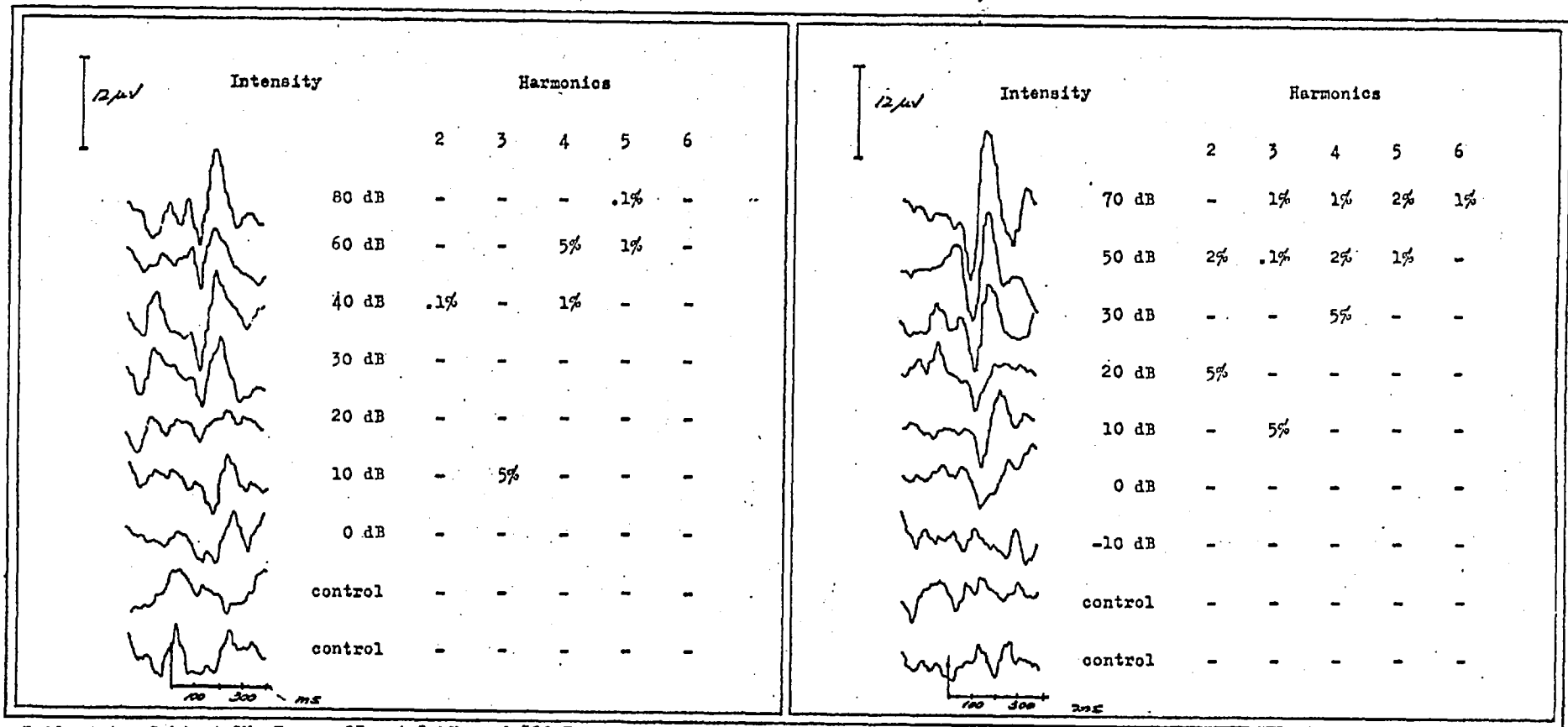


Table 4-1. Subject CH, F, age 23, at 2 kHz and 500 Hz.

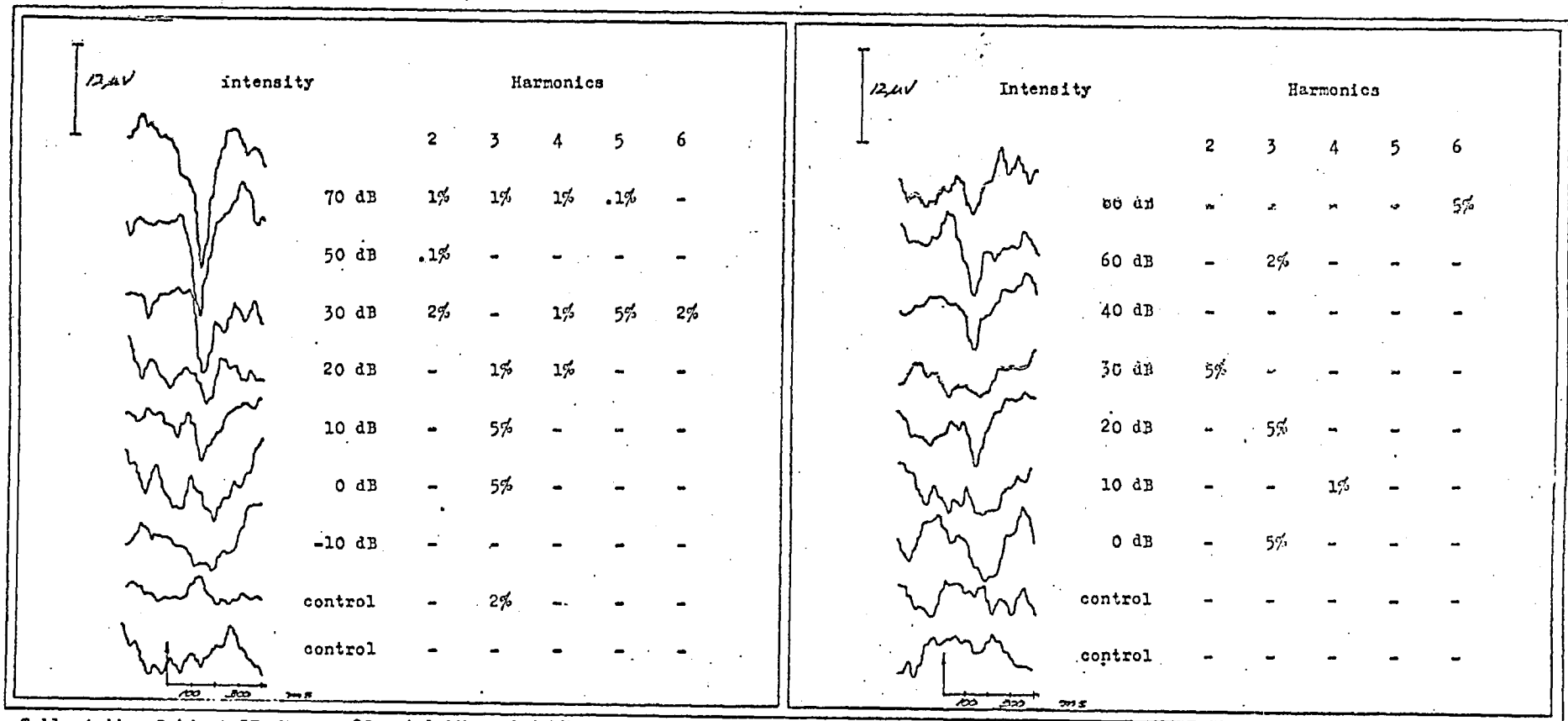


Table 4-ii. Subject GF, M, age 28, at 1 kHz and 4 kHz.

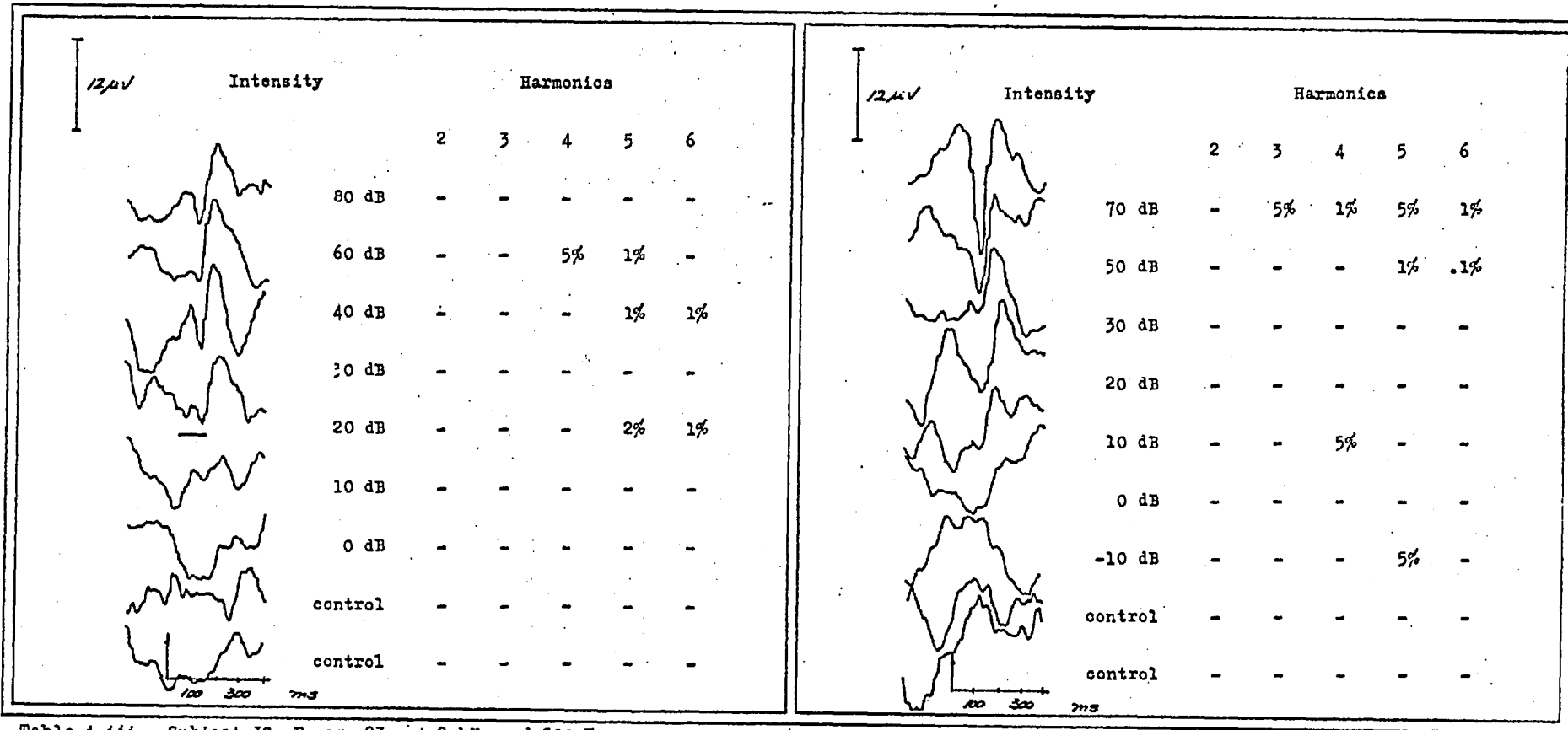


Table 4-iii. Subject JS, F, age 23, at 2 kHz and 500 Hz.

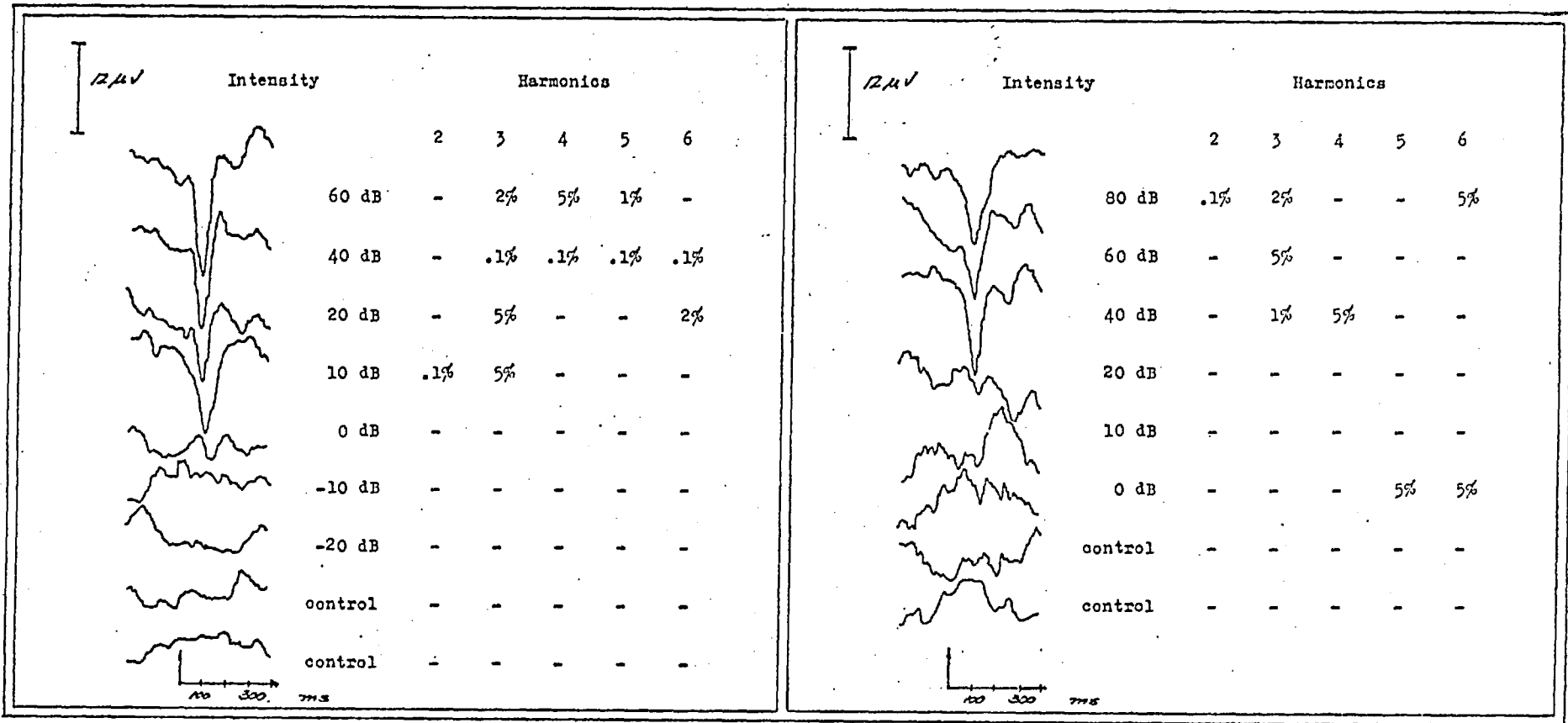


Table 4-iv. Subject CR, F, age 31, at 1 kHz and 4 kHz.



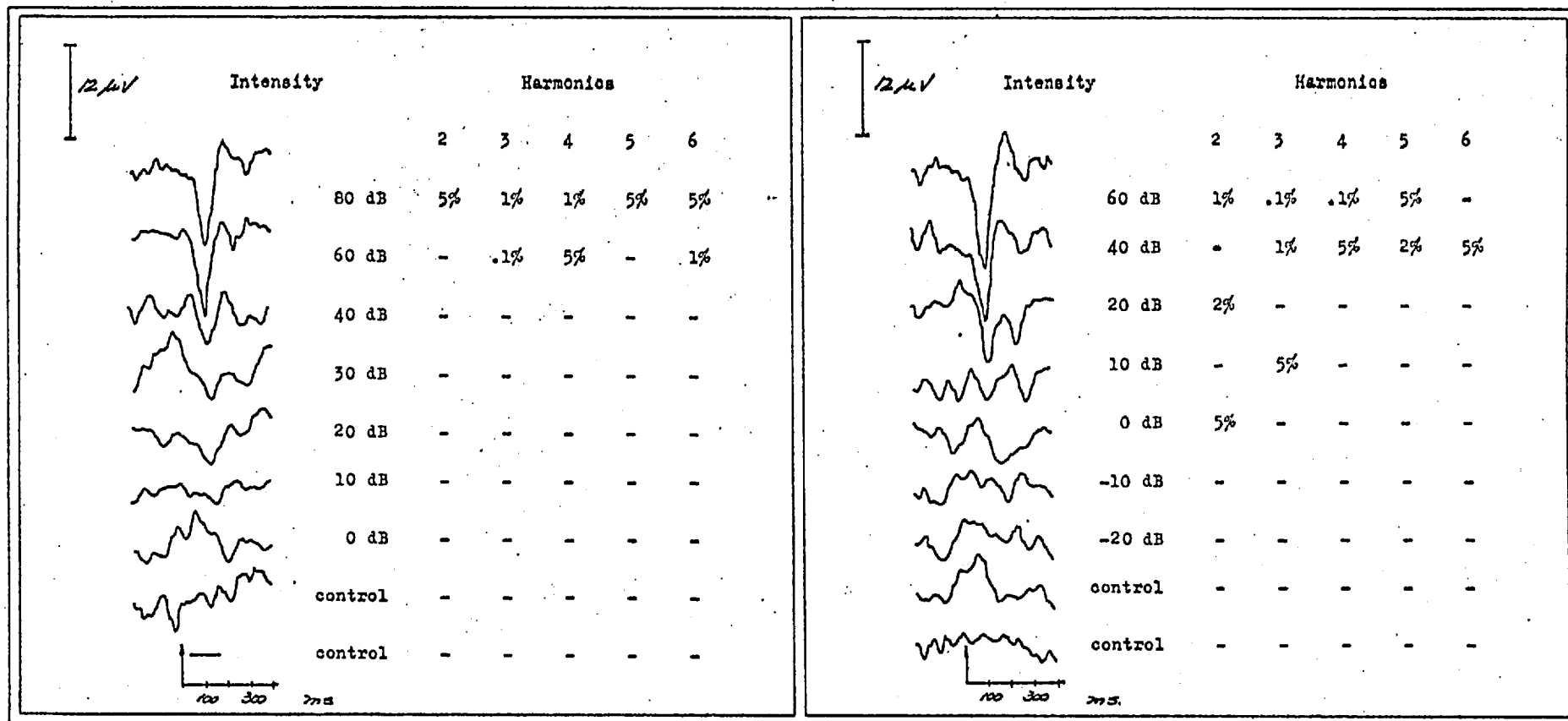


Table 4-v. Subject FN, M, age 28, at 2 kHz and 500 Hz.

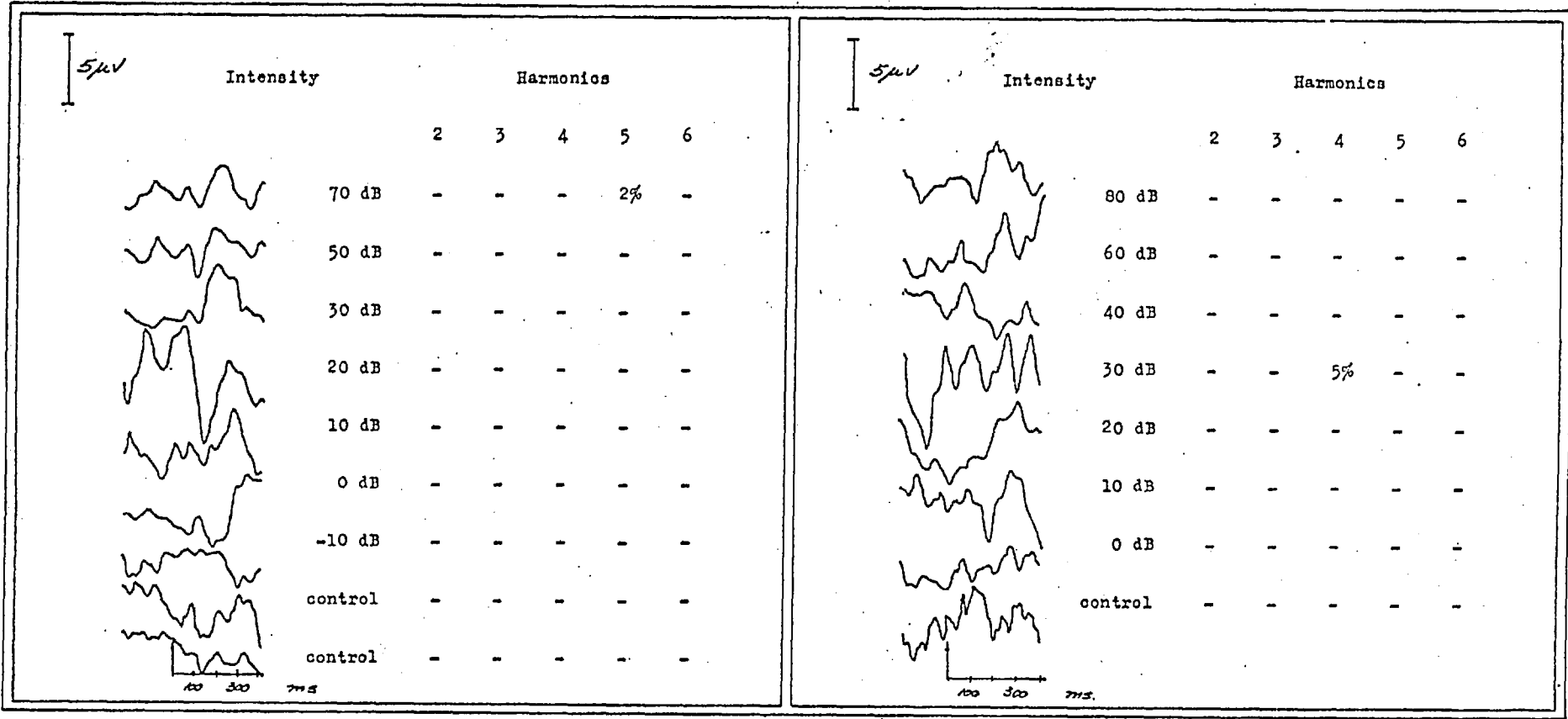


Table 4-vi. Subject TB, M, age 20, at 1 kHz and 4 kHz.

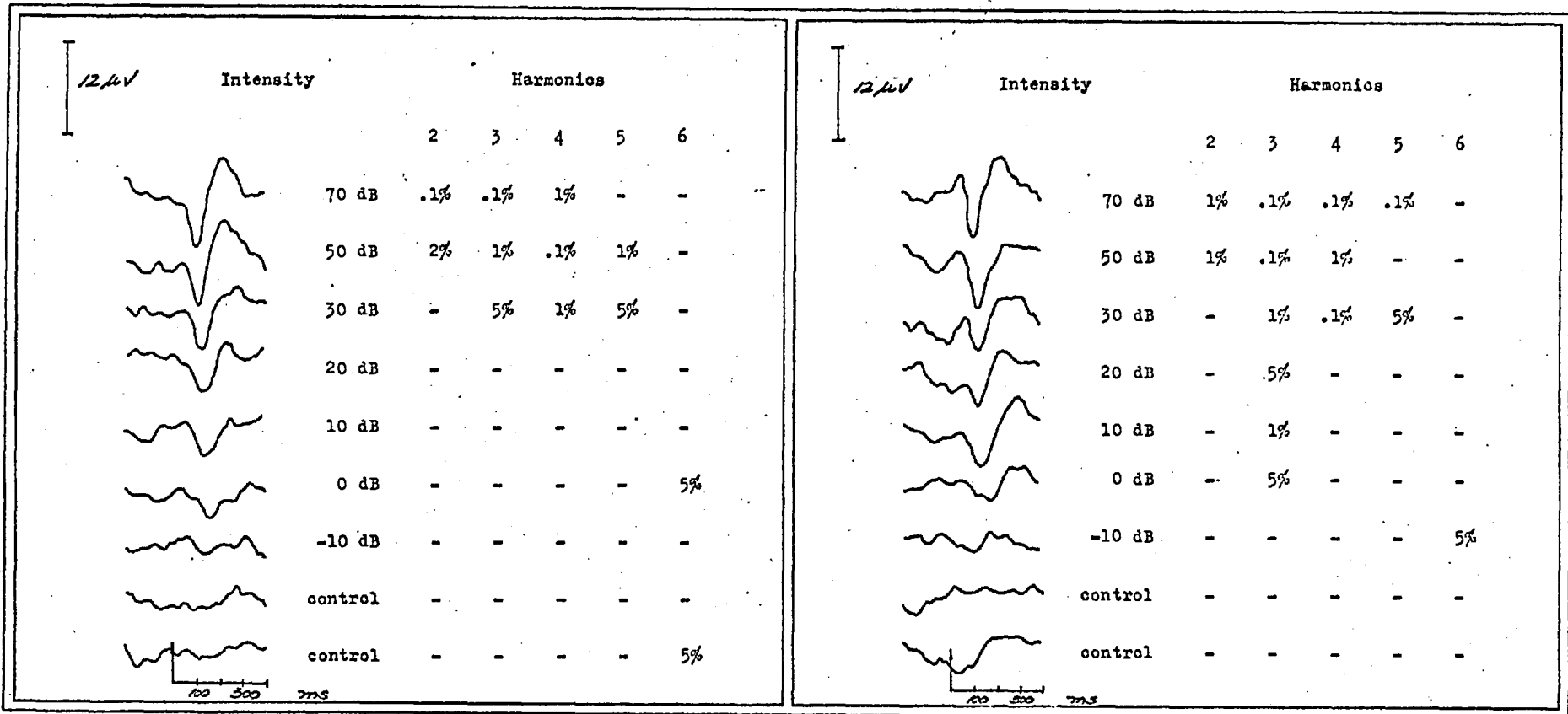


Table 4-vii. Subject E0, M, age 31, at 2 kHz and 500 Hz.

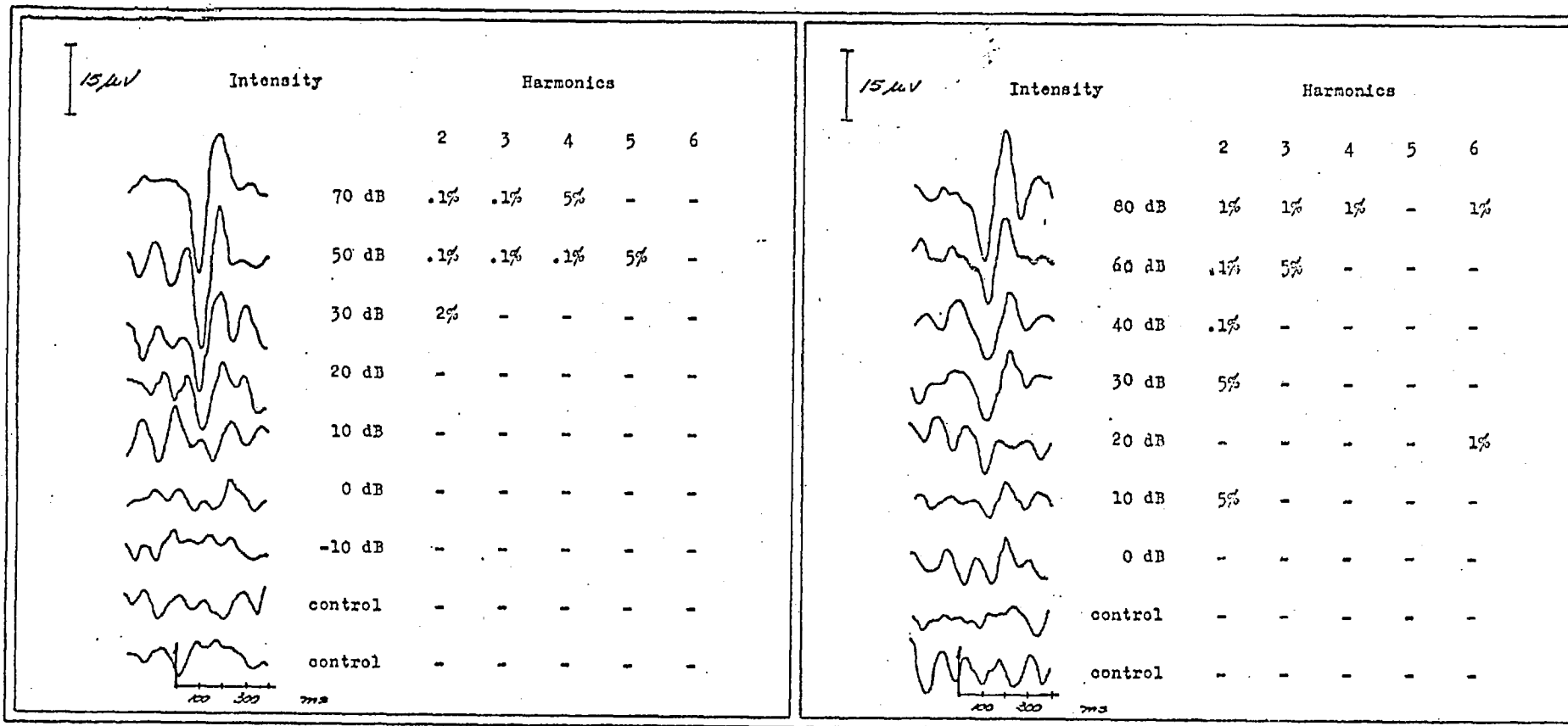


Table 4-viii. Subject JD, F, age 23, at 1 kHz and 4 kHz.

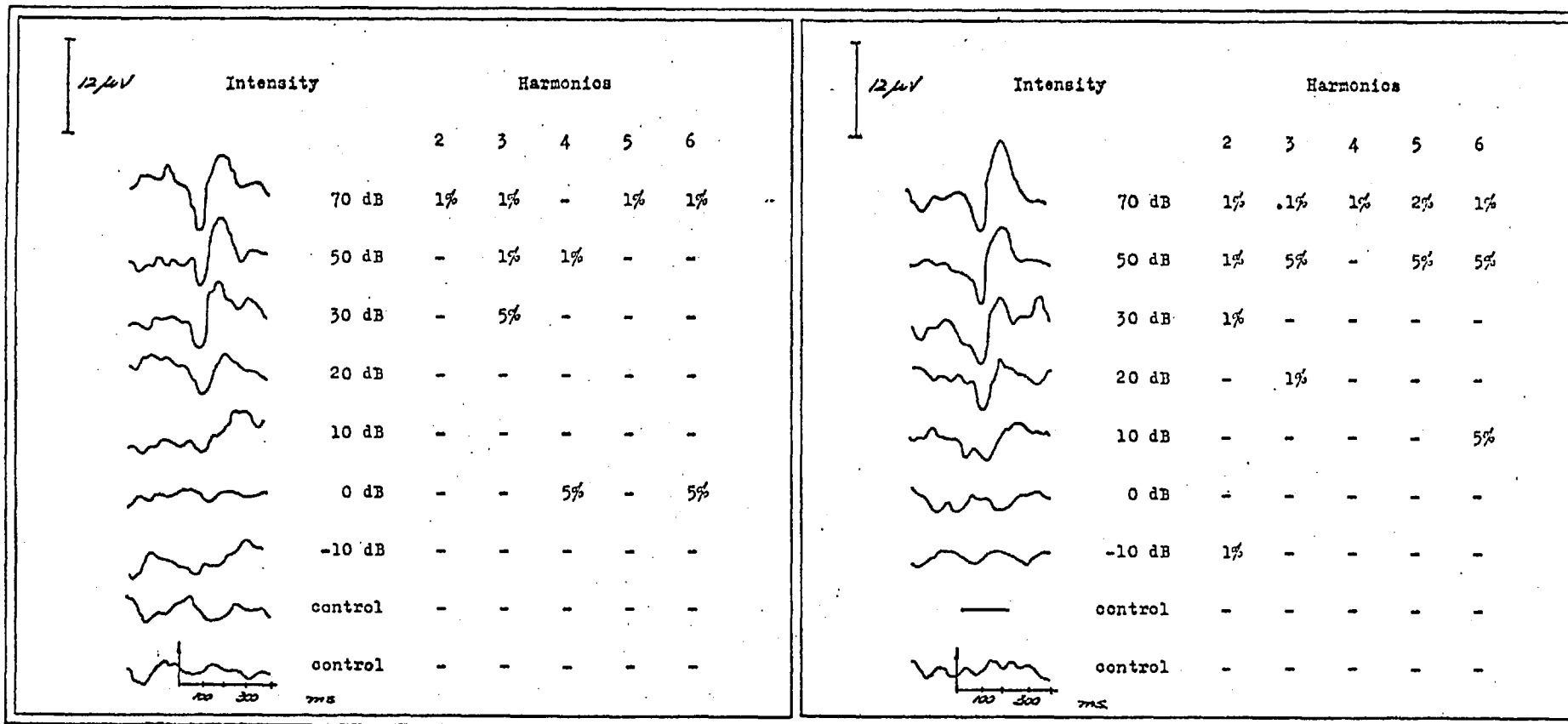


Table 4-ix. Subject DT, F, age 24, at 2 kHz and 500 Hz.

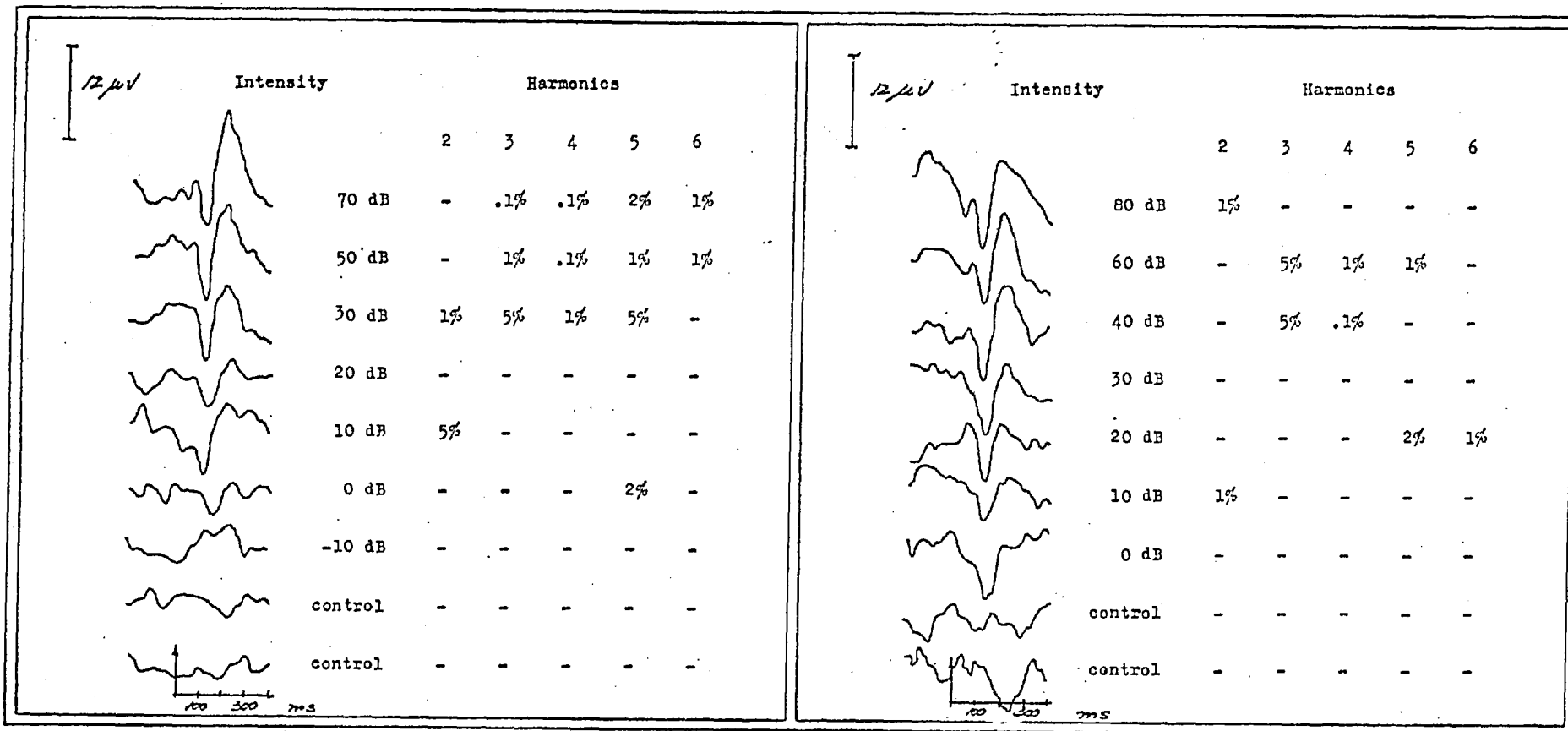


Table 4-x. Subject JN, M, age 30, at 1 kHz and 4 kHz.

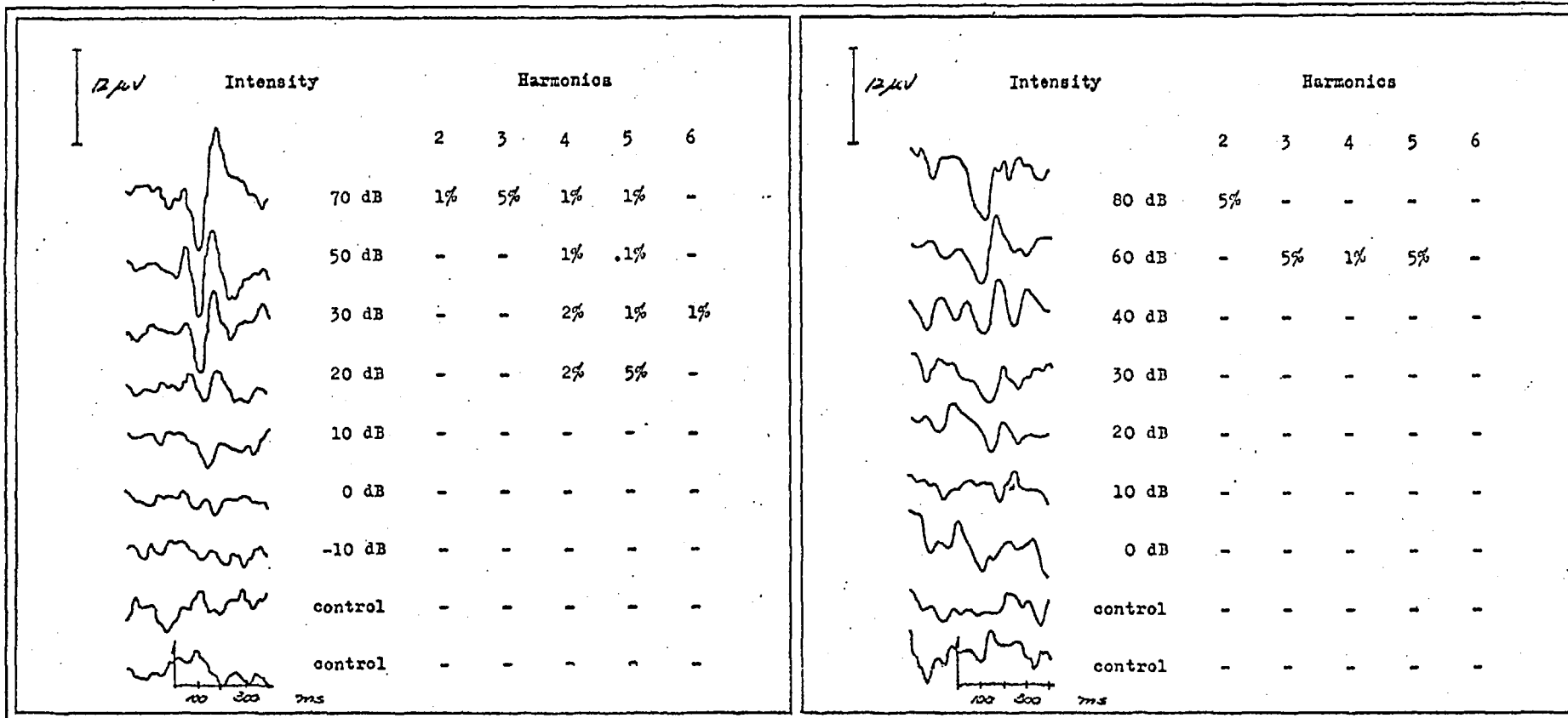


Table 4-xi. Subject VM, P, age 24, at 1 kHz and 4 kHz.

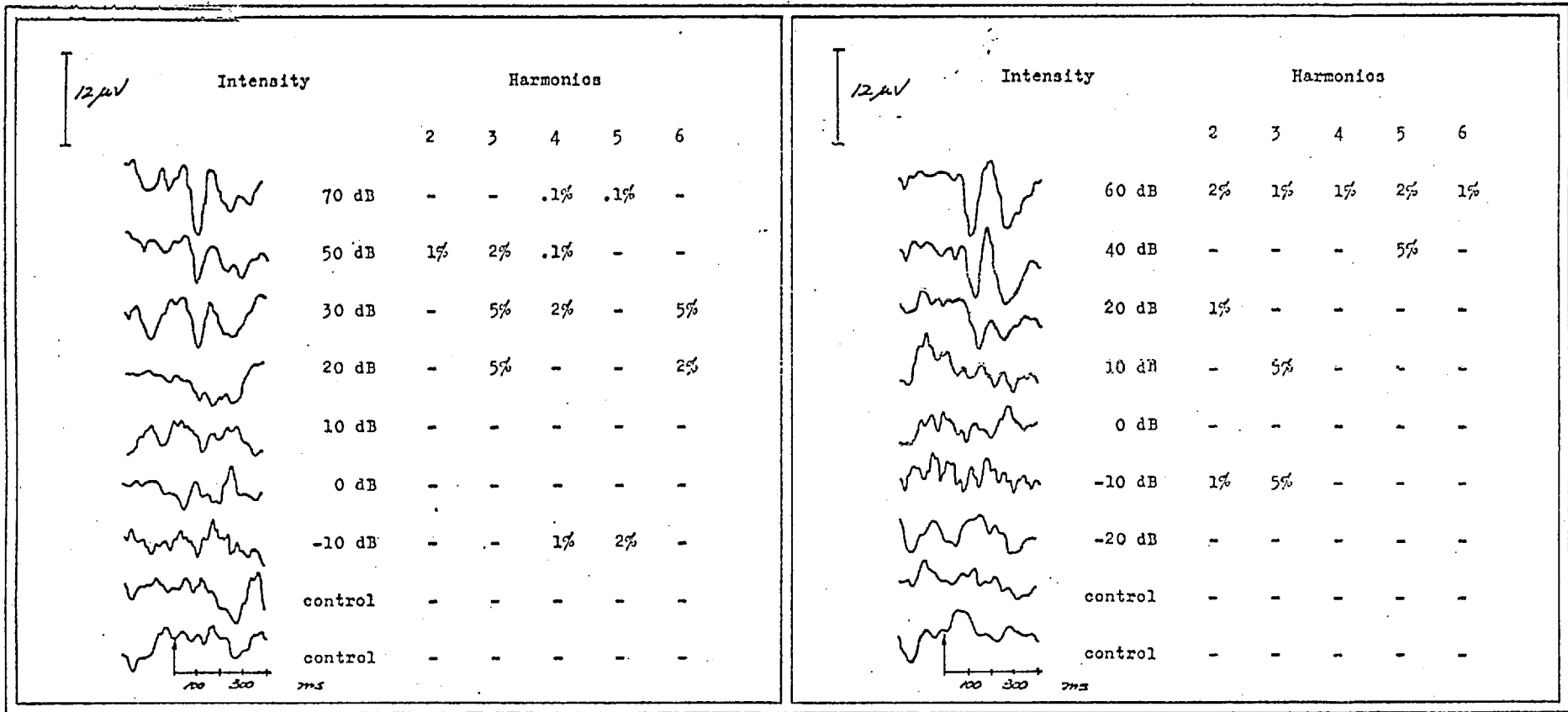


Table 4-xii. Subject SBa, F, age 20, at 2 kHz and 500 Hz.



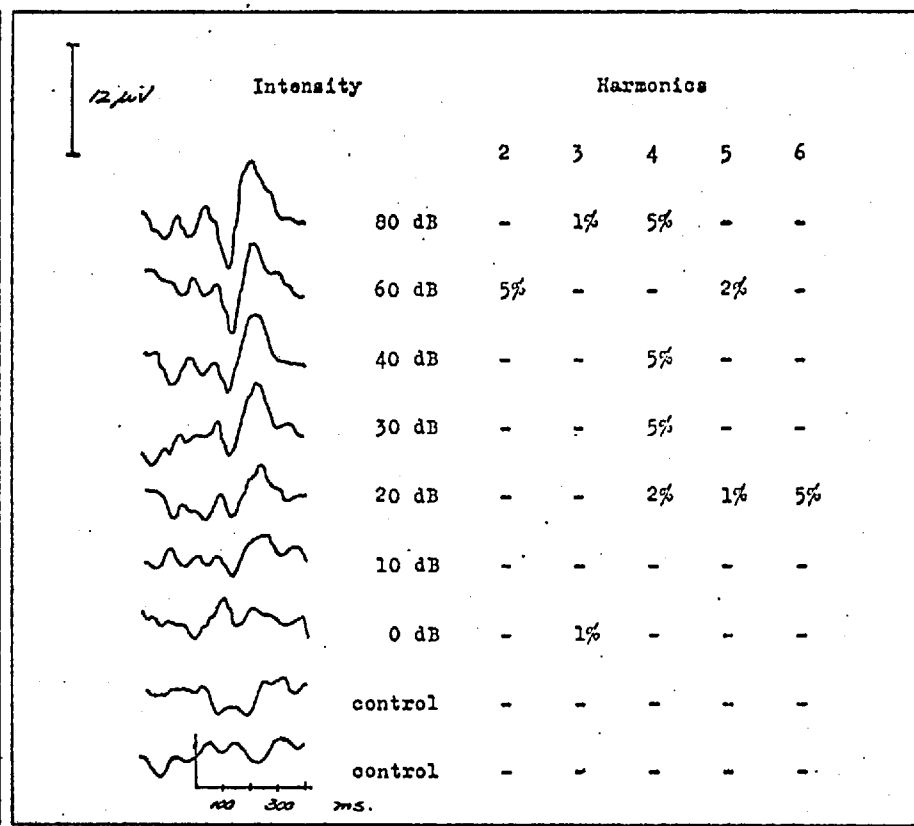
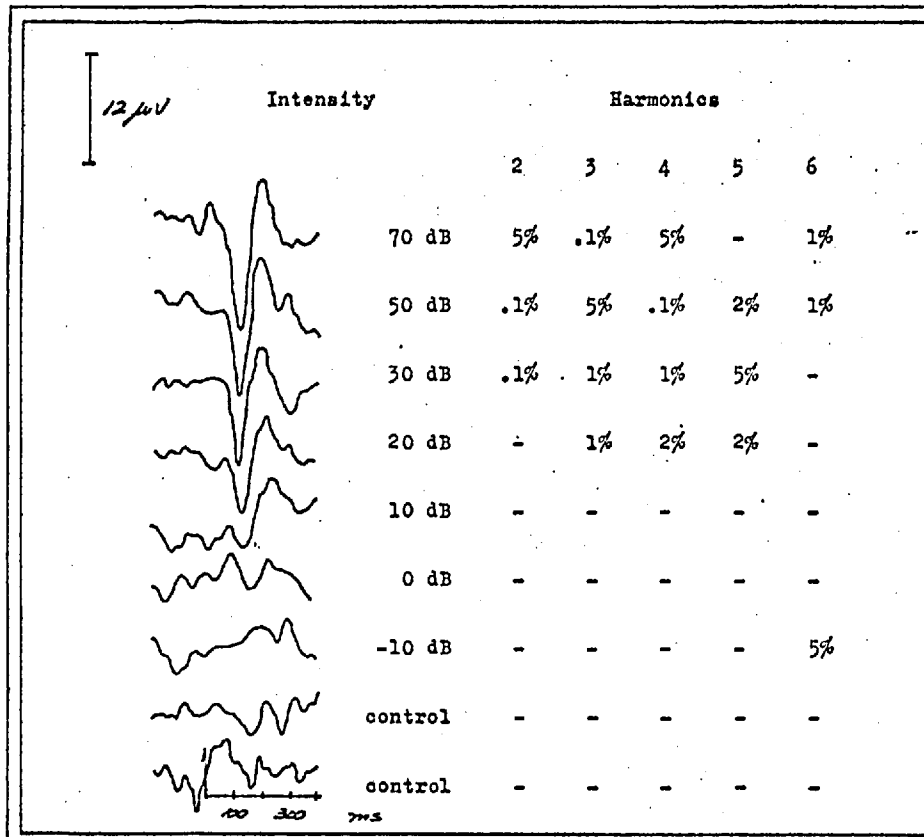


Table 4-xiii. Subject PC, M, age 24, at 1 kHz and 4 kHz.

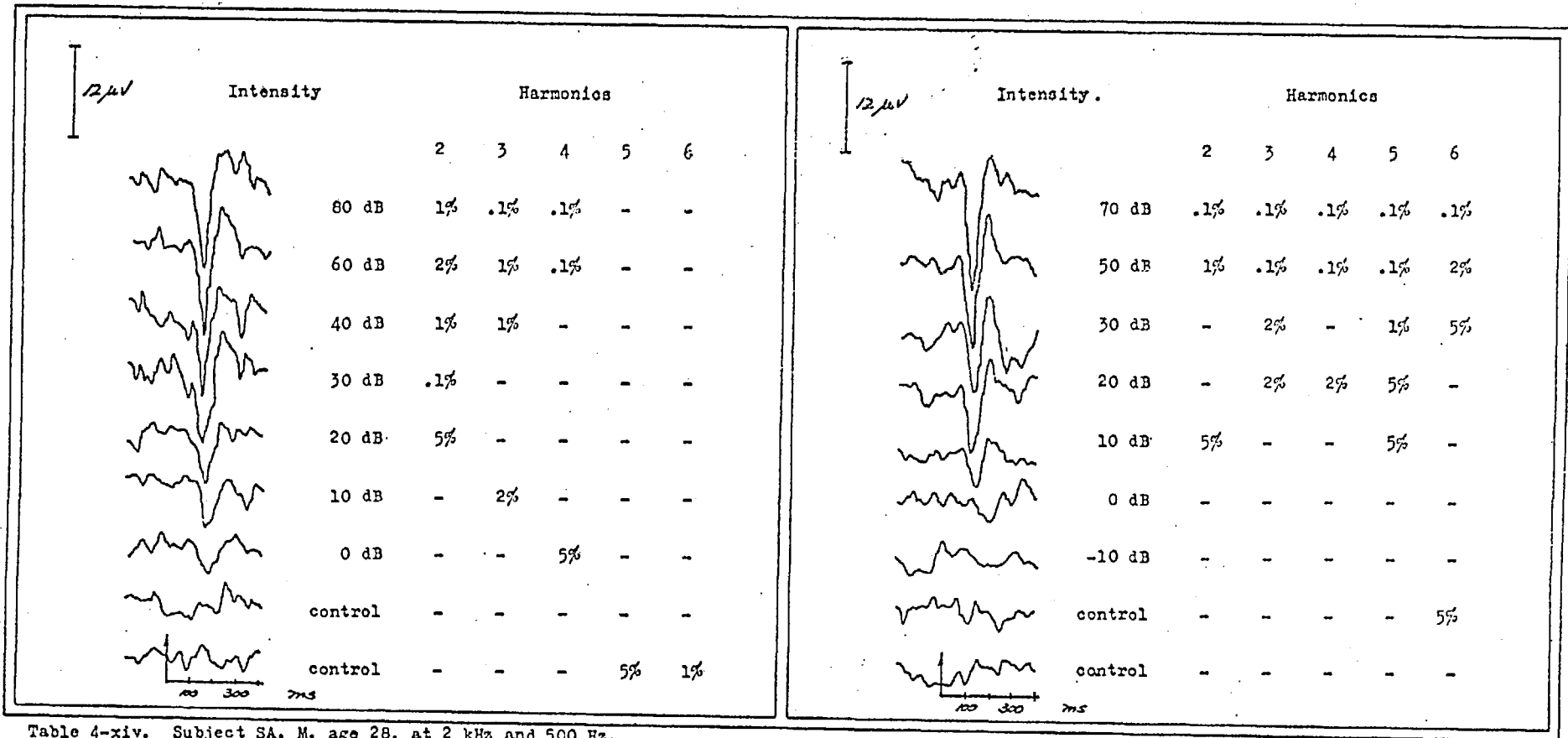


Table 4-xiv. Subject SA, M, age 28, at 2 kHz and 500 Hz.

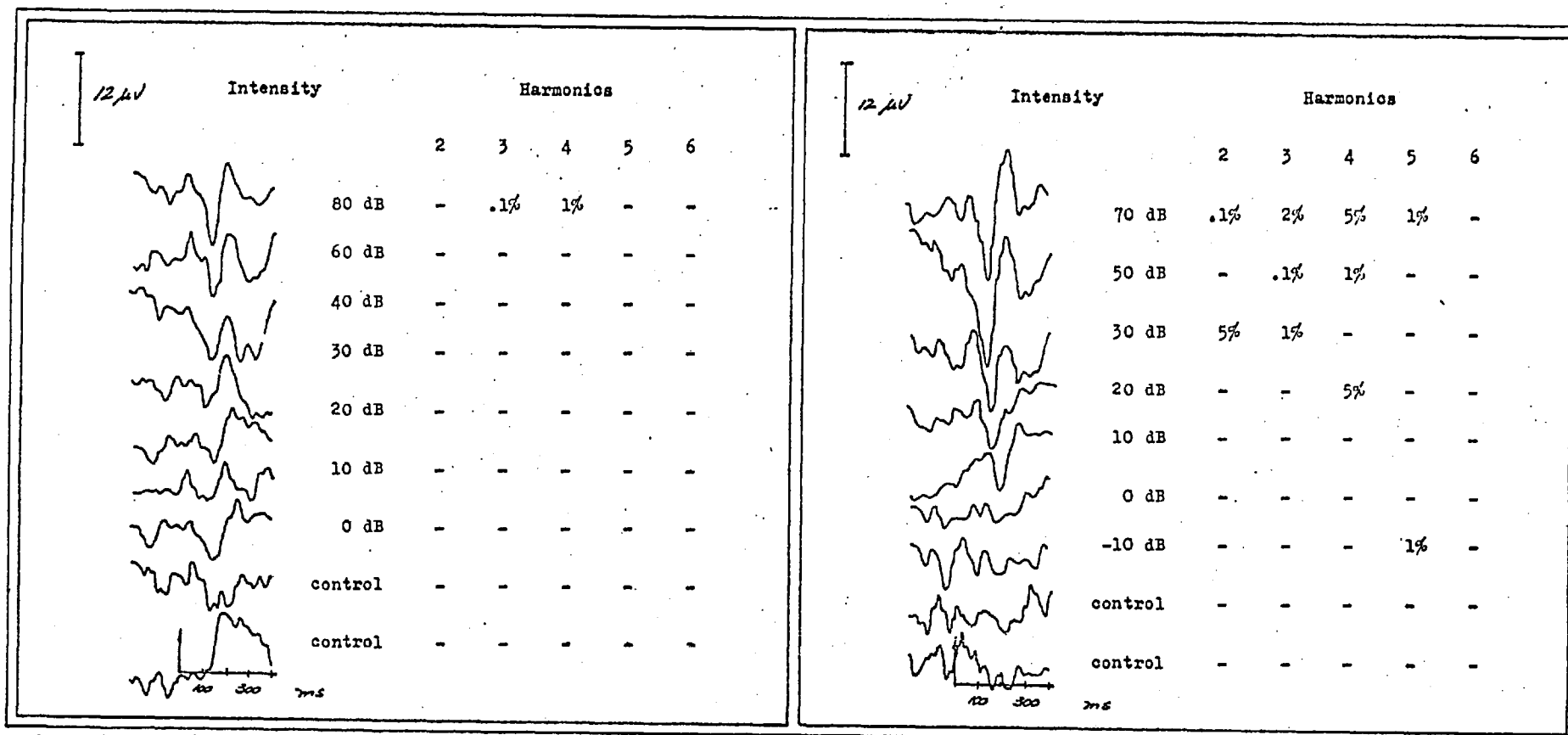


Table 4-xv. Subject DF, P, age 20, at 2 kHz and 500 Hz.

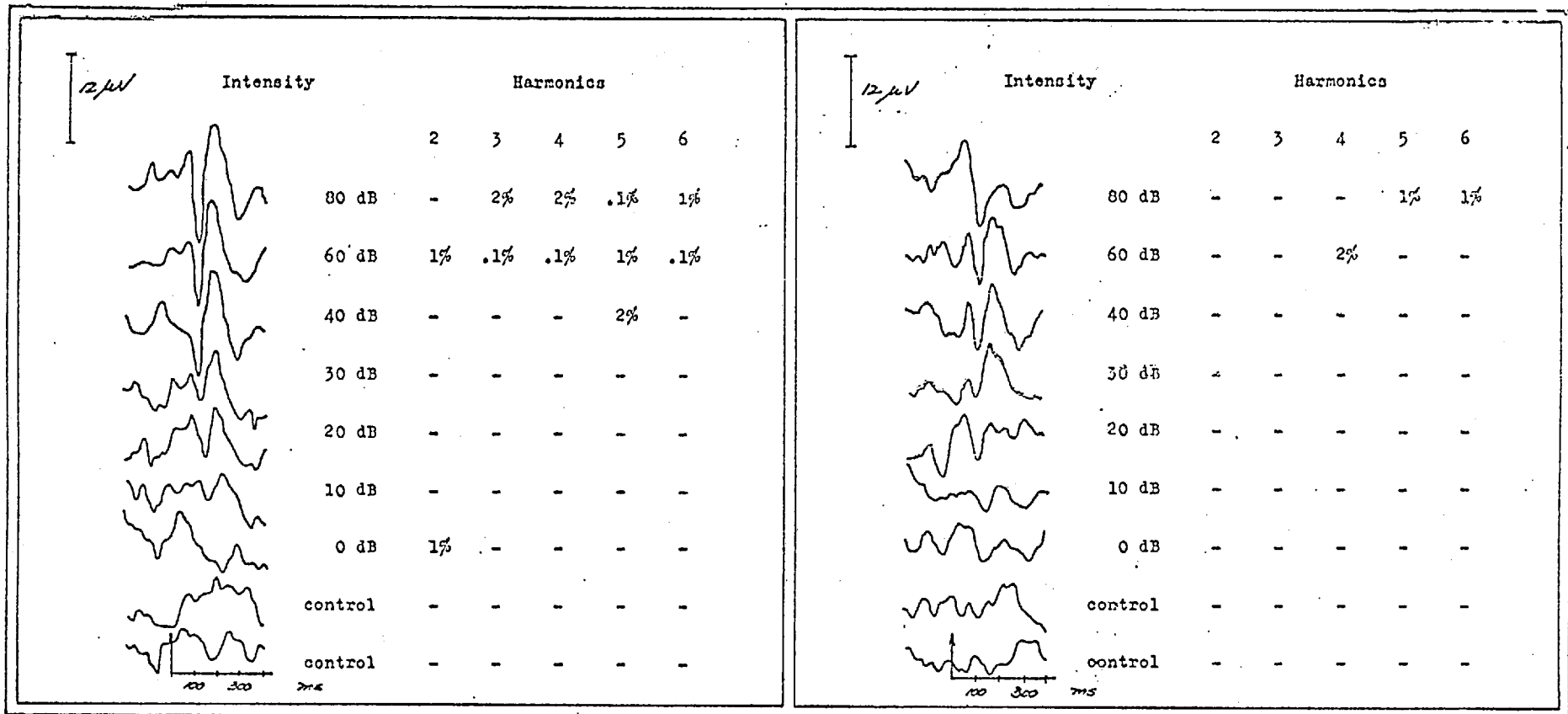


Table 4-xvi. Subject LS, F, age 20, at 1 kHz and 4 kHz.

Tables 4-xvii to 4-lxxii

The Off-line  $\chi^2$  Study

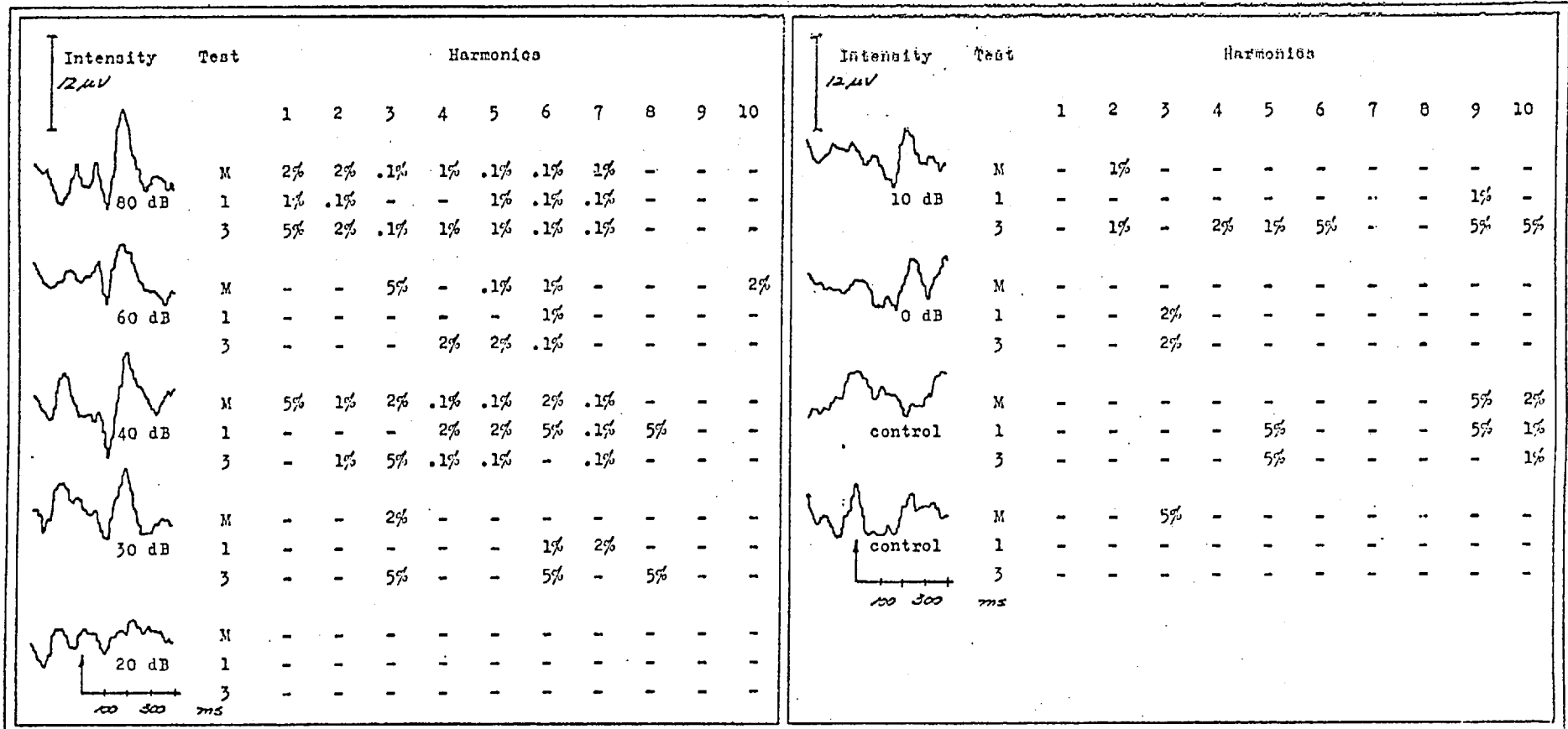


Table 4-xvii. Subject CH, F, age 23, at 2 kHz.

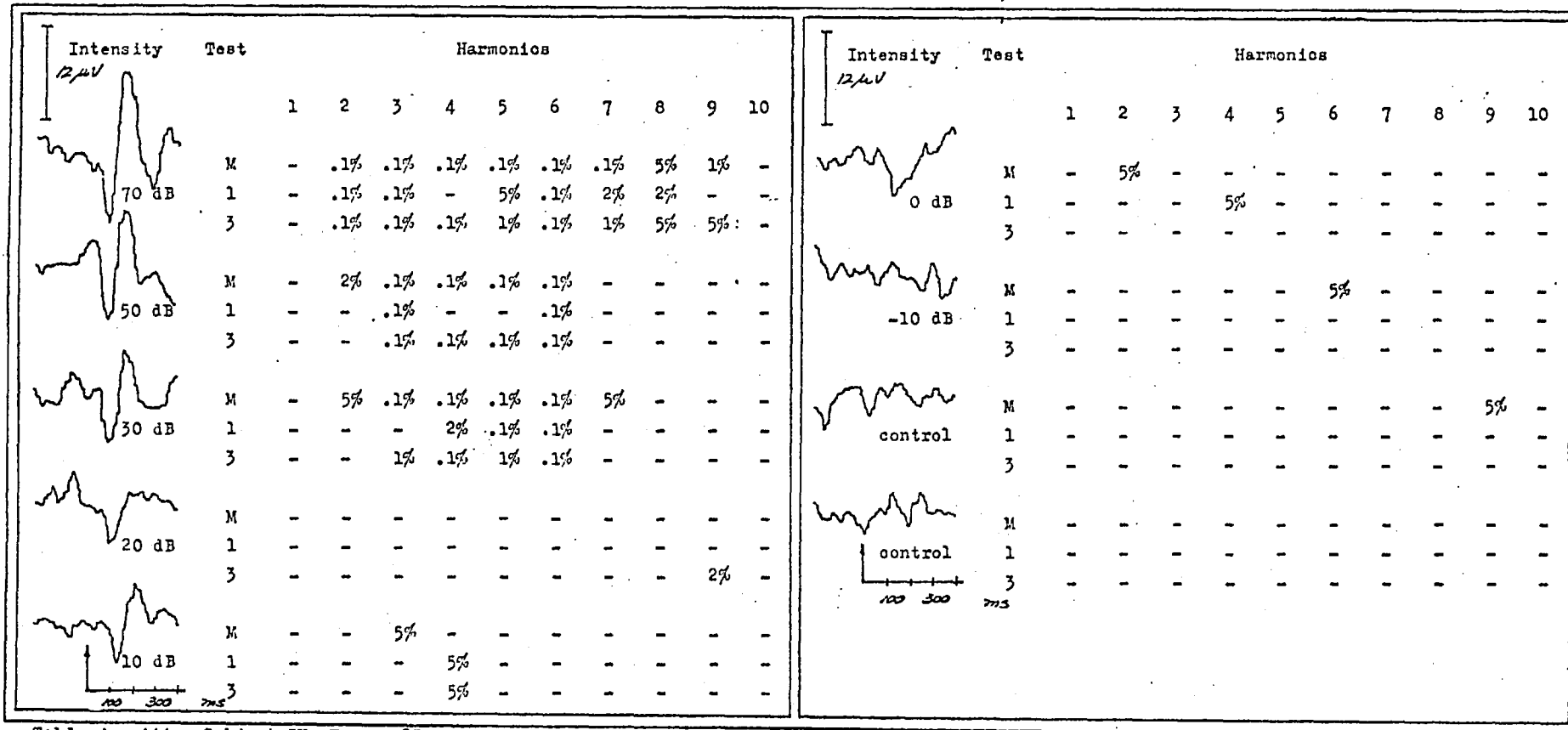


Table 4-xviii. Subject CH, F, age 23, at 500 Hz.

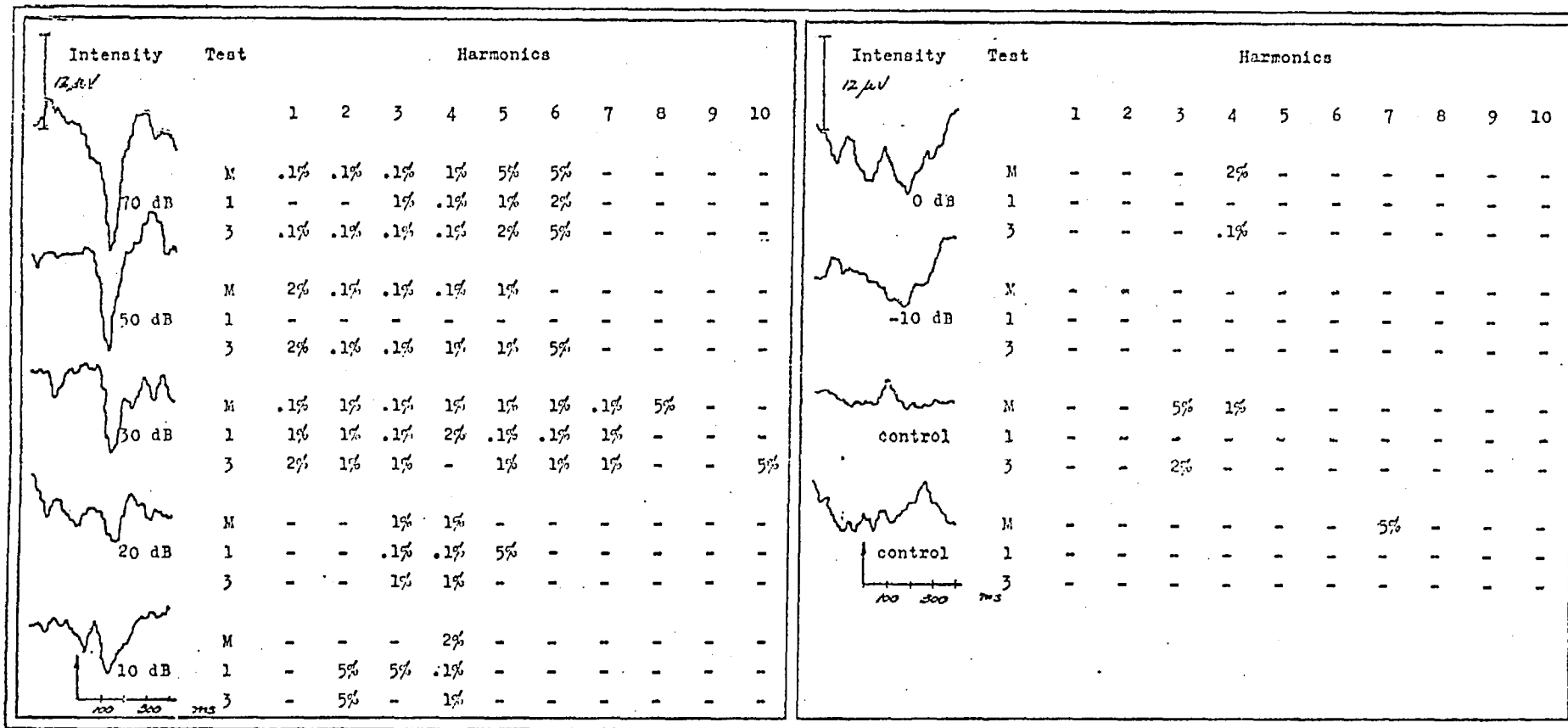


Table 4-xix. Subject GF, M, age 28, at 1 kHz.



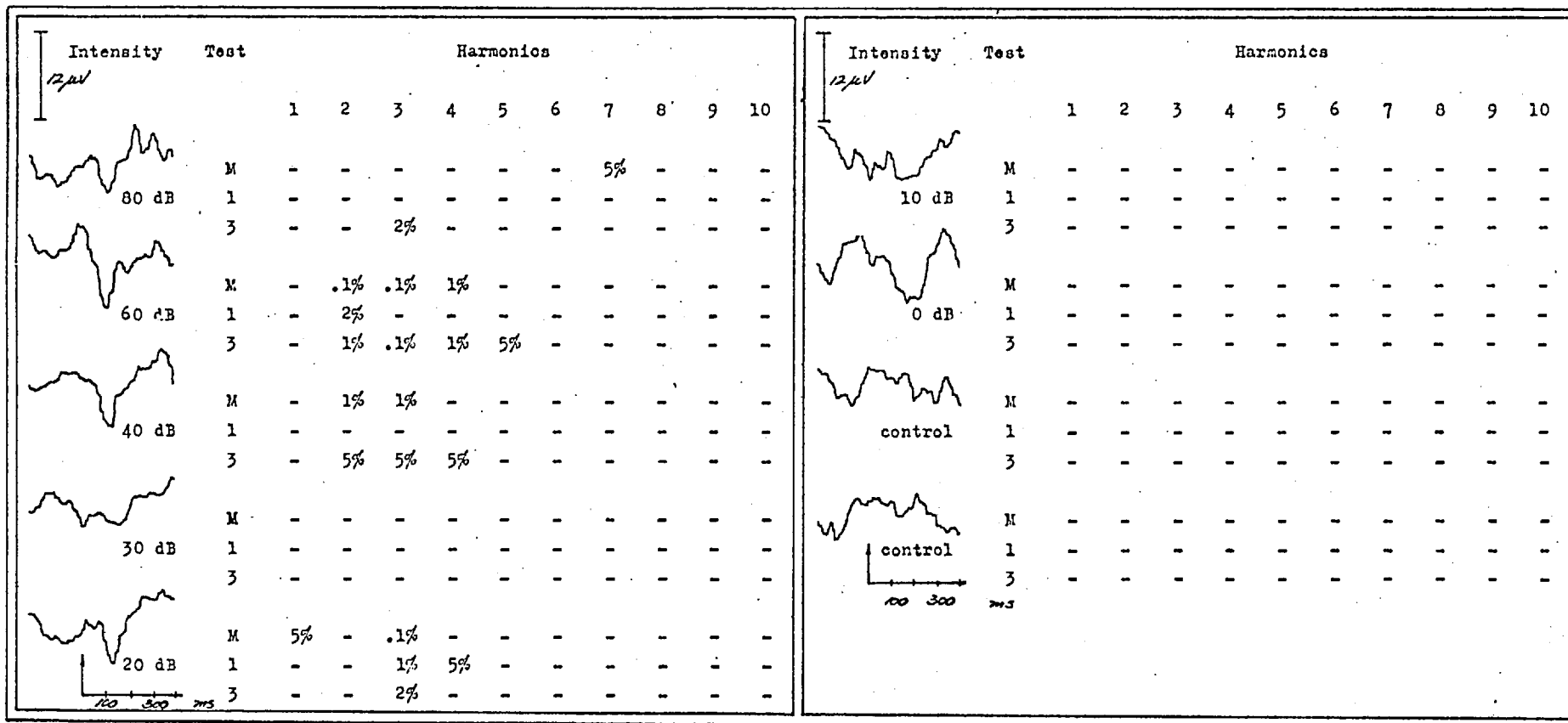


Table 4-xx. Subject GF, M, age 28, at 4 kHz.

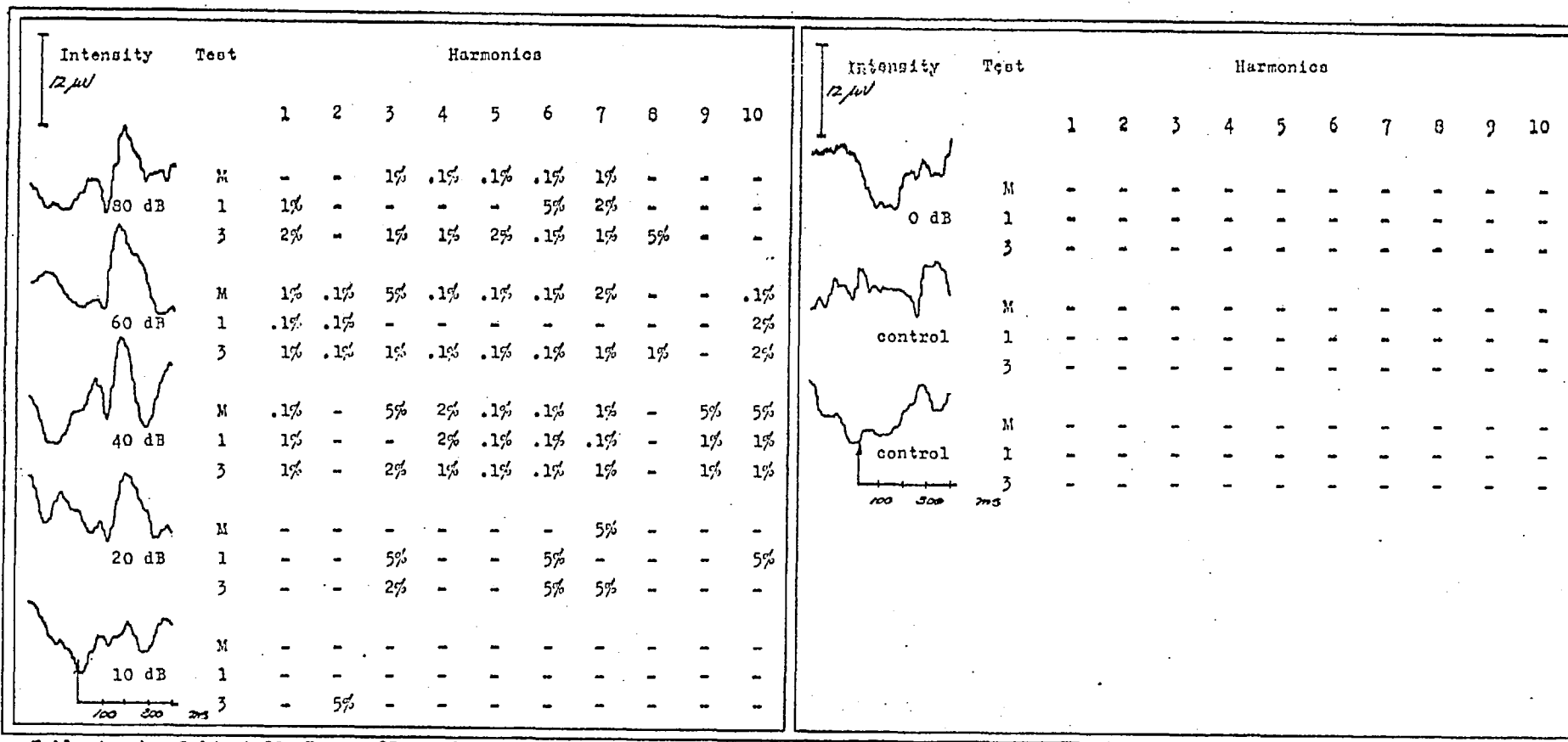


Table 4-xxi. Subject JS, F, age 23, at 2 kHz.

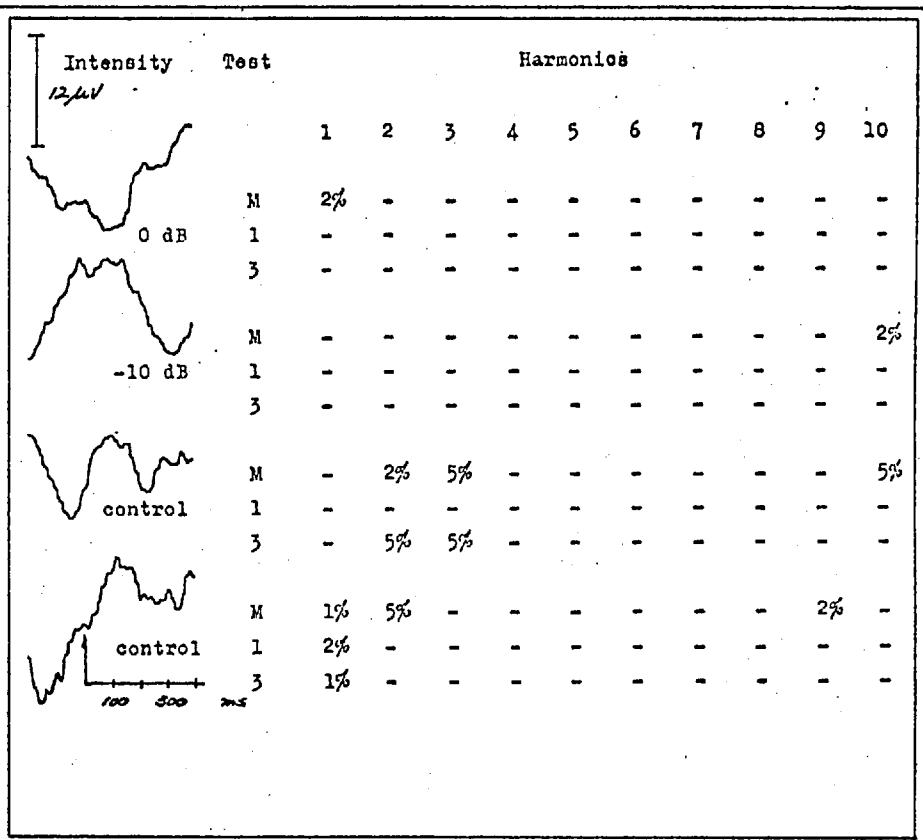
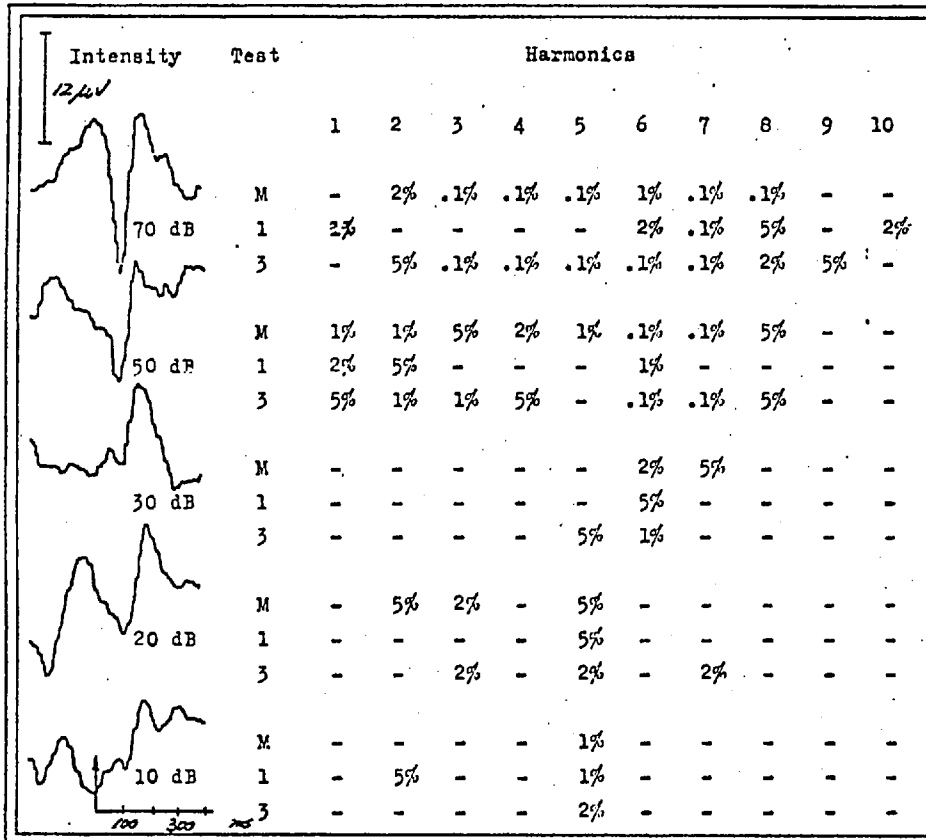


Table 4-xxii. Subject JS, F, age 23, at 500 Hz.

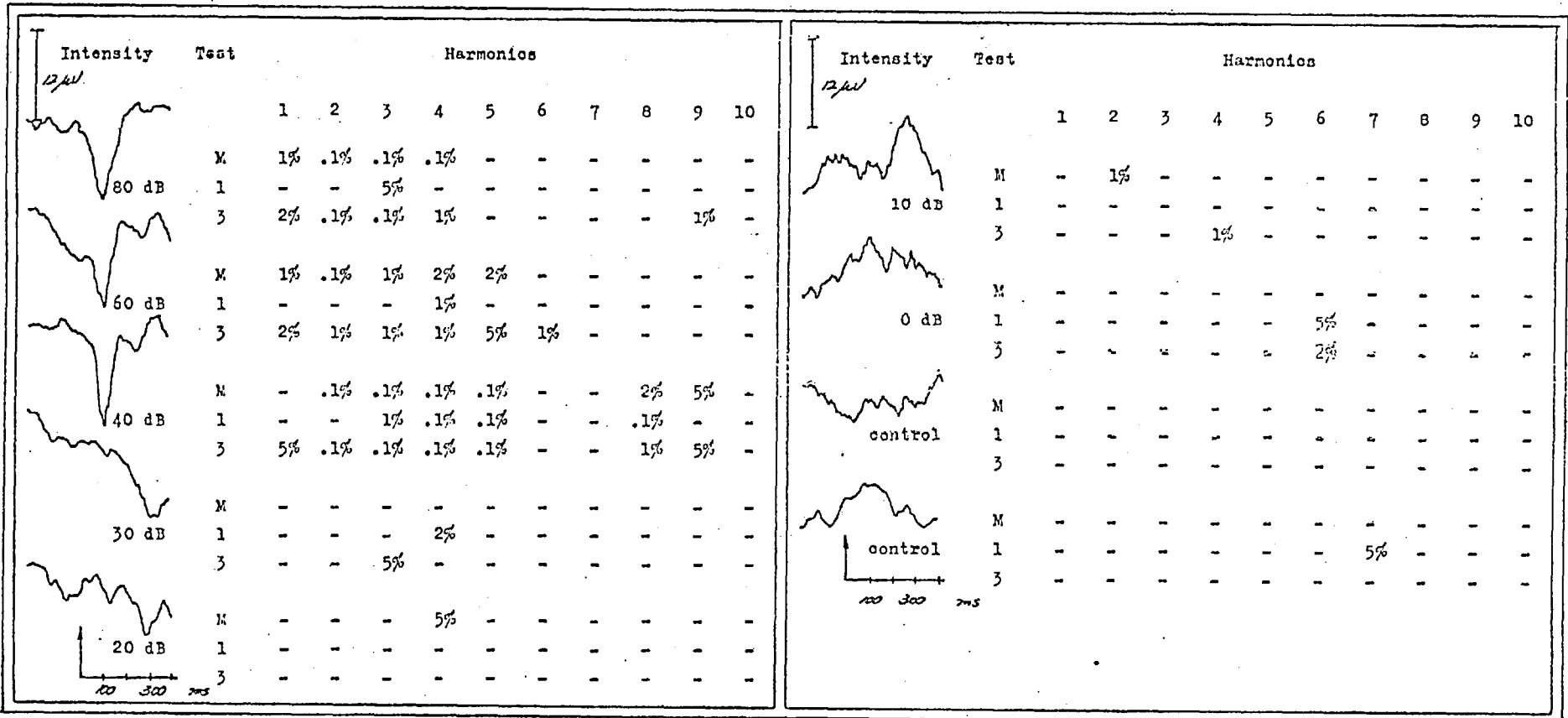


Table 4-xxiii. Subject CR, F, age 31, at 4 kHz.

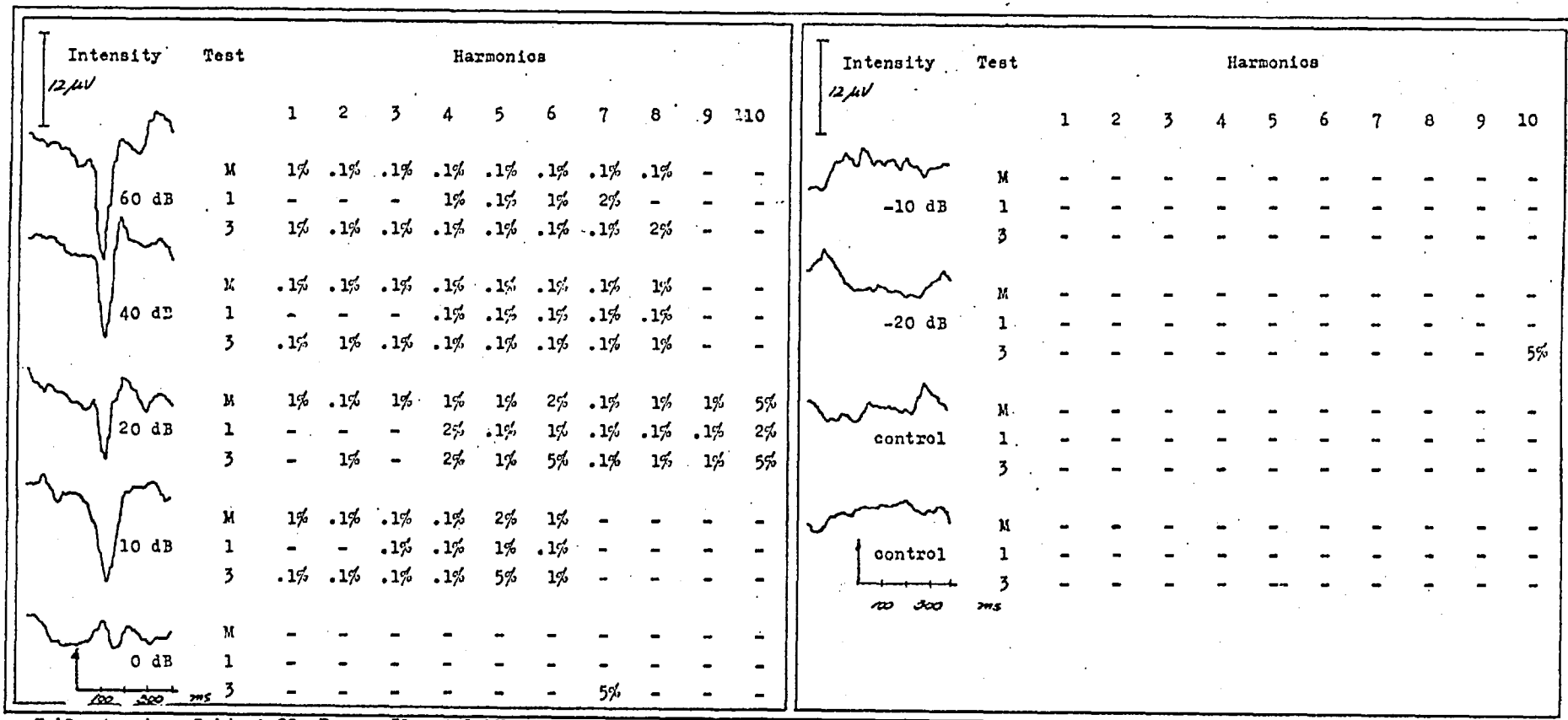
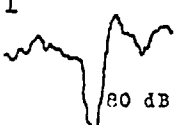
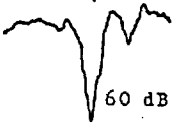
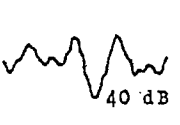
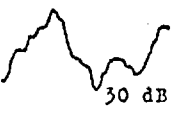
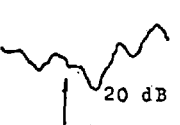


Table 4-xxiv. Subject CR, F, age 31, at 1 kHz.

Intensity	Test	Harmonics									
		1	2	3	4	5	6	7	8	9	10
80 dB 	M	.1%	.1%	.1%	.1%	.1%	.1%	.1%	-	-	-
	1	-	-	-	.1%	.1%	.1%	.1%	5%	-	-
	3	1%	1%	.1%	.1%	.1%	.1%	1%	-	-	.5%
60 dB 	M	.1%	.1%	.1%	.1%	1%	-	-	-	2%	-
	1	-	-	-	1%	2%	-	-	-	1%	-
	3	.1%	.1%	.1%	.1%	.1%	-	-	-	5%	-
40 dB 	M	-	-	5%	5%	5%	-	5%	1%	-	-
	1	-	-	1%	1%	-	-	-	-	-	-
	3	-	-	1%	-	-	-	-	-	-	-
30 dB 	M	2%	5%	-	-	-	-	-	-	-	-
	1	5%	5%	-	-	-	-	-	-	-	-
	3	-	1%	-	-	-	-	-	-	-	-
20 dB 	M	1%	2%	5%	-	-	5%	-	-	-	-
	1	-	-	-	-	-	2%	-	-	2%	-
	3	2%	5%	-	-	-	2%	-	-	-	-

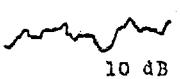

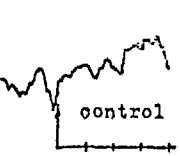
Intensity	Test	Harmonics									
		1	2	3	4	5	6	7	8	9	10
10 dB 	M	-	-	-	-	-	-	-	-	-	-
	1	-	-	-	-	-	-	-	-	-	2%
	3	-	-	-	-	-	-	-	-	-	1%
0 dB 	M	-	-	-	-	-	-	-	-	-	-
	1	-	-	-	-	-	-	-	-	1%	-
	3	-	-	-	-	-	-	-	-	2%	-
control 	M	-	-	-	-	-	-	-	-	-	-
	1	-	-	-	-	-	-	-	-	5%	-
	3	-	-	-	-	-	-	-	-	5%	-

Table 4-xxv. Subject FN, M, age 28, at 2 kHz.

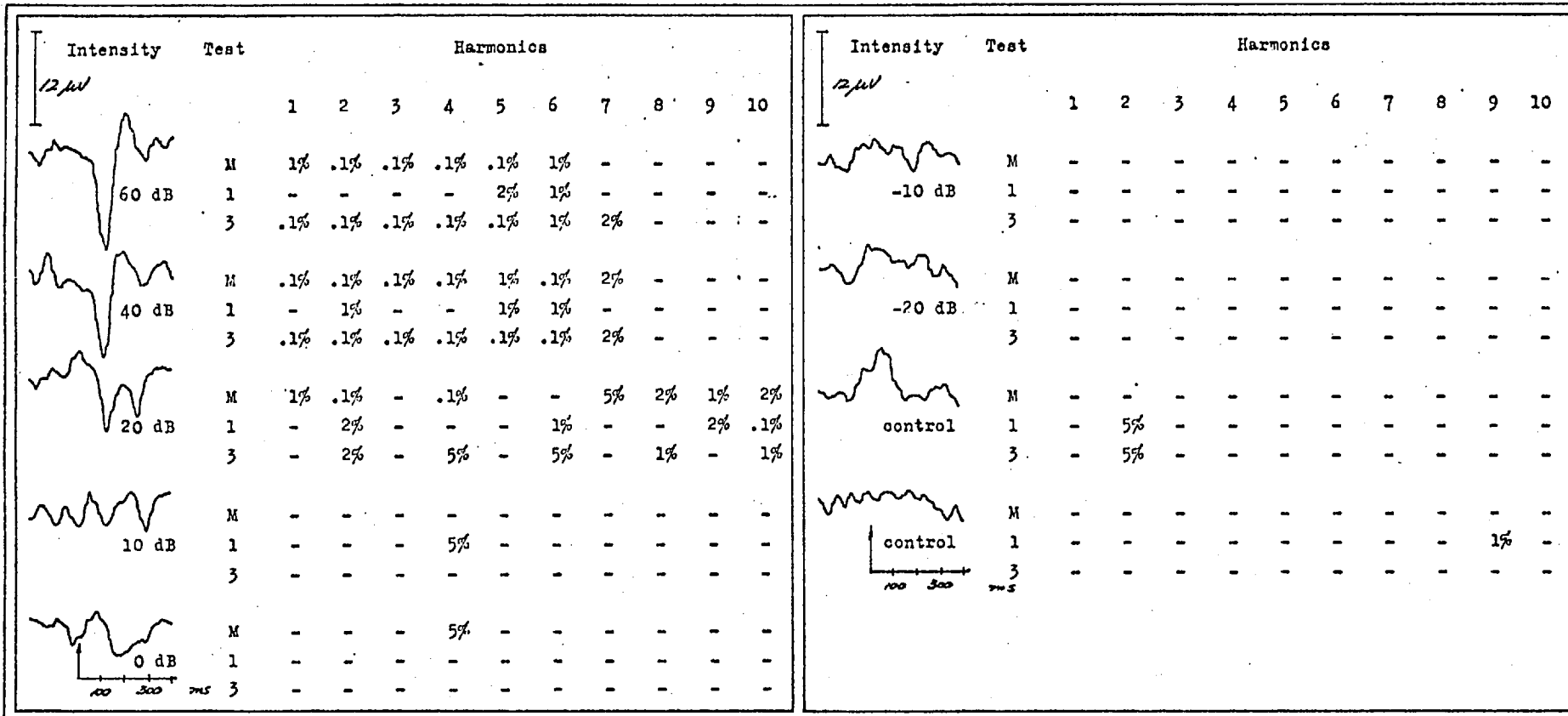


Table 4-xxvi. Subject FN, M, age 28, at 500 Hz.

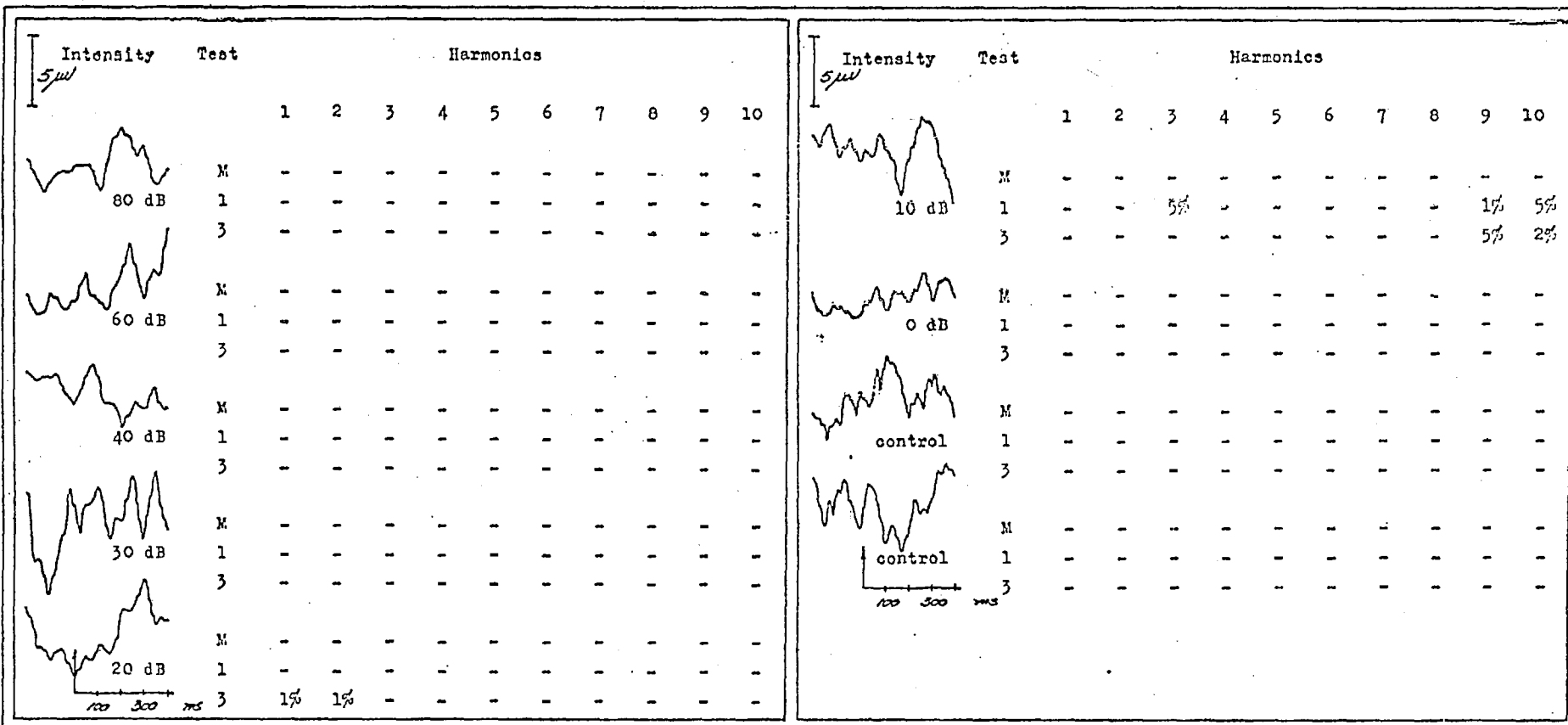


Table 4-xxvii. Subject TB, M, age 20, at 4 kHz.



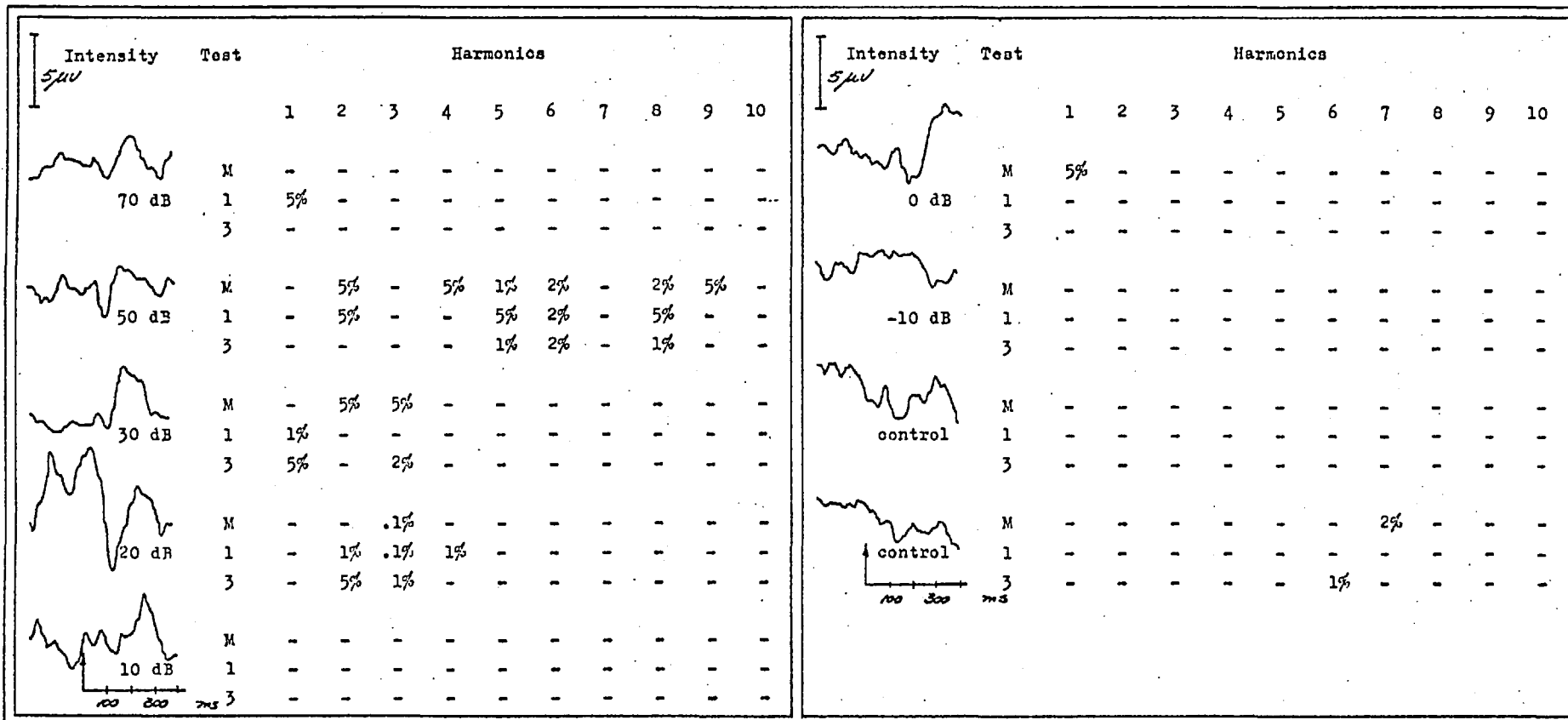


Table 4-xxviii. Subject TB, M, age 20, at 1 kHz.

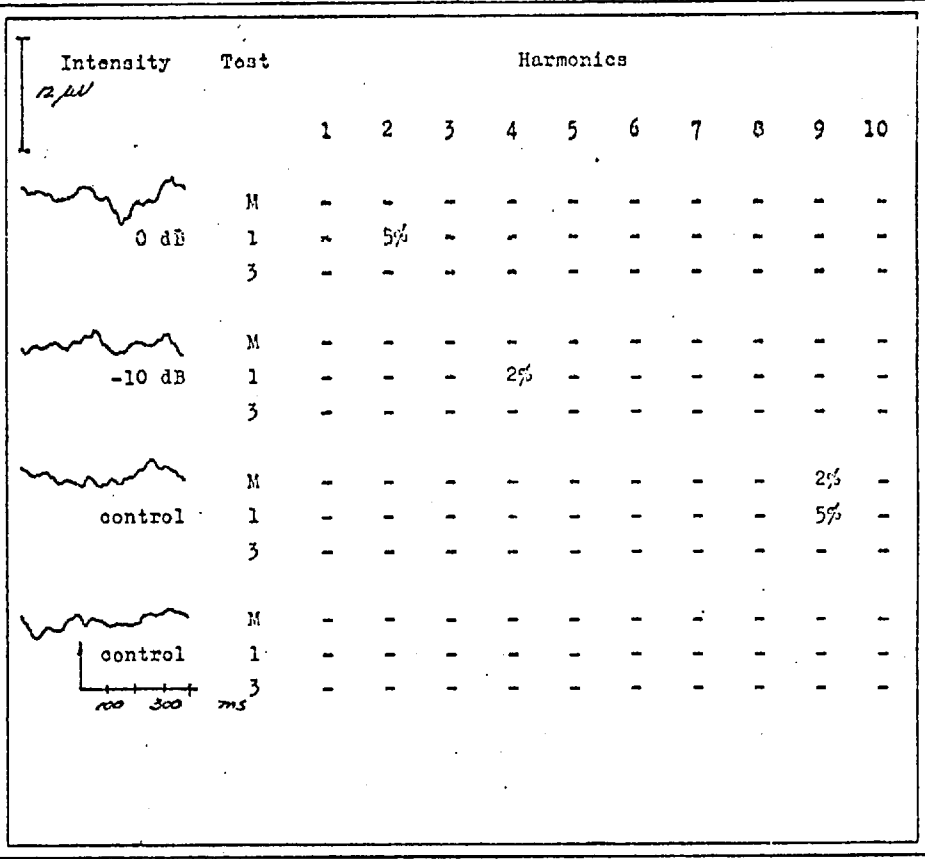
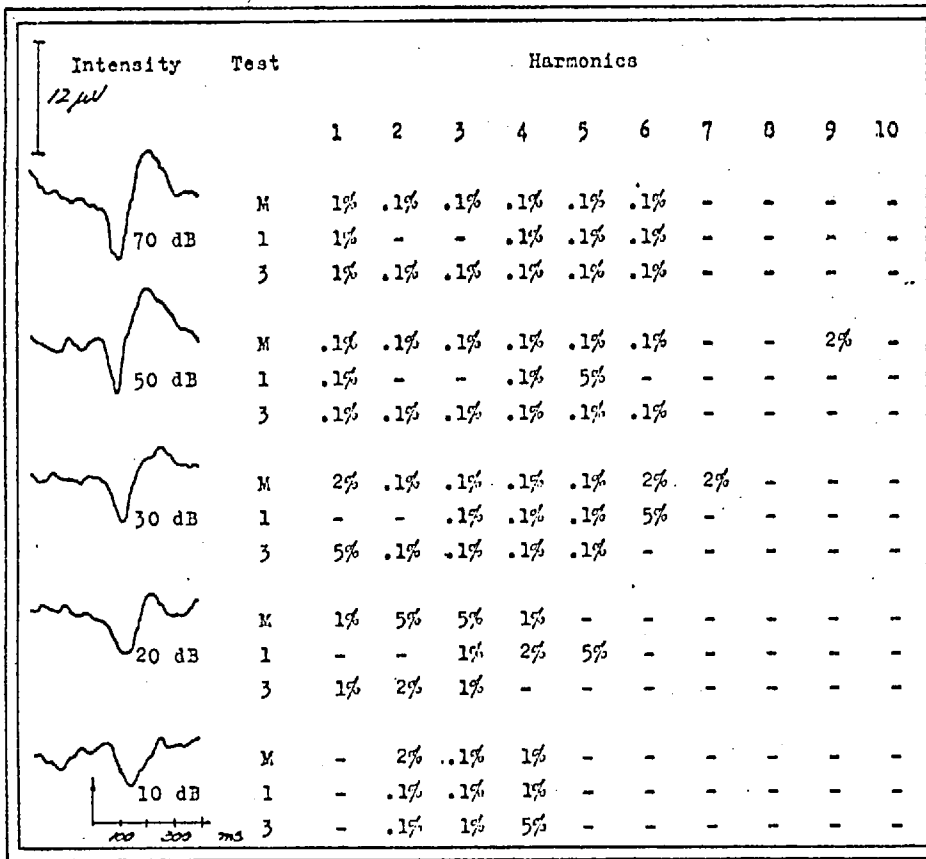


Table 4-xxix. Subject BO, K, age 31, at 2 kHz.

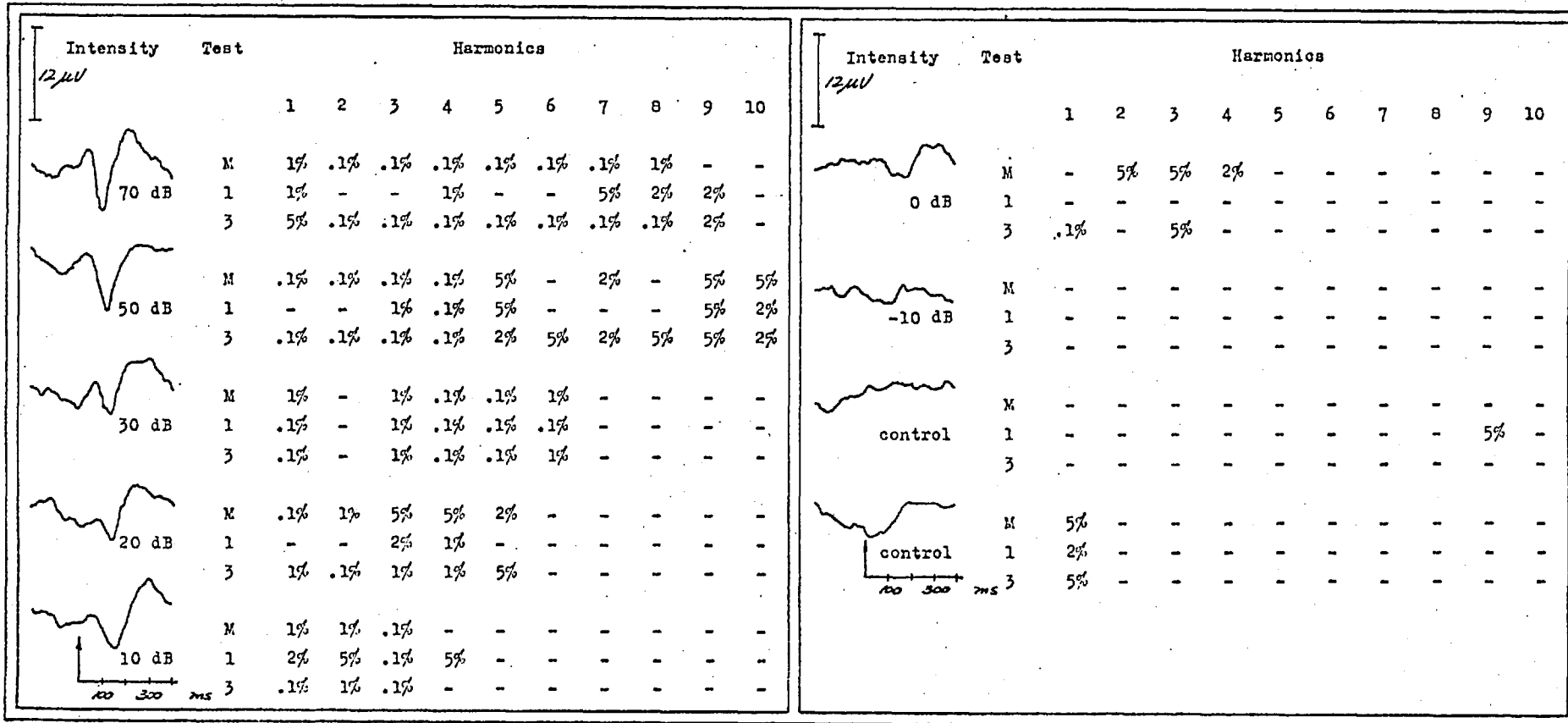


Table 4-xxx. Subject BO, M, age 31, at 500 Hz.

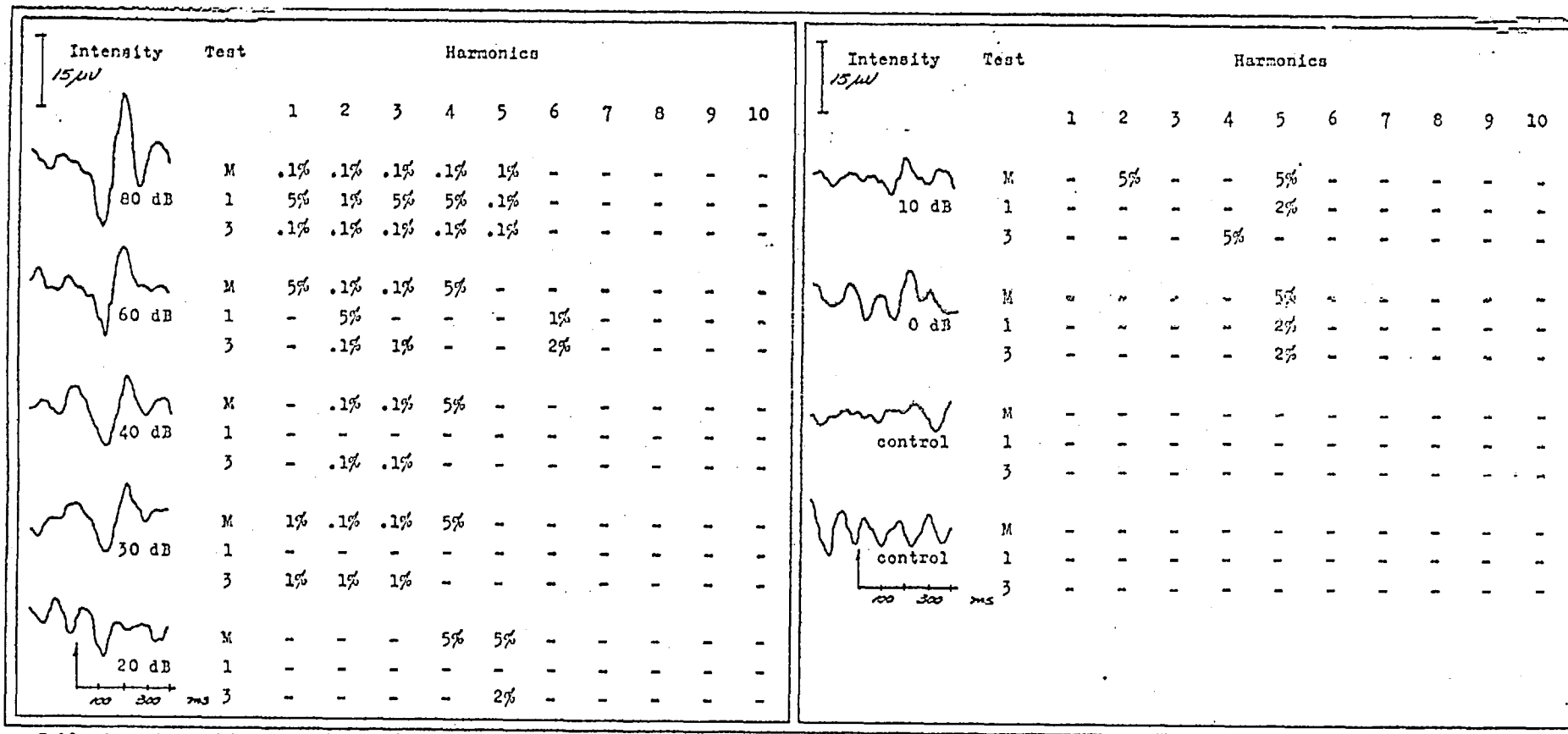


Table 4-xxx1. Subject JD, F, age 23, at 4 kHz.

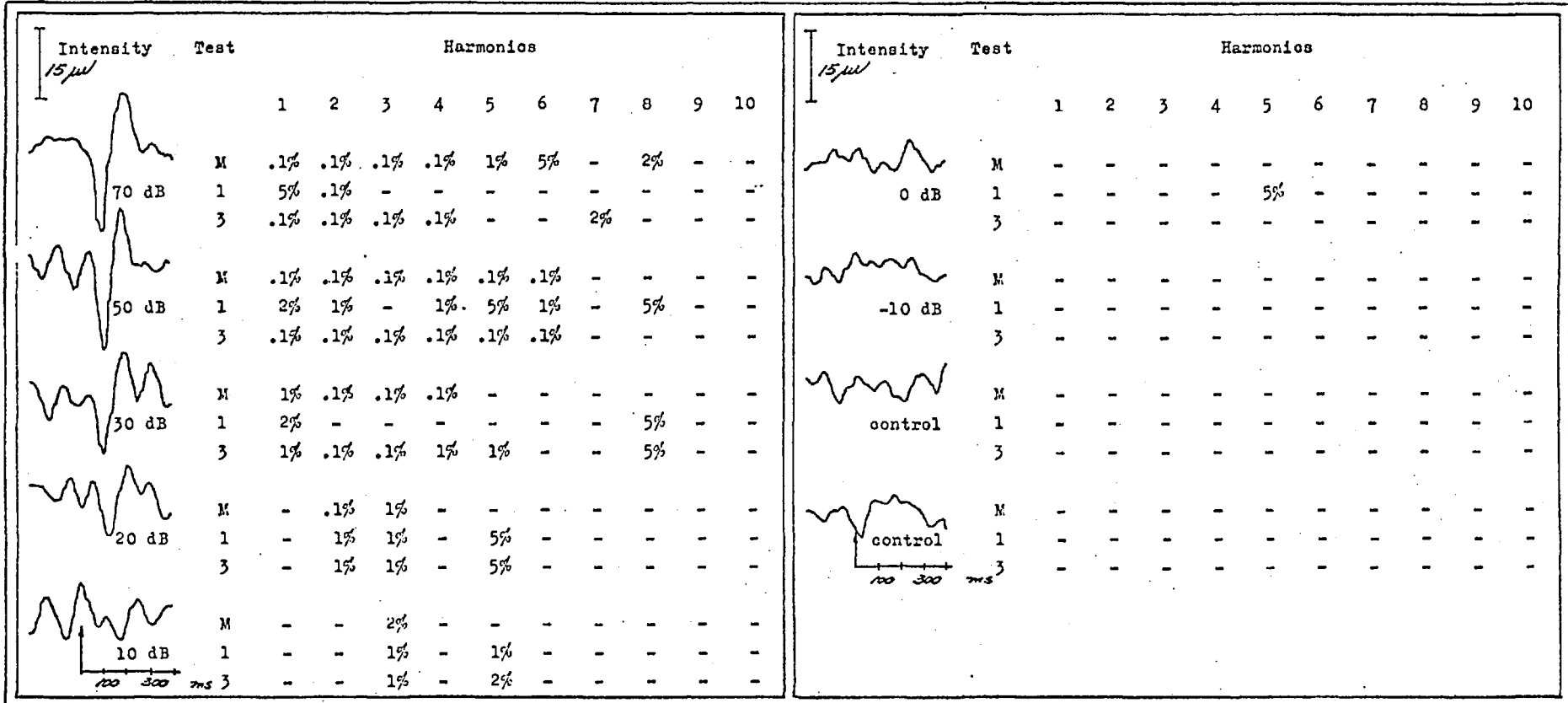
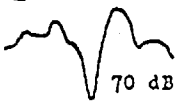
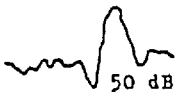
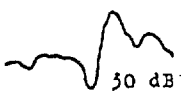
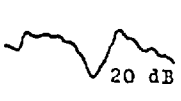
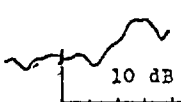


Table 4-xxxii. Subject JD, F, age 23, at 1 kHz.

Intensity <i>12 μV</i>	Test	Harmonics									
		1	2	3	4	5	6	7	8	9	10
 70 dB	M	-	.1%	.1%	.1%	.1%	.1%	.1%	-	-	-
	1	-	-	5%	-	5%	-	-	-	-	-
	3	-	.1%	.1%	.1%	5%	.1%	.1%	-	-	-
 50 dB	M	2%	.1%	.1%	.1%	.1%	-	-	5%	-	-
	1	1%	.1%	-	-	5%	2%	2%	5%	-	-
	3	2%	.1%	.1%	.1%	.1%	1%	1%	5%	-	-
 30 dB	M	-	1%	.1%	.1%	.1%	5%	-	-	-	-
	1	1%	.1%	-	-	-	-	-	-	-	-
	3	5%	.1%	.1%	.1%	1%	-	-	-	-	-
 20 dB	M	-	1%	1%	1%	-	-	-	-	-	-
	1	-	-	-	1%	-	-	-	-	-	-
	3	5%	-	1%	.1%	-	-	-	-	-	-
 10 dB	M	-	-	-	-	-	-	-	-	-	-
	1	-	-	-	-	-	-	-	-	-	-
	3	-	-	-	-	-	-	-	-	-	-

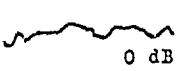
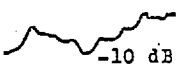
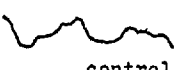
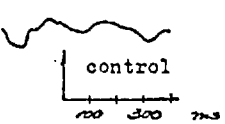
Intensity <i>12 μV</i>	Test	Harmonics									
		1	2	3	4	5	6	7	8	9	10
 0 dB	M	-	-	-	-	-	-	-	-	-	-
	1	-	-	-	-	-	-	-	-	-	-
	3	-	-	-	-	-	-	-	-	-	-
 -10 dB	M	-	-	-	-	-	-	-	-	-	-
	1	-	-	-	-	-	-	-	-	-	-
	3	-	-	-	-	-	-	-	-	-	-
 control	M	-	-	-	-	-	-	-	-	-	-
	1	-	-	-	-	-	-	-	-	-	-
	3	-	-	-	-	-	-	-	-	-	-
 control <i>100 300 ms</i>	M	-	-	-	-	-	-	-	-	-	-
	1	-	-	-	-	-	-	-	-	-	-
	3	-	-	-	-	-	-	-	-	-	-

Table 4-xxxiii. Subject DT, F, age 24, at 2 kHz.

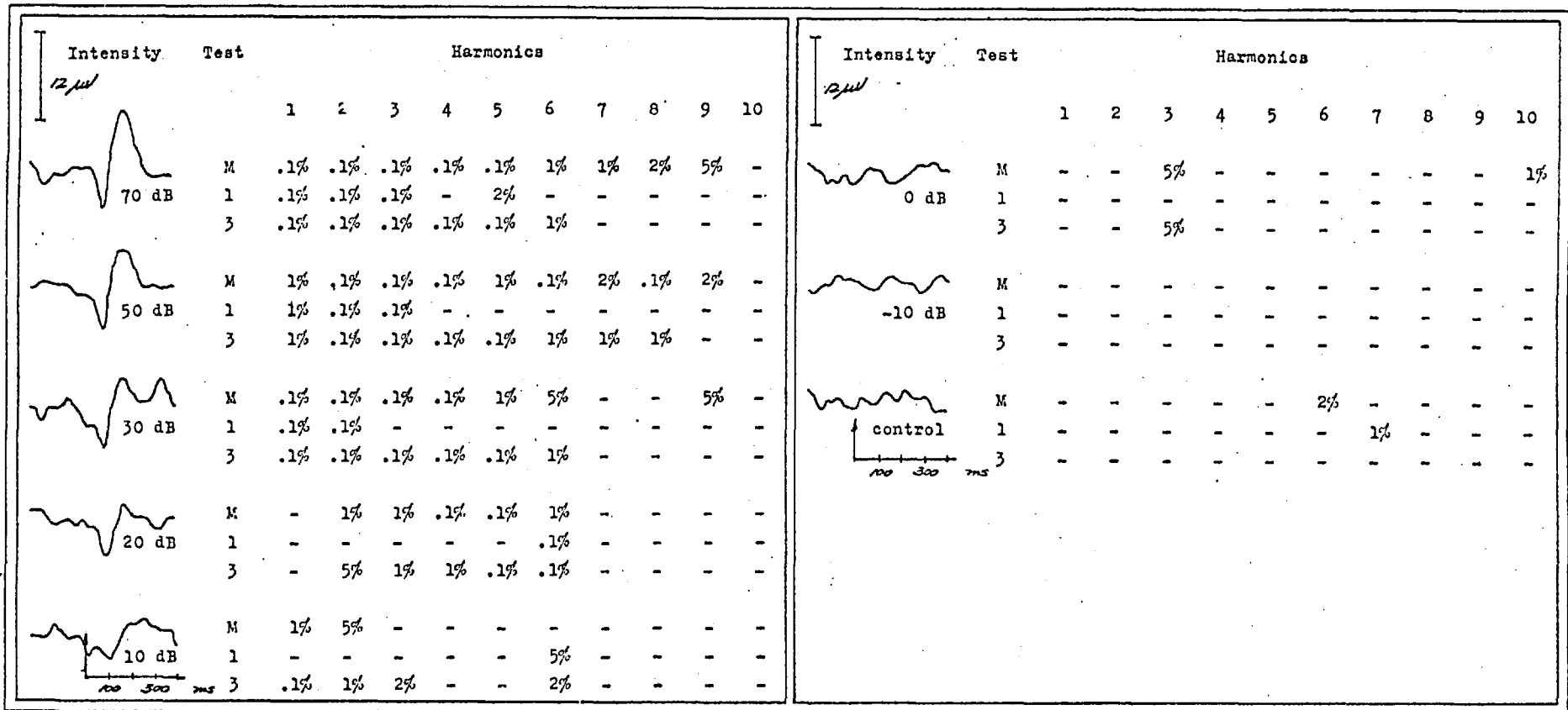


Table 4-xxxiv. Subject DT, F, age 24, at 500 Hz.

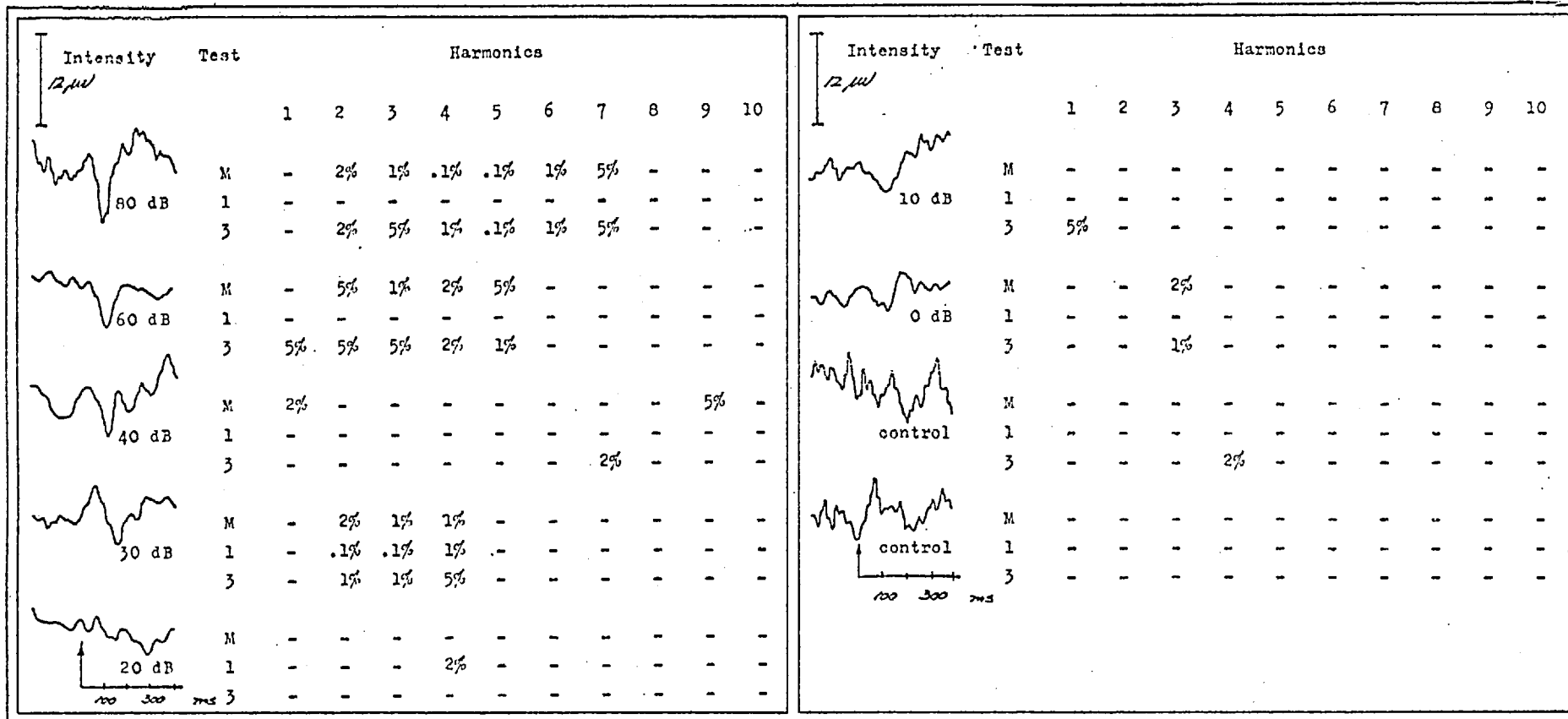


Table 4-xxxv. Subject SB, M, age 18, at 4 kHz.



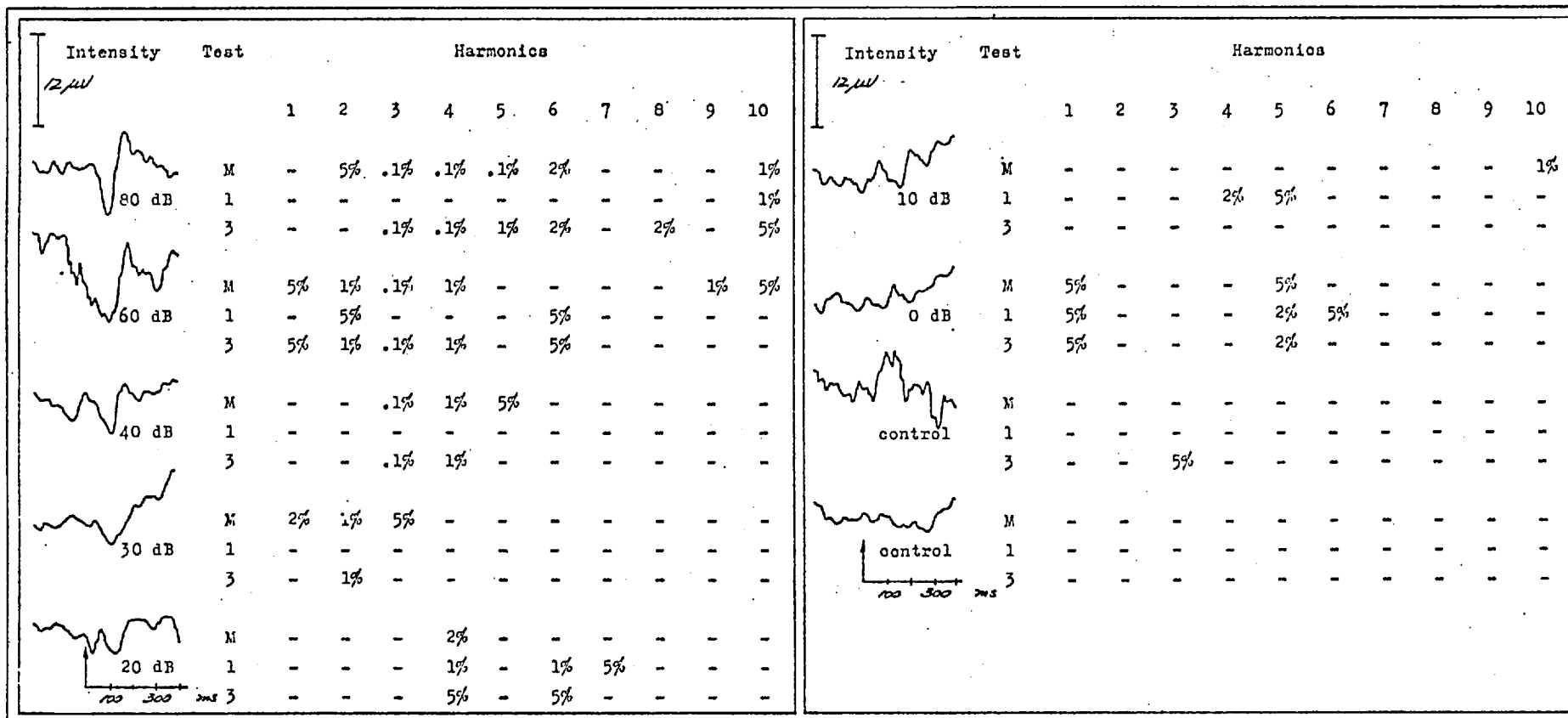
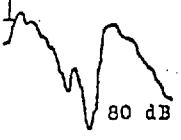


Table 4-xxxvi. Subject SB, M, age 18, at 1 kHz.

Intensity <i>12 μV</i>	Test	Harmonics										
		1	2	3	4	5	6	7	8	9	10	
	M	-	1%	.1%	.1%	.1%	.1%	.1%	.1%	5%	-	-
	1	5%	-	-	-	2%	1%	1%	-	-	-	-
	3	2%	1%	.1%	5%	.1%	.1%	.1%	-	-	-	-
60 dB	M	-	1%	.1%	.1%	.1%	.1%	.1%	-	-	-	-
	1	-	-	-	.1%	.1%	1%	5%	-	-	-	-
	3	-	.1%	1%	.1%	.1%	1%	1%	-	-	-	-
40 dB	M	-	1%	1%	.1%	.1%	2%	-	.1%	-	-	-
	1	5%	-	-	1%	-	5%	2%	5%	-	-	-
	3	-	5%	-	.1%	1%	1%	1%	5%	-	-	-
30 dB	M	-	2%	1%	1%	-	-	-	-	1%	-	-
	1	-	-	-	-	-	-	-	5%	.1%	-	-
	3	-	5%	2%	1%	-	-	-	-	1%	-	-
20 dB	M	-	-	1%	.1%	.1%	.1%	.1%	2%	-	-	-
	1	-	-	5%	.1%	1%	.1%	2%	5%	-	-	-
	3	-	-	.1%	.1%	-	1%	5%	-	.1%	-	-

Intensity <i>12 μV</i>	Test	Harmonics										
		1	2	3	4	5	6	7	8	9	10	
10 dB	M	2%	-	-	-	-	-	-	-	-	-	-
	1	-	-	-	-	-	-	-	-	-	-	-
	3	2%	5%	5%	-	-	-	-	-	-	-	-
0 dB	M	-	-	-	5%	-	-	-	-	-	-	-
	1	-	-	-	2%	-	-	-	-	-	-	-
	3	-	-	-	5%	-	-	-	-	-	-	-
control	M	-	-	-	-	-	-	-	-	-	-	-
	1	-	-	-	-	-	-	-	-	-	-	-
	3	-	-	-	-	-	-	-	-	-	-	-
control	M	-	-	-	-	-	-	-	-	-	-	-
	1	-	-	-	-	-	-	-	-	-	-	-
	3	-	-	-	-	-	-	-	-	-	-	-

Table 4-xxxvii. Subject JN, M, age 30, at 4 kHz.

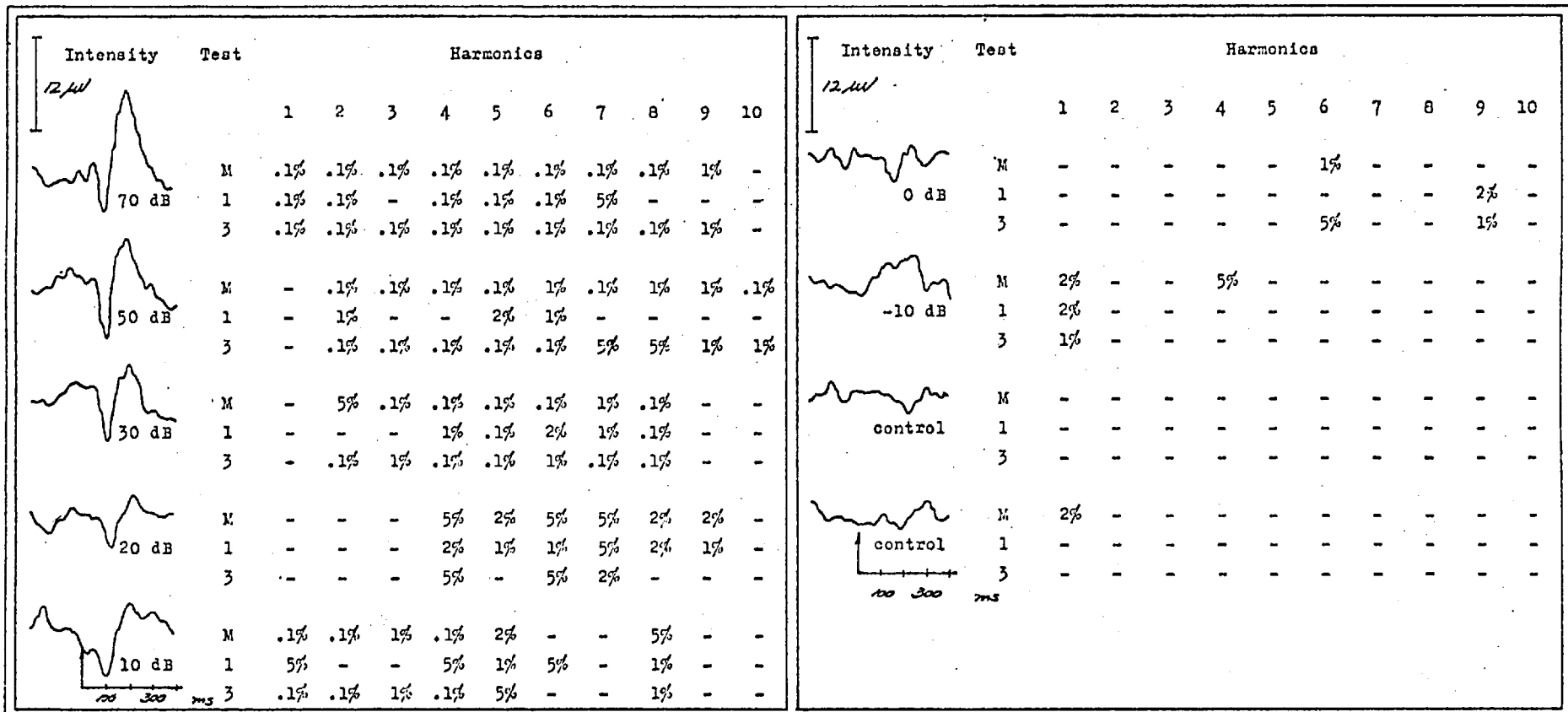


Table 4-xxxviii. Subject JN, M, age 30, at 1 kHz.

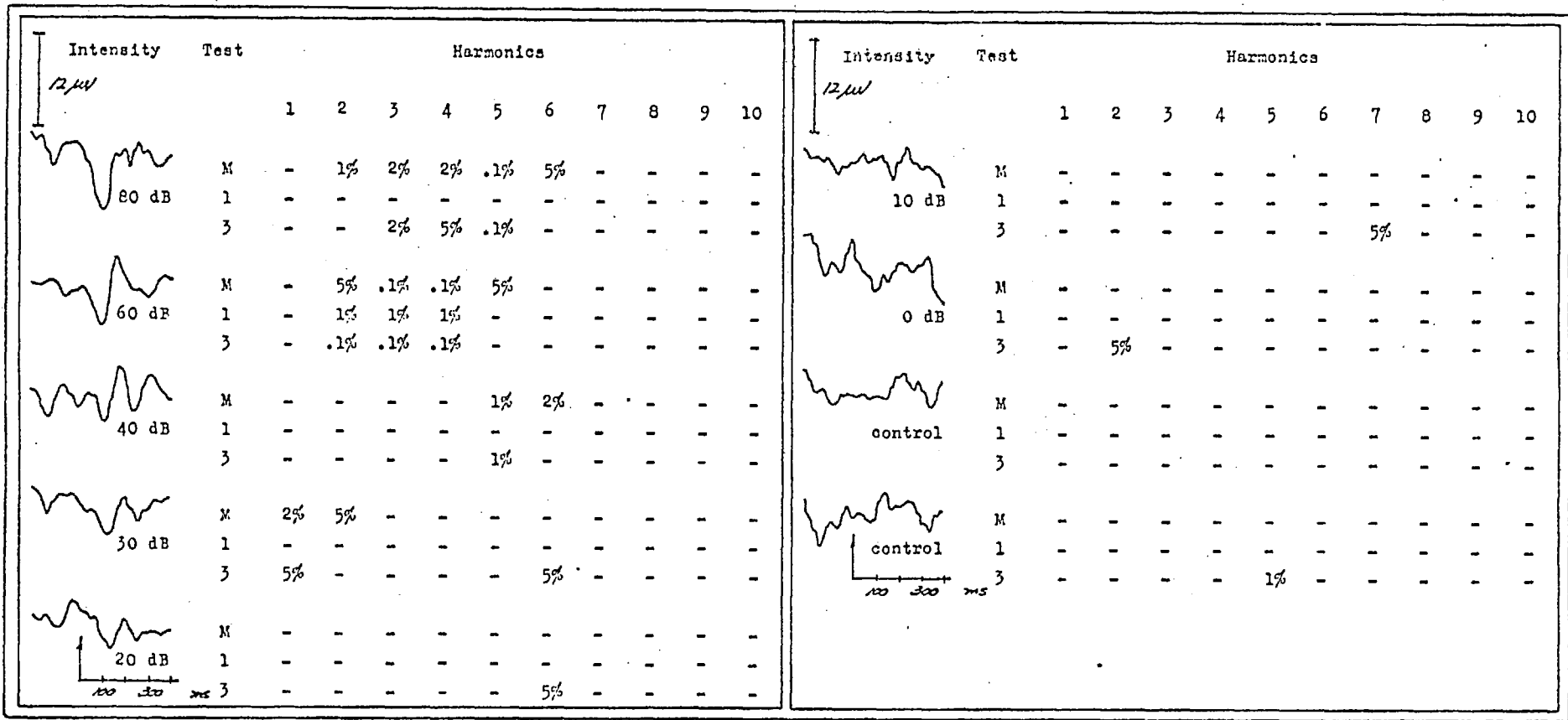
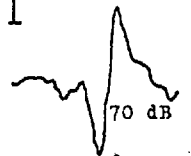
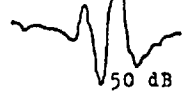
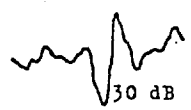
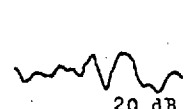



Table 4-xxxix. Subject VM, F, age 24, at 4 kHz.

Intensity <i>12 μV</i>	Test	Harmonics									
		1	2	3	4	5	6	7	8	9	10
 70 dB	M	.1%	.1%	.1%	.1%	.1%	.1%	-	-	-	-
	1	2%	.1%	-	-	-	.1%	-	-	-	-
	3	2%	.1%	1%	.1%	.1%	.1%	-	-	-	-
 50 dB	M	-	-	1%	.1%	.1%	1%	1%	5%	-	-
	1	-	-	-	-	-	-	5%	-	-	-
	3	-	-	5%	.1%	.1%	.1%	1%	-	-	-
 30 dB	M	-	-	2%	.1%	.1%	1%	5%	5%	-	-
	1	-	-	-	-	-	2%	1%	-	-	-
	3	-	-	-	.1%	1%	1%	1%	-	-	-
 20 dB	M	-	-	-	1%	2%	5%	-	-	-	-
	1	-	-	-	5%	5%	-	-	-	-	-
	3	-	-	-	5%	-	-	-	-	-	-
 10 dB	M	-	-	-	-	-	-	-	-	-	-
	1	5%	-	-	-	-	-	-	-	-	-
	3	1%	-	-	-	-	-	-	-	-	-

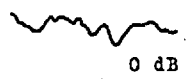
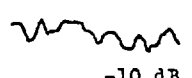

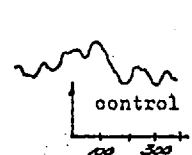
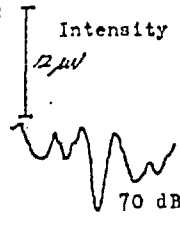
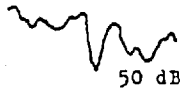
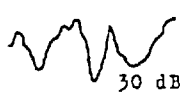


Intensity <i>12 μV</i>	Test	Harmonics									
		1	2	3	4	5	6	7	8	9	10
 0 dB	M	-	-	-	-	-	-	-	-	-	-
	1	-	-	-	-	-	-	-	-	-	-
	3	-	-	-	-	-	-	-	-	-	-
 -10 dB	M	-	-	-	-	-	-	-	-	-	-
	1	5%	-	-	-	-	-	-	-	-	-
	3	-	-	-	-	-	-	-	-	-	-
 control	M	-	-	-	-	-	-	-	-	-	-
	1	-	-	-	-	-	-	-	-	-	-
	3	5%	-	1%	-	-	-	-	-	-	-
 control	M	-	-	-	-	-	-	-	-	-	-
	1	-	-	-	-	-	-	-	-	-	-
	3	-	2%	-	-	-	-	-	-	-	-

Table 4-x1. Subject VM, F, age 24, at 1 kHz.

Intensity <i>12 μV</i>	Test	Harmonics									
		1	2	3	4	5	6	7	8	9	10
 70 dB	M	-	-	-	1%	.1%	.1%	-	-	5%	-
	1	-	-	-	-	1%	.1%	-	-	-	-
	3	-	-	-	1%	.1%	.1%	-	-	-	-
 50 dB	M	-	-	-	1%	.1%	.1%	.1%	-	5%	-
	1	-	-	-	-	-	-	-	-	-	-
	3	-	-	-	5%	.1%	.1%	1%	-	1%	-
 30 dB	M	-	-	5%	5%	1%	2%	1%	-	-	-
	1	-	5%	-	-	-	-	-	-	-	-
	3	-	5%	5%	-	1%	-	2%	-	-	-
 20 dB	M	-	-	-	-	-	-	-	2%	5%	-
	1	-	-	5%	-	-	-	-	-	-	-
	3	-	-	-	-	-	-	5%	-	-	-
 10 dB	M	-	-	-	-	-	-	-	-	-	-
	1	-	-	-	-	-	-	-	-	-	-
	3	-	-	-	-	-	-	-	-	-	-

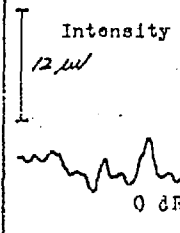



Intensity <i>12 μV</i>	Test	Harmonics									
		1	2	3	4	5	6	7	8	9	10
 0 dB	M	-	-	-	-	-	-	-	-	1%	-
	1	-	-	-	-	-	-	-	-	-	-
	3	-	-	-	-	-	-	-	-	1%	-
 -10 dB	M	-	-	-	-	-	-	-	-	-	-
	1	-	-	-	-	-	-	-	-	-	-
	3	-	-	-	-	-	-	-	-	-	-
 control	M	-	-	-	-	-	-	-	-	-	5%
	1	-	-	-	-	-	-	-	2%	-	2%
	3	-	-	-	-	-	-	-	2%	-	5%
 control	M	-	-	-	-	-	-	-	-	-	-
	1	-	-	-	-	-	-	-	-	-	-
	3	-	-	-	-	-	-	-	-	-	-

Table 4-x11. Subject SBa, F, age 20, at 2 kHz.

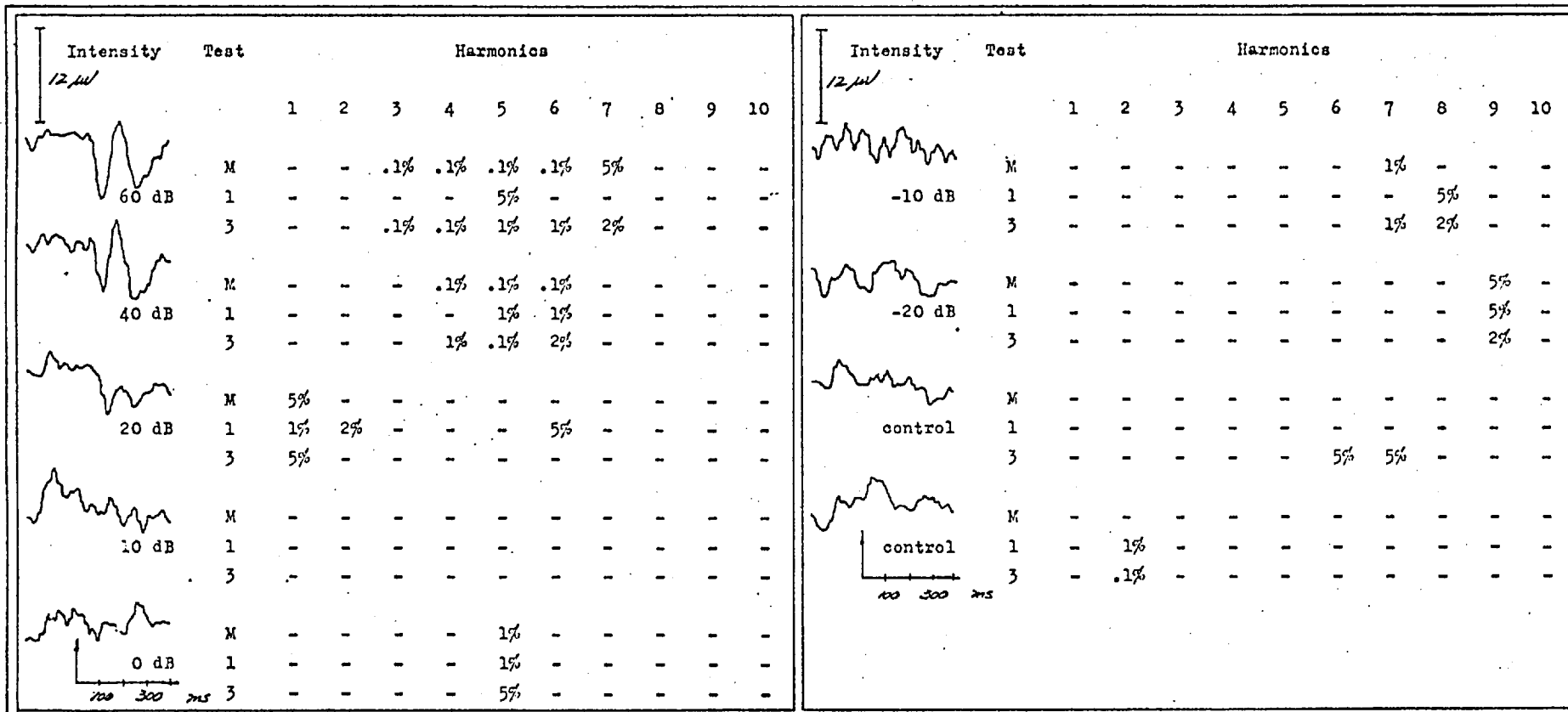


Table 4-xlii. Subject SBA, F, age 20, at 500 Hz.

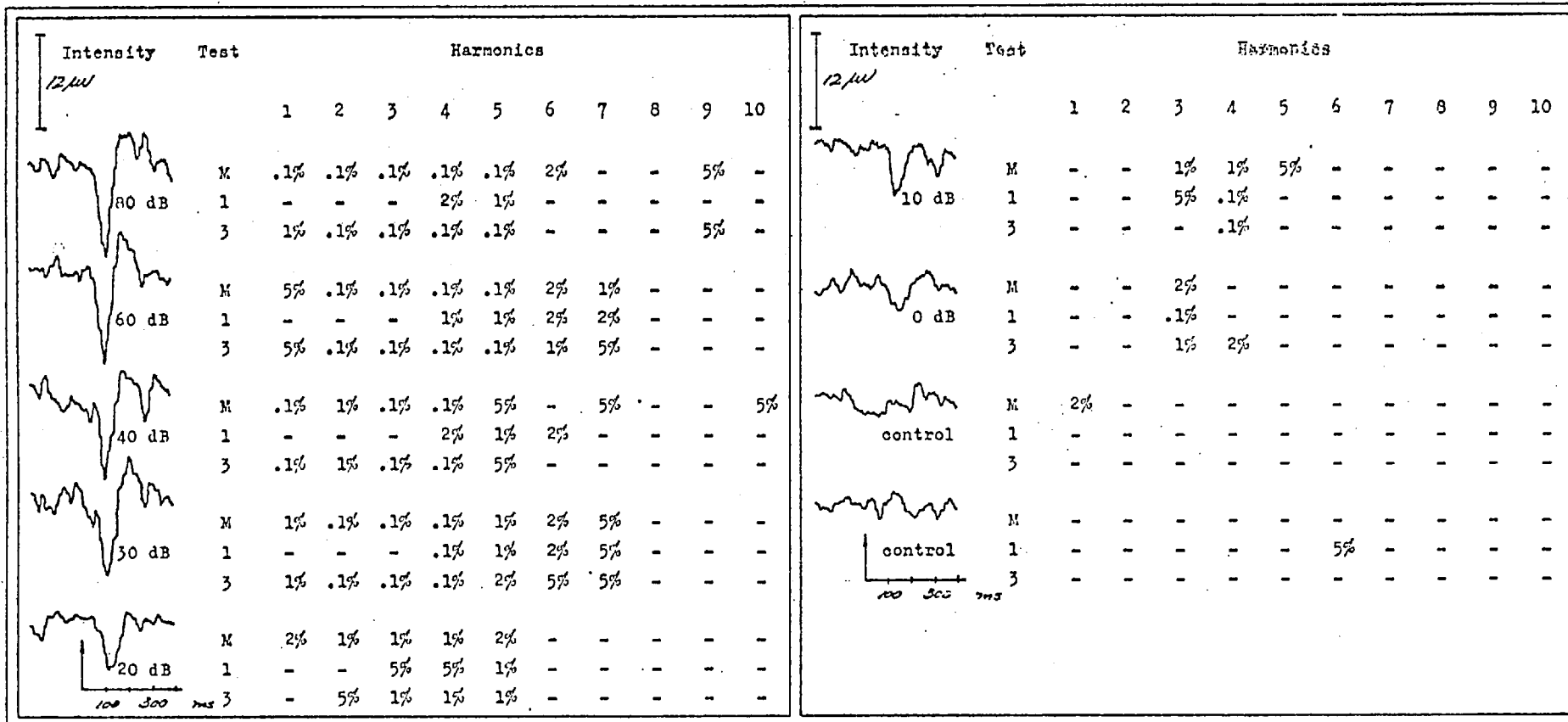


Table 4-xliiii. Subject SA, M, age 20, at 2 kHz.



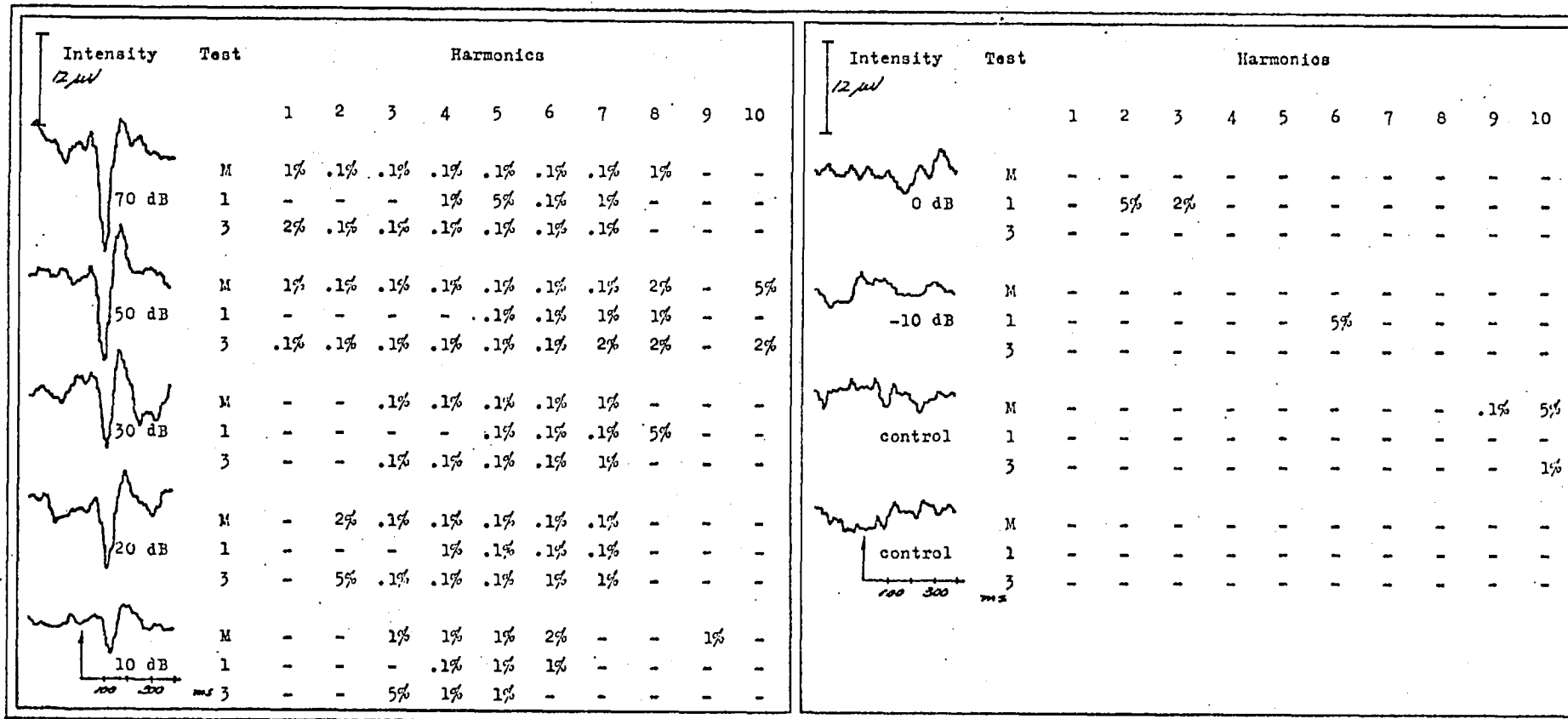


Table 4-xliv. Subject SA, M, age 28, at 500 Hz.

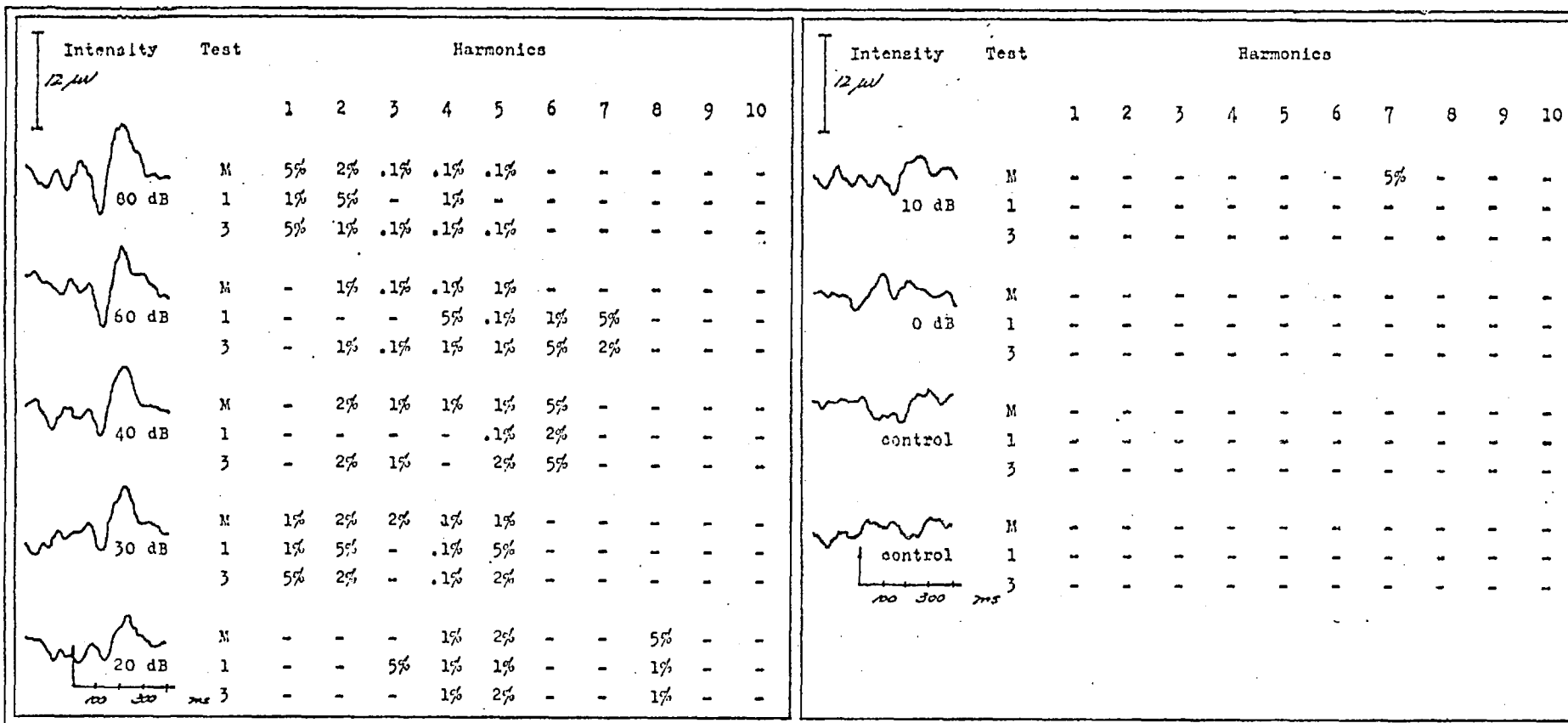


Table 4-xlv. Subject PC, M, age 24, at 4 kHz.

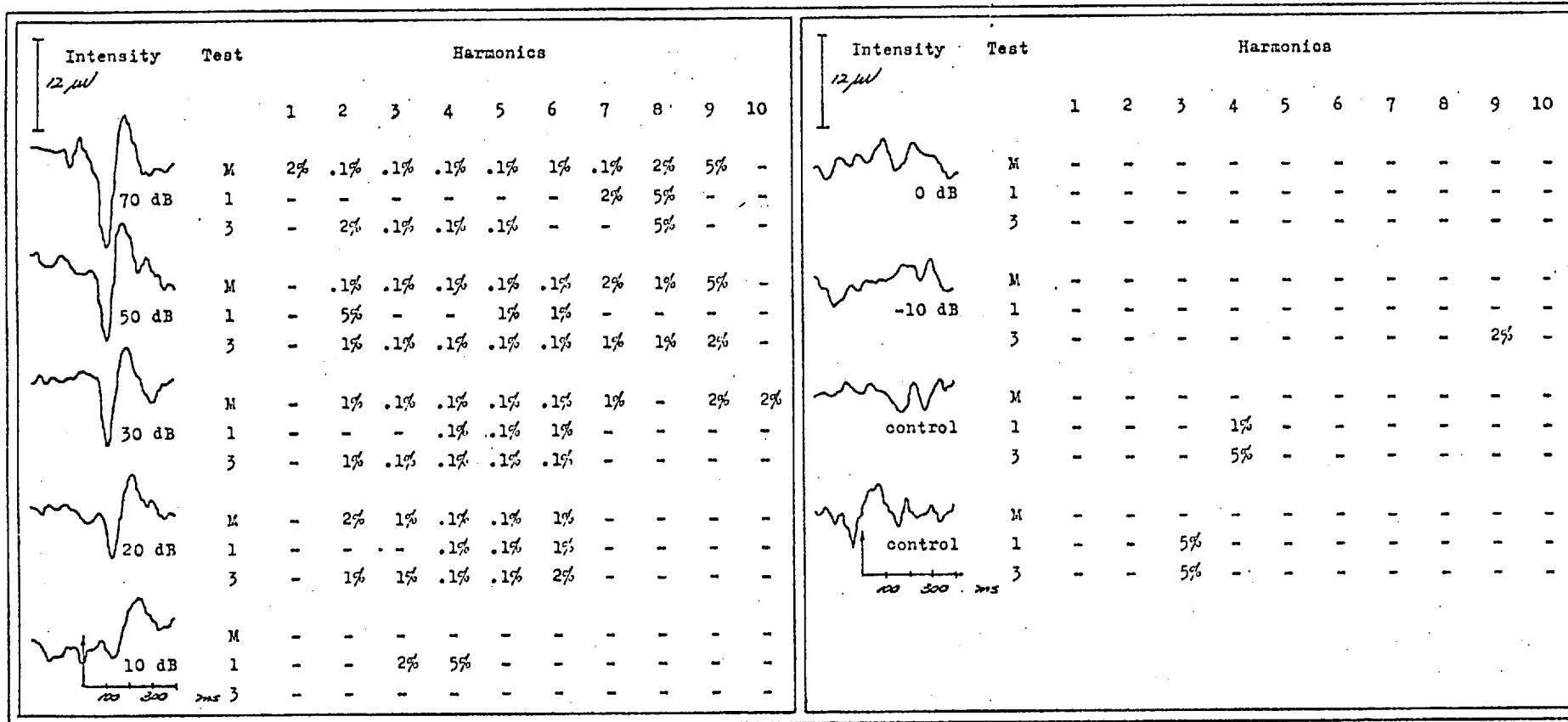


Table 4-xlvi. Subject PC, M, age 24, at 1 kHz.

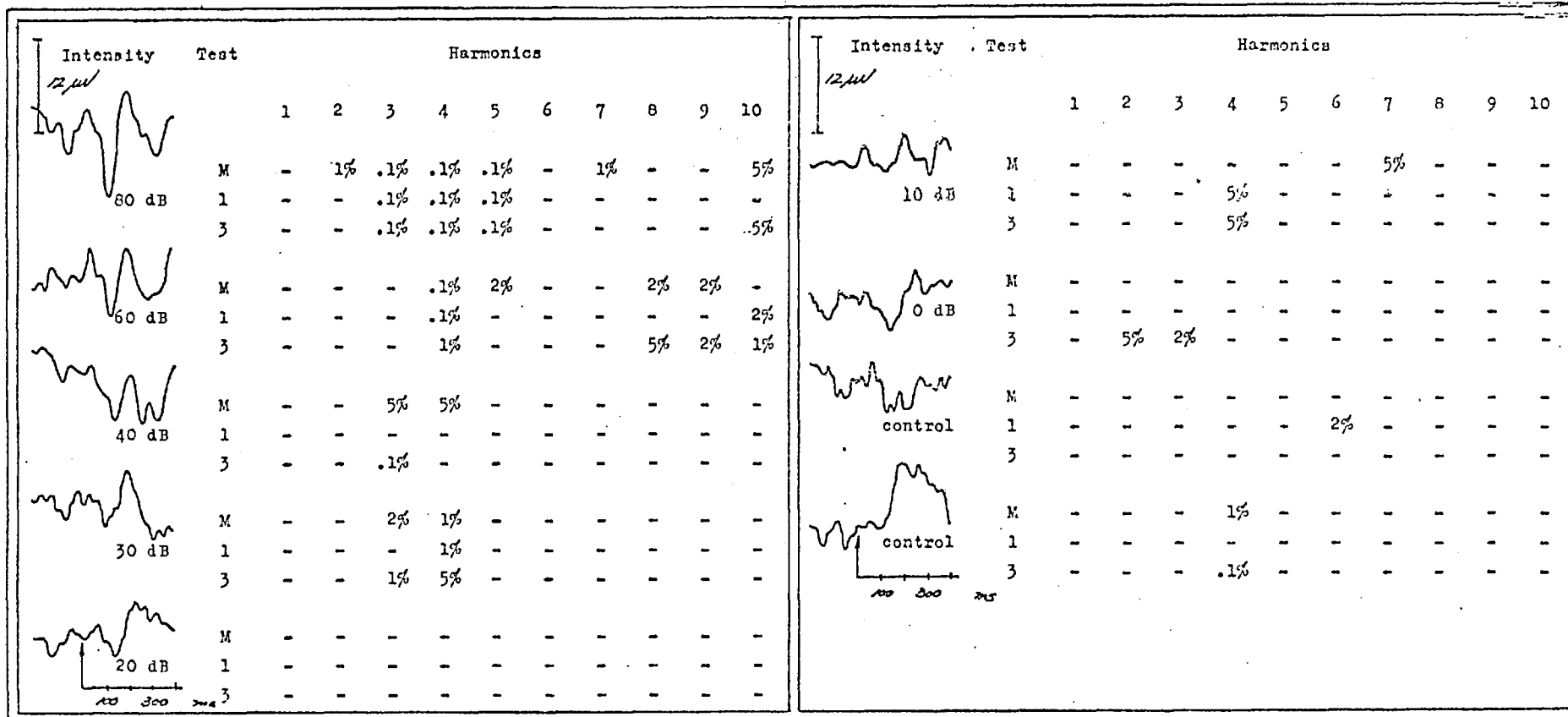


Table 4-xlvii. Subject DP, F, age 20, at 2 kHz.

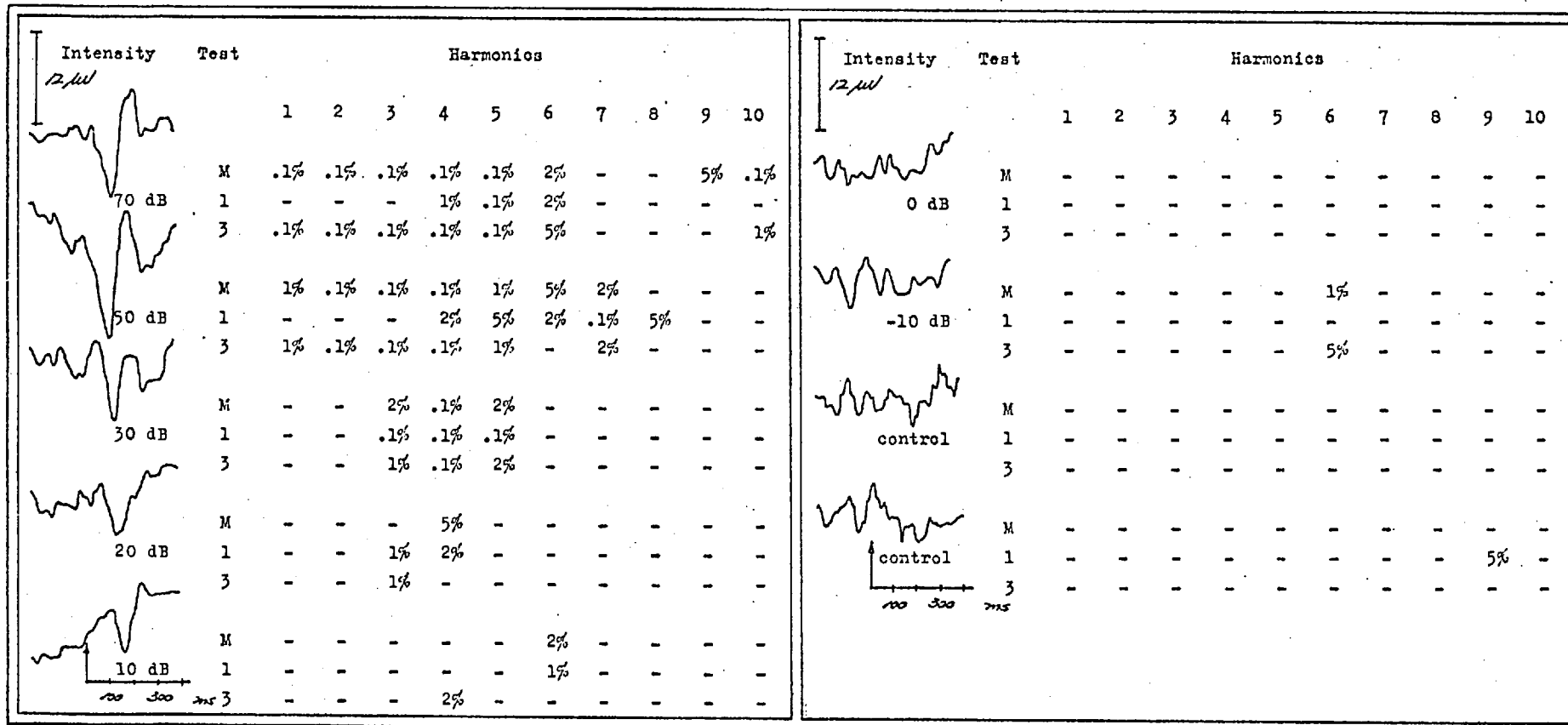


Table 4-xlviii. Subject DF, F, age 20, at 500 Hz.

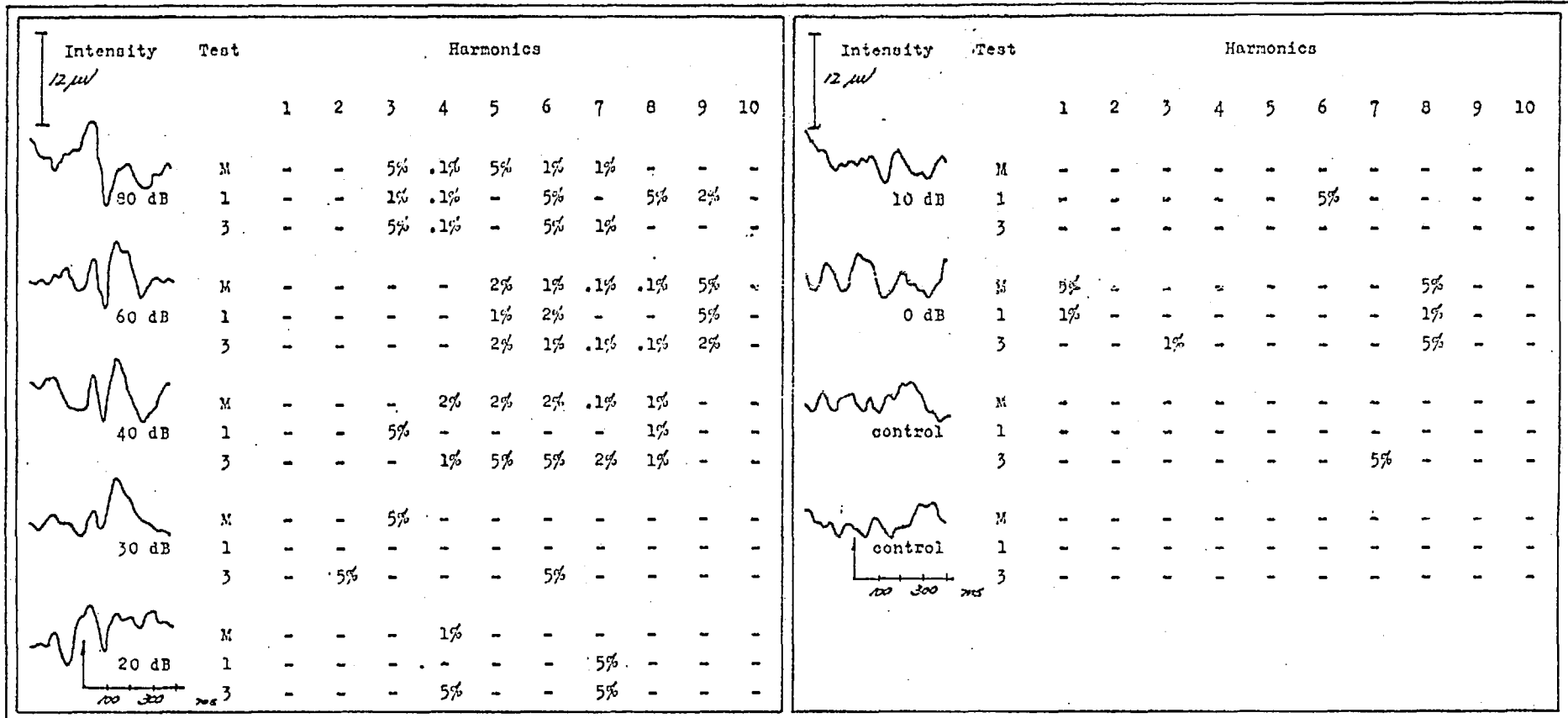


Table 4-xlix. Subject LS, F, age 20, at 4 kHz.

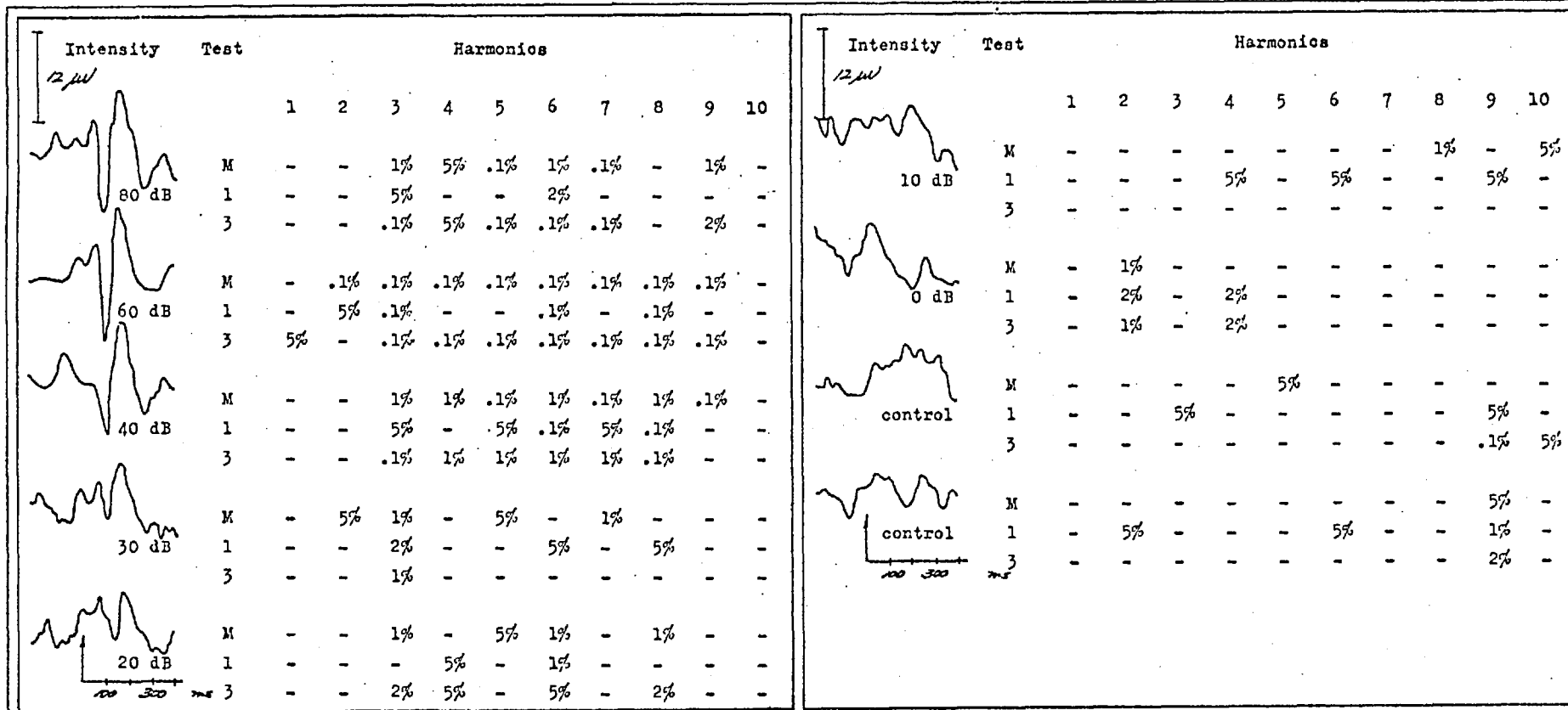


Table 4-1. Subject LS, F, age 20, at 1 kHz.

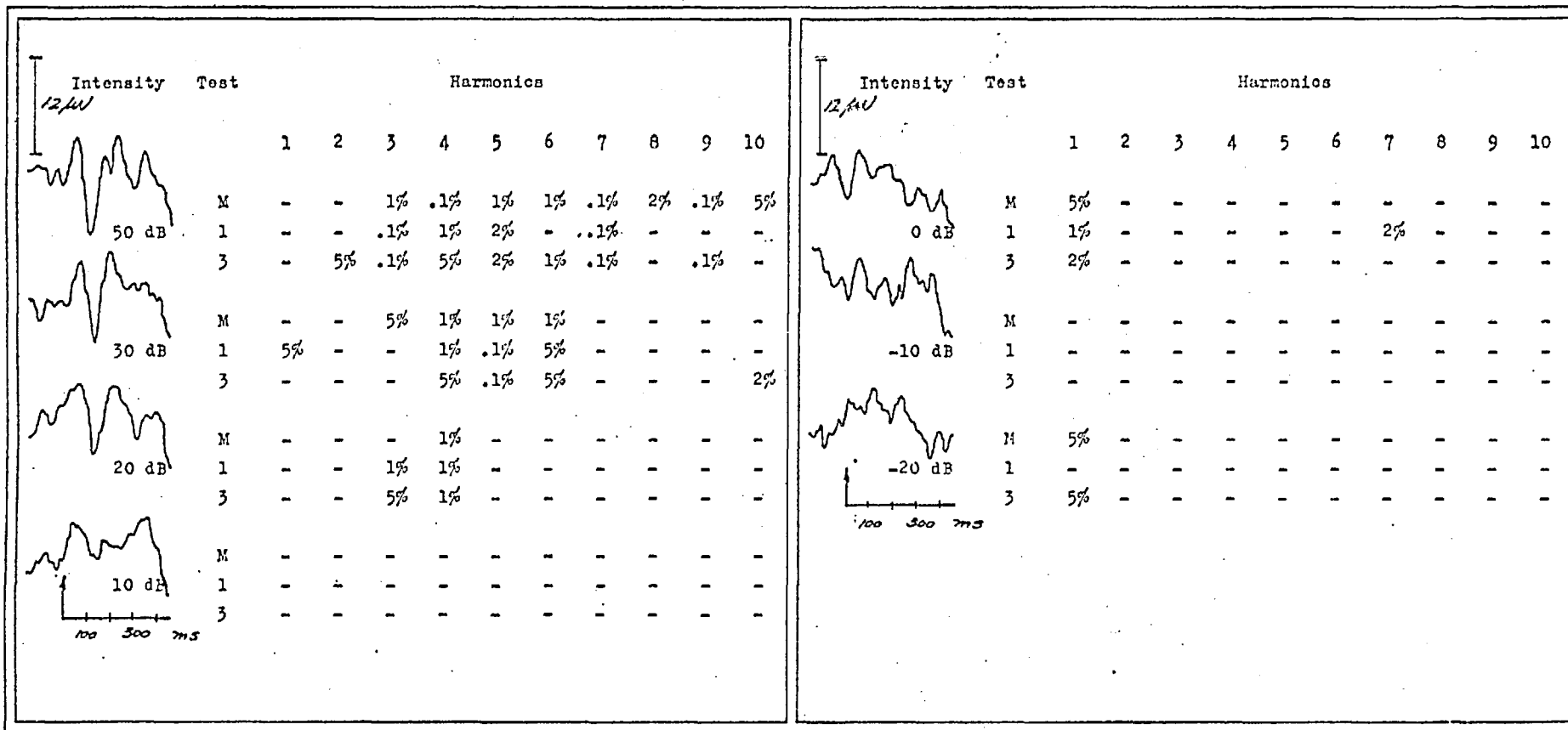


Table 4-11. Subject GP, M, age 18, at 500 Hz.



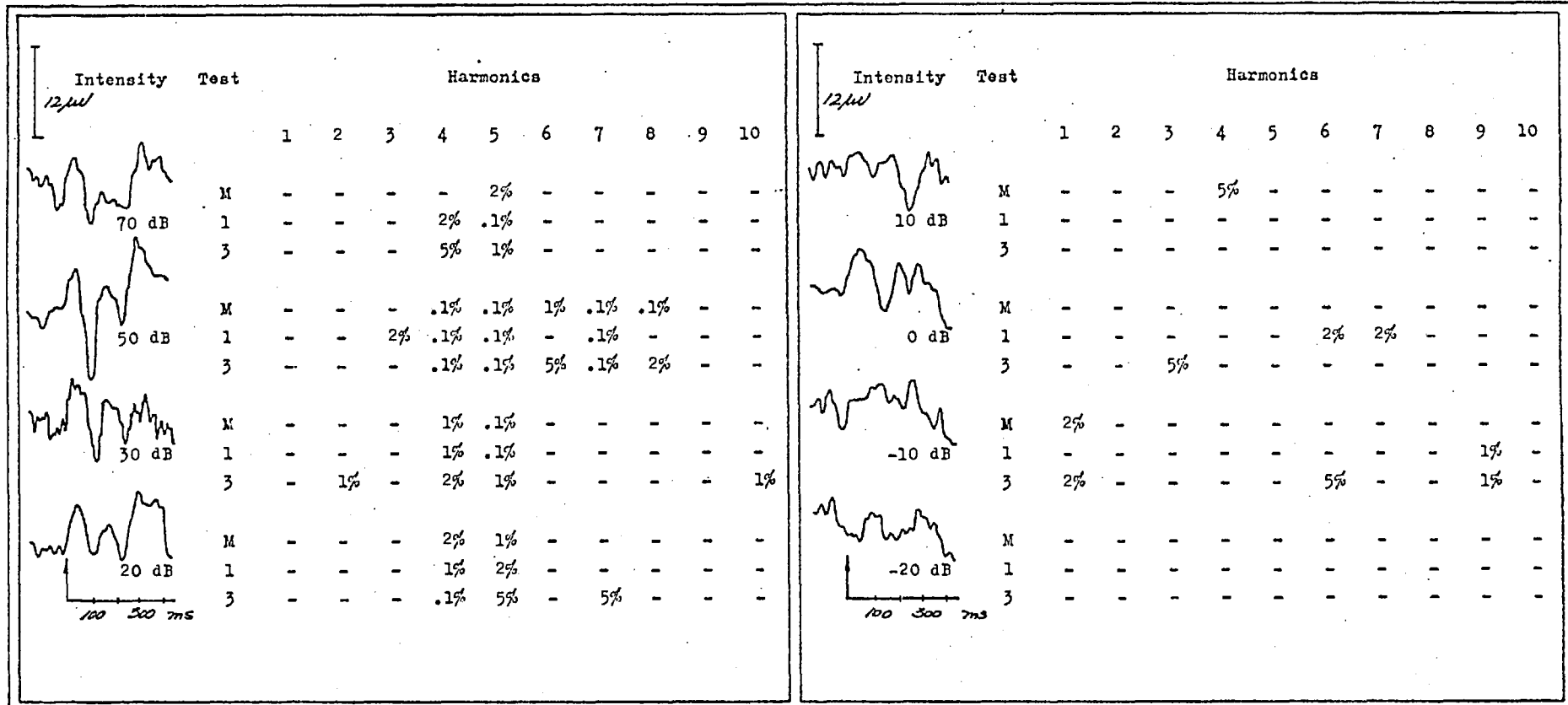

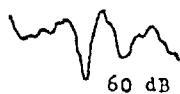
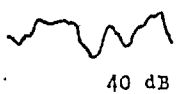
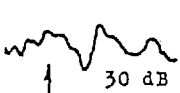


Table 4-111. Subject EB, F, age 18, at 1 kHz.

Intensity <i>12 μV</i>	Test	Harmonics									
		1	2	3	4	5	6	7	8	9	10
 80 dB	M	-	1%	.1%	.1%	.1%	-	-	-	-	1%
	1	-	2%	.1%	.1%	.1%	-	-	-	-	2%
	3	-	-	.1%	.1%	.1%	-	-	-	-	1%
 60 dB	M	-	-	.1%	.1%	.1%	.1%	-	2%	-	-
	1	-	-	1%	.1%	.1%	2%	-	-	-	-
	3	-	-	1%	.1%	.1%	5%	-	1%	-	-
 40 dB	M	5%	5%	-	1%	2%	-	-	-	-	-
	1	-	-	-	-	-	-	-	-	-	-
	3	5%	5%	-	5%	1%	-	-	-	-	-
 30 dB	M	-	-	.1%	1%	2%	-	-	-	-	-
	1	-	-	.1%	1%	.1%	-	-	-	-	-
	3	-	-	1%	1%	1%	-	-	-	-	-
<i>100 300 ms</i>											


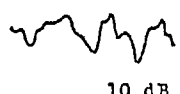

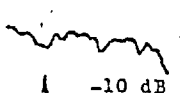
Intensity <i>12 μV</i>	Test	Harmonics									
		1	2	3	4	5	6	7	8	9	10
 20 dB	M	-	-	.1%	1%	2%	1%	-	-	-	1%
	1	-	-	.1%	.1%	1%	5%	-	-	-	-
	3	-	-	1%	.1%	1%	-	-	-	-	1%
 10 dB	M	-	-	-	-	-	-	-	-	-	-
	1	-	-	-	-	-	-	-	-	-	-
	3	-	-	-	-	-	-	-	5%	-	-
 0 dB	M	-	5%	5%	1%	-	-	-	-	-	5%
	1	-	-	2%	.1%	-	-	-	-	-	-
	3	-	5%	-	1%	-	-	-	-	-	1%
 -10 dB	M	-	-	-	-	-	-	-	-	-	-
	1	-	-	-	-	-	-	-	-	-	-
	3	-	-	-	-	-	-	-	-	-	-
<i>100 300 ms</i>											

Table 4-1111. Subject SH, F, age 20, at 2 kHz.

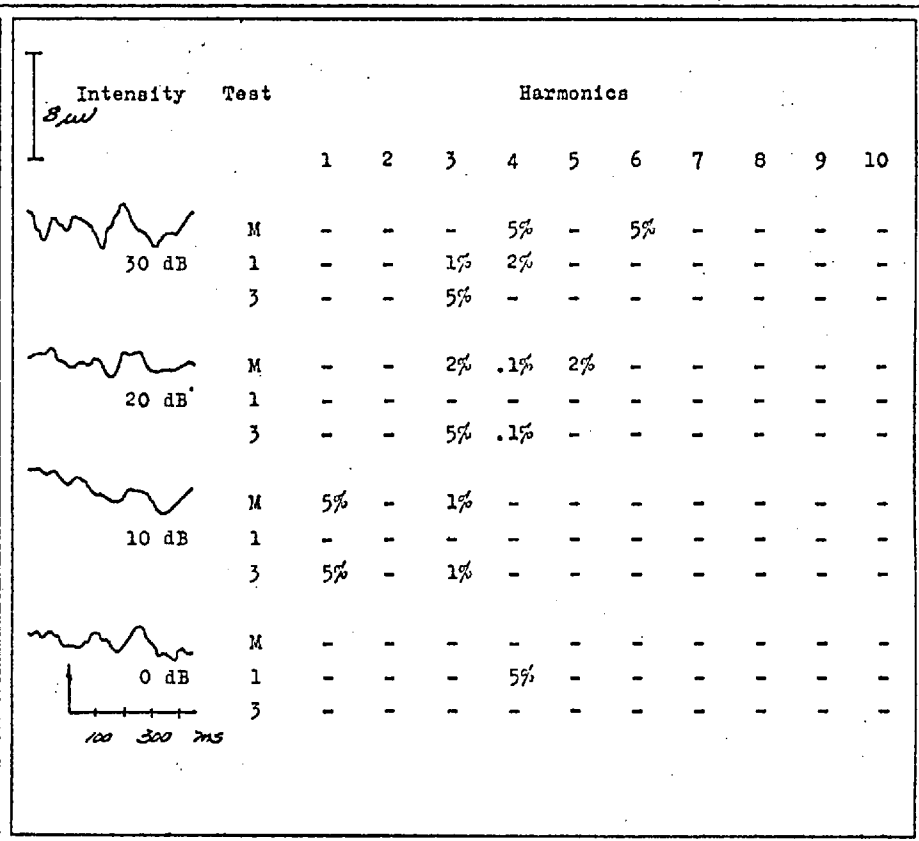
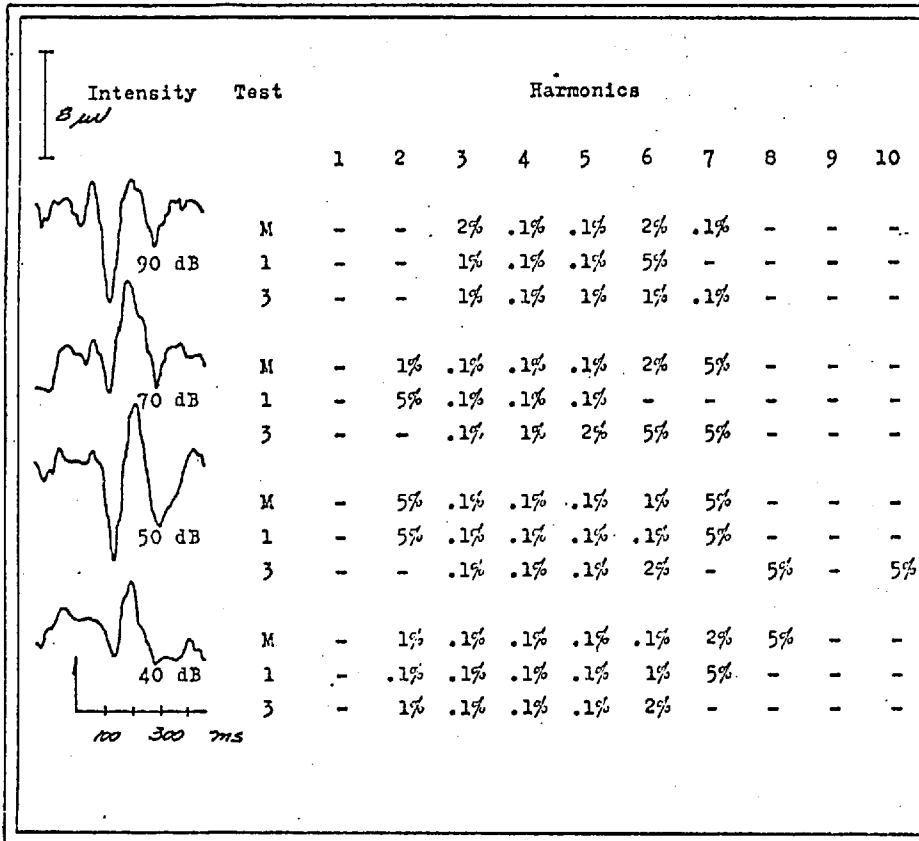


Table 4-11v. Subject RB, F, age 20, at 2 kHz.

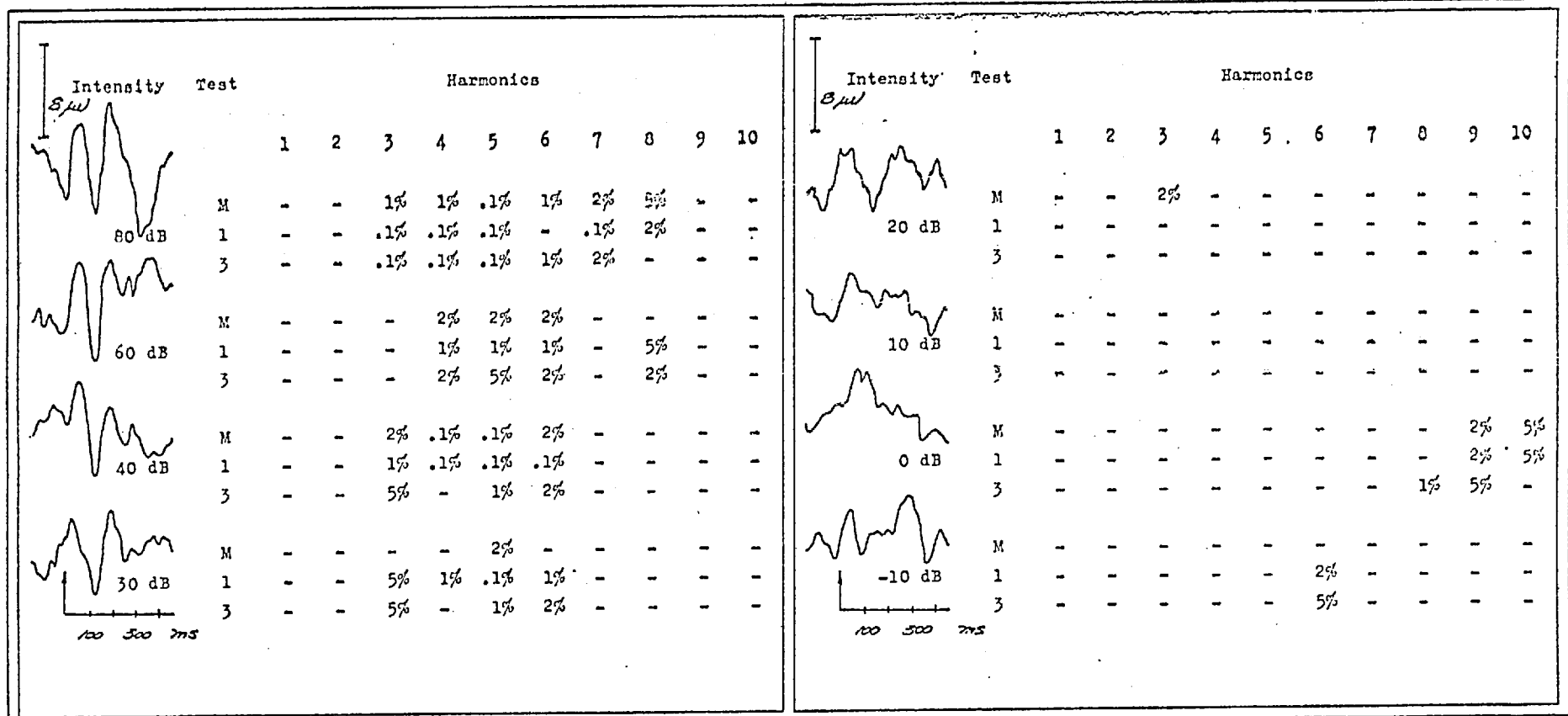


Table 4-1v. Subject AP, F, age 20, at 4 kHz.

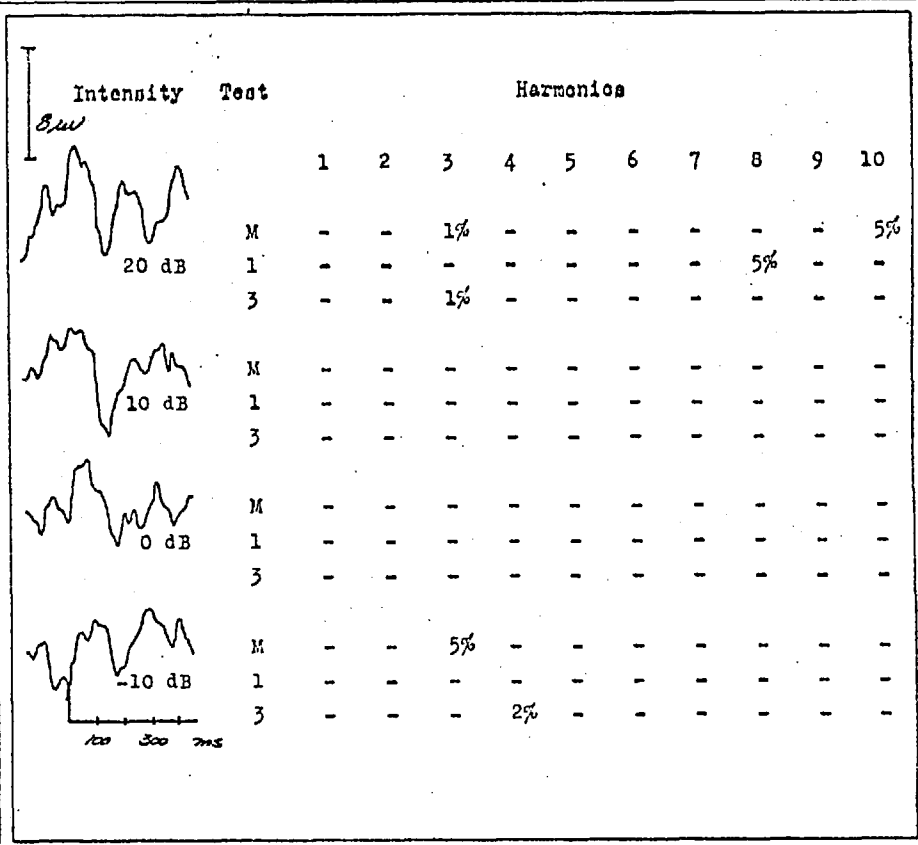
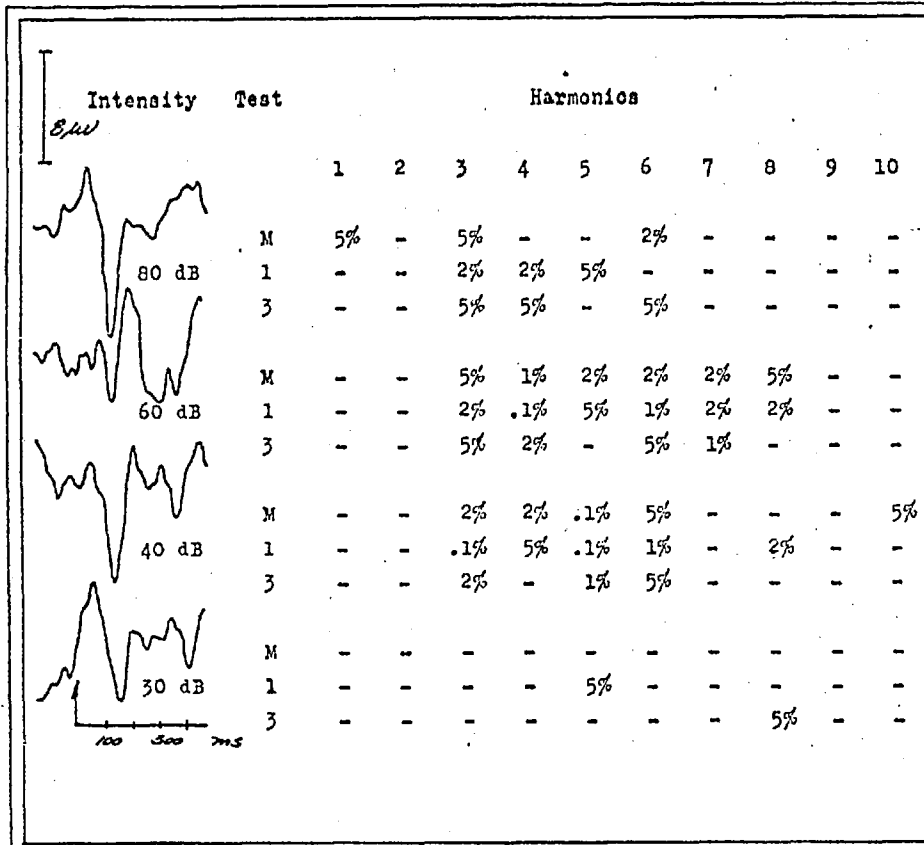


Table 4-lvi. Subject AP, F, age 20, at 1 kHz.

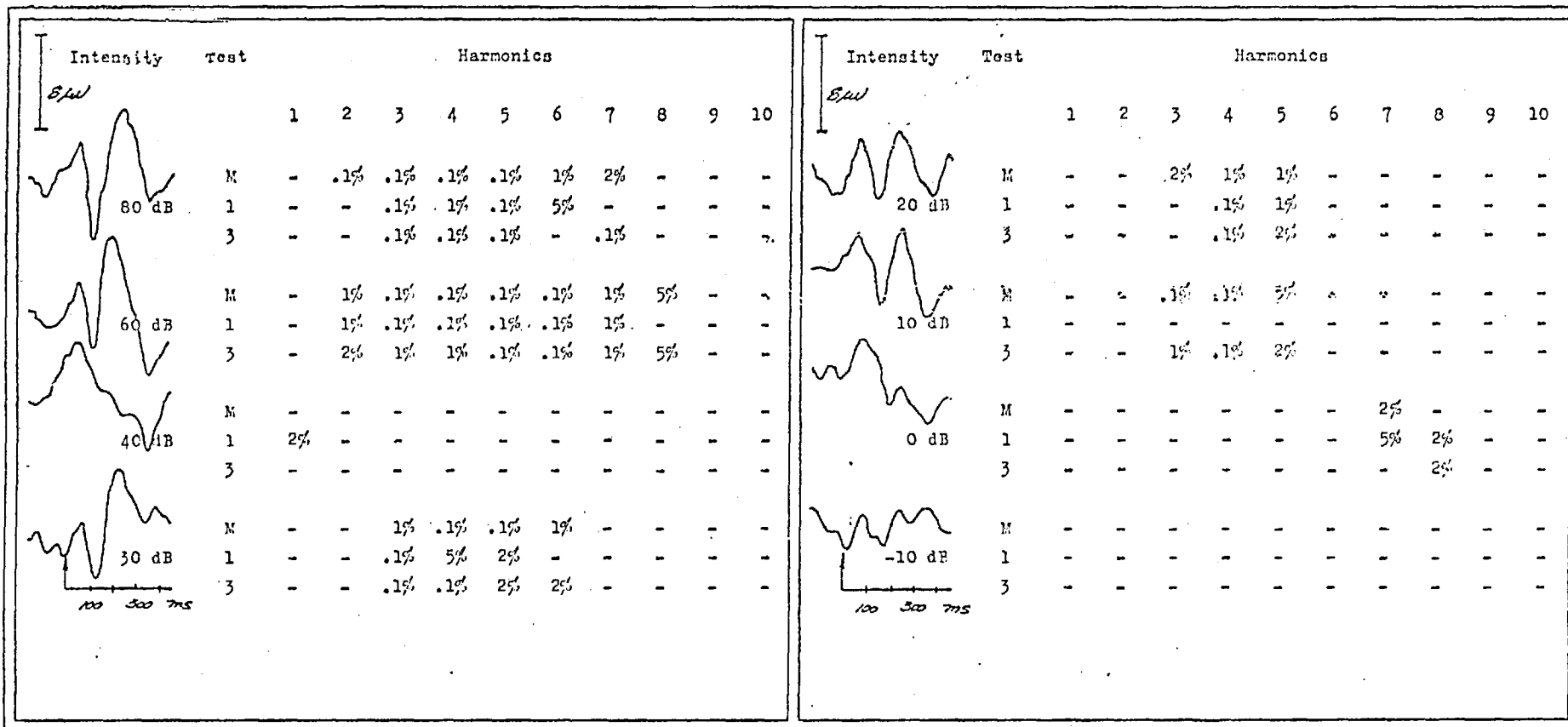


Table 4-lvii. Subject GD, F, age 19, at 2 kHz.

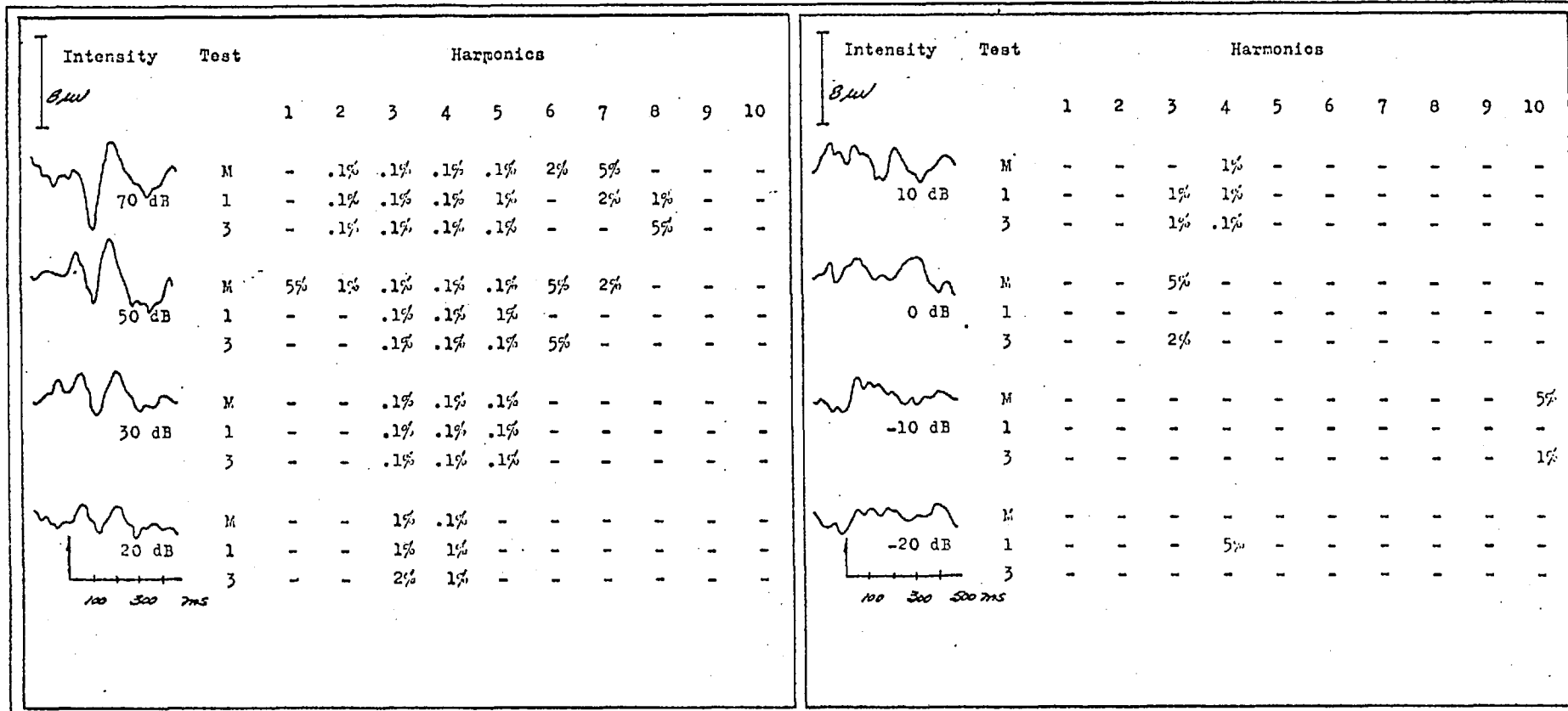


Table 4-lviii. Subject GD, F, age 19, at 500 Hz.

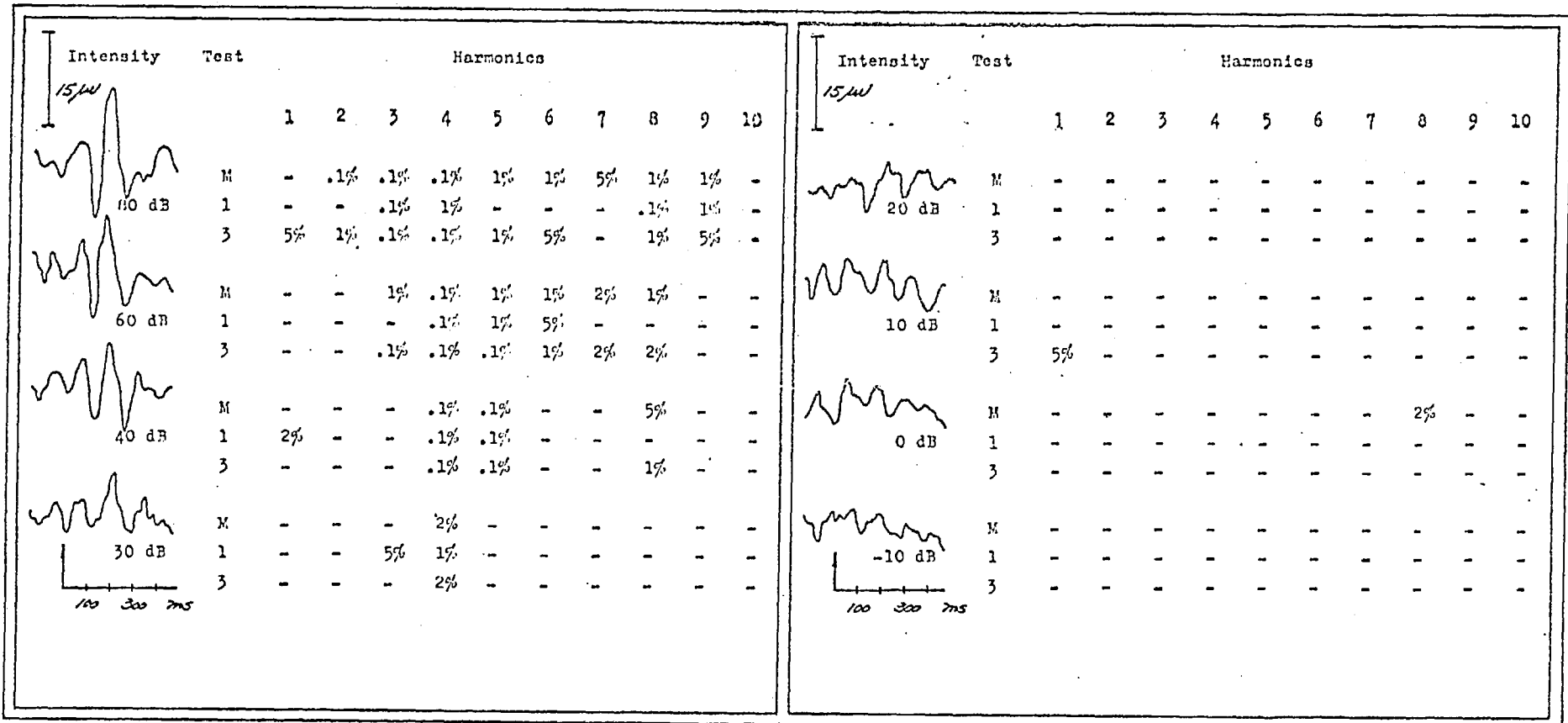


Table 4-lix. Subject KC, F, age 20, at 1 kHz.



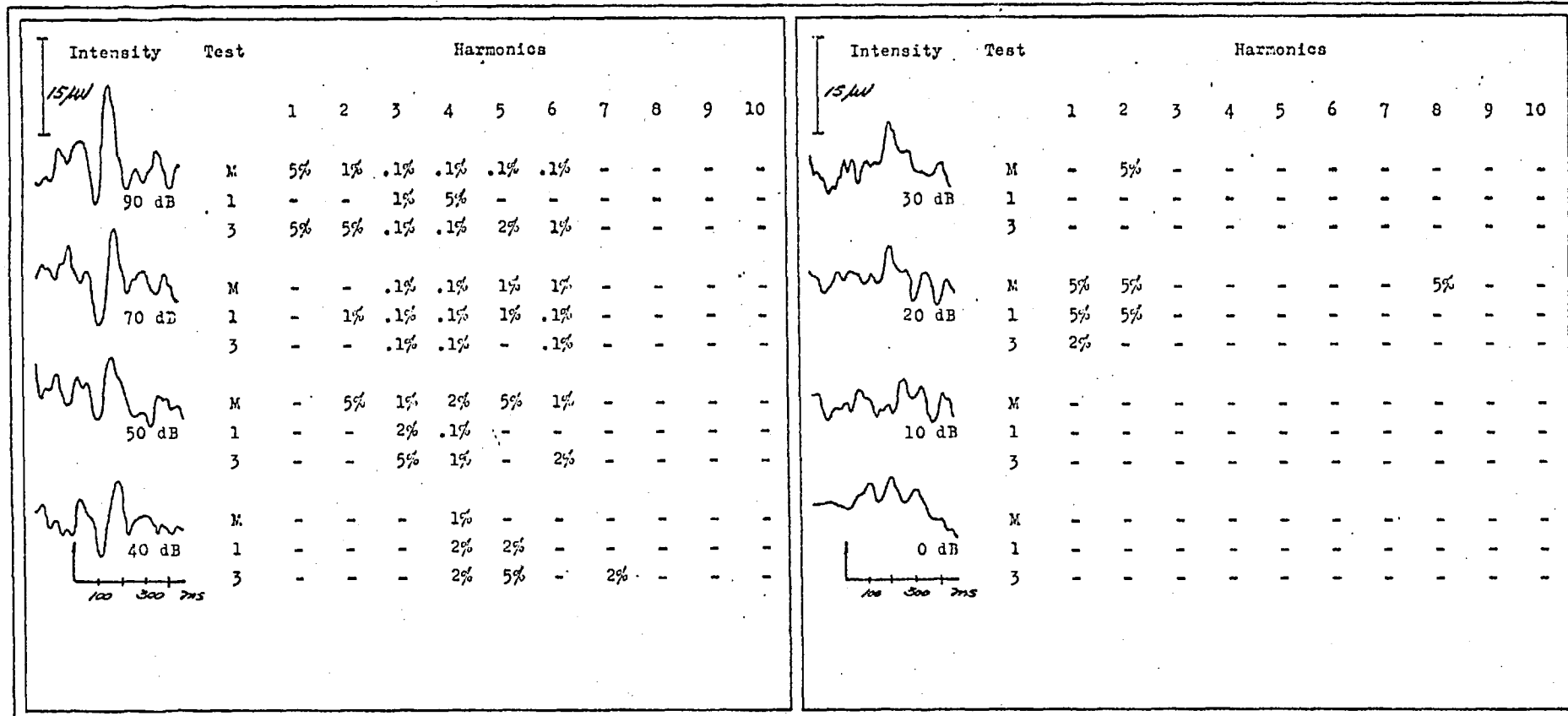


Table 4-1x. Subject KC, F, age 20, at 4 kHz.

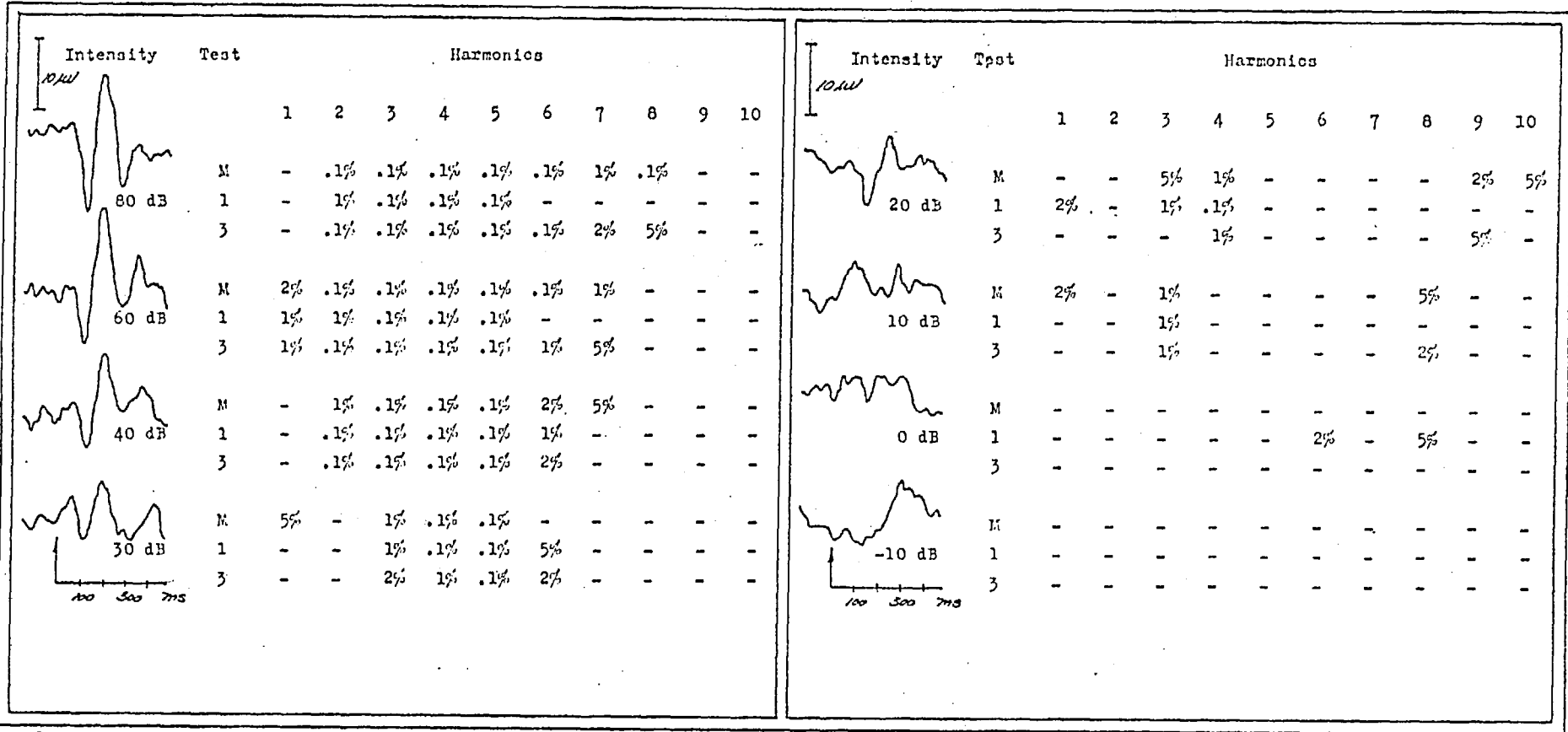


Table 4-1xi. Subject SC, F, age 22, at 2 kHz.

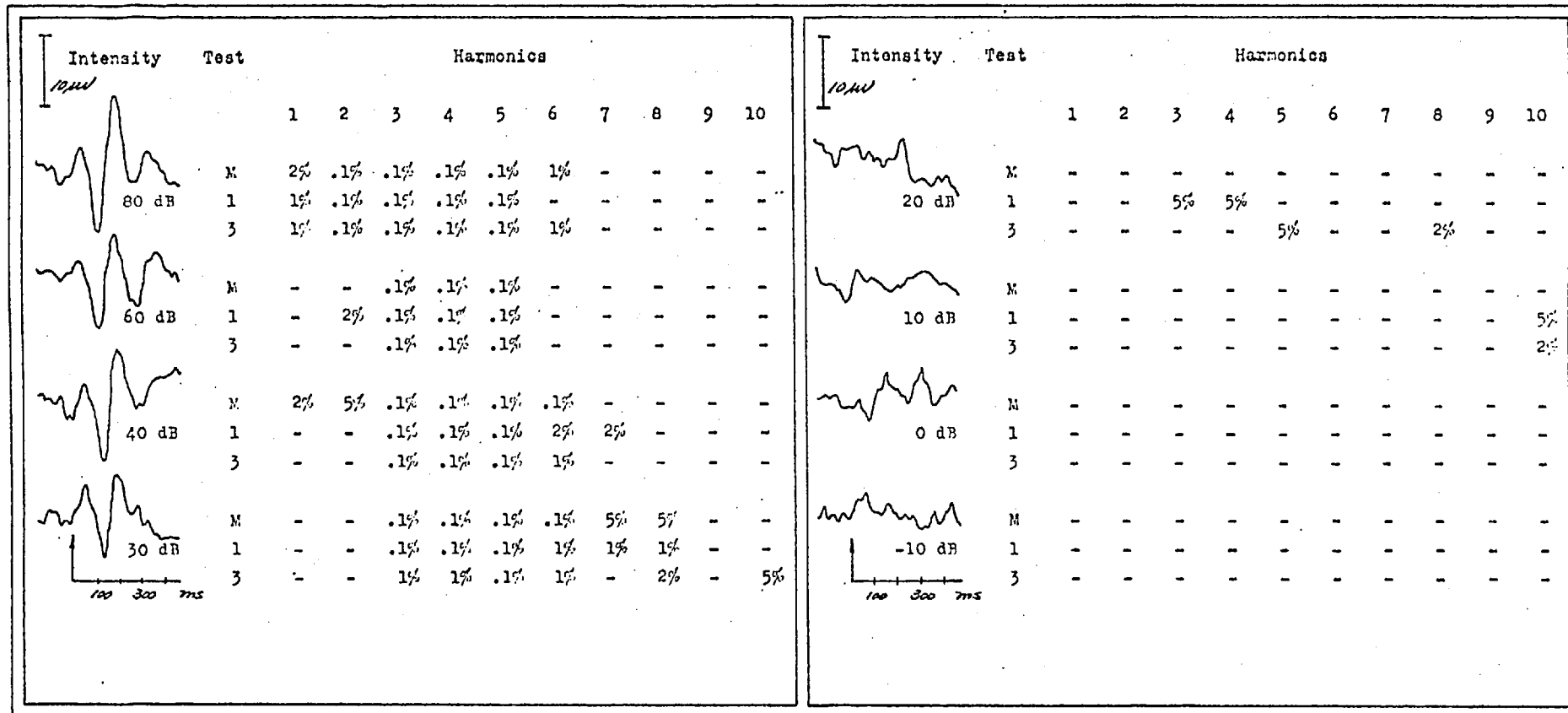


Table 4-lxii. Subject SC, F, age 22, at 500 Hz.

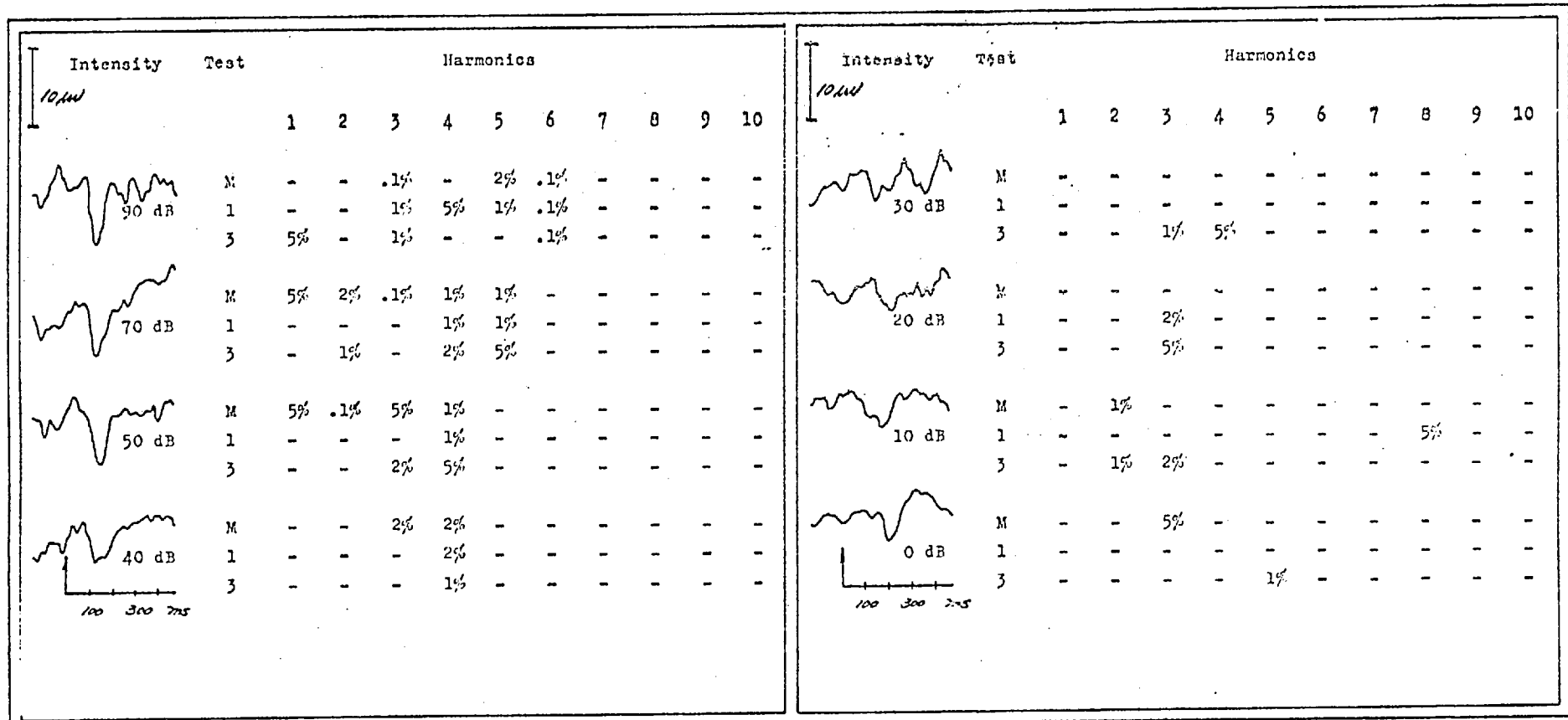


Table 4-1xiii. Subject AR, M, age 19, at 1 kHz.

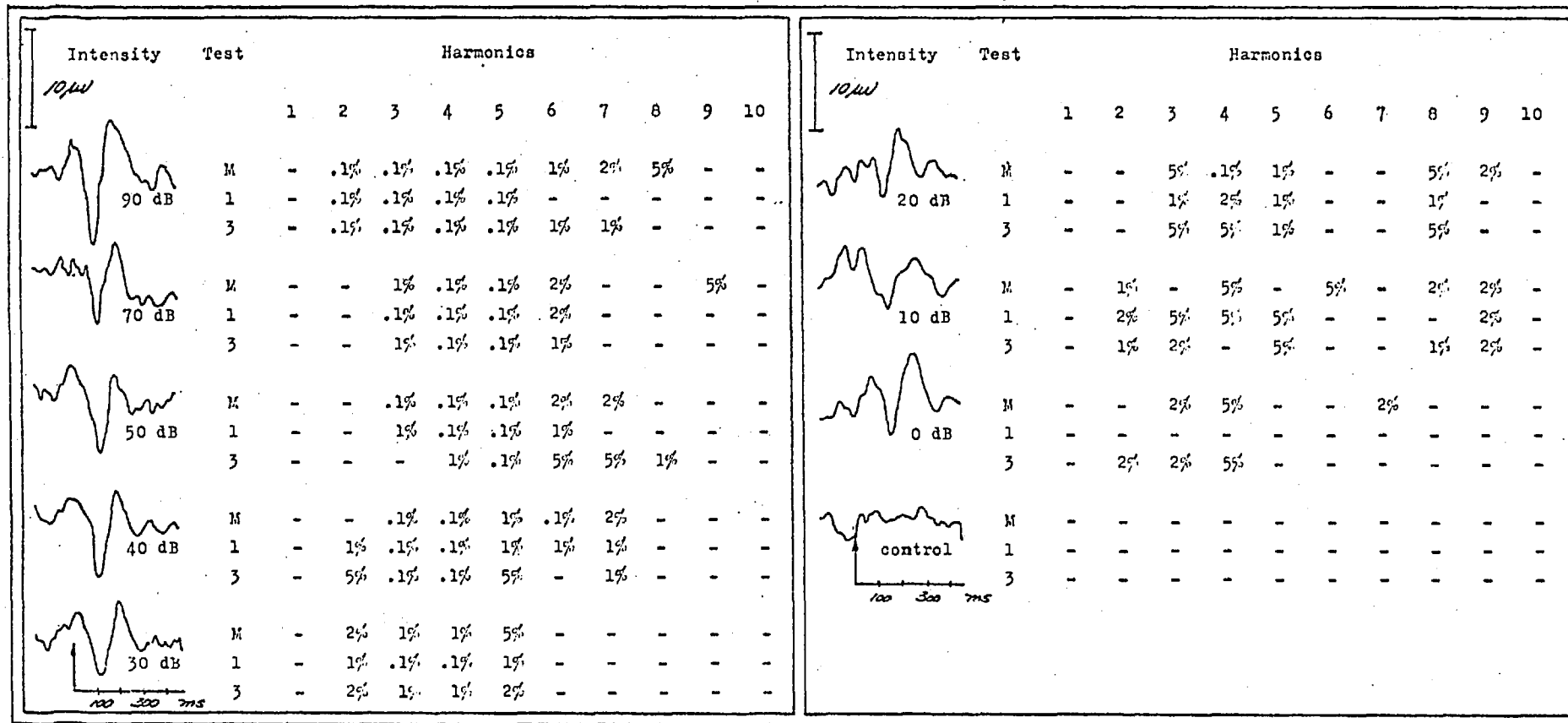


Table 4-lxiv Subject R.W., M, age 19, at 4 kHz.

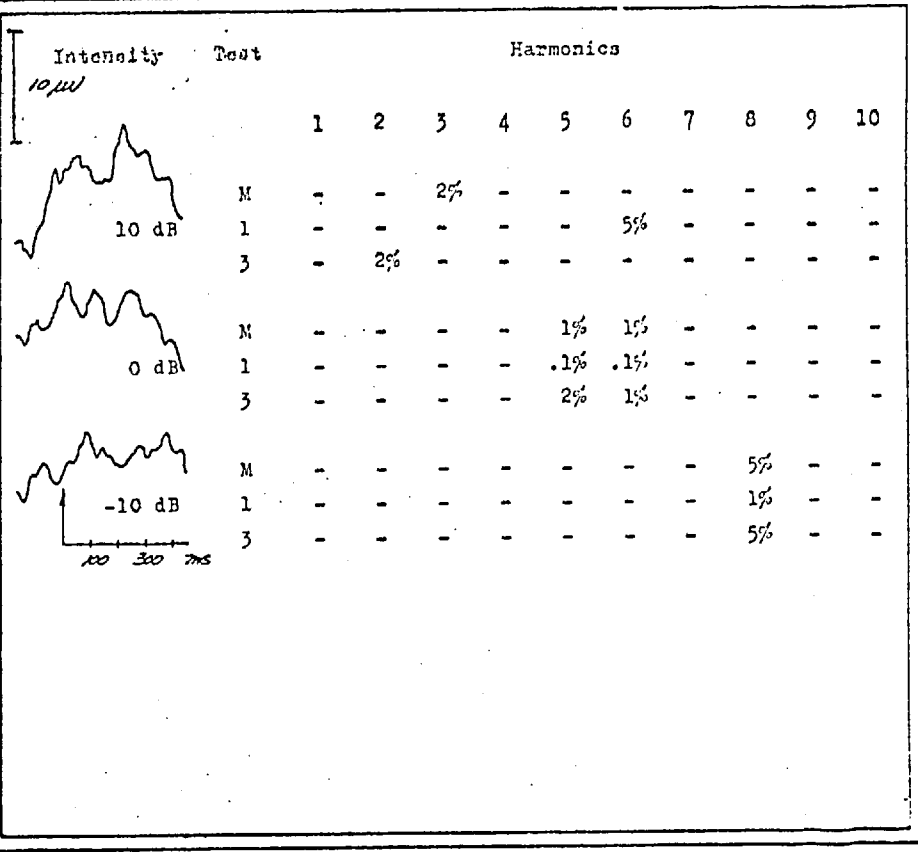
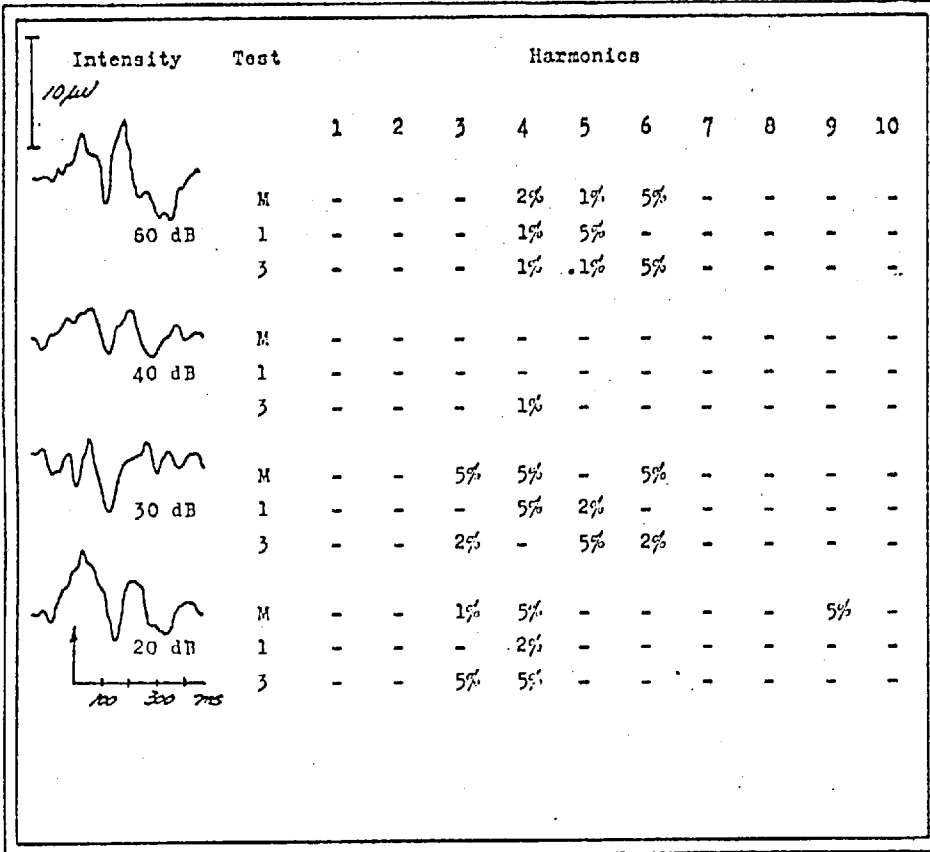


Table 4-lxv. Subject CK, F, age 19, at 2 kHz.

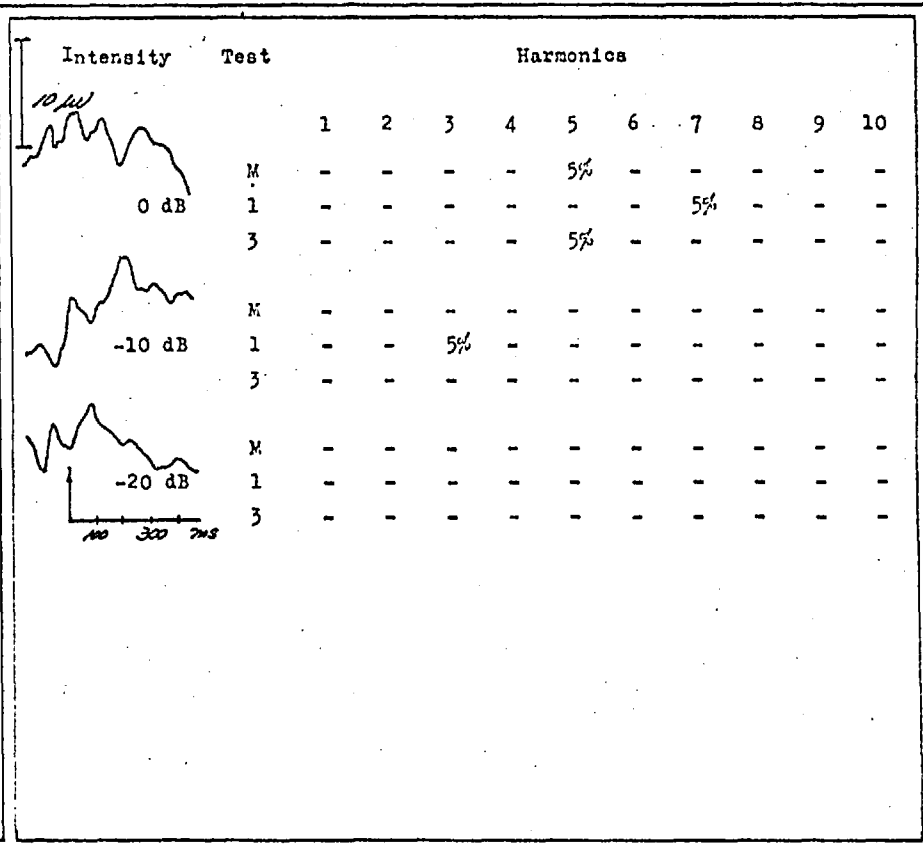
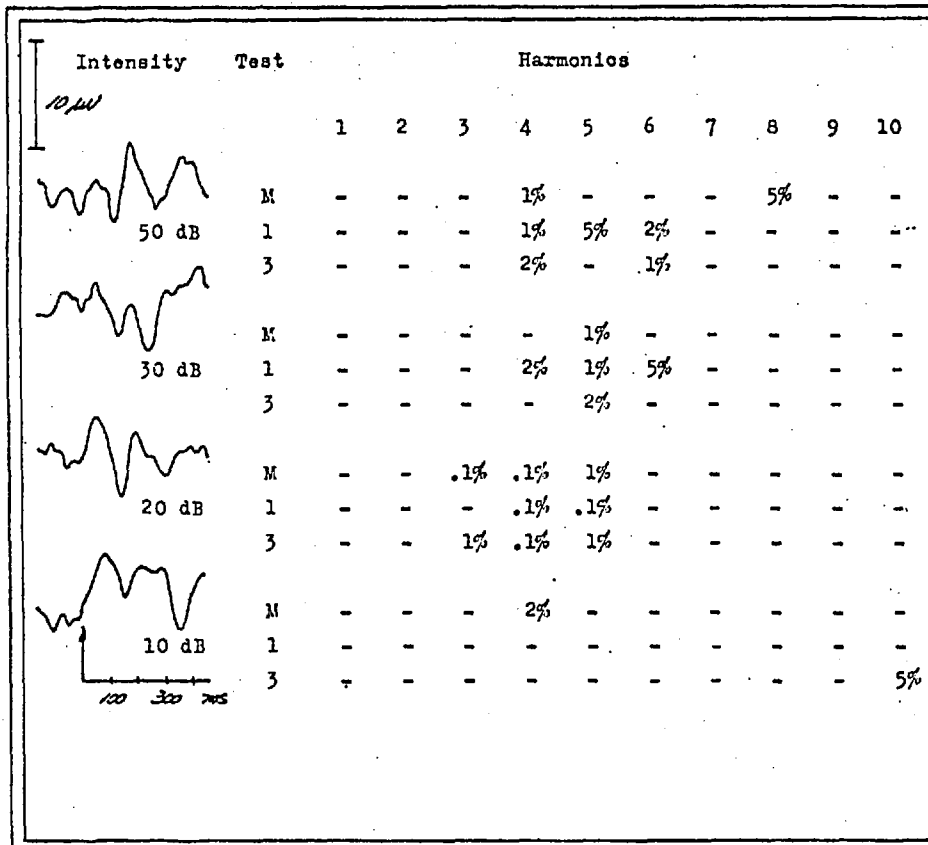


Table 4-lxvi. Subject CK, F, age 19, at 500 Hz.

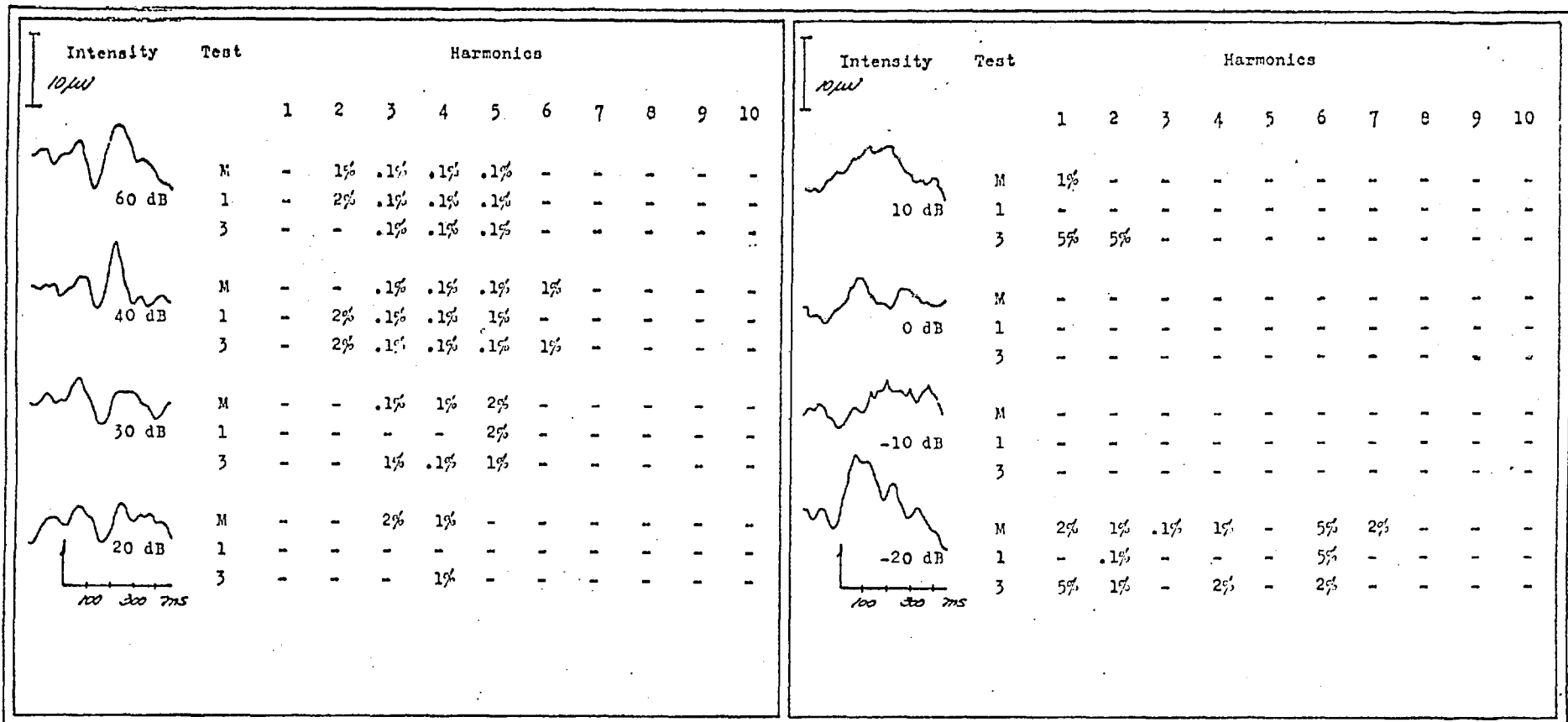


Table 4-lxvii. Subject SR, M, age 20, at 500 Hz.



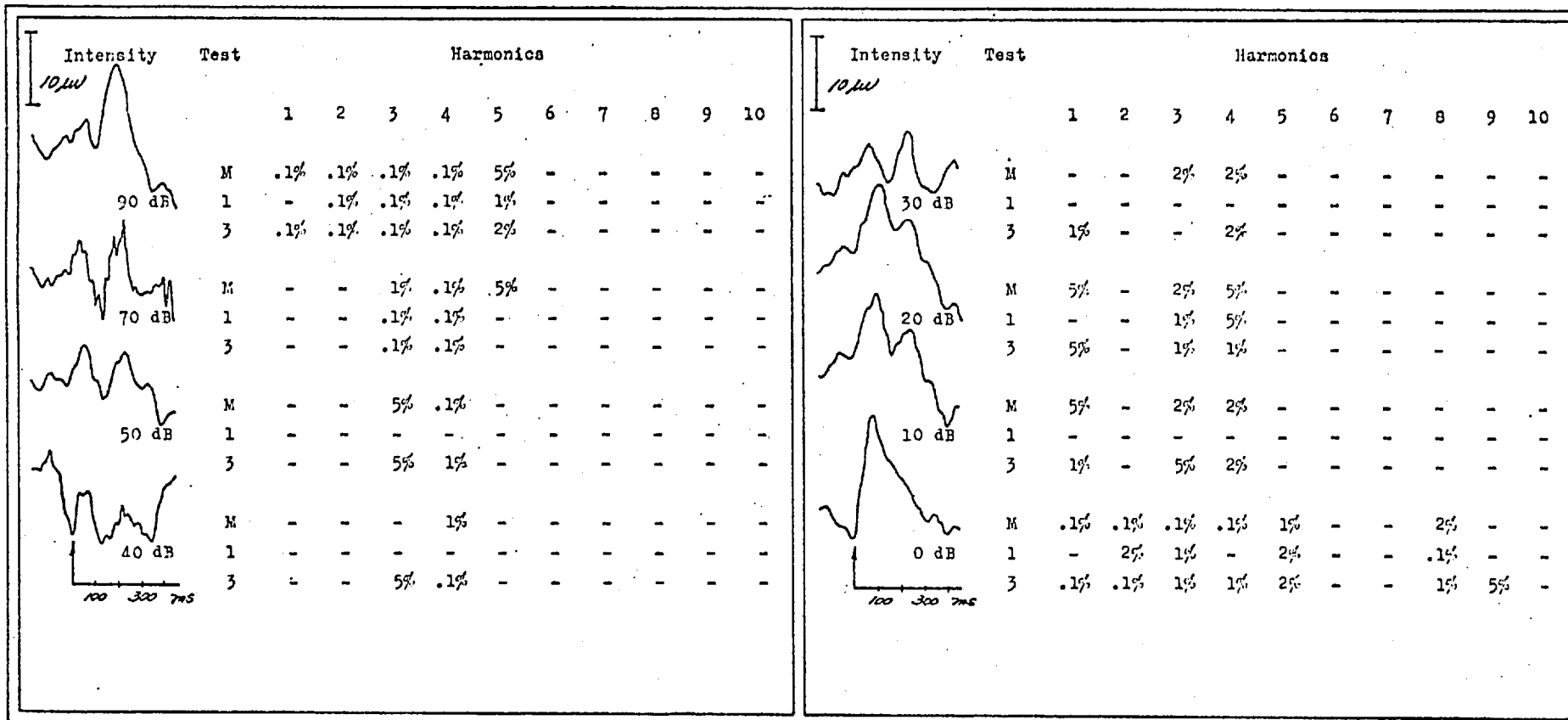


Table 4-lxviii. Subject SR, M, age 20, at 2 kHz.

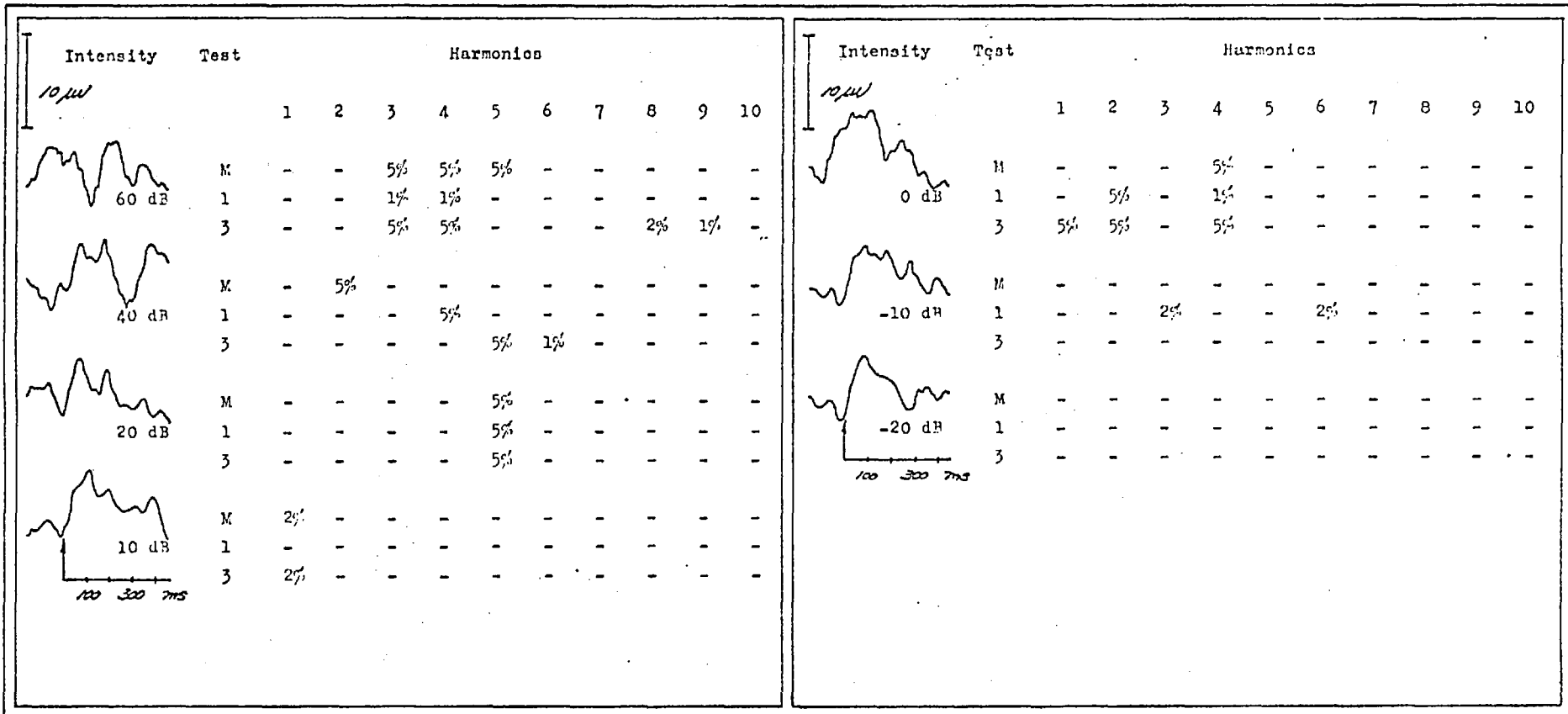


Table 4-lxix. Subject BS, F, age 23, at 4 kHz.

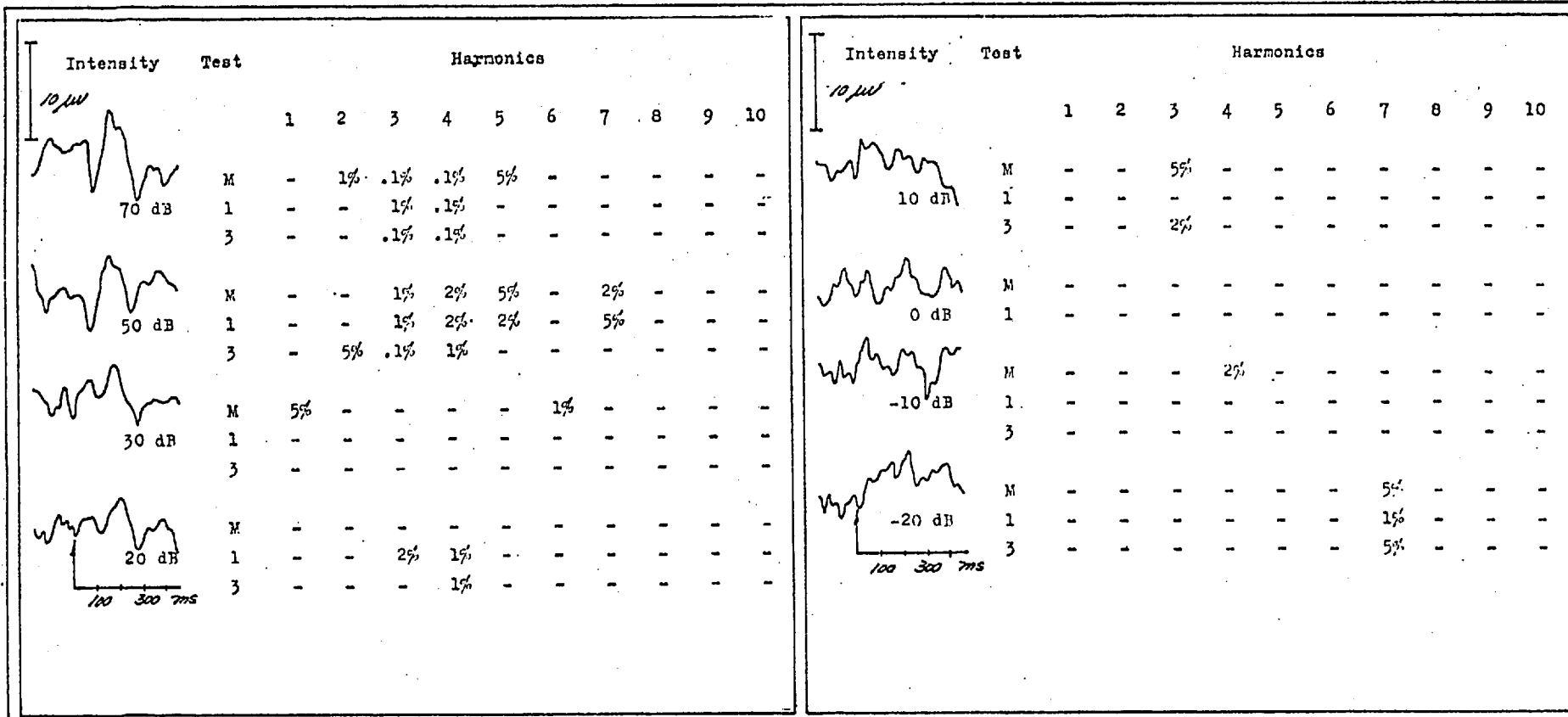


Table 4-lxx. Subject BS, F, age 23, at 1 kHz.

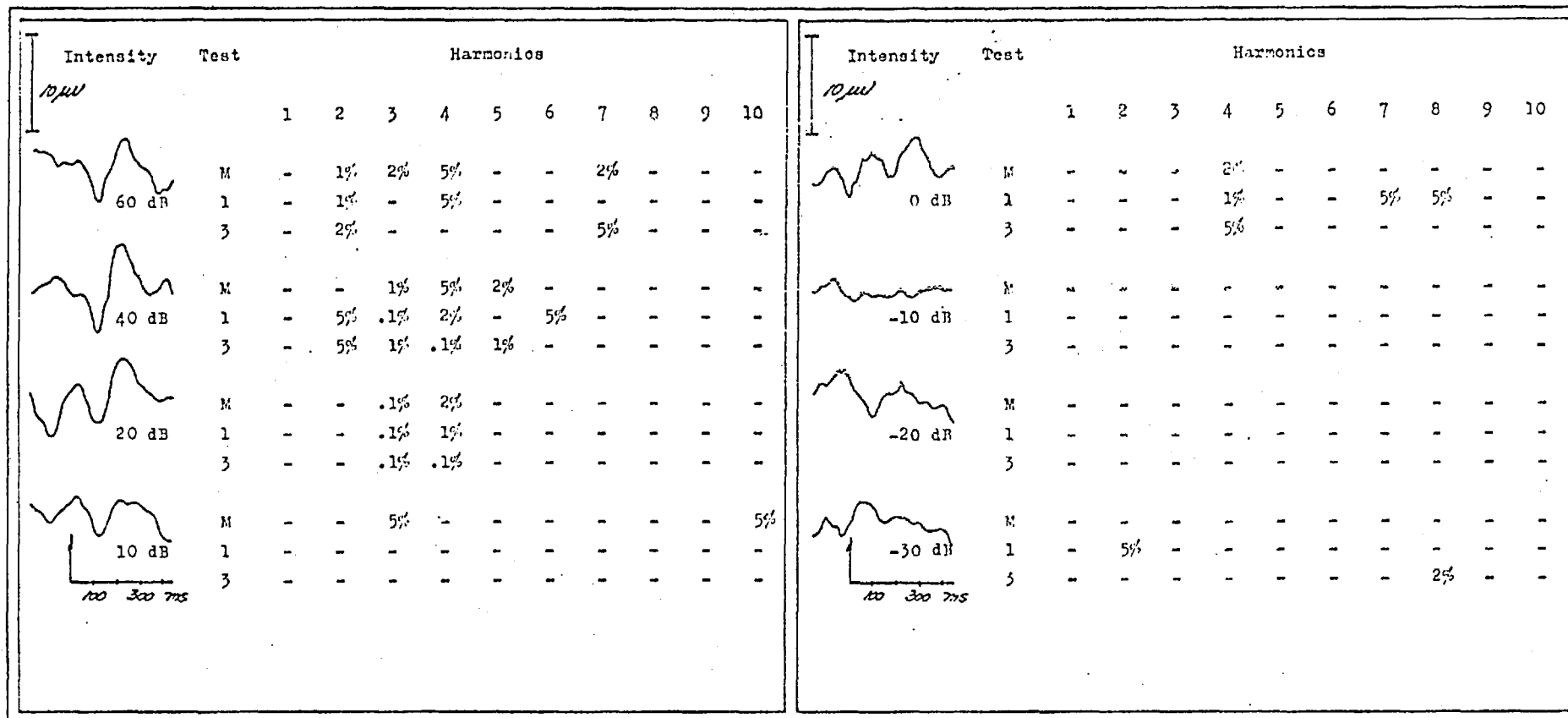


Table 4-lxxi. Subject TR, M, age 31, at 4 kHz.

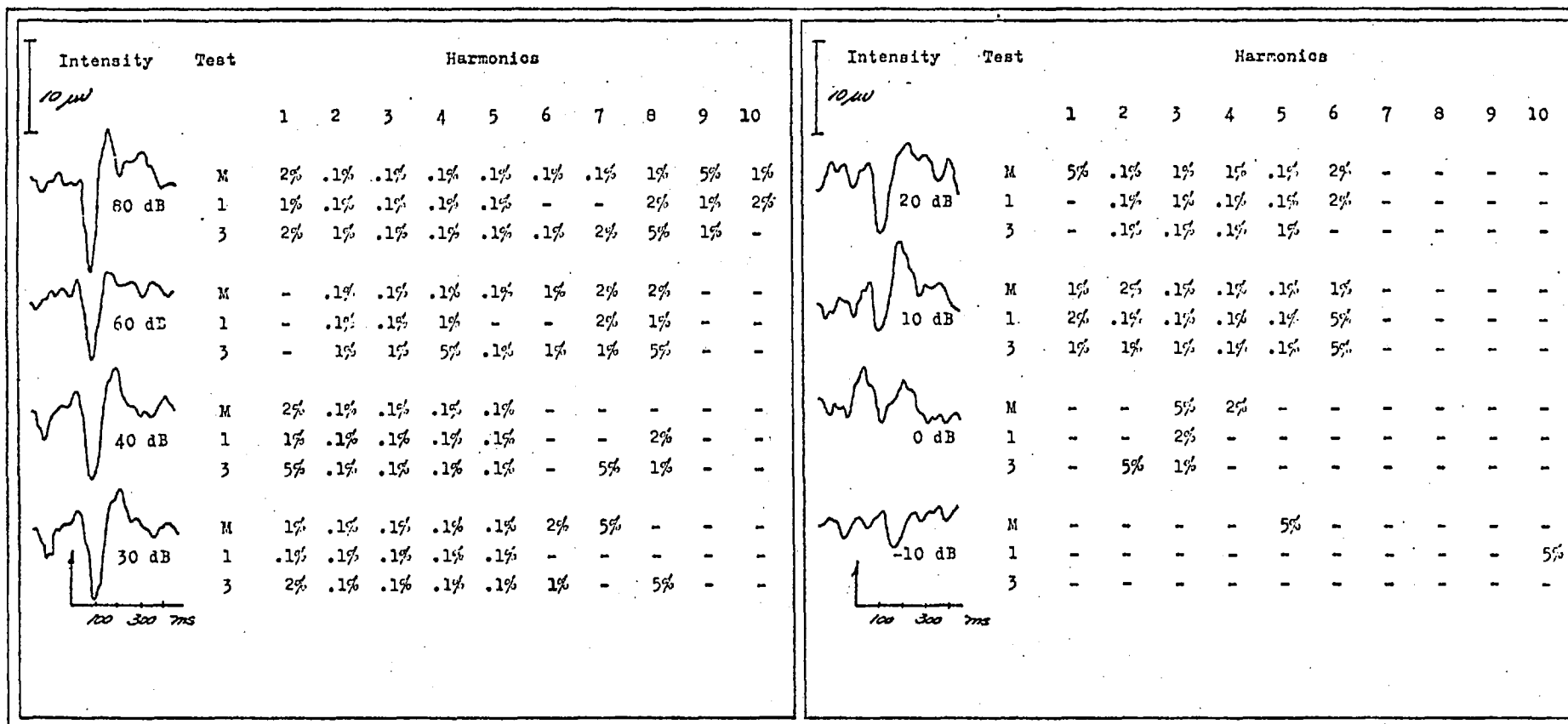


Table 4-1xxii. Subject TR, M, age 31, at 1 kHz.

Tables 4-lxxiii to 4-cxxviii

The Phase Vector Approach

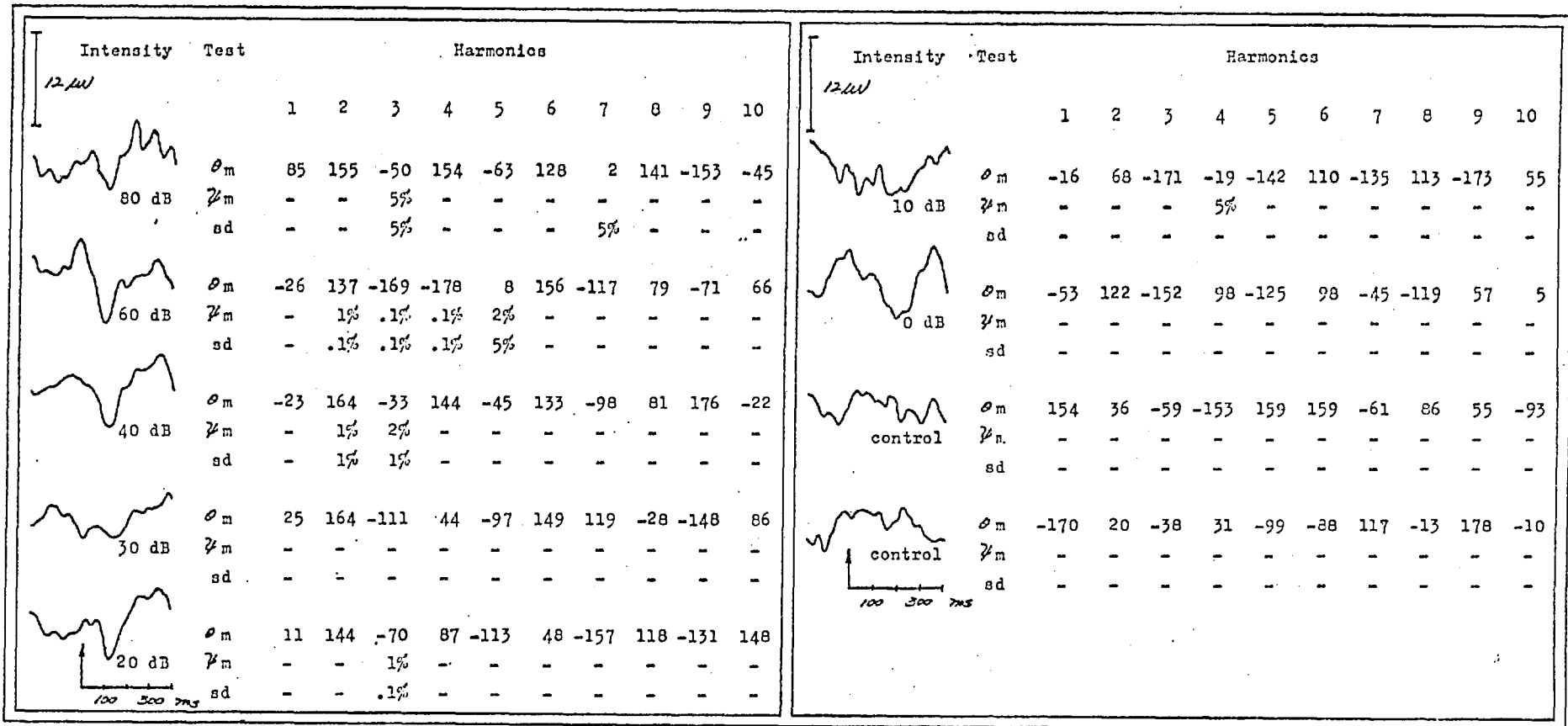


Table 4-lxxiii. Subject GF, M, age 28, at 4 kHz.

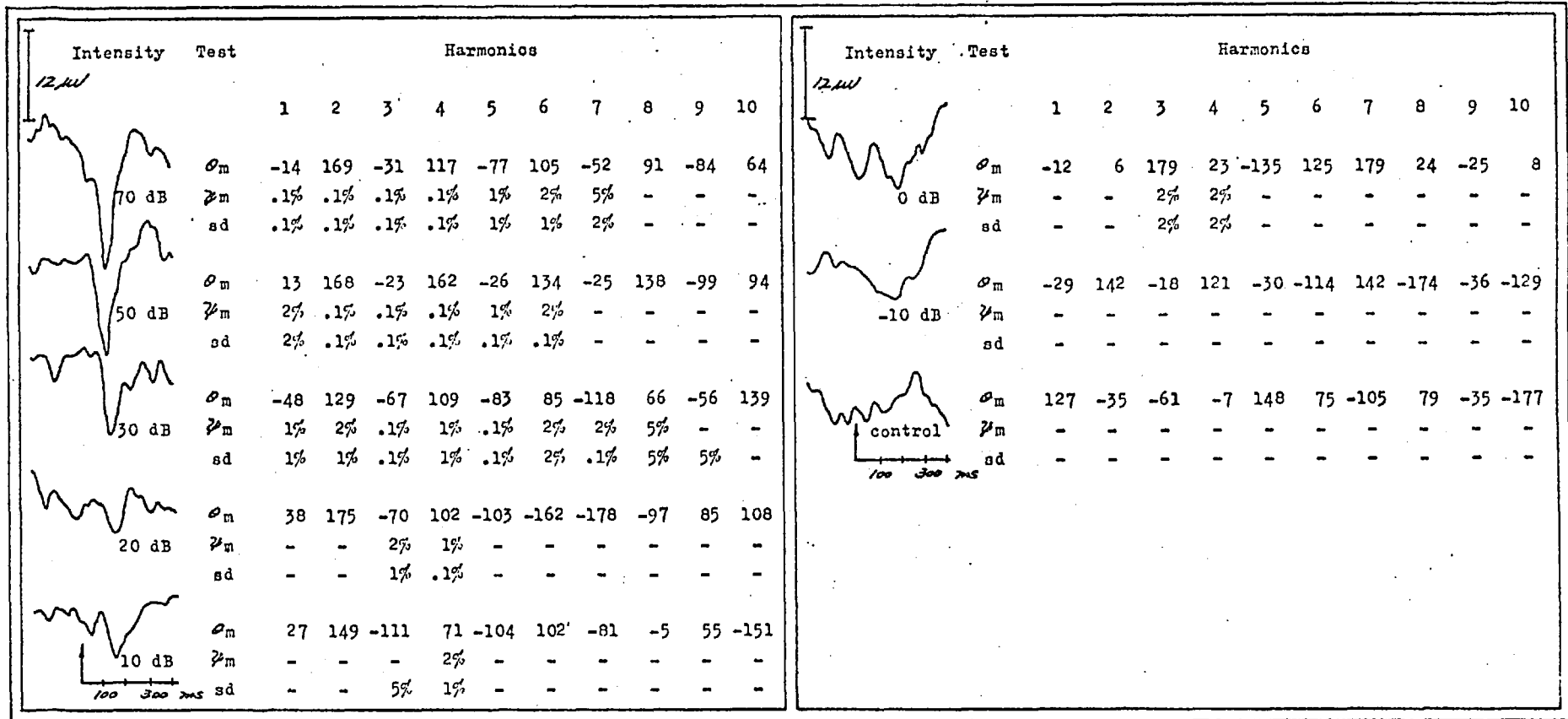


Table 4-1xxiv. Subject GF, M, age 28, at 1 kHz.



Intensity	Test	Harmonics									
		1	2	3	4	5	6	7	8	9	10
70 dB	$\phi_m$	65	-159	-4	171	-69	155	-4	137	-42	78
	$\psi_m$	-	1%	.1%	.1%	.1%	.1%	.1%	.1%	5%	-
	sd	-	.1%	.1%	.1%	.1%	.1%	.1%	.1%	-	-
50 dB	$\phi_m$	65	-144	28	-172	-2	143	-34	141	-106	127
	$\psi_m$	1%	.1%	2%	2%	.1%	.1%	.1%	2%	-	-
	sd	.1%	.1%	.1%	5%	.1%	.1%	.1%	.1%	-	-
30 dB	$\phi_m$	109	-102	42	163	-36	135	-76	105	-42	87
	$\psi_m$	-	-	-	-	2%	1%	-	-	-	-
	sd	-	-	-	-	2%	1%	-	-	-	-
20 dB	$\phi_m$	67	-153	55	109	-116	31	-170	49	-48	-173
	$\psi_m$	-	5%	2%	-	2%	-	-	-	-	-
	sd	-	2%	1%	-	2%	-	-	-	-	-
10 dB	$\phi_m$	60	-132	-21	122	-74	85	-91	126	154	10
	$\psi_m$	-	-	-	-	2%	-	-	-	-	-
	sd	-	-	-	-	1%	2%	2%	-	-	-
0 dB	$\phi_m$	44	179	-36	149	-81	-126	143	-27	-23	-101
	$\psi_m$	5%	5%	-	-	-	-	-	-	-	-
	sd	-	-	-	-	-	-	-	-	-	-
-10 dB	$\phi_m$	157	-44	132	2	-139	138	3	-157	-6	72
	$\psi_m$	-	-	-	-	-	-	-	5%	-	5%
	sd	-	-	-	-	-	-	-	2%	-	5%
control	$\phi_m$	119	-30	-177	-82	39	166	-126	37	-123	30
	$\psi_m$	-	2%	-	-	-	-	-	-	-	-
	sd	5%	1%	-	-	-	-	-	-	-	-
control	$\phi_m$	133	-20	179	33	-79	137	-63	7	-142	19
	$\psi_m$	1%	2%	-	-	-	-	-	-	2%	-
	sd	.1%	1%	-	-	-	-	-	-	2%	-

Table 4-lxxv. Subject JS, F, age 23, at 500 Hz.

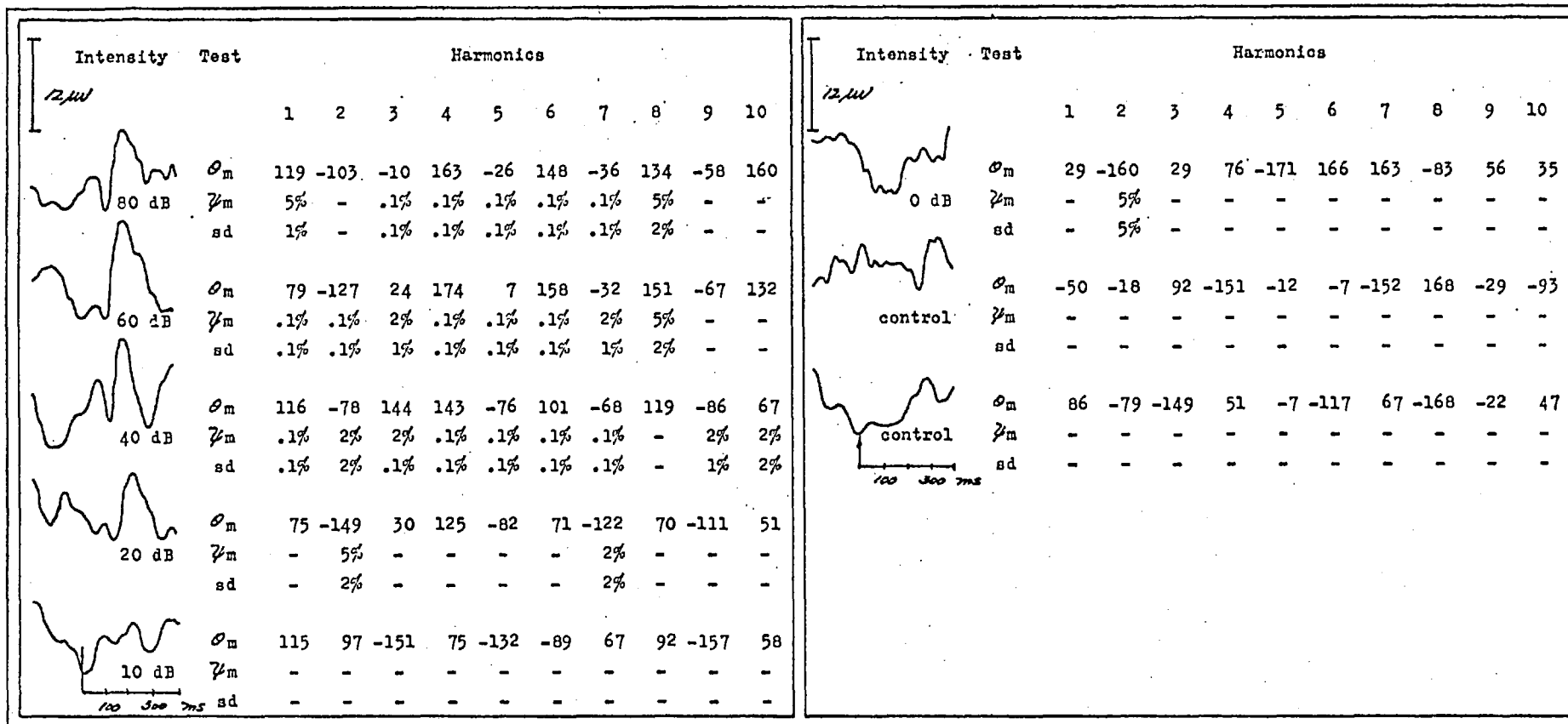


Table 4-lxxvi. Subject JS, F, age 23, at 2 kHz.

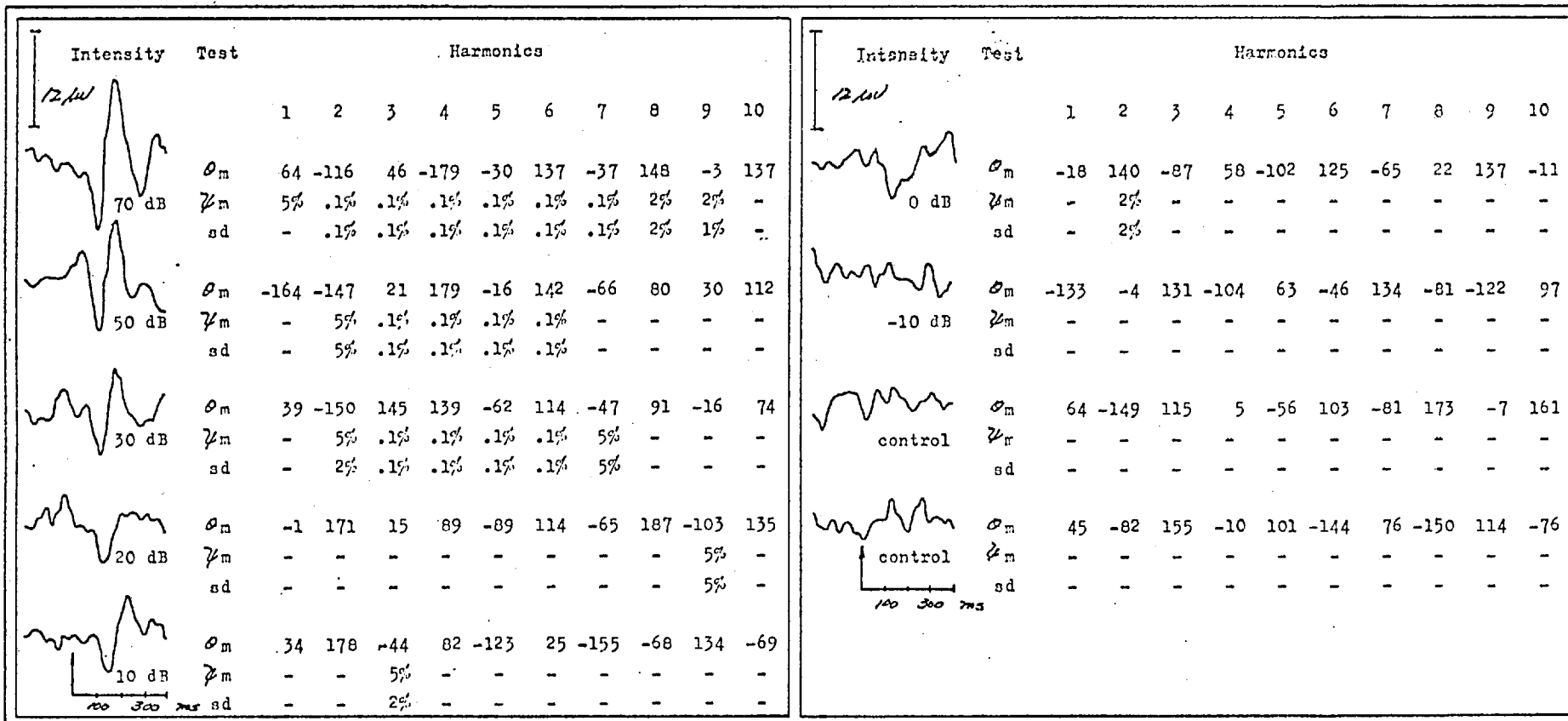


Table 4-lxxvii. Subject GH, F, age 23, at 500 Hz.

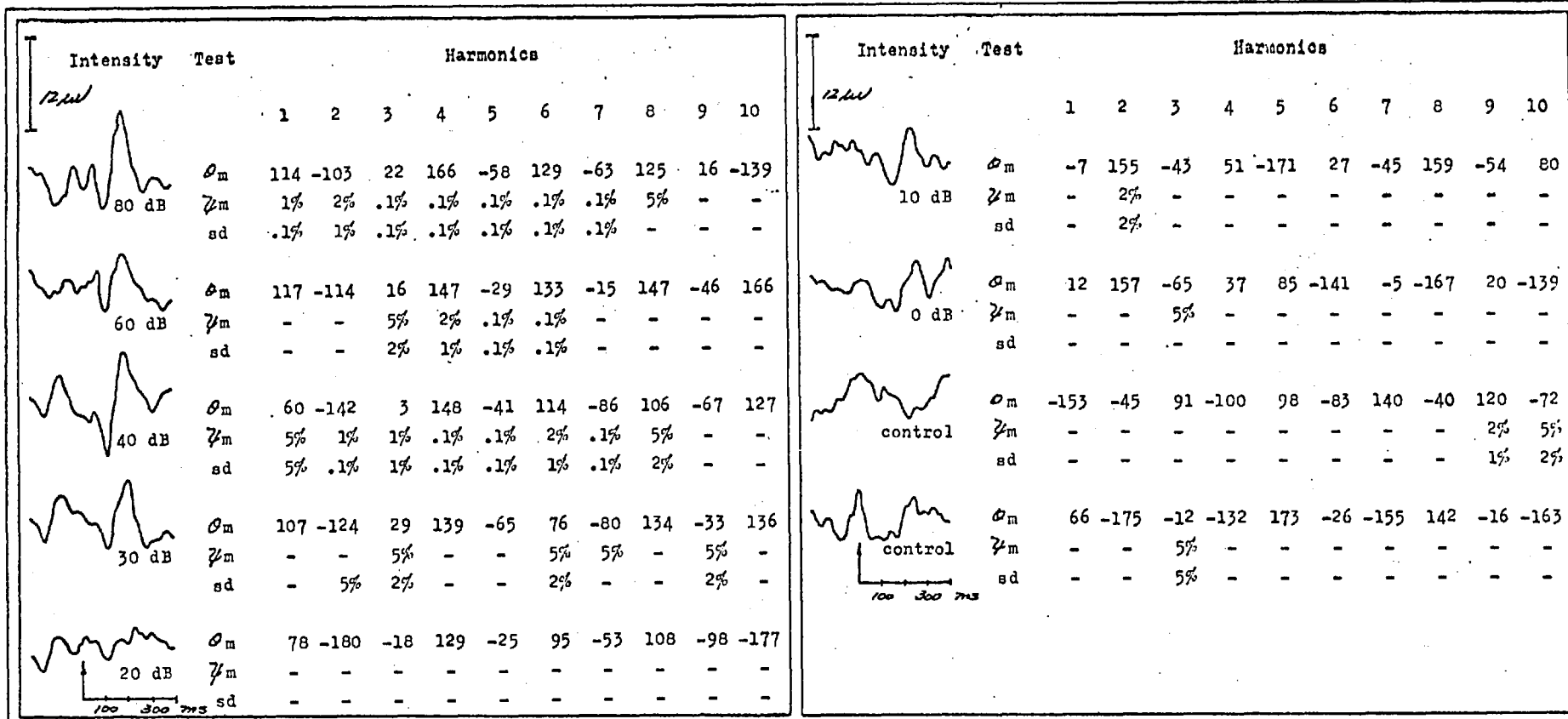


Table 4-1xxviii. Subject CH, F, age 23, at 2 kHz.

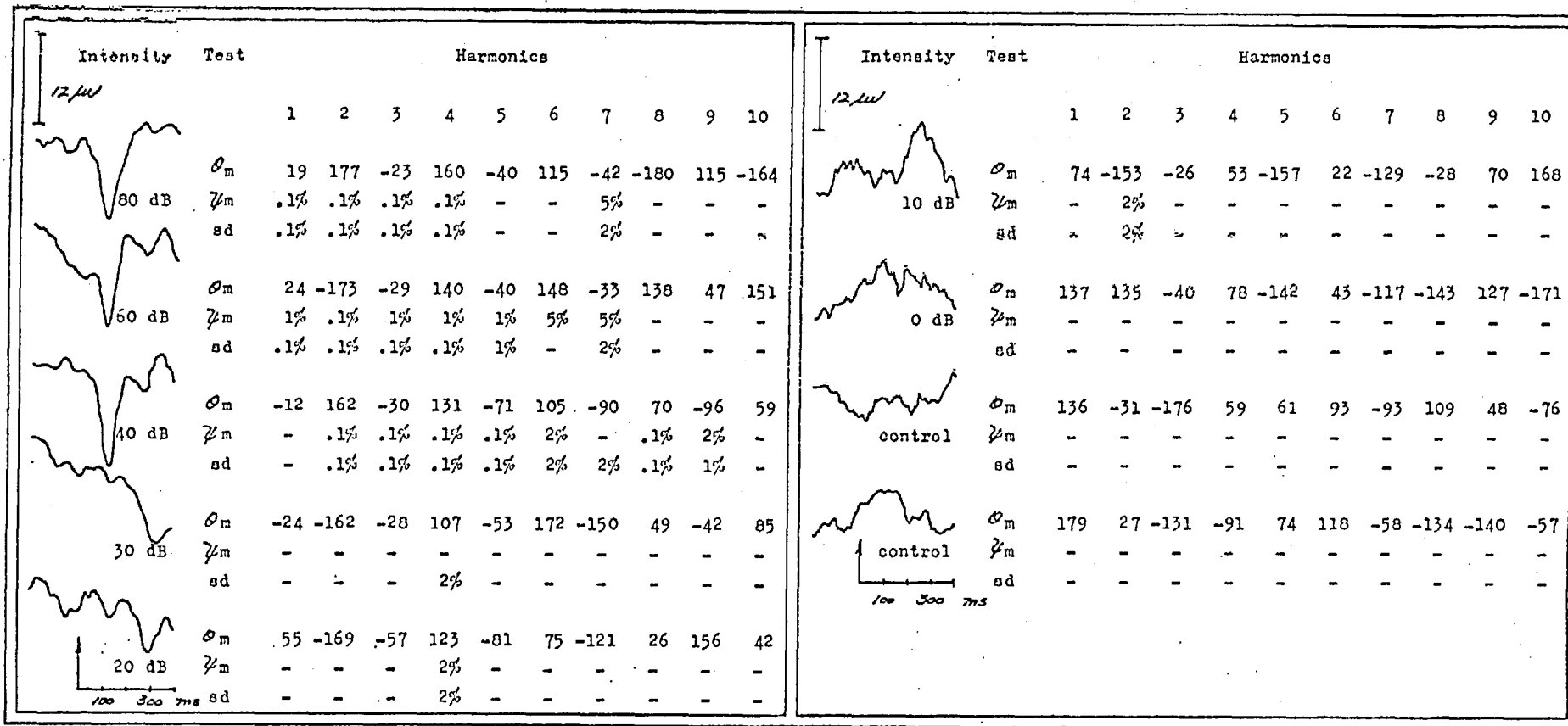


Table 4-lxxix. Subject CR, F, age 31, at 4 kHz.

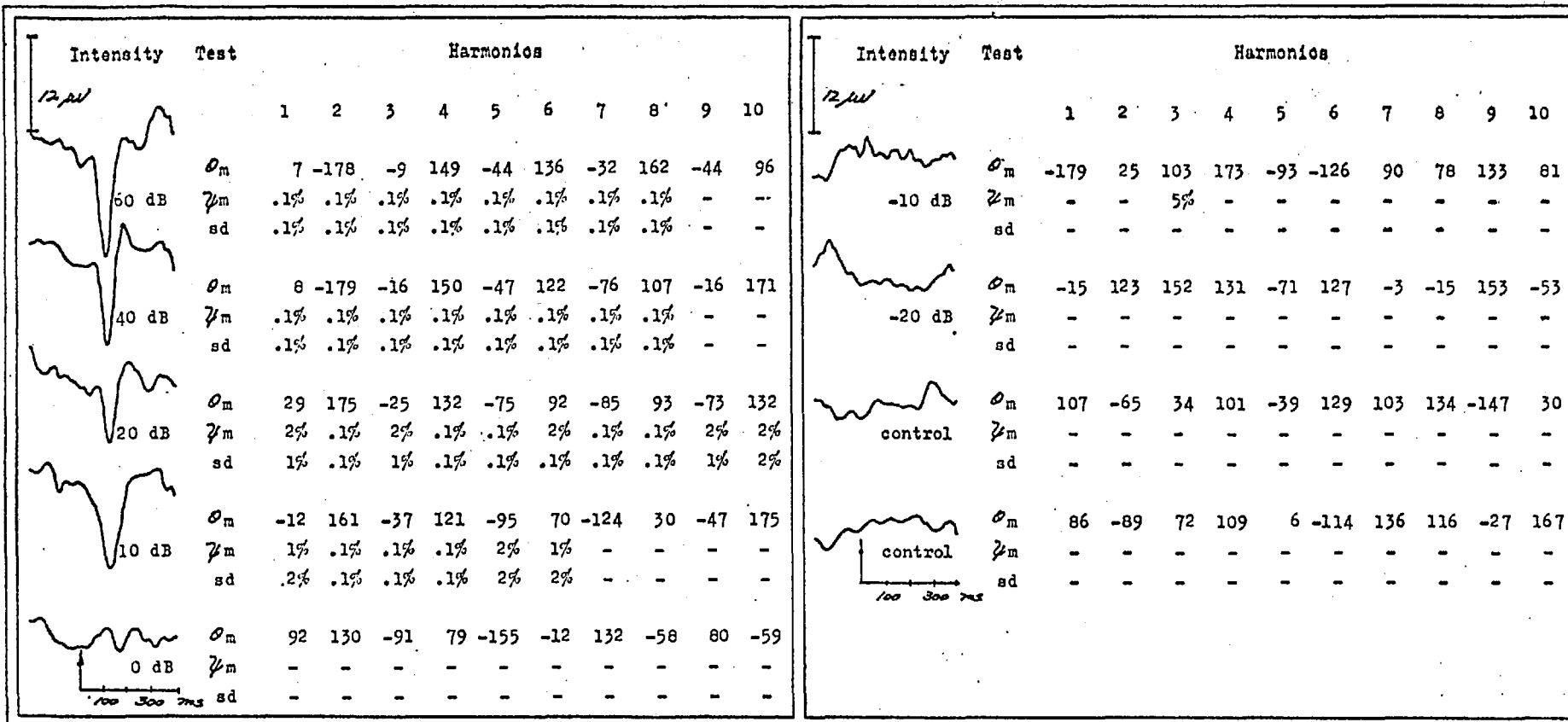


Table 4-lxxx. Subject CR, F, age 31, at 1 kHz.

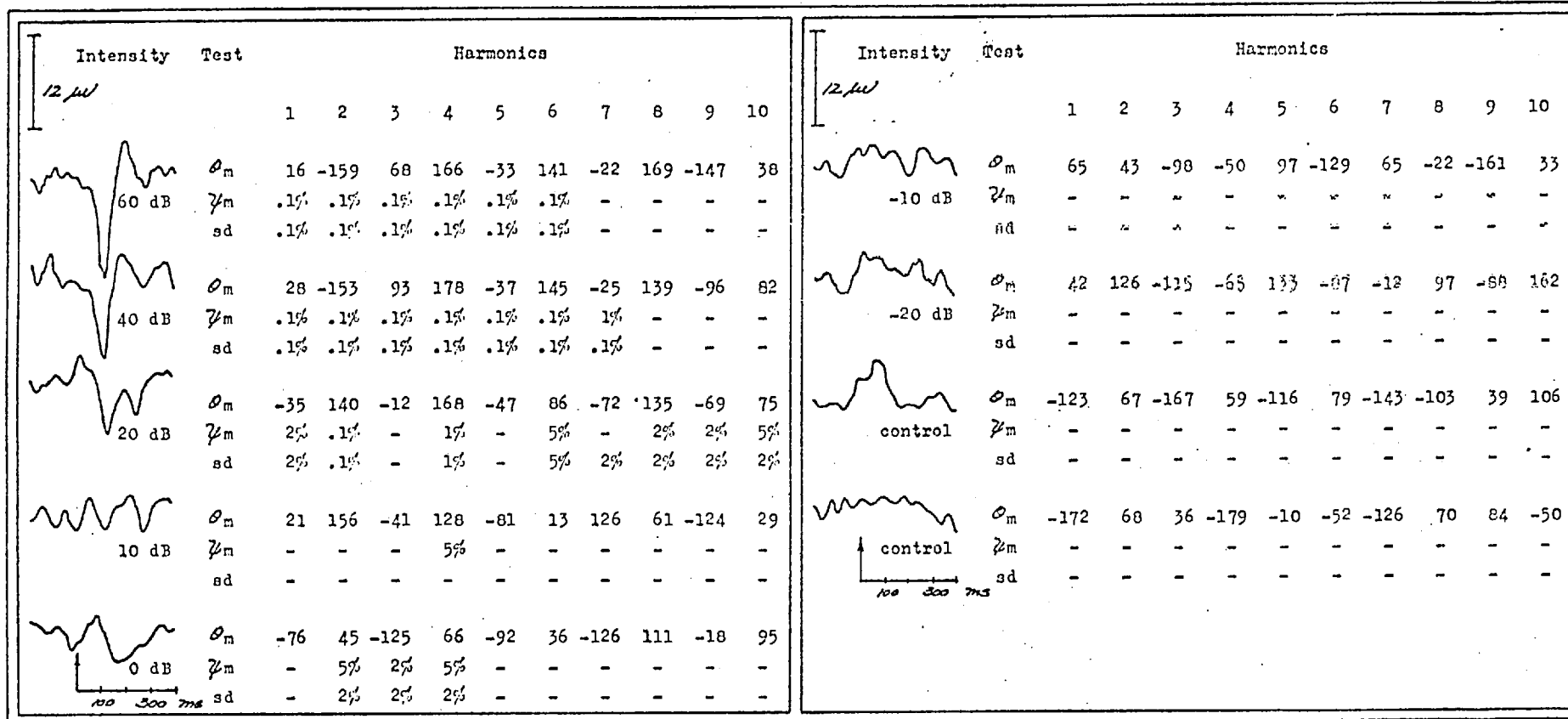


Table 4-lxxxii. Subject FN, M, age 28, at 500 Hz.

Intensity	Test	Harmonics									
		1	2	3	4	5	6	7	8	9	10
12 $\mu$ 80 dB	$O_m$	144	-173	-159	143	-51	116	-76	124	-26	139
	$\psi_m$	.1%	.1%	.1%	.1%	.1%	.1%	.1%	-	-	5%
	sd	.1%	.1%	.1%	.1%	.1%	.1%	.1%	-	-	5%
60 dB	$O_m$	-3	172	-63	161	-35	103	-103	143	-81	92
	$\psi_m$	.1%	.1%	.1%	.1%	.1%	-	5%	-	2%	5%
	sd	.1%	.1%	.1%	.1%	.1%	-	2%	-	-	2%
40 dB	$O_m$	-147	170	-46	107	-86	98	37	-122	94	105
	$\psi_m$	-	-	2%	2%	5%	-	-	-	-	-
	sd	-	-	1%	.1%	2%	-	-	-	-	-
30 dB	$O_m$	-66	128	-2	91	-137	46	-110	-2	155	-34
	$\psi_m$	2%	2%	-	-	-	-	-	-	-	-
	sd	2%	2%	-	-	-	-	-	-	-	-
20 dB	$O_m$	98	177	-40	117	-138	40	-137	88	-74	20
	$\psi_m$	2%	2%	5%	-	-	-	-	-	5%	-
	sd	2%	2%	2%	-	-	-	-	-	-	-

Intensity	Test	Harmonics									
		1	2	3	4	5	6	7	8	9	10
12 $\mu$ 10 dB	$O_m$	-22	134	-54	166	-148	-17	-89	150	48	-128
	$\psi_m$	-	-	-	-	-	-	-	-	-	-
	sd	-	-	-	-	-	-	-	-	-	-
0 dB	$O_m$	-160	69	-142	-99	-27	128	-58	172	48	-128
	$\psi_m$	-	-	-	-	-	-	-	-	-	-
	sd	-	-	-	-	-	5%	-	5%	-	-
control	$O_m$	84	-56	-143	150	-15	101	-137	45	56	-167
	$\psi_m$	-	-	-	-	-	-	2%	-	-	-
	sd	-	-	-	-	-	-	1%	-	-	-

Table 4-lxxxii. Subject FN, M, age 28, at 2 kHz.



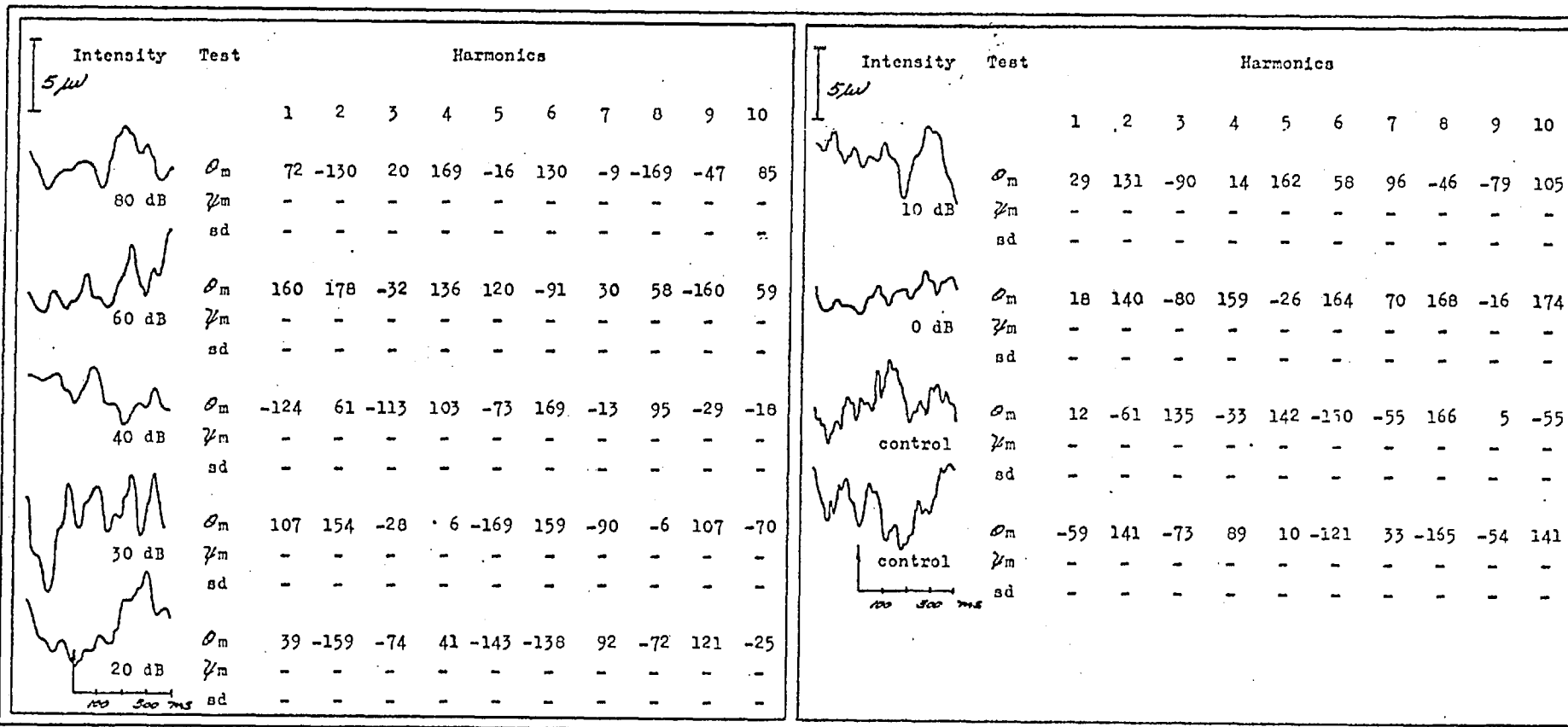


Table 4-lxxxiii. Subject TB, M, age 20, at 4 kHz.

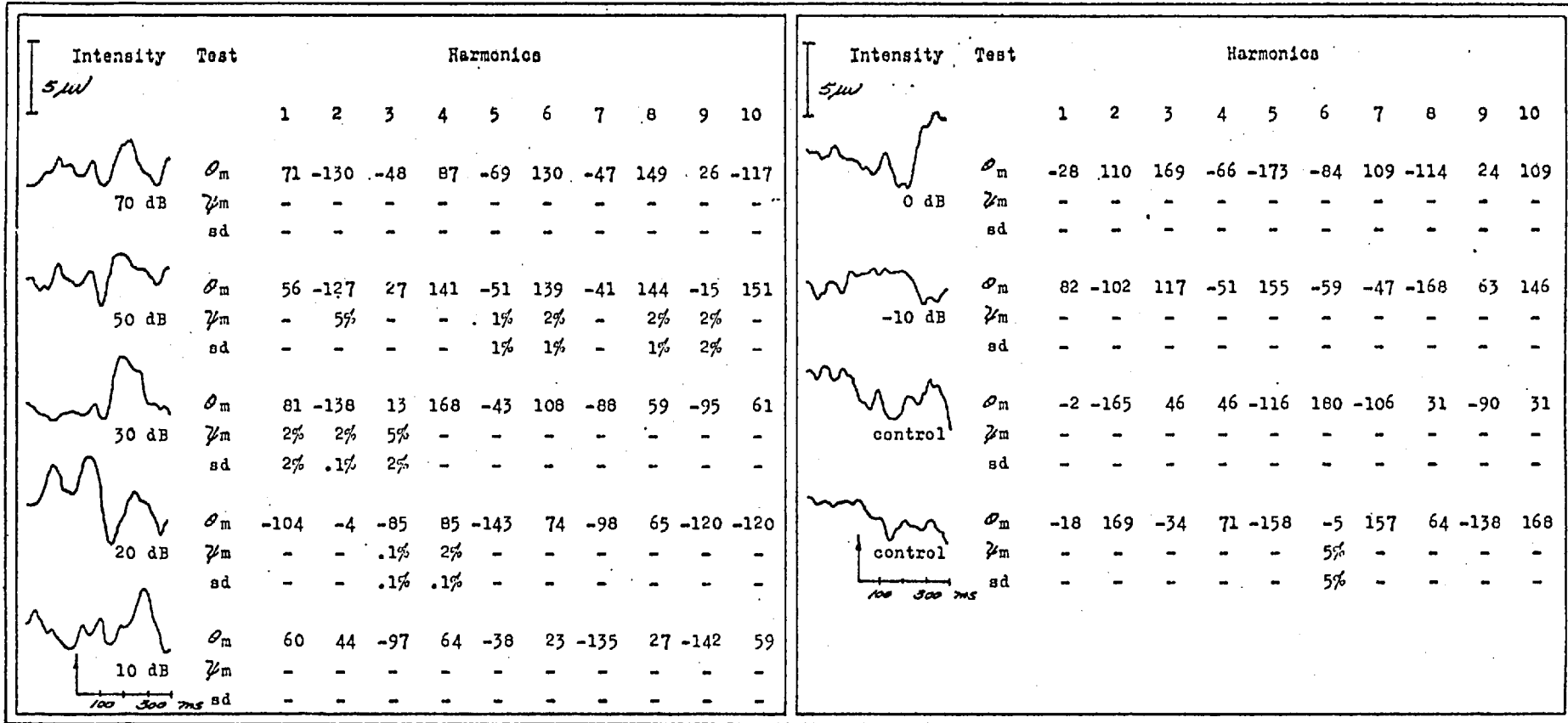


Table 4-lxxxiv. Subject TB, M, age 20, at 1 kHz.

Intensity	Test	Harmonics									
		1	2	3	4	5	6	7	8	9	10
70 dB	$\phi_m$	61	-158	-15	159	-14	-172	28	-148	45	-174
	$\psi_m$	.1%	.1%	.1%	.1%	.1%	.1%	.1%	.1%	5%	-
	sd	.1%	.1%	.1%	.1%	.1%	.1%	.1%	.1%	5%	-
50 dB	$\phi_m$	13	167	-31	137	-44	143	-5	137	-61	97
	$\psi_m$	.1%	.1%	.1%	.1%	2%	5%	2%	2%	2%	5%
	sd	.1%	.1%	.1%	.1%	1%	2%	1%	2%	1%	-
30 dB	$\phi_m$	53	-164	-73	99	-75	108	-43	22	-166	-48
	$\psi_m$	1%	2%	.1%	.1%	.1%	.1%	-	-	-	-
	sd	.1%	2%	1%	.1%	.1%	.1%	-	-	-	-
20 dB	$\phi_m$	24	-167	-38	98	-115	91	-114	34	-124	53
	$\psi_m$	.1%	.1%	1%	1%	2%	-	-	-	-	-
	sd	.1%	.1%	.1%	.1%	1%	-	-	-	-	-
10 dB	$\phi_m$	28	147	-87	66	-115	80	22	-93	114	97
	$\psi_m$	.1%	.1%	.1%	5%	-	-	-	-	-	-
	sd	.1%	.1%	.1%	2%	-	-	-	-	-	-

Intensity	Test	Harmonics									
		1	2	3	4	5	6	7	8	9	10
0 dB	$\phi_m$	71	143	-119	45	116	-133	-1	115	-73	88
	$\psi_m$	5%	5%	2%	-	-	-	-	-	-	-
	sd	-	2%	1%	5%	-	-	-	-	-	-
-10 dB	$\phi_m$	61	-167	4	-136	-103	127	-63	37	-98	-91
	$\psi_m$	-	-	-	-	-	5%	-	-	-	-
	sd	-	-	-	-	-	5%	-	-	-	-
control	$\phi_m$	143	-99	-34	163	5	-85	139	23	-94	87
	$\psi_m$	-	-	-	-	-	-	-	-	-	-
	sd	-	-	-	-	-	-	-	-	-	-
control	$\phi_m$	63	-113	67	-89	-151	94	-60	-97	144	-43
	$\psi_m$	-	-	-	-	-	-	-	-	-	-
	sd	-	-	-	-	-	-	-	-	-	-

Table 4-lxxxv. Subject BO, M, age 31, at 500 Hz.

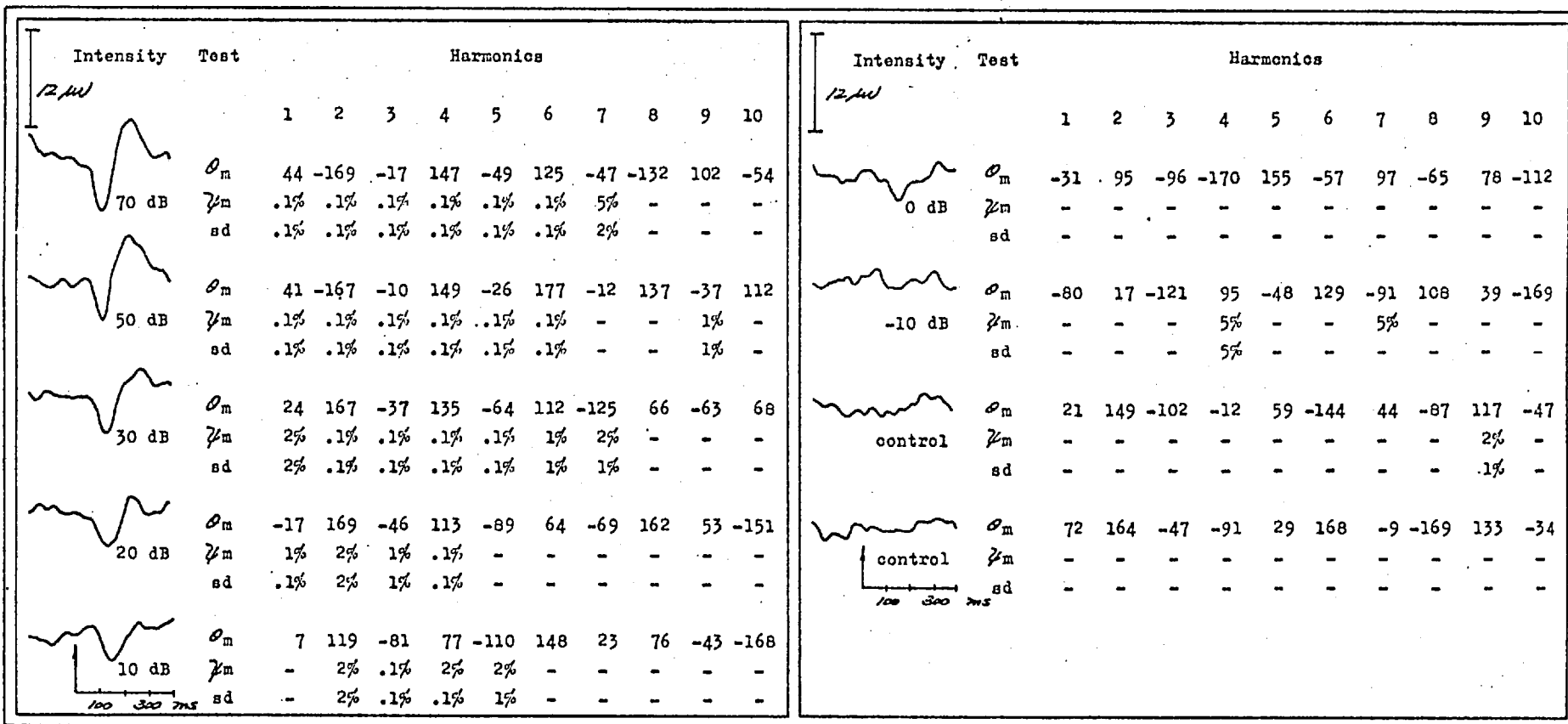


Table 4-lxxxvi. Subject BO, M, age 31, at 2 kHz.

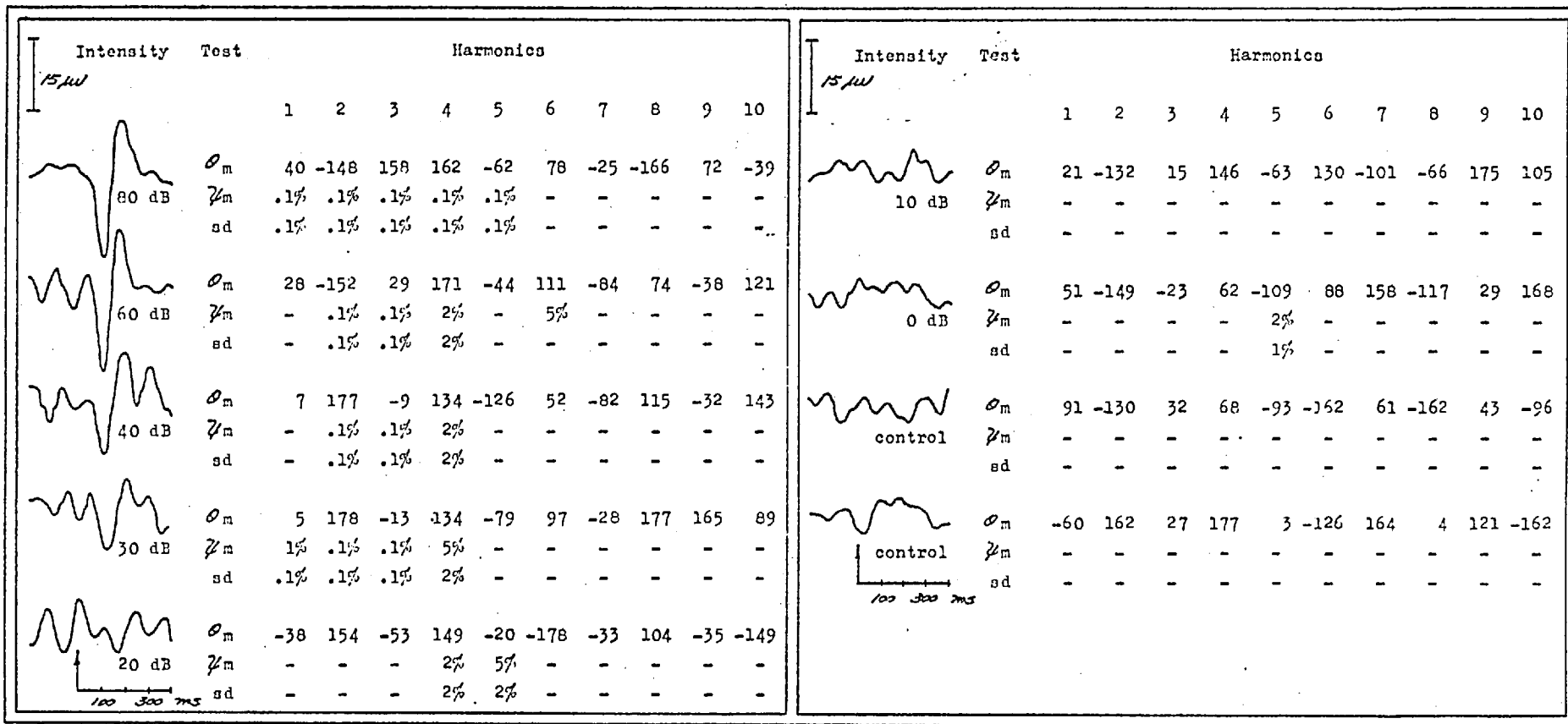


Table 4-lxxxvii. Subject JD, F, age 23 at 4 kHz.

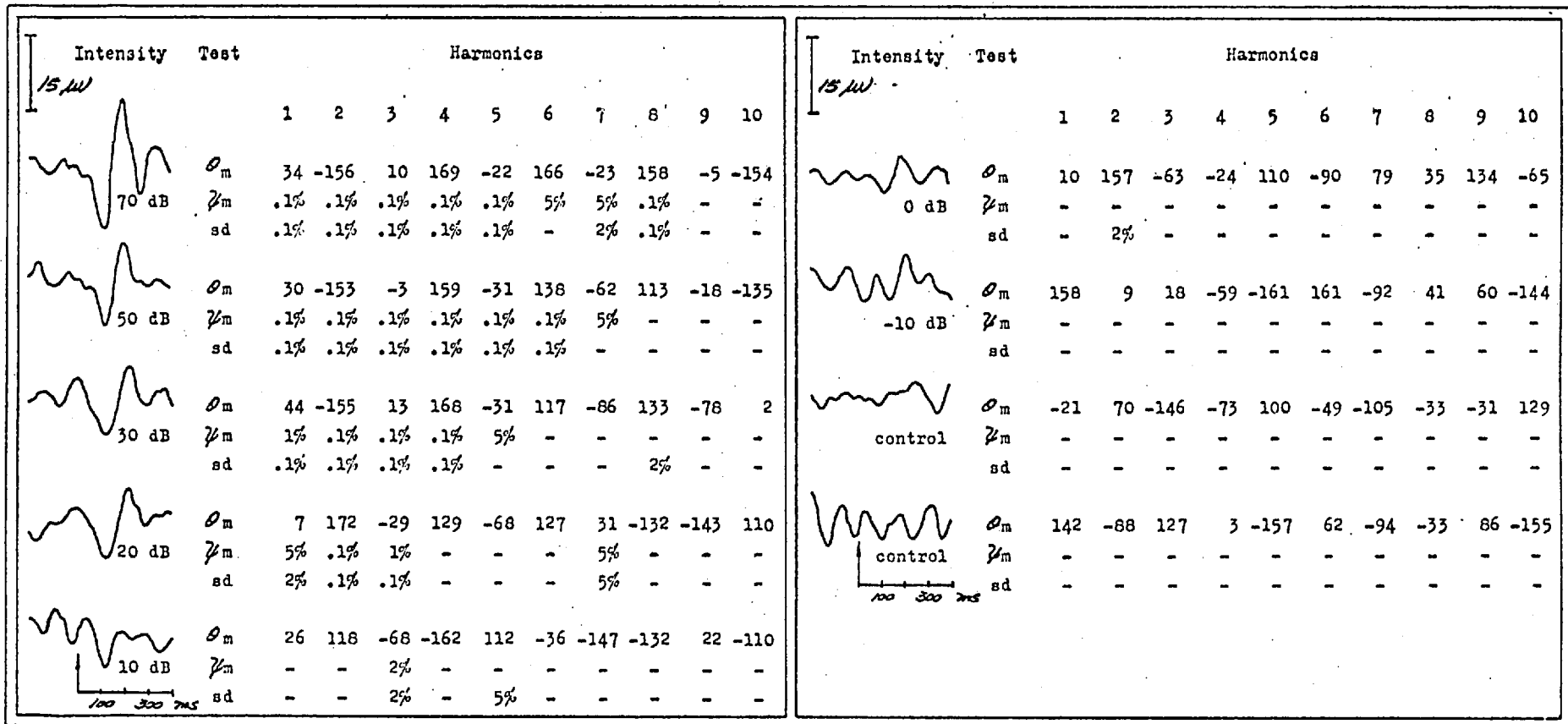


Table 4-1xxxviii. Subject JD, F, age 23, at 1 kHz.

Intensity	Test	Harmonics									
		1	2	3	4	5	6	7	8	9	10
12.4W 70 dB	$\phi_m$	100	-118	22	173	-21	157	-5	-167	48	131
	$\psi_m$	.1%	.1%	.1%	.1%	.1%	.1%	2%	2%	5%	-
	sd	.1%	.1%	.1%	.1%	.1%	.1%	2%	2%	5%	-
50 dB	$\phi_m$	67	-123	32	-163	20	-179	12	174	-7	168
	$\psi_m$	.1%	.1%	.1%	.1%	.1%	.1%	2%	.1%	1%	-
	sd	.1%	.1%	.1%	.1%	.1%	.1%	2%	.1%	.1%	-
30 dB	$\phi_m$	53	-138	31	179	-23	133	-21	177	-18	176
	$\psi_m$	.1%	.1%	.1%	.1%	.1%	-	-	-	-	-
	sd	.1%	.1%	.1%	.1%	.1%	-	-	-	-	-
20 dB	$\phi_m$	18	-148	5	170	-18	143	-58	129	5	-108
	$\psi_m$	5%	1%	.1%	.1%	.1%	1%	-	-	-	5%
	sd	-	1%	.1%	.1%	.1%	1%	-	-	-	5%
10 dB	$\phi_m$	-2	-169	-16	135	-103	79	-80	-179	37	-88
	$\psi_m$	2%	2%	-	-	-	-	-	-	-	-
	sd	2%	5%	-	-	-	-	-	-	-	-
12.4W 0 dB	$\phi_m$	-22	101	-131	27	-51	-163	20	-86	47	-134
	$\psi_m$	-	-	-	-	-	-	-	-	-	2%
	sd	-	-	-	-	-	-	-	-	-	1%
-10 dB	$\phi_m$	-9	-154	57	-69	127	-79	69	145	69	-99
	$\psi_m$	-	-	-	-	-	-	-	-	-	-
	sd	-	-	-	-	-	-	-	-	-	-
control	$\phi_m$	113	-39	130	-38	99	-76	95	133	-57	101
	$\psi_m$	-	-	-	-	-	5%	-	-	-	-
	sd	-	-	-	-	-	2%	-	-	-	-

Table 4-lxxxix. Subject DT, F, age 24, at 500 Hz.

Intensity	Test	Harmonics										
		1	2	3	4	5	6	7	8	9	10	
	70 dB	$O_m$	29	-158	20	-179	-45	152	3	-171	54	-153
		$\psi_m$	5%	.1%	.1%	.1%	.1%	.1%	.1%	2%	-	-
		sd	-	.1%	.1%	.1%	.1%	.1%	.1%	2%	-	-
	50 dB	$O_m$	104	-113	17	165	-38	132	-39	149	4	163
		$\psi_m$	.1%	.1%	.1%	.1%	.1%	2%	2%	2%	5%	-
	sd	.1%	.1%	.1%	.1%	.1%	2%	2%	1%	2%	2%	
	30 dB	$O_m$	84	-126	22	159	-38	142	-40	157	54	-29
	$\psi_m$	2%	.1%	.1%	.1%	.1%	5%	-	-	-	-	-
	sd	1%	.1%	.1%	.1%	.1%	2%	-	-	-	-	-
	20 dB	$O_m$	9	-160	-2	153	-24	-19	4	-29	162	29
	$\psi_m$	2%	2%	.1%	.1%	-	-	-	-	-	-	-
	sd	2%	1%	.1%	.1%	-	-	-	-	-	-	-
	10 dB	$O_m$	49	171	-35	72	-85	121	-67	59	-140	30
	$\psi_m$	-	-	-	-	-	-	-	-	-	-	-
	sd	-	-	-	-	-	-	-	-	-	-	-

Intensity	Test	Harmonics										
		1	2	3	4	5	6	7	8	9	10	
	0 dB	$O_m$	135	120	-55	67	-58	83	-171	32	77	-122
		$\psi_m$	-	-	-	-	-	-	-	-	-	-
		sd	-	-	-	-	-	-	-	-	-	-
	-10 dB	$O_m$	47	-165	57	-121	31	-129	48	-33	-178	-105
		$\psi_m$	-	-	-	-	-	-	-	-	-	-
	sd	-	-	-	-	-	-	-	-	-	-	
	control	$O_m$	87	113	-56	97	-56	-161	-96	119	-76	-170
	$\psi_m$	-	-	-	-	-	-	-	-	-	-	-
	sd	-	-	-	-	-	-	-	-	5%	-	-
	control	$O_m$	-149	-97	75	-58	154	61	101	-145	-46	178
	$\psi_m$	-	-	-	-	-	-	-	-	-	-	-
	sd	-	-	-	-	-	-	-	-	-	-	-

Table 4-rc. Subject DT, F, ate 24 at 2 kHz.



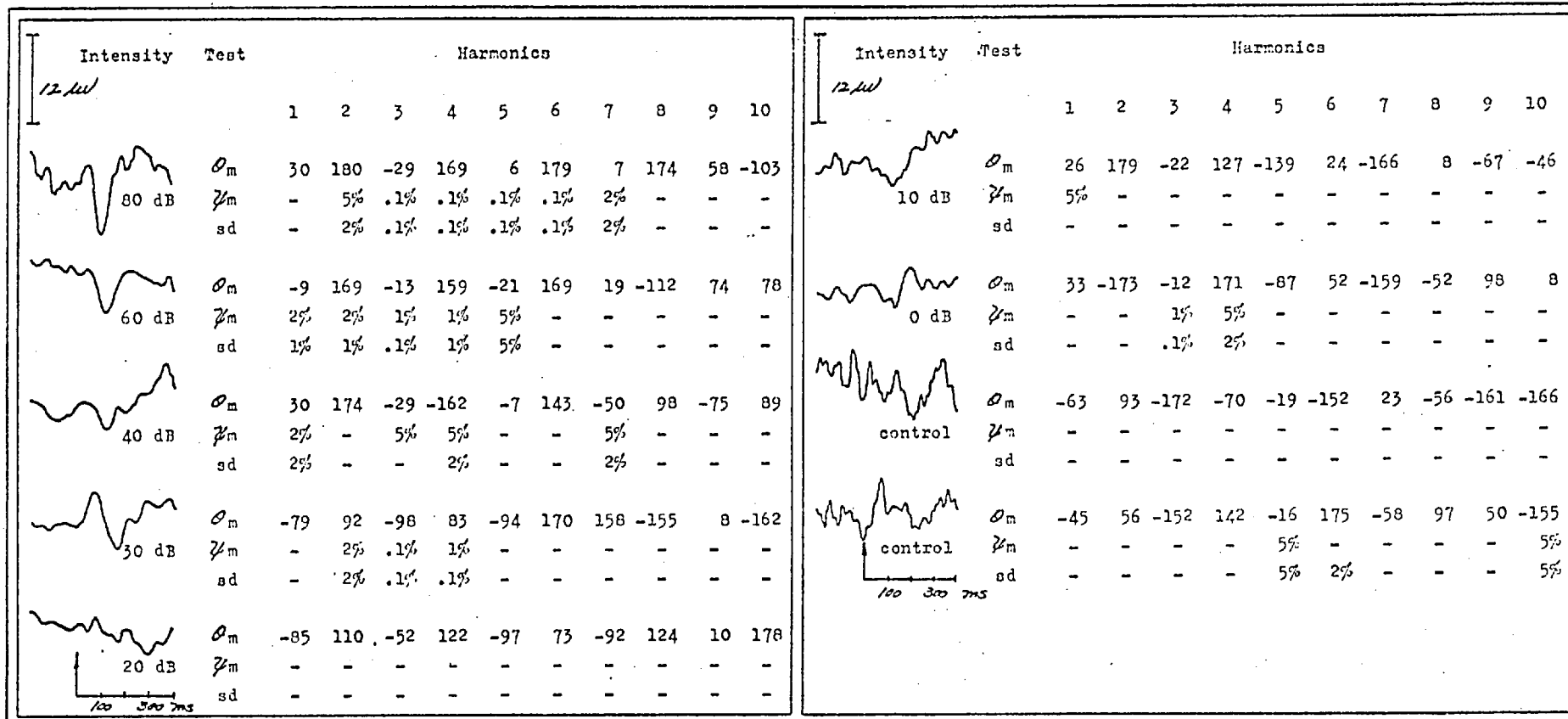


Table 4-xci. Subject SB, M, age 18, at 4 kHz.

Intensity <i>12 μV</i>	Test	Harmonics									
		1	2	3	4	5	6	7	8	9	10
	$\phi_m$	53	-157	7	177	-2	179	-26	30	128	-83
80 dB	$\psi_m$	-	2%	.1%	.1%	.1%	2%	-	-	-	1%
	sd	-	1%	.1%	.1%	.1%	1%	-	-	-	1%
	$\phi_m$	22	-138	14	162	-7	89	-37	168	19	-161
60 dB	$\psi_m$	2%	.1%	.1%	.1%	5%	-	-	-	2%	-
	sd	.1%	.1%	.1%	.1%	-	-	-	-	1%	-
	$\phi_m$	13	179	-60	179	-7	120	-125	101	-115	80
40 dB	$\psi_m$	-	5%	.1%	.1%	5%	-	-	-	-	-
	sd	2%	5%	.1%	.1%	-	-	-	-	-	-
	$\phi_m$	16	162	-4	104	-52	100	85	-99	7	140
30 dB	$\psi_m$	5%	.1%	2%	-	-	-	-	-	-	-
	sd	-	.1%	1%	-	-	-	-	-	-	-
	$\phi_m$	70	-150	-54	98	-109	76	-92	122	38	-119
20 dB	$\psi_m$	-	-	-	2%	-	-	5%	-	-	-
	sd	-	-	-	1%	-	-	5%	-	-	-

Intensity <i>12 μV</i>	Test	Harmonics									
		1	2	3	4	5	6	7	8	9	10
	$\phi_m$	44	-132	-97	80	-122	-15	69	170	-29	148
10 dB	$\psi_m$	-	-	-	5%	5%	-	-	-	-	2%
	sd	-	-	-	2%	-	-	-	-	-	2%
	$\phi_m$	46	-103	137	-86	70	-110	29	148	-65	133
0 dB	$\psi_m$	-	-	-	-	5%	-	-	-	-	-
	sd	-	-	-	2%	2%	-	-	-	-	-
	$\phi_m$	161	-29	135	-60	132	-15	-63	127	-81	35
control	$\psi_m$	-	-	-	-	-	-	-	-	5%	-
	sd	-	-	-	-	-	-	-	-	2%	-
	$\phi_m$	-89	-49	117	-160	-161	26	-155	42	-28	152
control	$\psi_m$	-	-	-	5%	-	-	-	-	-	-
	sd	-	-	-	-	-	-	-	-	-	-

Table 4-xcii. Subject SB, M, age 18, at 1 kHz.

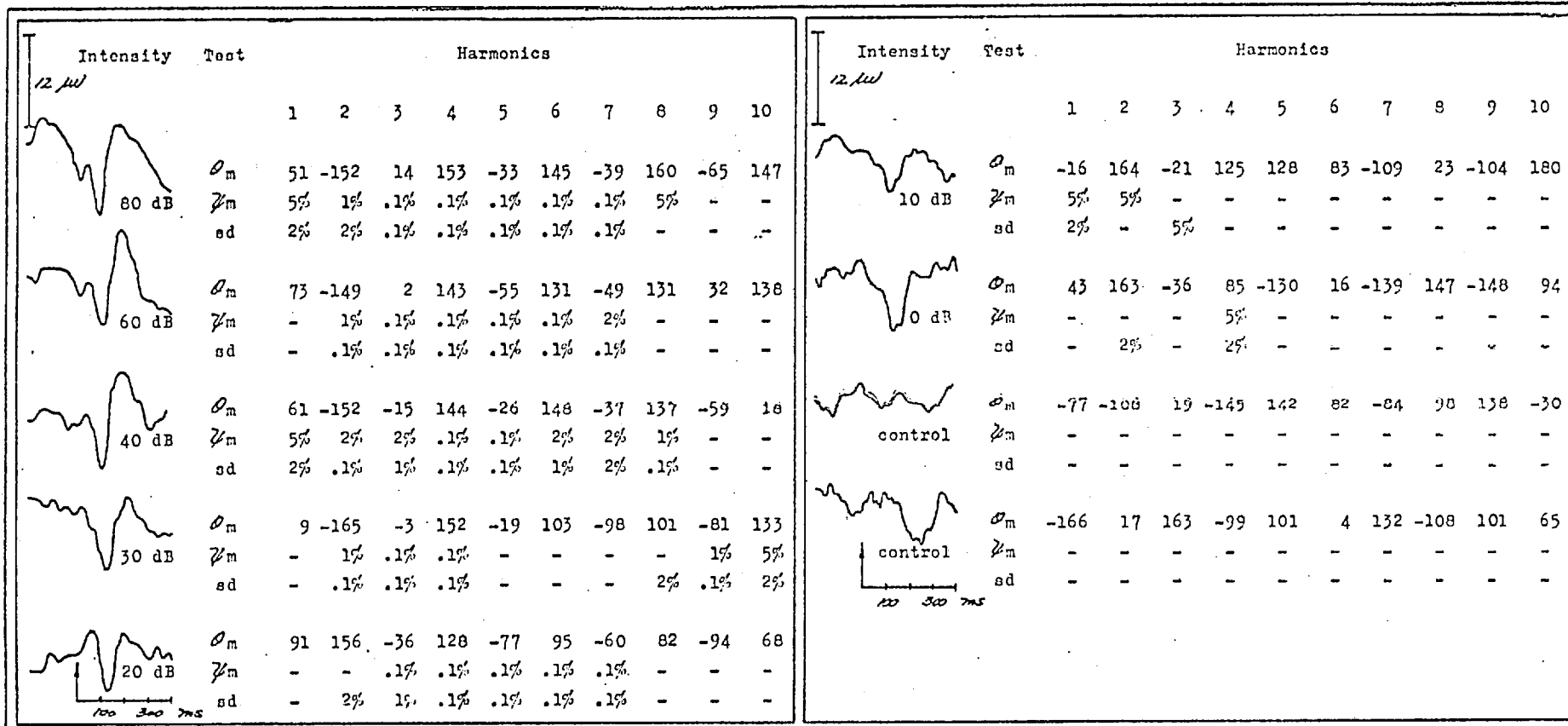


Table 4-xciii. Subject JN, M, age 30, at 4 kHz.

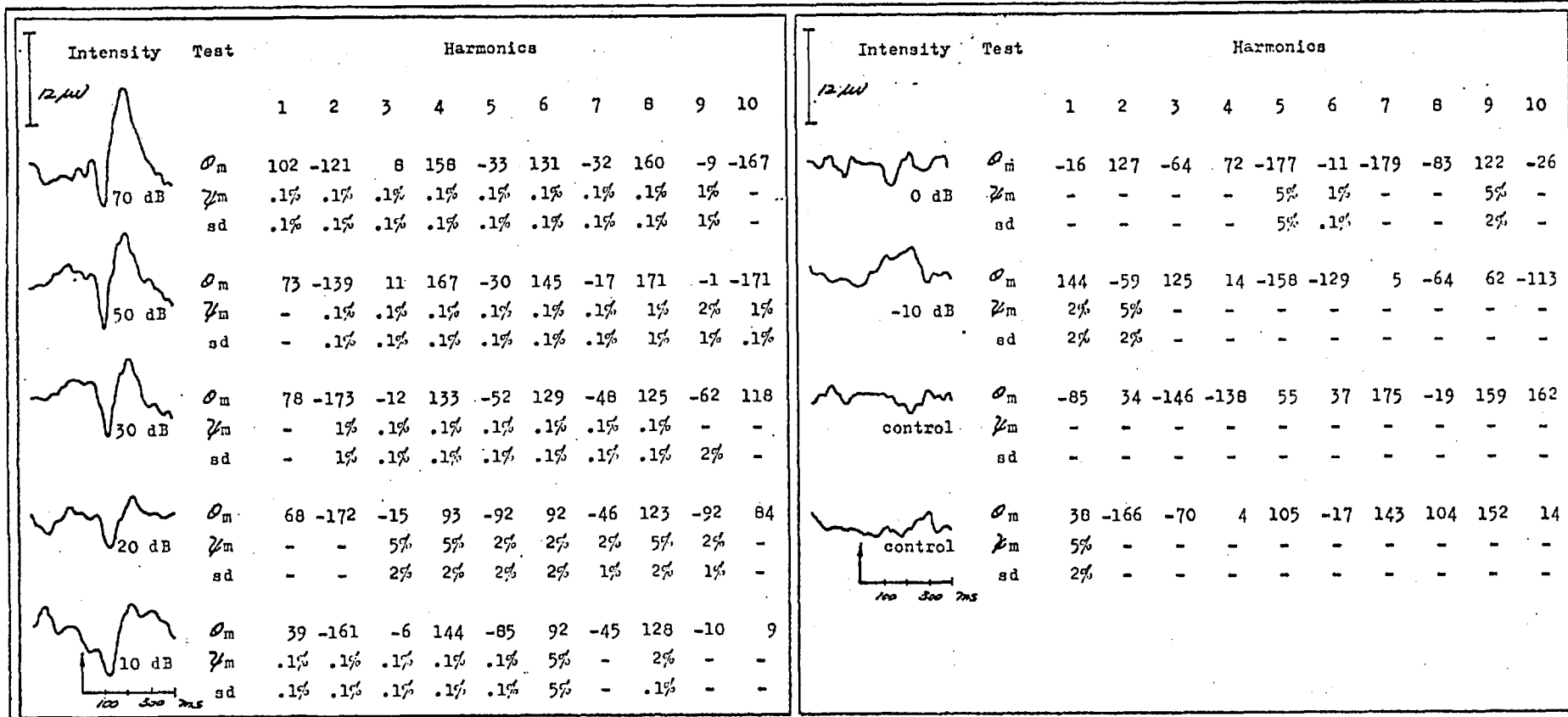


Table 4-xciv. Subject JN, M, age 30, at 1 kHz.

Intensity	Test	Harmonics									
		1	2	3	4	5	6	7	8	9	10
12 $\mu$ W 60 dB	$O_m$	3	173	7	-162	10	171	-10	130	-73	131
	$Z_m$	2%	.1%	.1%	2%	.1%	2%	-	-	-	-
	sd	2%	.1%	.1%	.1%	.1%	2%	-	-	-	-
60 dB	$O_m$	71	-124	46	-147	35	-174	-12	122	-67	116
	$Z_m$	-	1%	.1%	.1%	-	-	-	-	-	-
	sd	-	2%	.1%	.1%	-	-	-	-	-	-
40 dB	$O_m$	-12	-180	36	179	-39	140	-108	-7	60	-106
	$Z_m$	-	-	-	-	.1%	5%	-	-	-	-
	sd	-	-	-	-	.1%	-	-	-	-	-
30 dB	$O_m$	-14	-180	24	157	-71	105	-66	-124	81	-94
	$Z_m$	5%	5%	-	-	-	-	-	-	-	-
	sd	1%	-	-	2%	-	-	-	-	-	-
20 dB	$O_m$	-112	145	-62	-175	-47	93	-38	-48	23	39
	$Z_m$	-	-	-	-	-	-	-	-	-	-
	sd	5%	-	2%	-	-	-	-	-	-	-
12 $\mu$ W 10 dB	$O_m$	-63	60	-108	-20	110	-135	30	-136	41	115
	$Z_m$	-	-	-	-	-	-	-	-	-	-
	sd	-	-	-	-	-	-	-	-	-	-
0 dB	$O_m$	-51	157	-17	-178	76	-99	-43	156	3	-147
	$Z_m$	-	-	-	-	-	-	-	-	-	-
	sd	-	-	-	-	-	-	-	-	-	-
control	$O_m$	67	-157	-31	-69	-151	-22	120	-45	-103	36
	$Z_m$	-	-	-	-	-	-	-	-	-	-
	sd	-	-	-	-	-	-	-	-	-	-
control	$O_m$	56	-142	66	-56	101	-122	34	-143	5	132
	$Z_m$	-	-	-	-	-	-	-	-	-	-
	sd	-	-	-	-	-	-	-	-	-	-

Table 4-xcv. Subject VM, age 24, at 4 kHz.

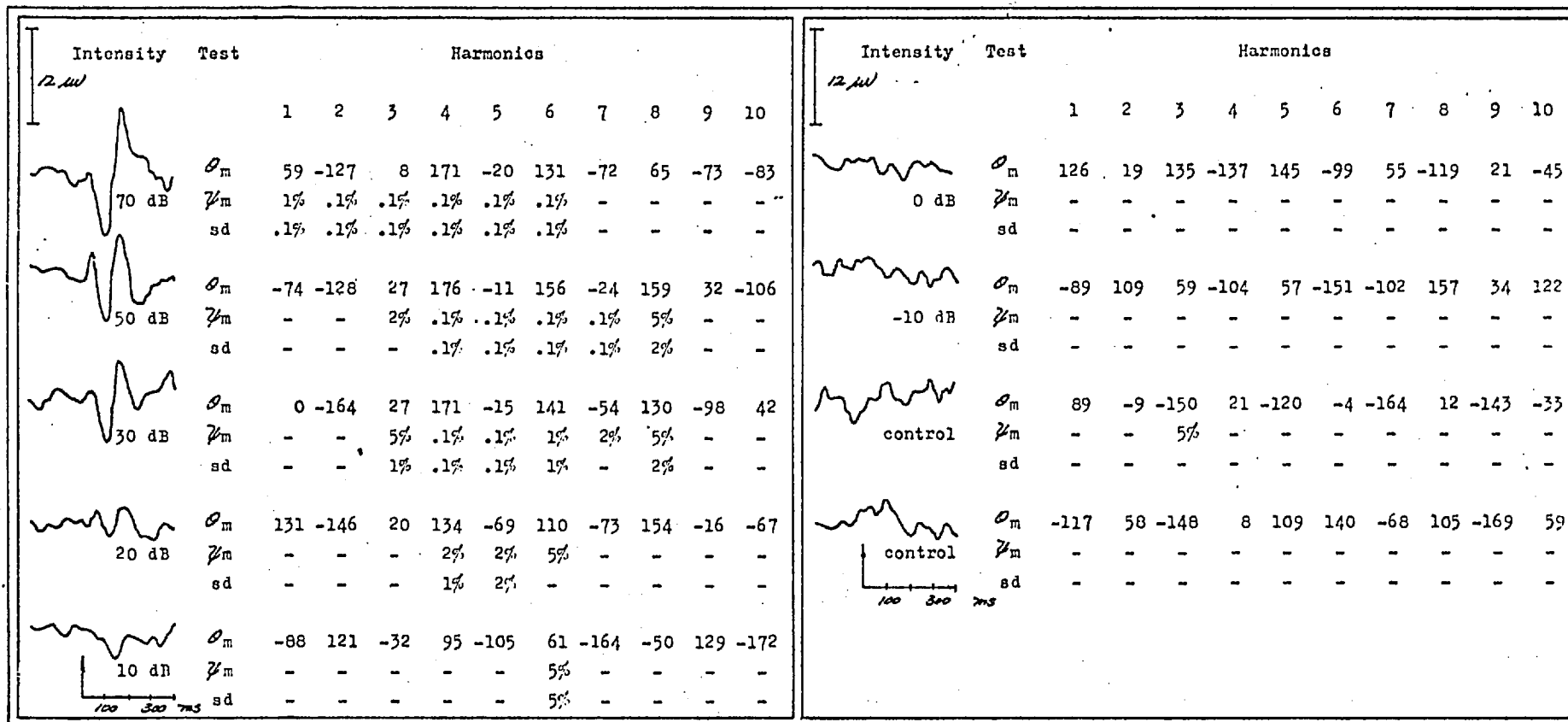


Table 4-xcvi. Subject VM, F, at 1 kHz.

Intensity	Test	Harmonics									
		1	2	3	4	5	6	7	8	9	10
12 $\mu$ V 60 dB	$O_m$	-76	-168	18	176	-40	140	-10	-172	15	115
	$\psi_m$	-	-	1%	.1%	.1%	.1%	2%	-	-	-
	sd	-	-	2%	.1%	.1%	.1%	5%	-	-	-
40 dB	$O_m$	-77	-171	45	-178	-35	132	-91	123	-7	-8
	$\psi_m$	-	-	2%	.1%	.1%	.1%	-	-	-	-
	sd	-	-	2%	.1%	.1%	.1%	5%	-	-	-
20 dB	$O_m$	-93	87	-61	105	-89	63	-110	33	-118	-22
	$\psi_m$	5%	-	-	-	-	-	5%	-	-	-
	sd	5%	-	-	-	-	-	5%	-	-	-
10 dB	$O_m$	-77	105	5	-130	63	-165	-18	156	-13	-114
	$\psi_m$	-	-	-	-	-	-	-	-	-	-
	sd	-	-	-	-	-	-	-	-	-	-
0 dB	$O_m$	-57	170	59	-80	86	-127	122	-95	81	-61
	$\psi_m$	-	-	-	-	-	-	-	-	-	-
	sd	-	-	-	-	-	-	-	-	-	-

Intensity	Test	Harmonics									
		1	2	3	4	5	6	7	8	9	10
12 $\mu$ V -10 dB	$O_m$	-55	-105	37	-154	-11	-39	-162	39	-112	147
	$\psi_m$	-	-	-	-	-	-	1%	2%	-	-
	sd	-	-	-	-	-	-	1%	2%	-	-
-20 dB	$O_m$	-159	-63	121	11	-169	-102	37	135	-54	133
	$\psi_m$	-	-	-	-	-	-	-	-	2%	-
	sd	-	-	-	5%	-	-	-	-	2%	-
control	$O_m$	-88	139	146	40	-114	-62	148	-95	96	-55
	$\psi_m$	-	-	-	-	-	-	-	-	-	-
	sd	-	-	-	-	-	-	-	-	5%	-
control	$O_m$	-167	47	-128	119	-31	153	-98	-16	157	3
	$\psi_m$	-	-	-	-	-	-	-	-	-	-
	sd	-	-	-	-	-	-	-	-	-	-

Table 4-xcvii. Subject SBa, F, age 20, at 500 Hz.

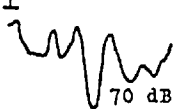
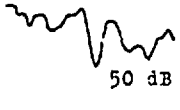
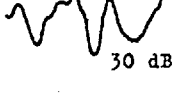
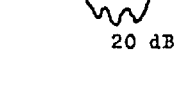
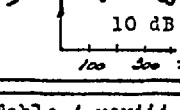

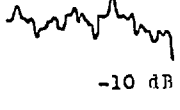

Intensity	Test	Harmonics									
		1	2	3	4	5	6	7	8	9	10
 70 dB	$\phi_m$	-47	175	-7	158	-38	140	-15	129	-137	-39
	$\psi_m$	-	-	-	.1%	.1%	.1%	-	-	-	-
	sd	-	-	-	.1%	.1%	.1%	-	-	-	-
	$\phi_m$	-78	123	-4	171	-11	163	-26	-174	32	-151
	$\psi_m$	-	-	2%	2%	.1%	.1%	.1%	-	2%	5%
sd	-	-	2%	-	.1%	.1%	.1%	-	2%	2%	
 50 dB	$\phi_m$	-78	113	9	-160	-4	159	-11	138	-132	46
	$\psi_m$	-	-	5%	5%	2%	2%	2%	-	-	-
	sd	-	-	2%	2%	5%	2%	1%	2%	-	-
 30 dB	$\phi_m$	-52	112	-61	131	-39	-162	3	128	-40	156
	$\psi_m$	2%	-	-	-	-	-	-	-	-	-
	sd	2%	-	-	-	-	-	-	-	-	5%
 20 dB	$\phi_m$	-77	102	-85	121	18	32	-144	64	132	-86
	$\psi_m$	-	-	-	-	-	-	-	-	-	-
	sd	-	-	-	-	-	-	-	-	-	-
 10 dB	$\phi_m$	-63	135	-136	-14	99	-53	-152	30	-167	48
	$\psi_m$	-	-	-	-	-	-	-	-	2%	-
	sd	-	-	-	-	-	-	-	-	2%	-
	$\phi_m$	176	70	-84	146	-45	171	-40	-169	-41	-117
	$\psi_m$	-	-	-	-	-	-	-	-	-	-
sd	-	-	-	-	-	-	-	-	-	-	
 0 dB	$\phi_m$	-47	44	93	-116	99	-104	24	-110	66	-107
	$\psi_m$	-	-	-	-	-	2%	-	-	-	-
	sd	-	-	-	-	-	2%	-	-	-	-
 -10 dB	$\phi_m$	-164	107	11	155	-112	141	-150	-30	149	-64
	$\psi_m$	-	-	-	-	-	-	-	-	5%	-
	sd	-	-	-	-	-	-	-	-	-	2%
 control	$\phi_m$	-	-	-	-	-	-	-	-	-	-
	$\psi_m$	-	-	-	-	-	-	-	-	-	-
	sd	-	-	-	-	-	-	-	-	-	-

Table 4-xcviii. Subject SBa, F, age 20, at 2 kHz.



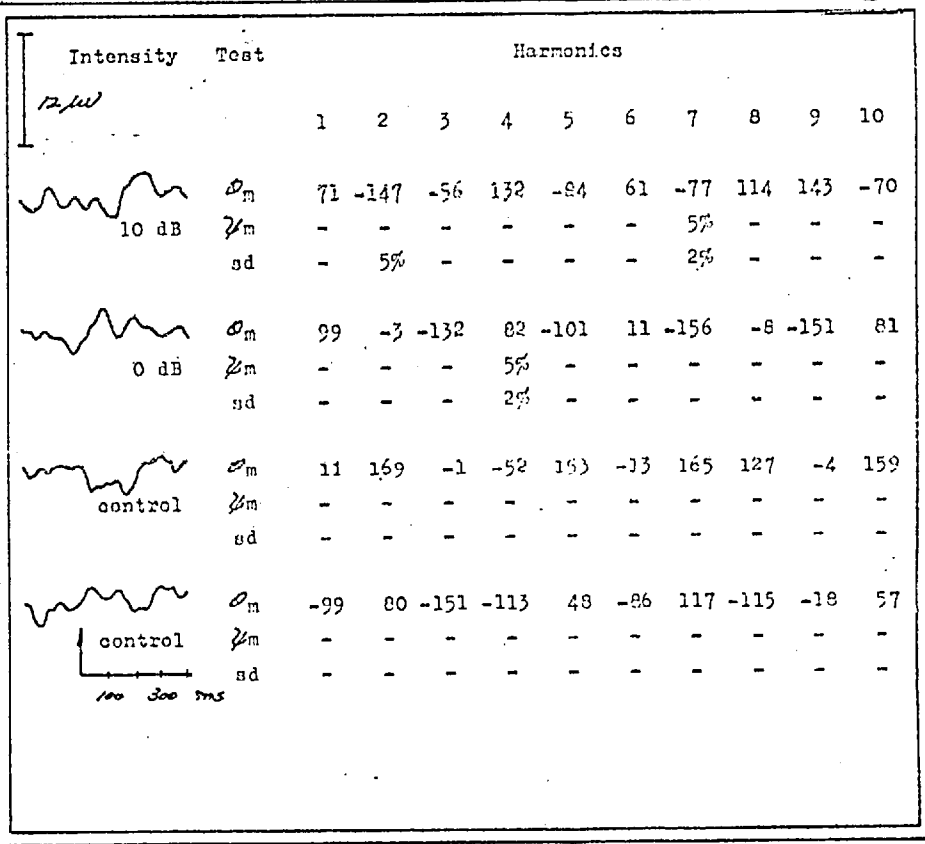
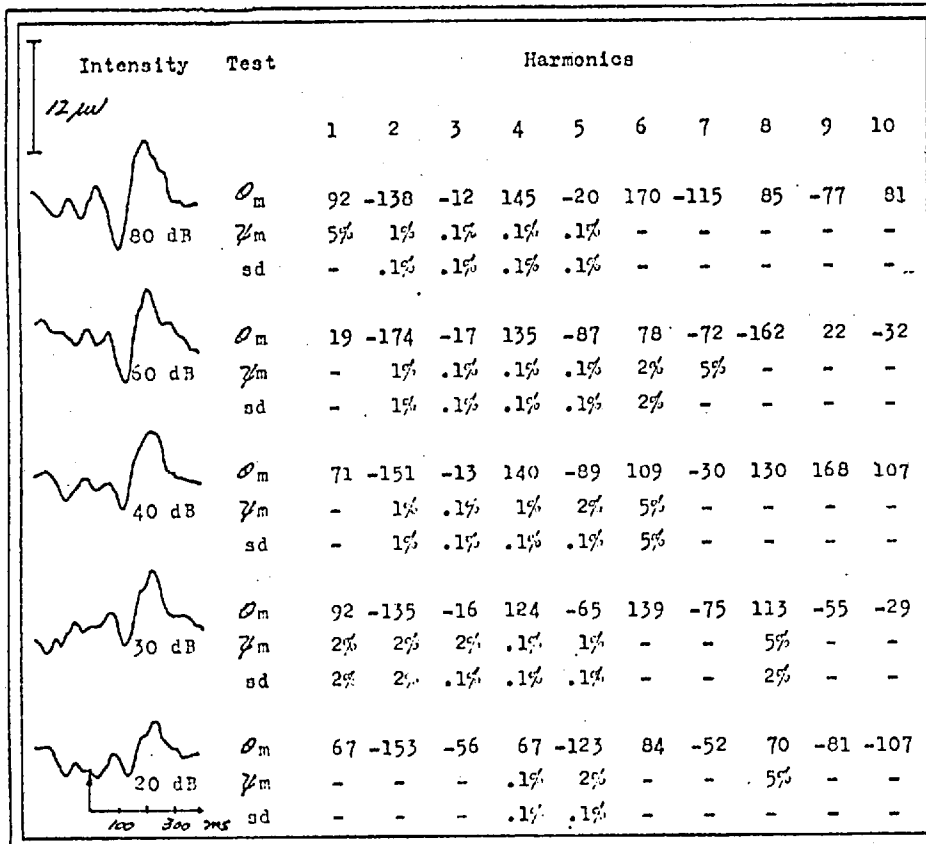


Table 4-xcix. Subject PC, M, age 24, at 4 kHz.

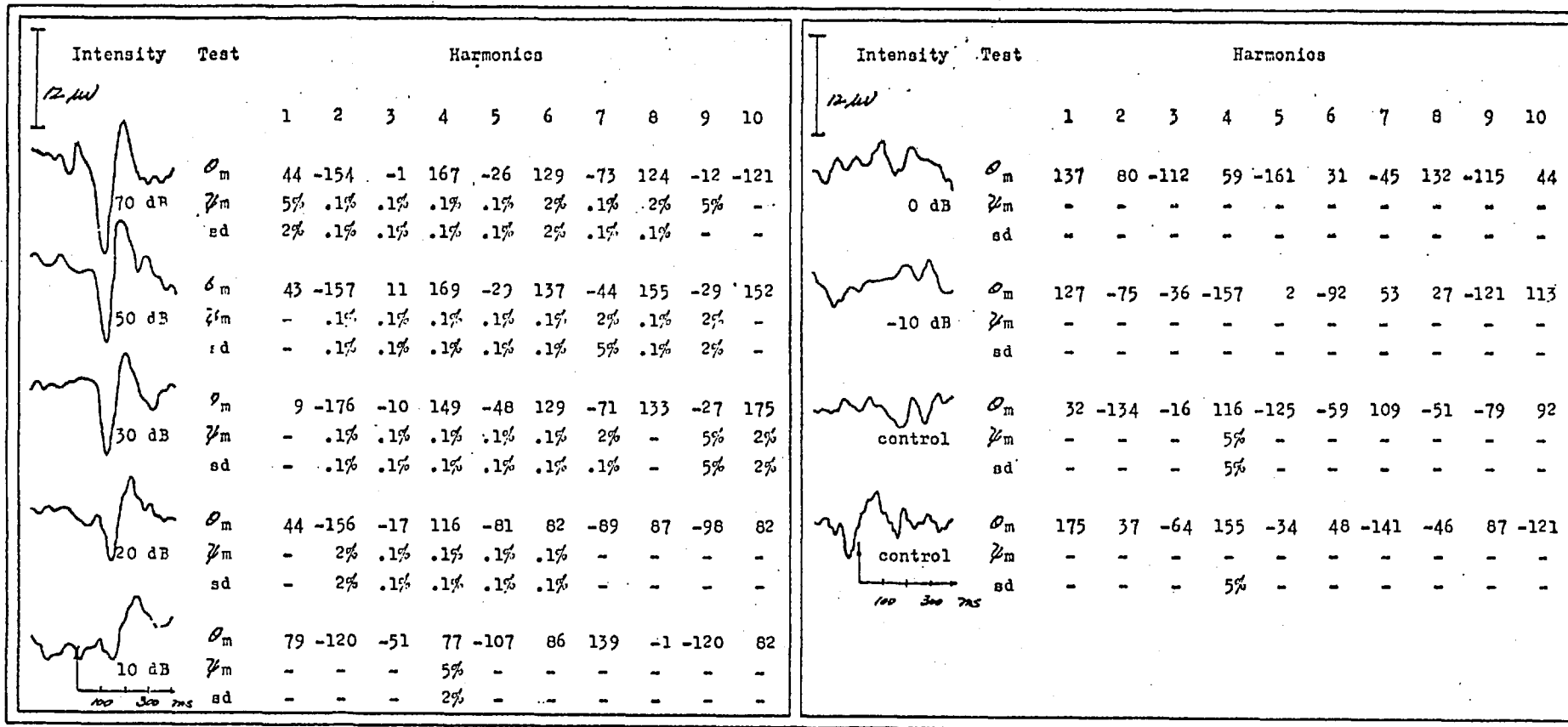


Table 4-c. Subject PC, M, age 24, at 1 kHz.

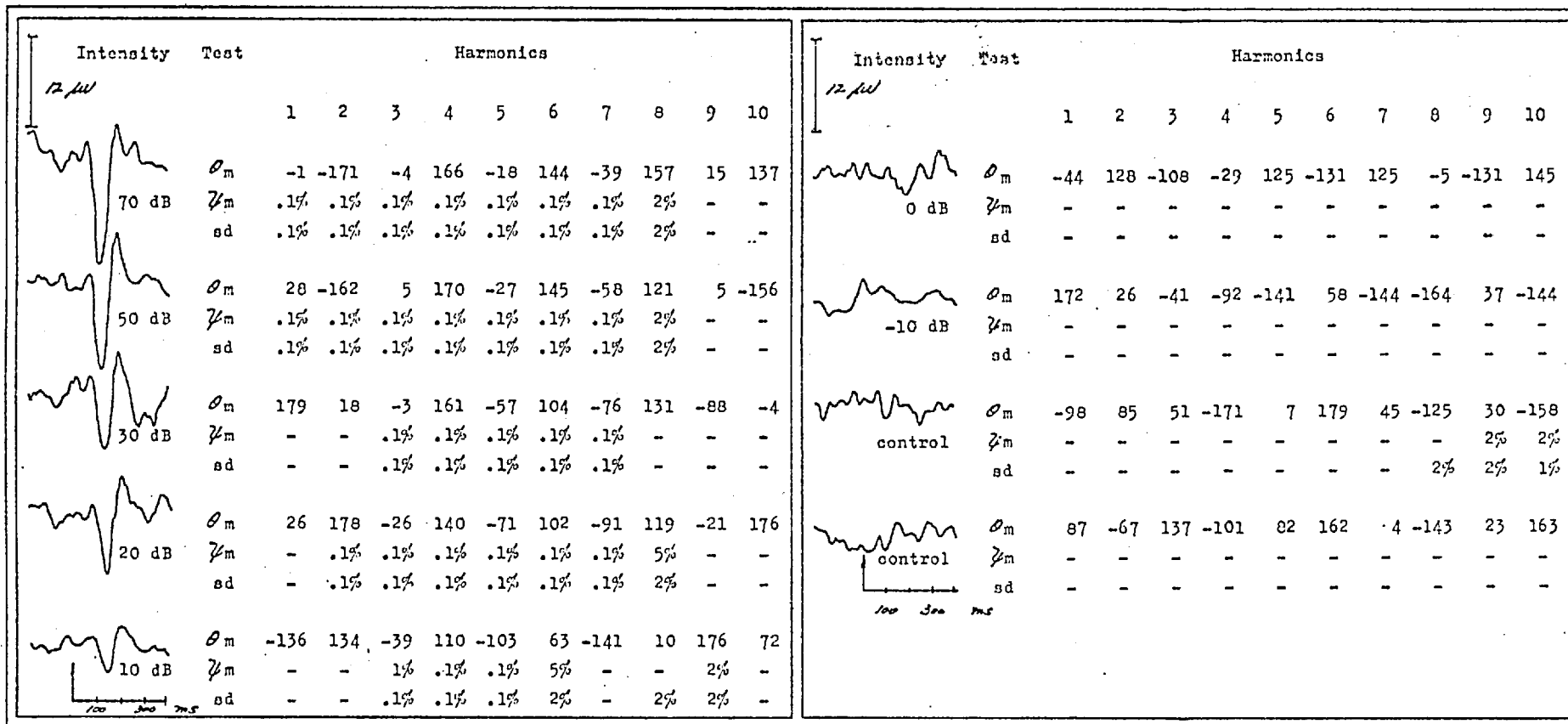


Table 4-ci. Subject SA, M, age 28, at 500 Hz.

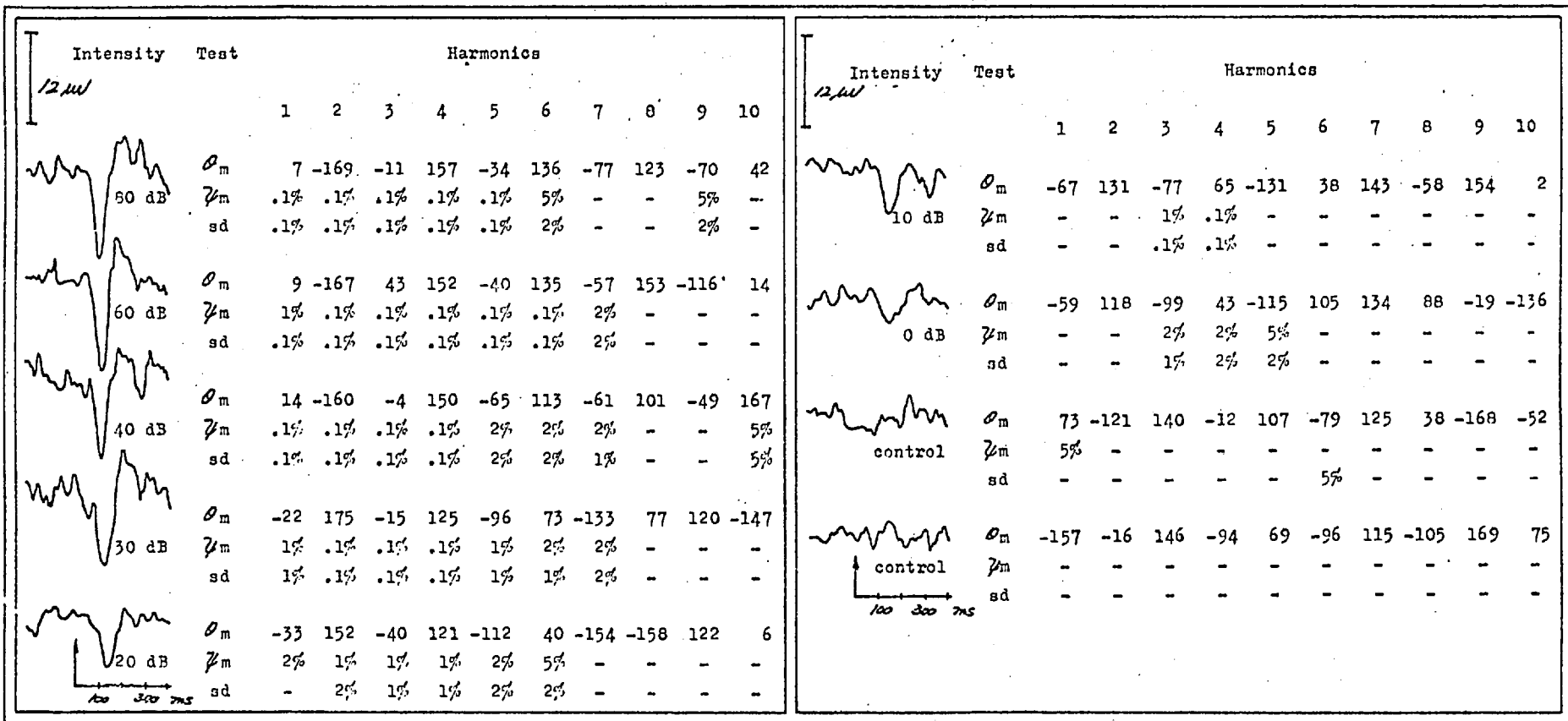


Table 4-cii. Subject SA, M, age 28, at 2 kHz.

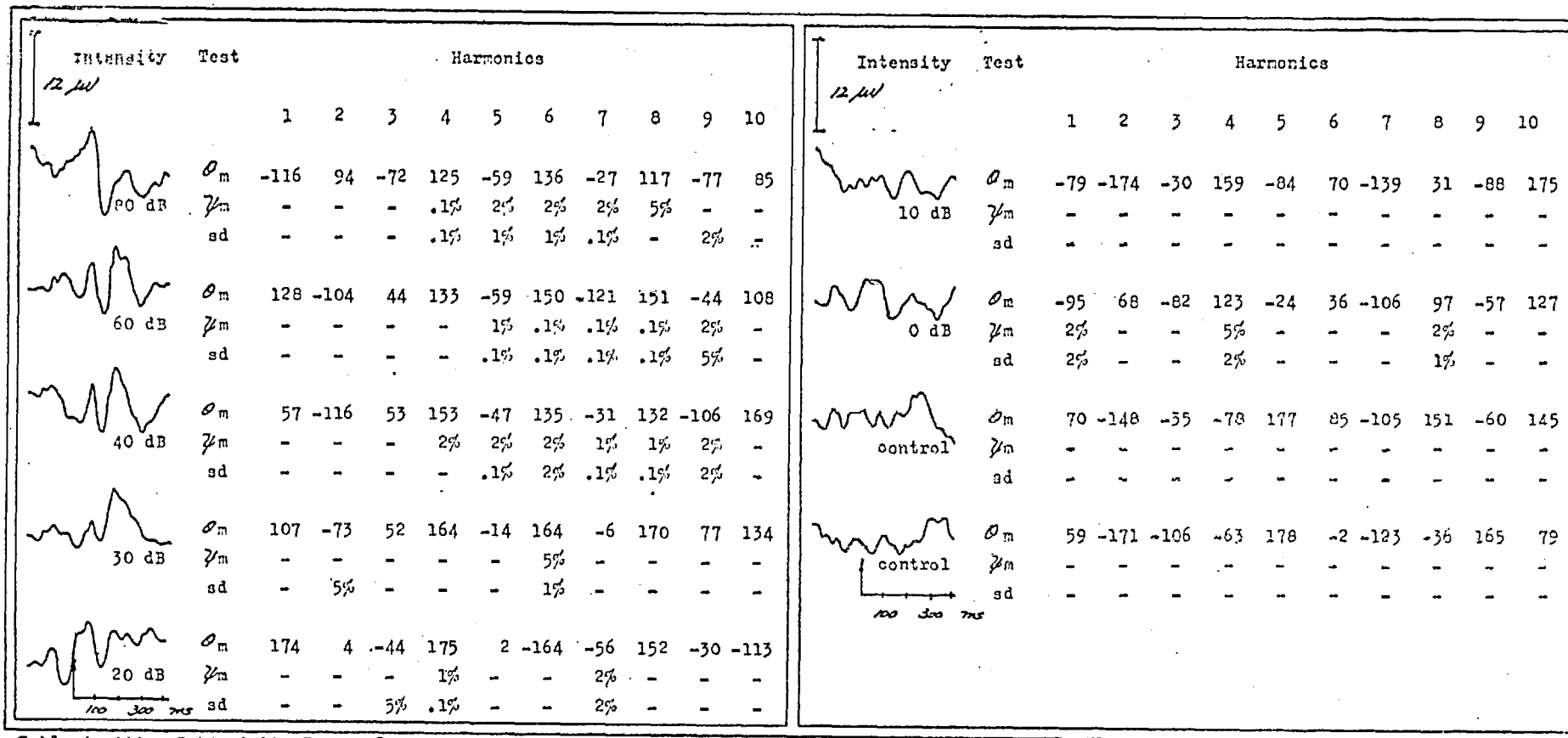


Table 4-ciii. Subject LS, F, age 20, at 4 kHz.

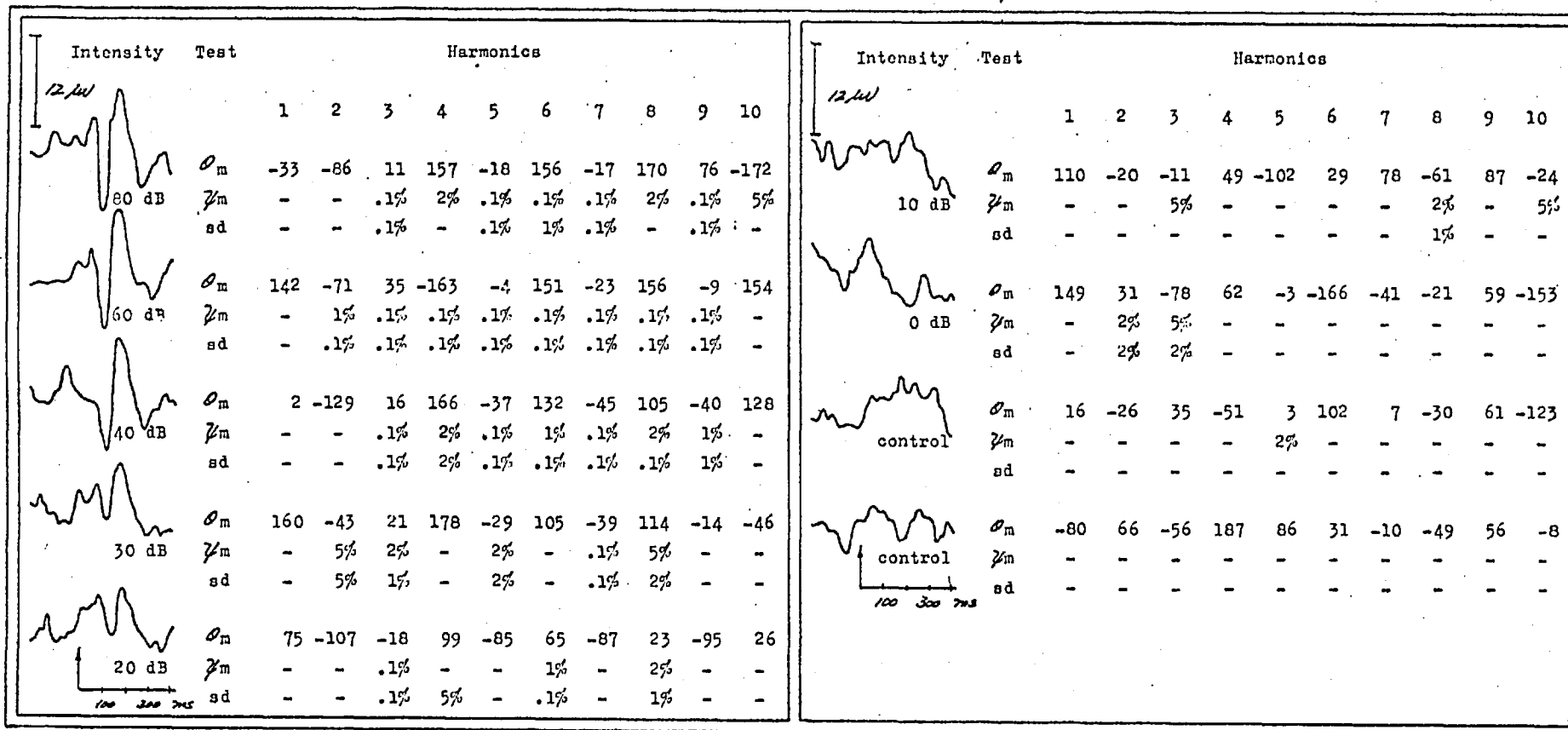


Table 4-civ. Subject LS, F, age 20, at 1 kHz.

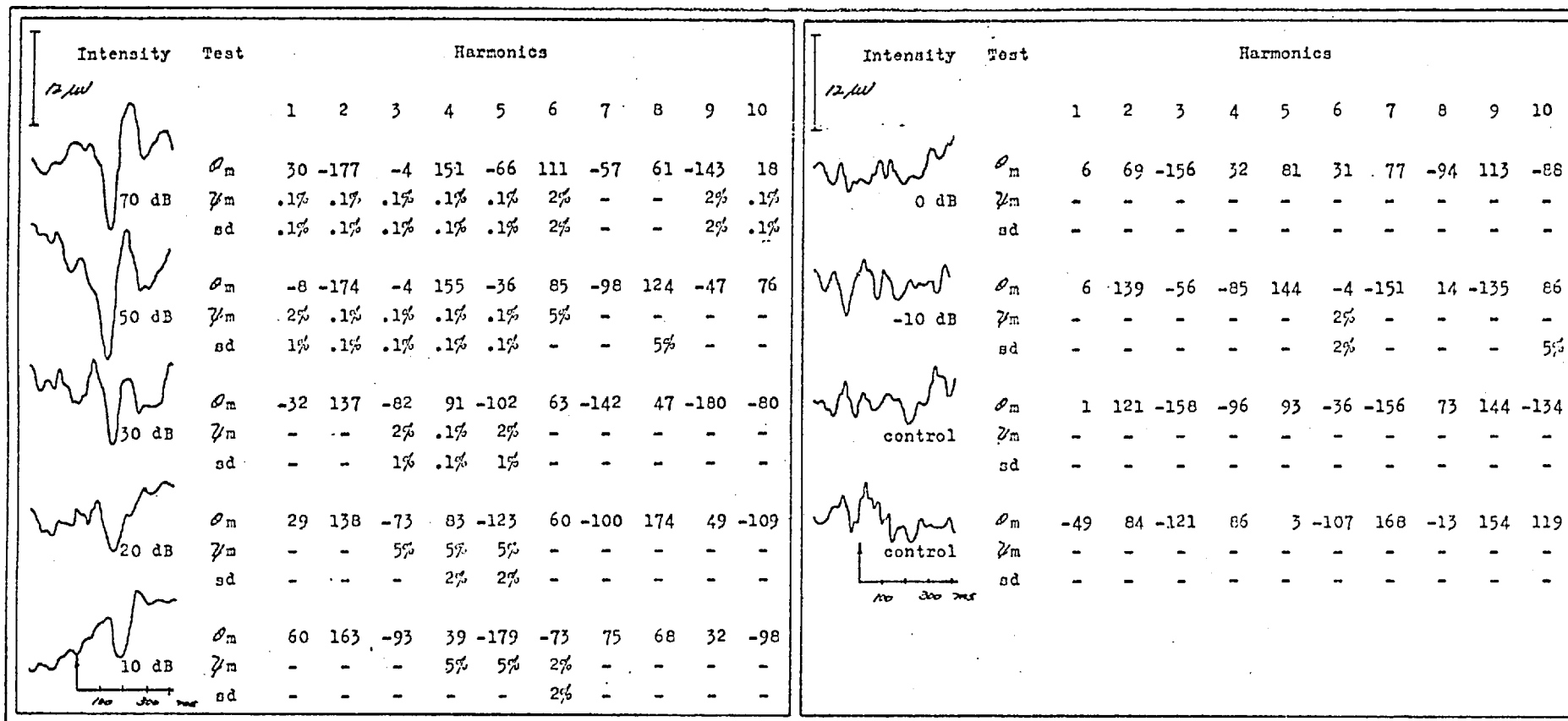
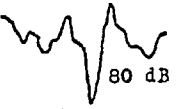

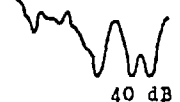




Table 4-cv. Subject DF, F, age 20, at 500 Hz.

Intensity <i>12 μV</i>	Test	Harmonics									
		1	2	3	4	5	6	7	8	9	10
 80 dB	$\phi_m$	-38	158	-39	120	-75	45	-145	11	177	18
	$\psi_m$	-	1%	.1%	.1%	.1%	-	5%	-	-	-
	sd	-	.1%	.1%	.1%	.1%	2%	2%	-	-	-
 60 dB	$\phi_m$	159	163	-38	123	-77	32	132	-45	-177	38
	$\psi_m$	-	-	5%	.1%	-	-	-	2%	5%	2%
	sd	-	-	-	.1%	-	-	-	1%	2%	1%
 40 dB	$\phi_m$	-81	132	-29	132	-118	9	105	46	-164	-68
	$\psi_m$	-	-	2%	-	-	-	-	-	-	-
	sd	-	-	-	-	-	-	-	-	-	-
 30 dB	$\phi_m$	176	179	-21	120	-90	58	12	-141	47	120
	$\psi_m$	-	-	2%	2%	-	-	-	-	-	-
	sd	-	-	1%	1%	-	-	-	-	-	-
 20 dB	$\phi_m$	21	155	-73	77	-130	39	40	-154	19	115
	$\psi_m$	-	-	-	-	-	-	-	-	-	-
	sd	-	-	-	-	-	-	-	-	-	-

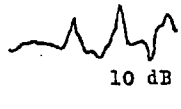
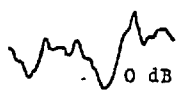


Intensity <i>12 μV</i>	Test	Harmonics									
		1	2	3	4	5	6	7	8	9	10
 10 dB	$\phi_m$	91	178	-28	142	-41	-28	129	-76	-33	65
	$\psi_m$	-	-	-	5%	-	-	-	-	-	-
	sd	-	-	-	5%	-	-	5%	-	-	-
 0 dB	$\phi_m$	32	158	-46	69	-127	-98	-44	-148	98	13
	$\psi_m$	-	-	-	-	-	-	-	-	-	-
	sd	-	-	-	-	-	-	-	-	-	-
 control	$\phi_m$	-29	91	-96	89	-60	98	-99	-62	7	146
	$\psi_m$	-	-	-	-	-	-	-	-	-	-
	sd	-	-	-	-	-	5%	-	-	-	-
 control	$\phi_m$	76	-101	38	180	-9	71	-123	-159	51	7
	$\psi_m$	-	-	-	2%	-	-	-	-	-	-
	sd	-	-	-	2%	-	-	-	-	-	-

Table 4-cvi. Subject DF, F, age 20, at 2 kHz.



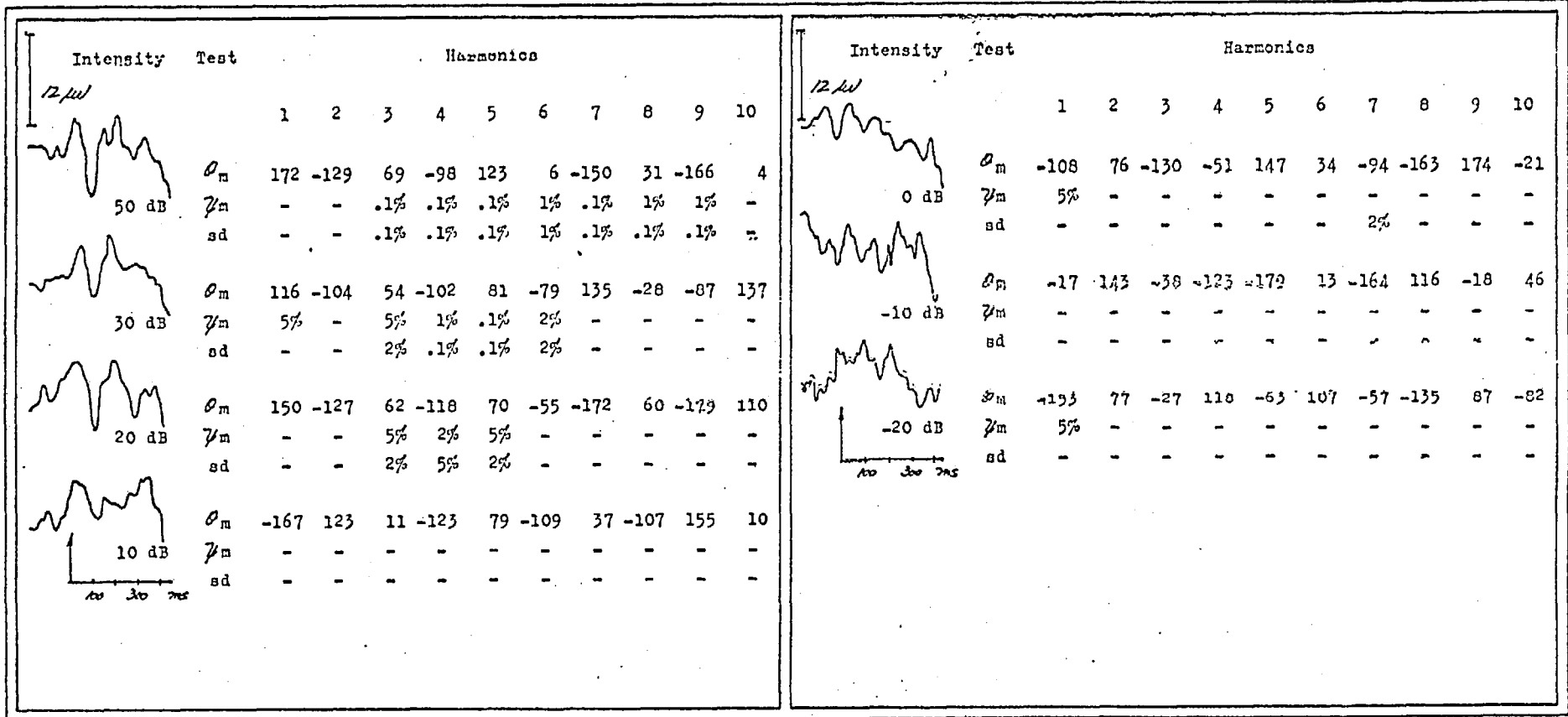


Table 4-cvii. Subject GP, M, age 18, at 500 Hz.

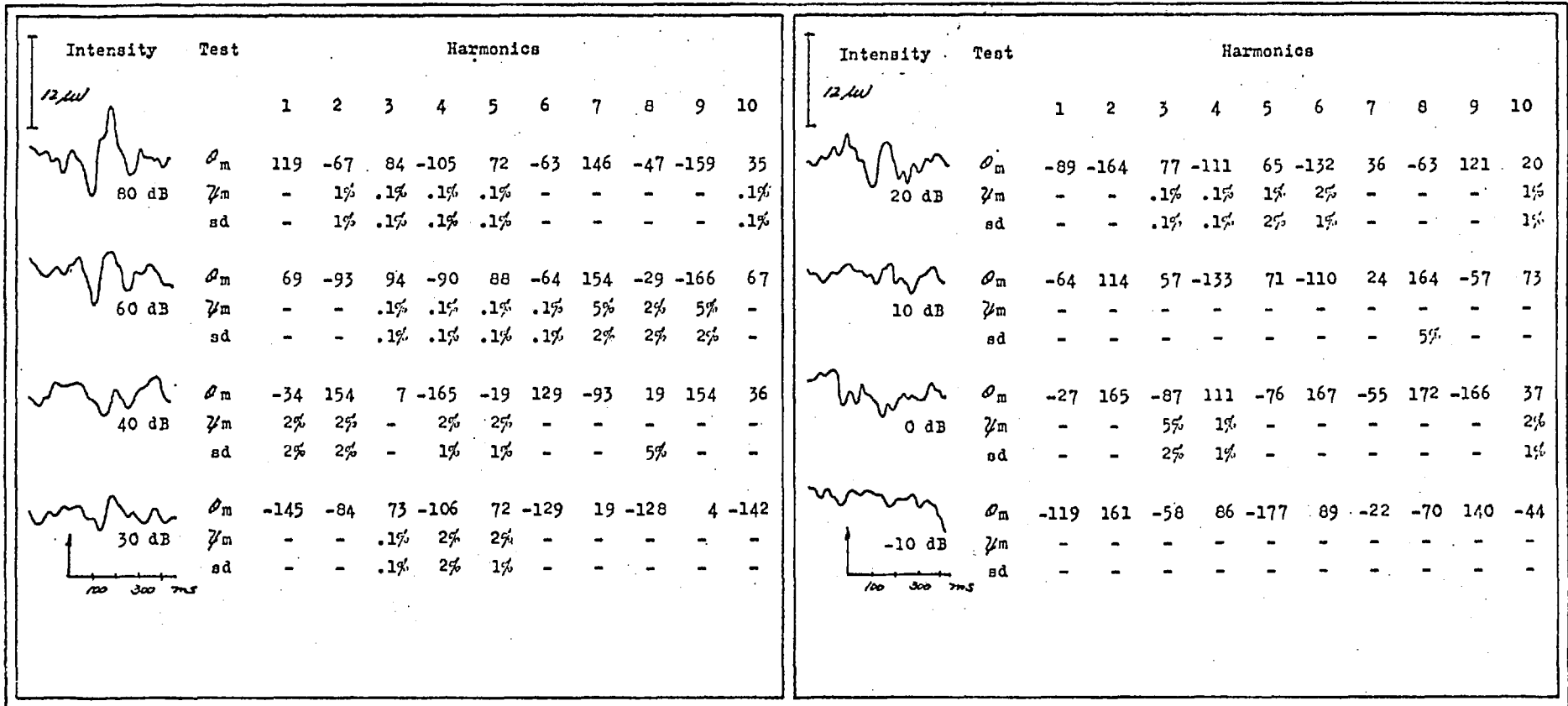


Table 4-oviii. Subject SH, F, age 20, at 2 kHz.

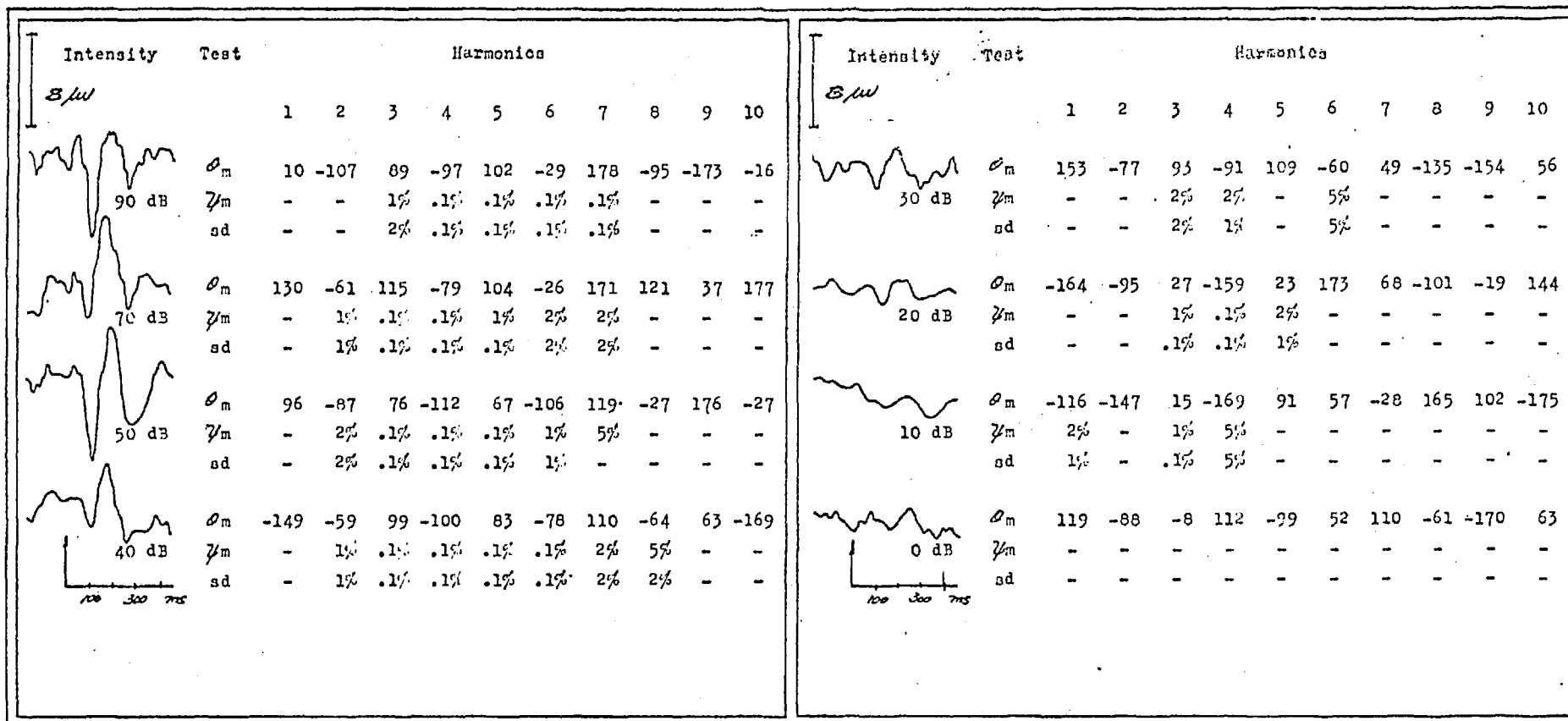


Table 4-cix. Subject RB, F, age 20, at 2 kHz.

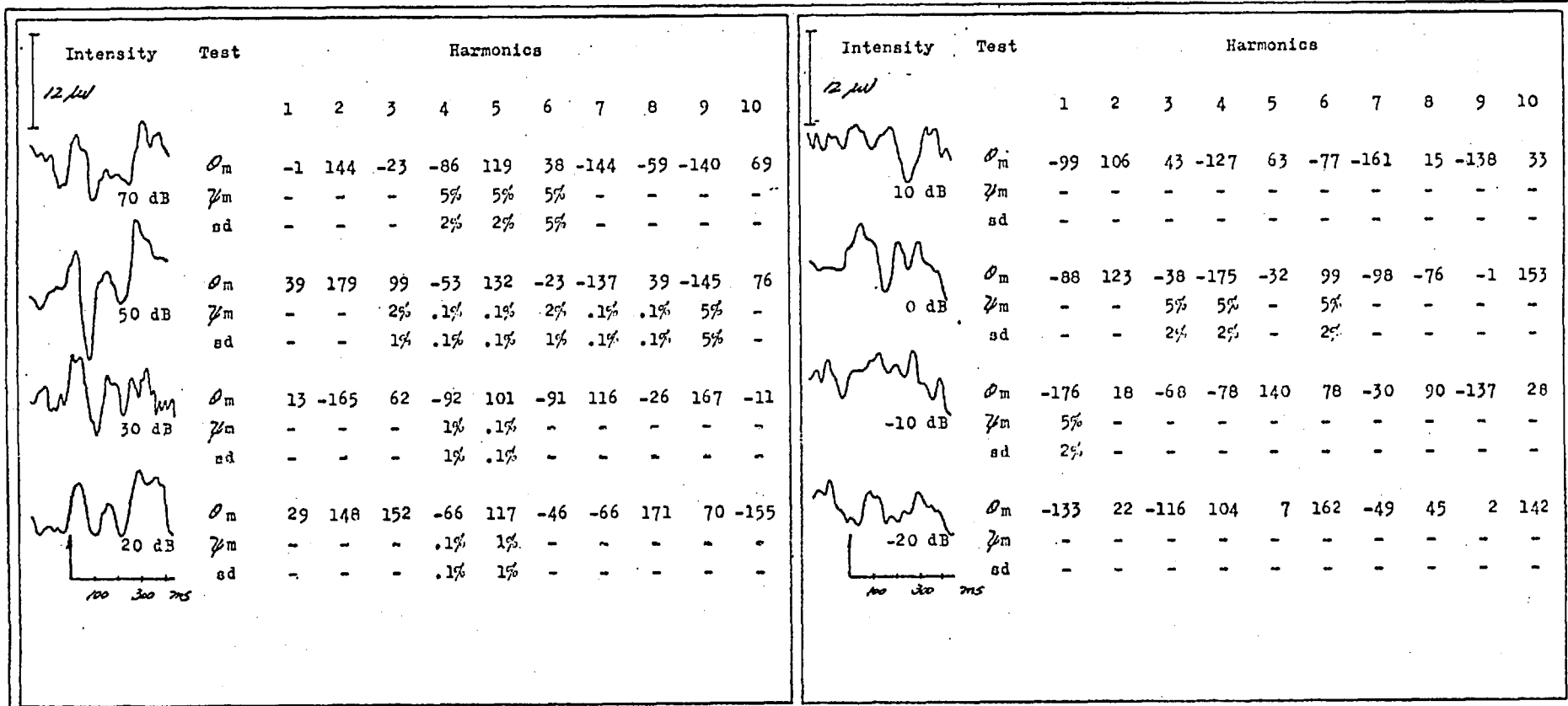


Table 4-cx. Subject EB, F, age 18, at 1 kHz.

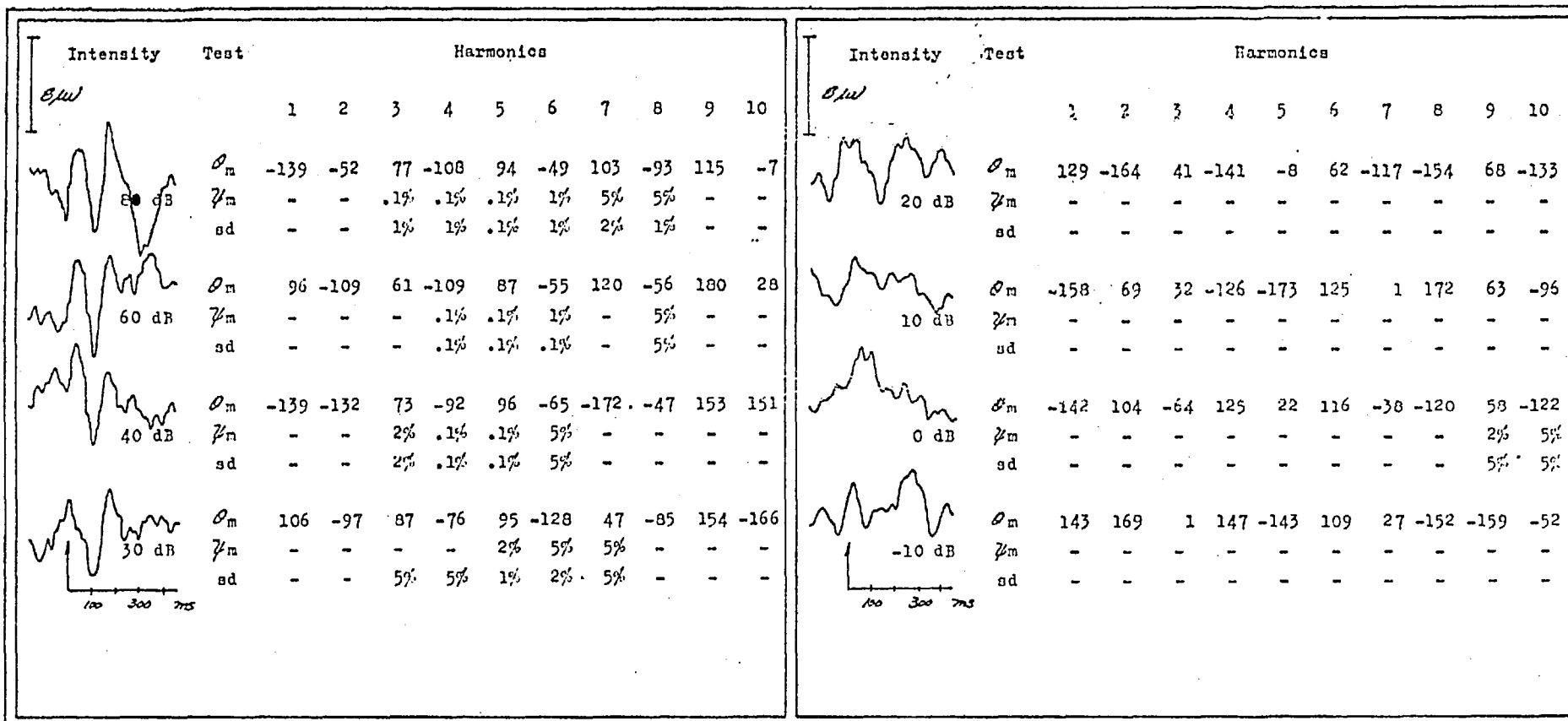


Table 4-cxi. Subject AP, F, age 20, at 4 kHz.

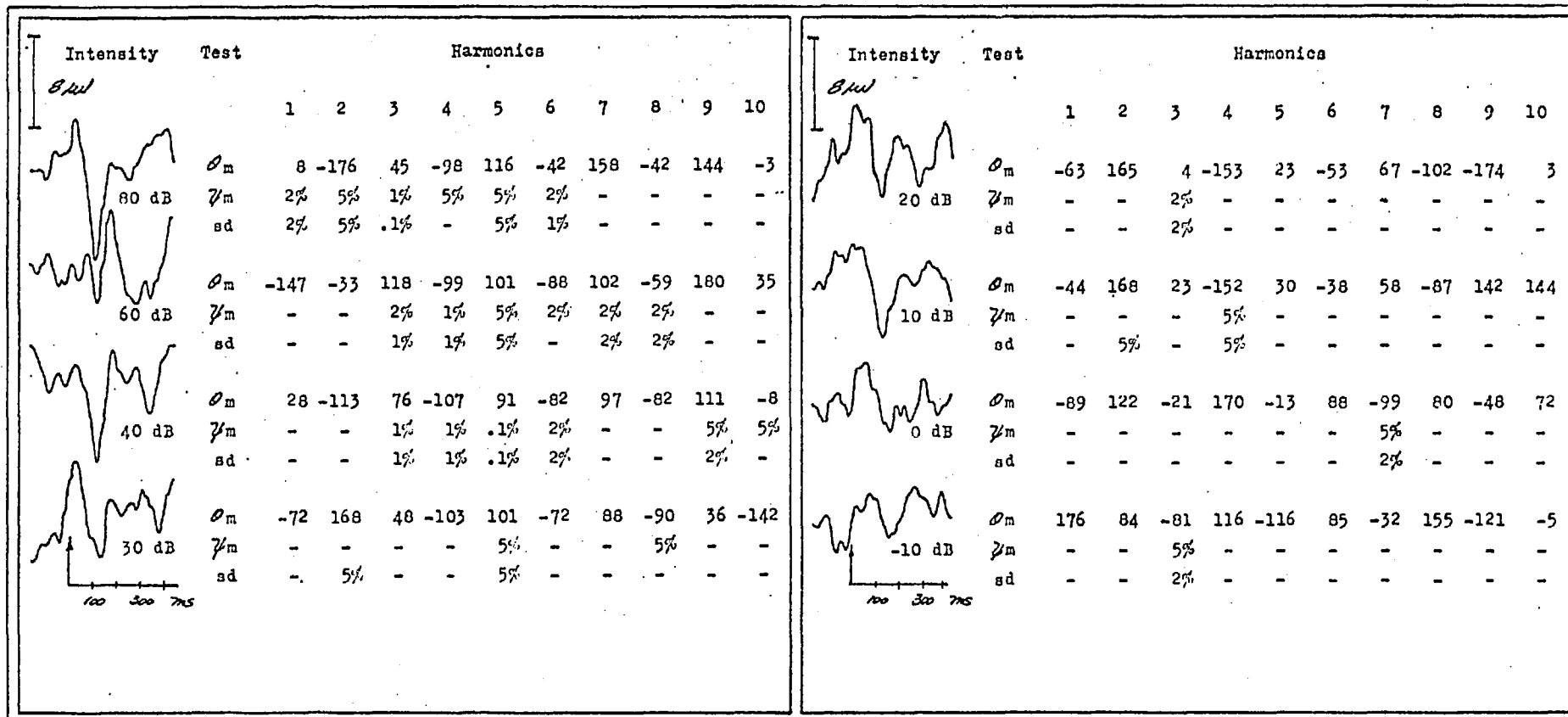


Table 4-cxii. Subject A<sup>2</sup>, F, age 20, at 1 kHz.

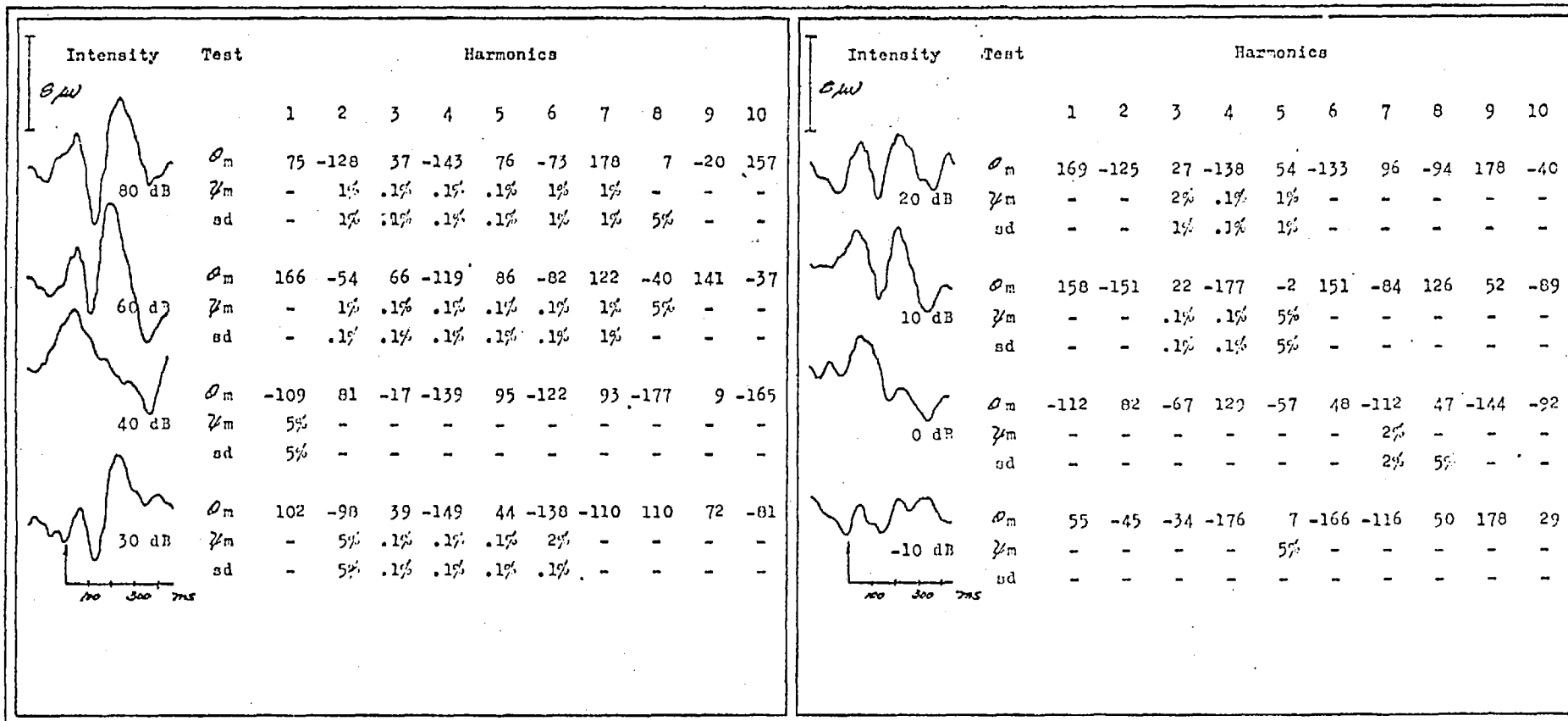
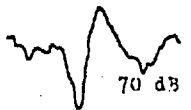

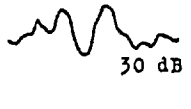
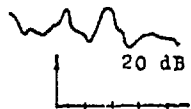


Table 4-cxiii. Subject GD, F, age 19, at 2 kHz.

Intensity <i>S<sub>μ</sub></i>	Test	Harmonics									
		1	2	3	4	5	6	7	8	9	10
70 dB 	<i>O<sub>m</sub></i>	134	-66	110	-57	151	103	-103	81	-89	161
	<i>μ<sub>m</sub></i>	5%	.1%	.1%	.1%	.1%	1%	5%	-	-	-
	<i>sd</i>	-	.1%	.1%	.1%	.1%	1%	5%	-	-	-
50 dB 	<i>O<sub>m</sub></i>	-177	-37	116	-69	135	-20	-162	7	111	-54
	<i>μ<sub>m</sub></i>	5%	2%	.1%	.1%	.1%	1%	5%	-	-	-
	<i>sd</i>	2%	1%	.1%	.1%	.1%	.1%	-	-	-	-
30 dB 	<i>O<sub>m</sub></i>	-159	-89	84	-93	109	-13	-47	153	-77	40
	<i>μ<sub>m</sub></i>	-	-	.1%	.1%	.1%	-	-	-	-	-
	<i>sd</i>	-	-	.1%	.1%	.1%	-	-	-	-	-
20 dB  100 300 ms	<i>O<sub>m</sub></i>	-129	-77	70	-114	62	81	-151	137	90	-109
	<i>μ<sub>m</sub></i>	-	-	2%	.1%	-	-	-	-	-	-
	<i>sd</i>	-	-	1%	.1%	-	-	-	-	-	-

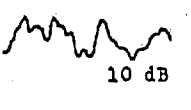
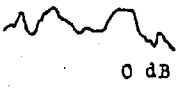
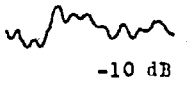
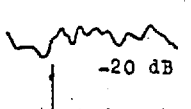
Intensity <i>S<sub>μ</sub></i>	Test	Harmonics									
		1	2	3	4	5	6	7	8	9	10
10 dB 	<i>O<sub>m</sub></i>	39	-133	58	-142	40	174	-62	-174	39	50
	<i>μ<sub>m</sub></i>	-	-	2%	.1%	-	-	-	-	-	-
	<i>sd</i>	-	-	2%	.1%	-	-	-	-	-	-
0 dB 	<i>O<sub>m</sub></i>	-170	170	-9	7	177	39	152	-46	107	135
	<i>μ<sub>m</sub></i>	-	5%	2%	-	-	-	-	-	-	-
	<i>sd</i>	-	-	2%	-	-	-	-	-	-	-
-10 dB 	<i>O<sub>m</sub></i>	-167	65	-103	-15	152	5	-21	172	149	26
	<i>μ<sub>m</sub></i>	-	-	-	-	-	-	-	-	-	5%
	<i>sd</i>	-	5%	-	-	-	-	-	-	-	2%
-20 dB  100 300 ms	<i>O<sub>m</sub></i>	143	-8	145	-54	159	26	-29	-154	161	-49
	<i>μ<sub>m</sub></i>	-	-	-	5%	-	-	-	-	-	-
	<i>sd</i>	-	-	-	5%	-	-	-	-	-	-

Table 4-cxiv. Subject GD, F, age 19, at 500 Hz.



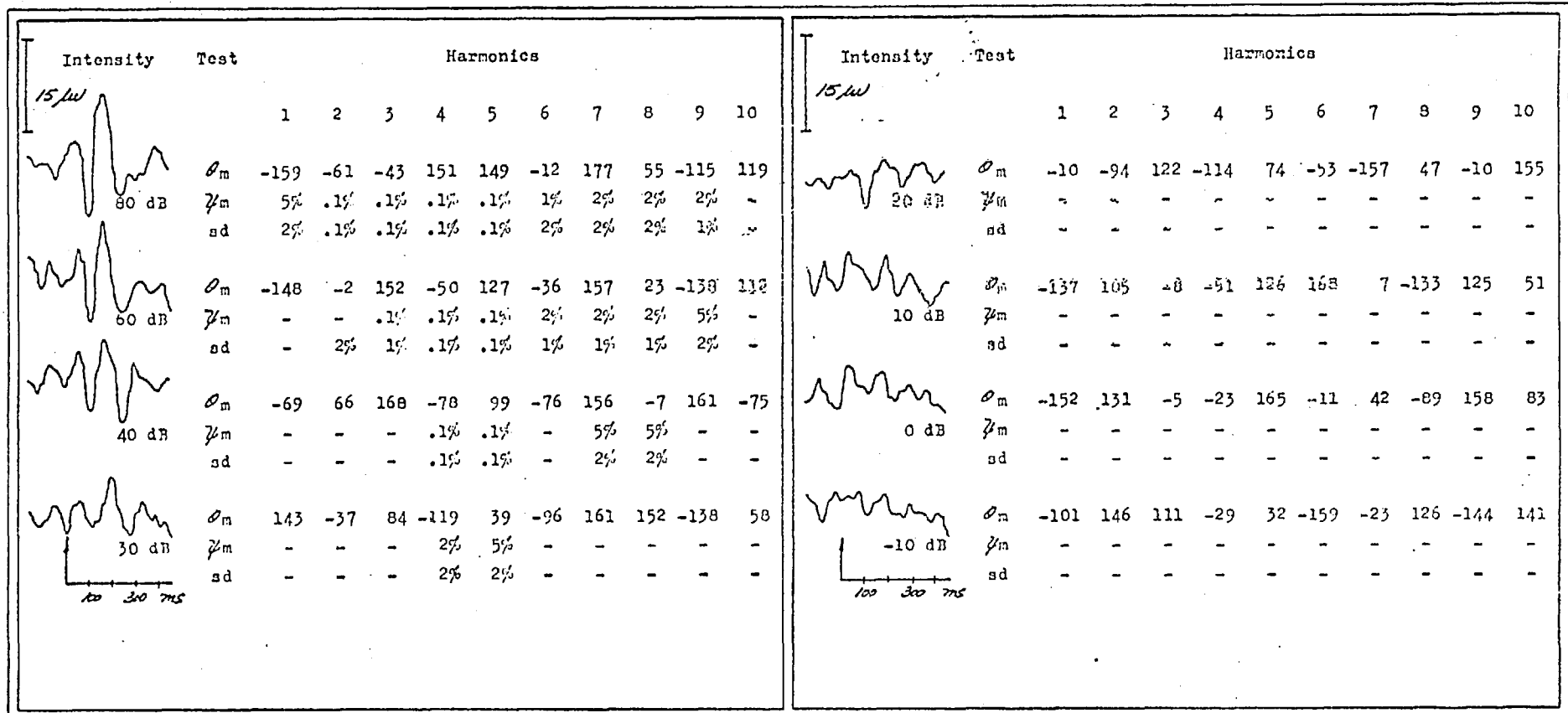


Table 4-exv. Subject KC, F, age 20, at 1 kHz.

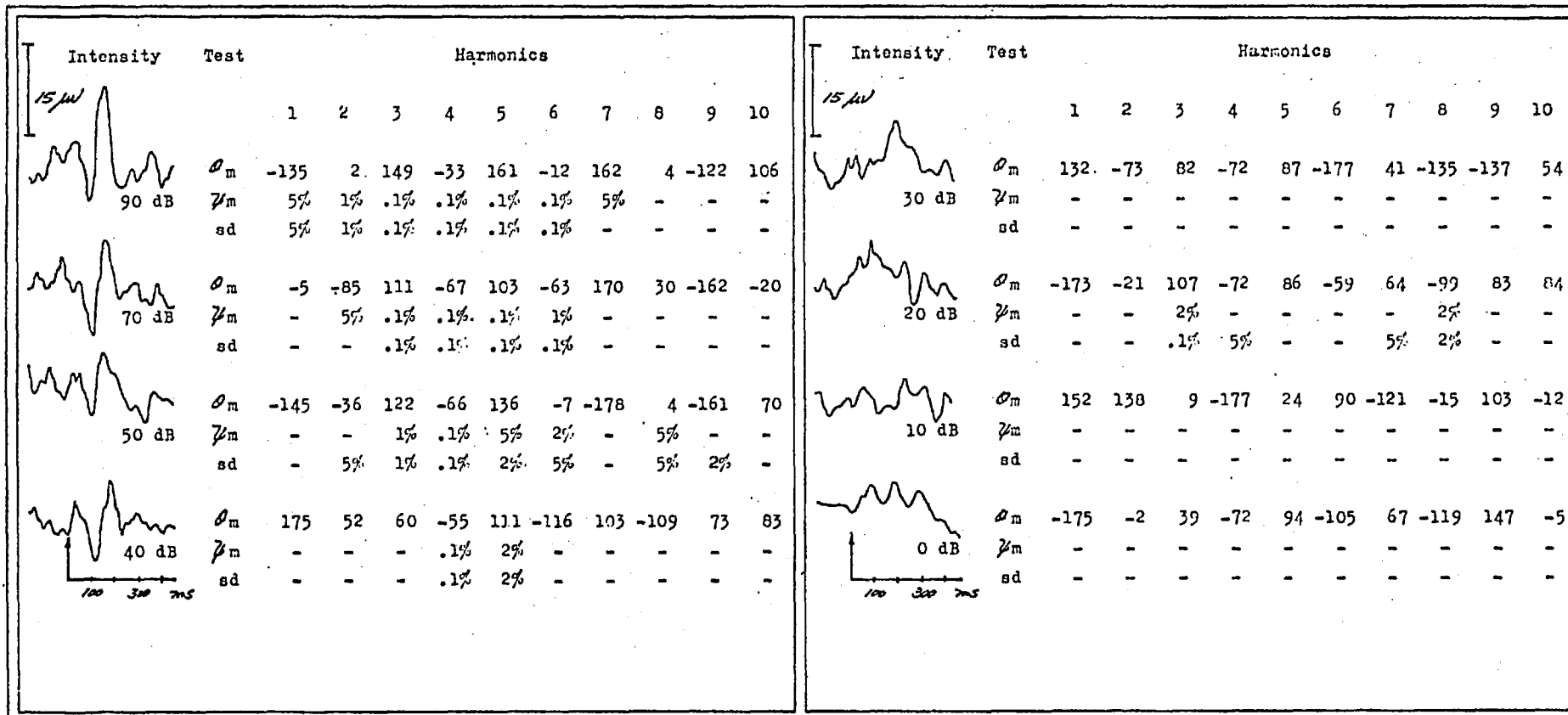


Table 4-orvi. Subject KC, F, age 20, ut 4 kHz.

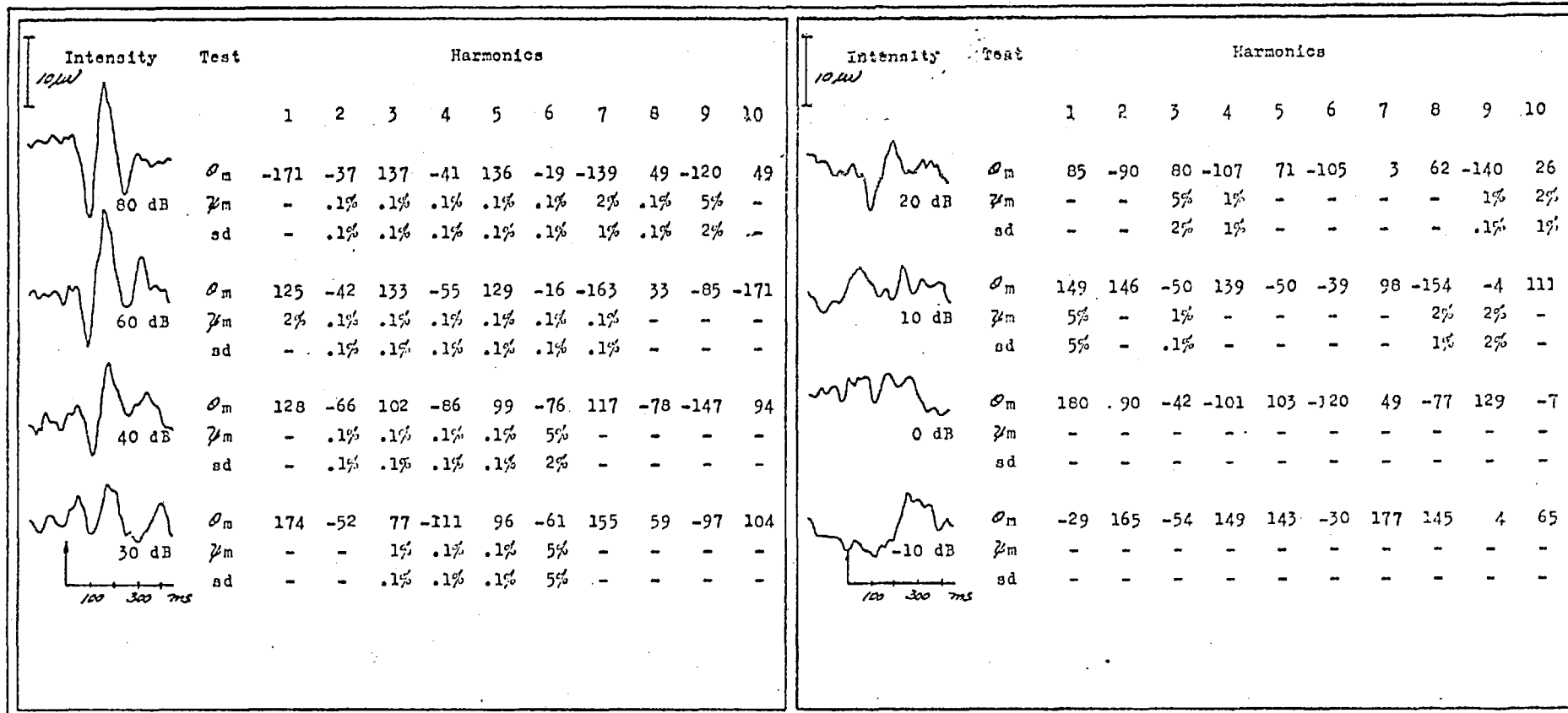


Table 4-cxvii. Subject SC, F, age 22, at 2 kHz.

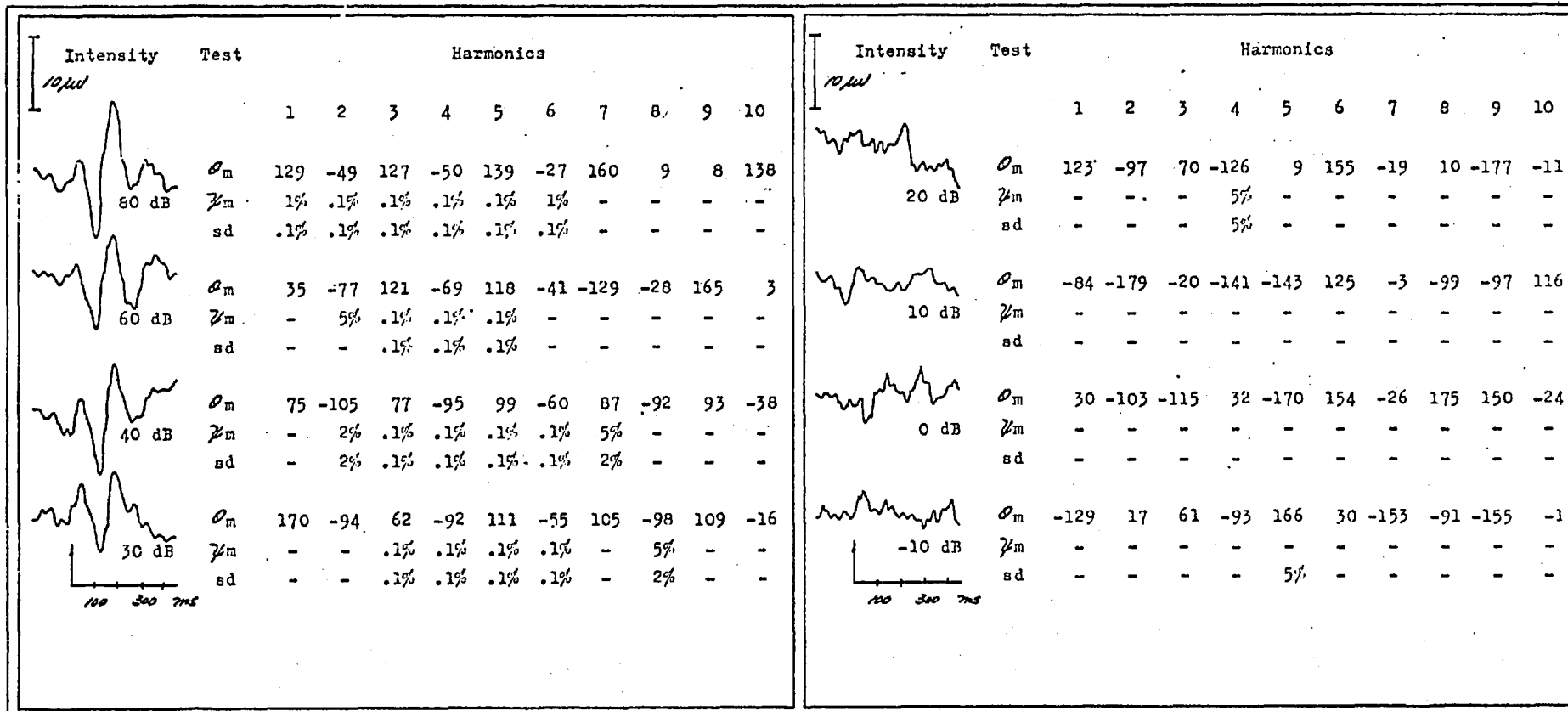
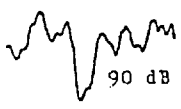
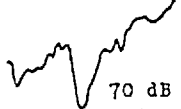
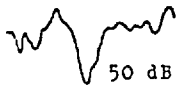
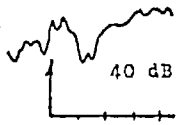
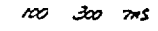


Table 4-cxviii. Subject SC, F, age 22, at 500 Hz.

Intensity <i>10 μV</i>	Test	Harmonics									
		1	2	3	4	5	6	7	8	9	10
 90 dB	$\phi_m$	12	-150	46	-116	89	-73	113	111	-87	125
	$\psi_m$	5%	-	.1%	5%	1%	.1%	-	-	-	-
	sd	-	-	.1%	5%	.1%	.1%	-	-	-	-
 70 dB	$\phi_m$	30	-161	42	-101	89	-72	129	-45	97	125
	$\psi_m$	5%	2%	1%	1%	.1%	-	-	-	-	-
	sd	1%	2%	.1%	1%	.1%	-	-	-	-	-
 50 dB	$\phi_m$	4	-167	34	-114	61	-129	78	-162	-10	102
	$\psi_m$	5%	1%	2%	2%	-	-	-	-	-	-
	sd	2%	.1%	2%	1%	-	-	-	-	-	-
 40 dB	$\phi_m$	53	-151	9	-145	80	-58	132	11	-130	89
	$\psi_m$	-	-	5%	2%	-	-	-	-	-	-
	sd	-	-	5%	1%	-	-	-	-	-	-
											

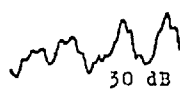

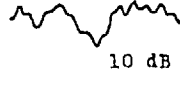

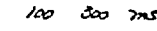
Intensity <i>10 μV</i>	Test	Harmonics									
		1	2	3	4	5	6	7	8	9	10
 30 dB	$\phi_m$	-7	-151	24	-165	4	-36	154	-54	145	44
	$\psi_m$	-	-	5%	5%	-	-	-	-	-	-
	sd	-	-	-	2%	-	-	-	-	-	-
 20 dB	$\phi_m$	9	89	-86	117	-91	72	-97	-168	-2	-156
	$\psi_m$	-	-	-	-	-	-	-	-	-	-
	sd	-	-	-	-	-	-	-	-	-	-
 10 dB	$\phi_m$	26	179	15	-132	-102	103	-96	87	26	-76
	$\psi_m$	-	1%	5%	-	-	-	-	5%	-	-
	sd	5%	.1%	-	-	-	-	-	-	-	-
 0 dB	$\phi_m$	49	134	-73	93	-154	8	156	-22	167	9
	$\psi_m$	-	-	5%	-	-	-	-	5%	-	-
	sd	-	-	2%	-	-	5%	-	5%	-	-
											

Table 4-cxix. Subject AR, M, age 19, at 1 kHz.

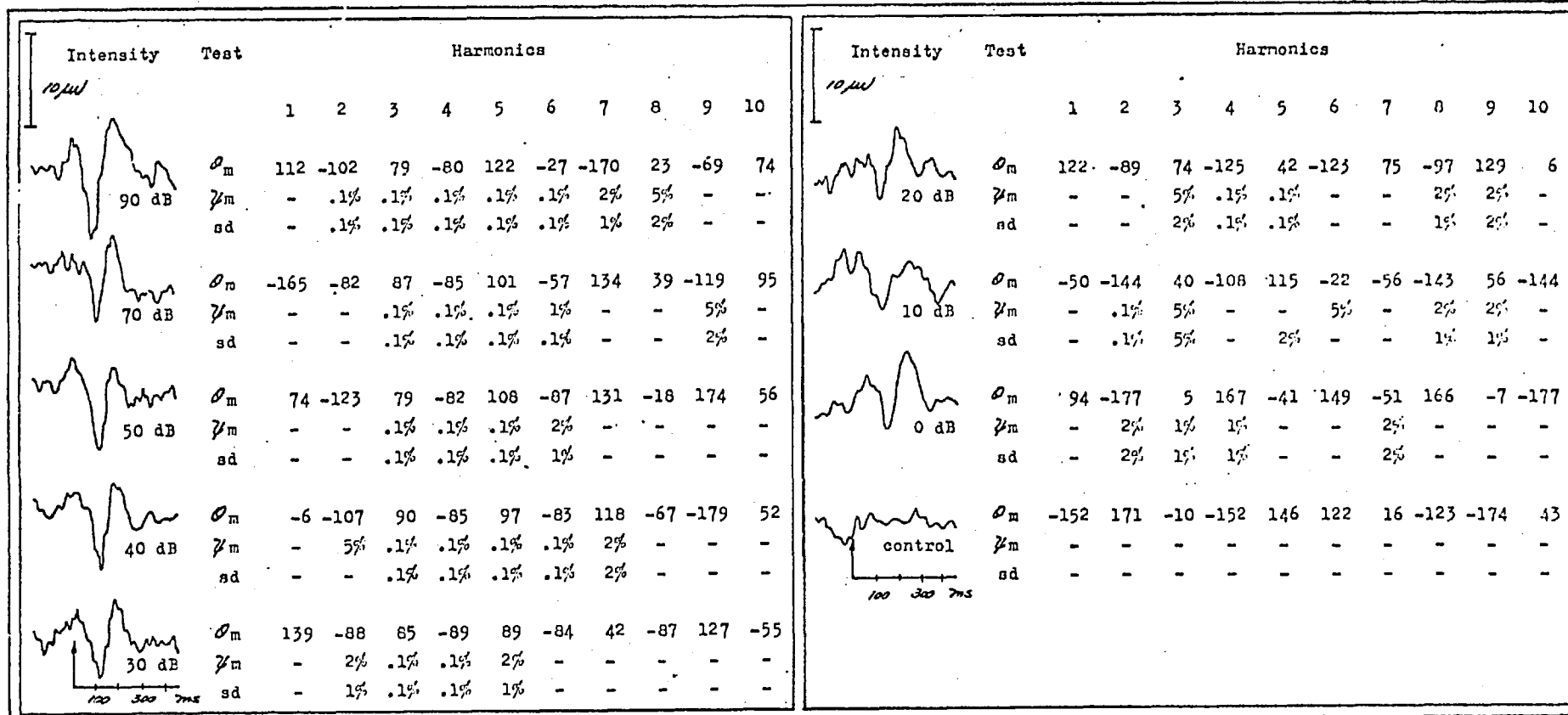


Table 4-cxx. Subject RW, M, age 19, at 4 kHz.

Intensity	Test	Harmonics									
		1	2	3	4	5	6	7	8	9	10
10 $\mu$ V											
50 dB	$\phi_m$	152	-84	119	-82	92	-55	116	-117	116	-32
	$\psi_m$	-	-	-	2%	5%	1%	-	-	-	-
	sd	-	-	-	1%	5%	2%	-	-	2%	-
30 dB	$\phi_m$	-39	141	106	-79	91	-106	49	89	116	-109
	$\psi_m$	-	-	-	-	.1%	2%	-	-	-	-
	sd	-	-	-	-	.1%	1%	-	-	-	-
20 dB	$\phi_m$	-92	162	31	-133	72	-114	42	172	-1	8
	$\psi_m$	-	-	.1%	.1%	2%	-	-	-	-	-
	sd	-	-	.1%	.1%	1%	-	-	-	-	-
10 dB	$\phi_m$	159	-23	-18	167	18	-124	-29	175	49	-128
	$\psi_m$	2%	-	5%	2%	-	-	-	-	-	-
	sd	1%	-	2%	2%	-	-	-	-	-	5%

Intensity	Test	Harmonics									
		1	2	3	4	5	6	7	8	9	10
10 $\mu$ V											
0 dB	$\phi_m$	-137	104	-64	53	-154	51	-94	34	-149	105
	$\psi_m$	-	-	-	-	5%	-	-	-	-	-
	sd	-	-	-	-	2%	-	-	-	-	-
-10 dB	$\phi_m$	-162	29	60	-96	114	164	9	-116	-173	124
	$\psi_m$	-	-	-	5%	-	-	-	-	-	-
	sd	-	-	-	5%	-	-	-	-	-	-
-20 dB	$\phi_m$	-144	-12	-56	138	58	-20	-67	-74	86	175
	$\psi_m$	-	-	-	-	-	-	-	-	-	-
	sd	-	-	-	-	-	-	-	-	-	-

Table 4-cxxi. Subject CK, F, age 19, at 500 Hz.

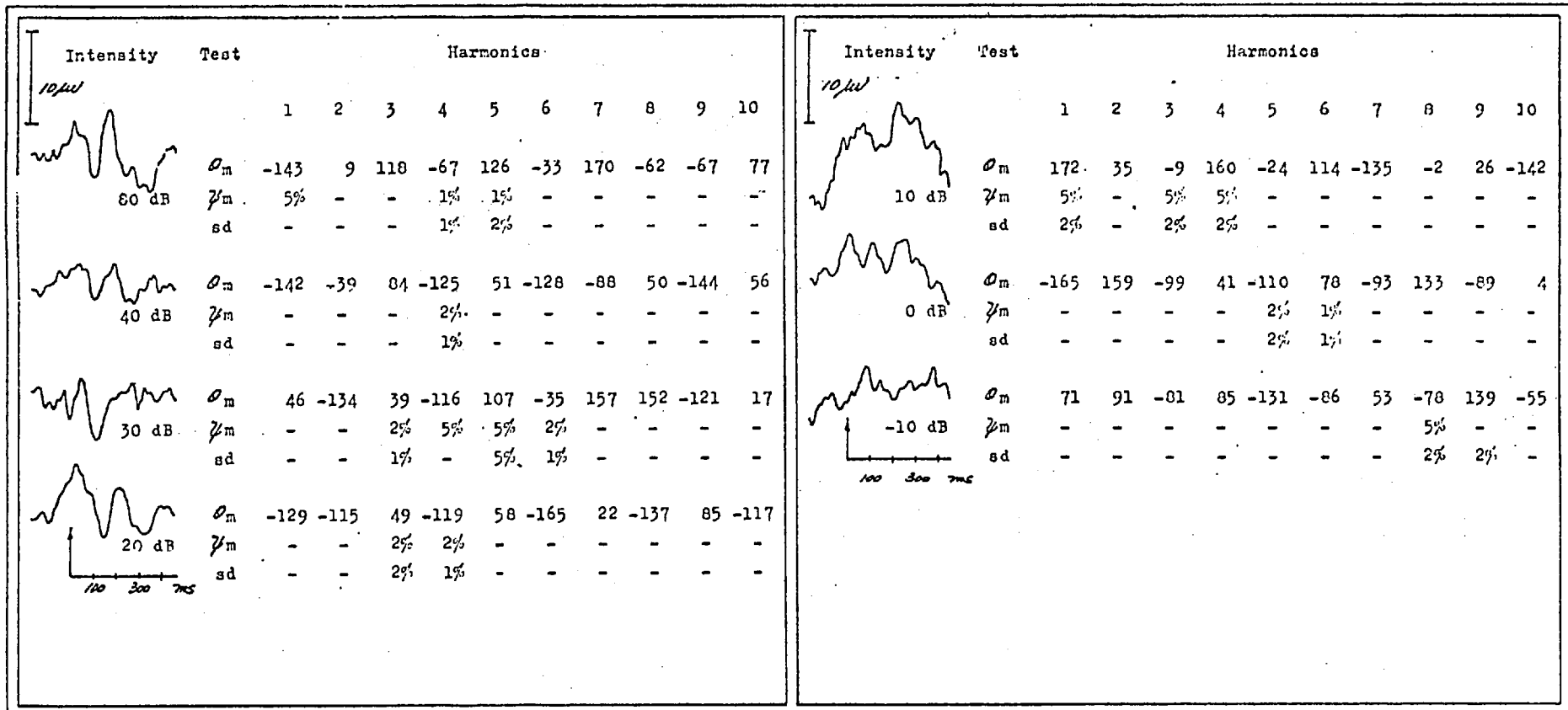


Table 4-cxxii. Subject CK, F, age 19, at 2 kHz.



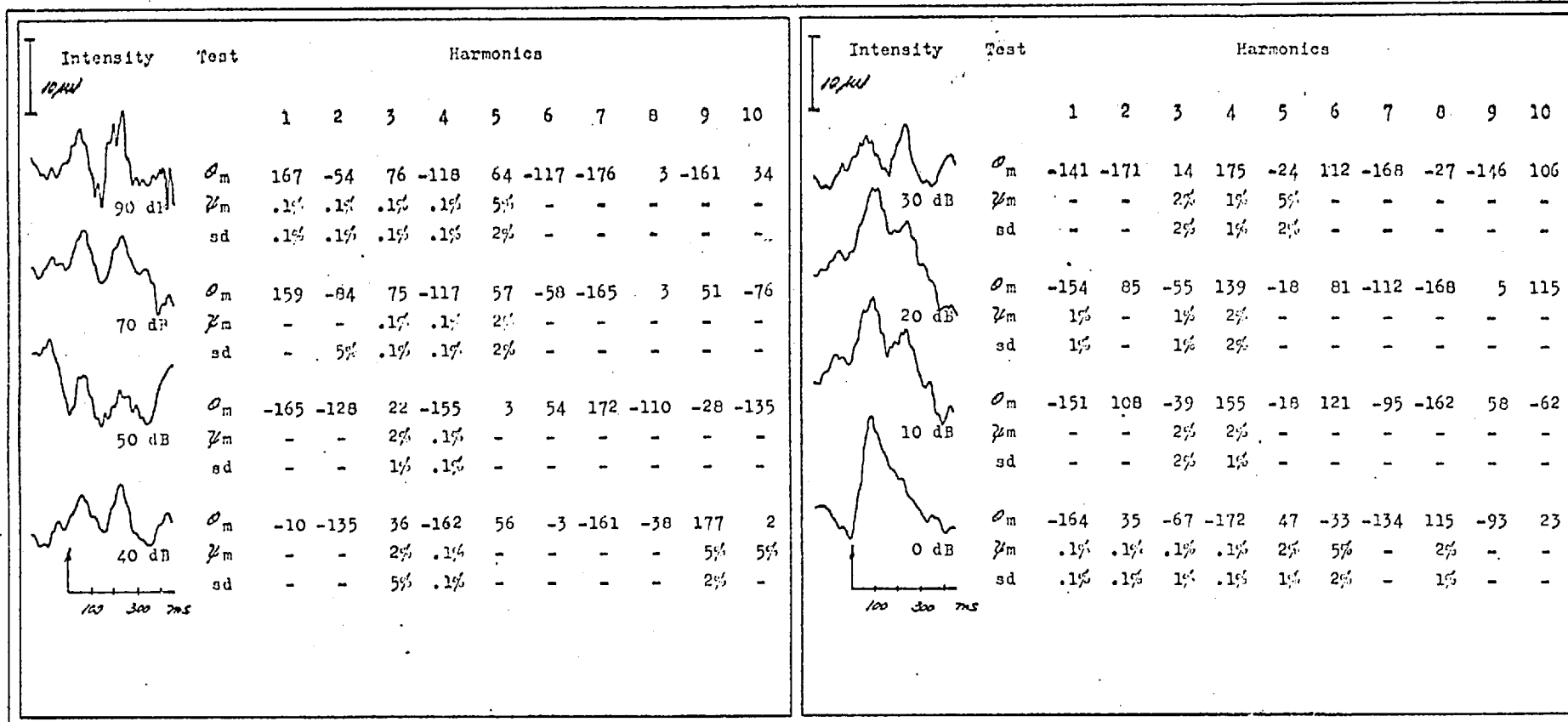
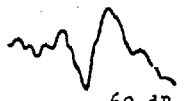

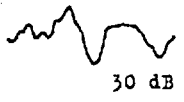
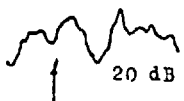
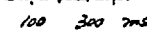


Table 4-cxxiii. Subject SR, M, age 20, at 2 kHz.

Intensity <i>10 μ</i>	Test	Harmonics									
		1	2	3	4	5	6	7	8	9	10
 60 dB	$\phi_m$	95	-117	67	-103	96	-91	139	-78	21	53
	$\psi_m$	-	2%	.1%	.1%	.1%	-	-	-	-	-
	sd	-	1%	.1%	.1%	.1%	-	-	-	-	-
 40 dB	$\phi_m$	165	-71	64	-143	31	-157	44	-81	154	62
	$\psi_m$	-	5%	.1%	.1%	.1%	.1%	-	-	-	-
	sd	-	-	.1%	.1%	.1%	.1%	-	-	-	-
 30 dB	$\phi_m$	-91	139	-2	-165	45	-130	37	153	2	11
	$\psi_m$	-	-	.1%	.1%	.1%	-	-	-	-	-
	sd	-	-	.1%	.1%	.1%	-	-	-	-	-
 20 dB	$\phi_m$	-151	-174	-6	165	-39	79	-57	-137	68	-143
	$\psi_m$	-	-	2%	2%	5%	-	-	-	-	-
	sd	-	-	1%	1%	5%	-	-	-	-	-
											

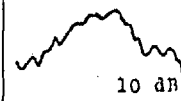
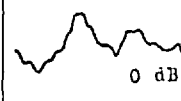
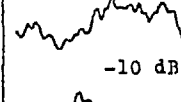
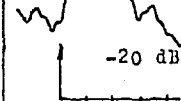
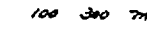
Intensity <i>10 μ</i>	Test	Harmonics									
		1	2	3	4	5	6	7	8	9	10
 10 dB	$\phi_m$	170	-5	92	-104	85	-141	-33	-163	78	-77
	$\psi_m$	5%	2%	-	-	-	-	-	-	-	-
	sd	5%	2%	-	-	-	-	-	-	-	-
 0 dB	$\phi_m$	-164	82	-36	138	39	-64	144	-23	47	167
	$\psi_m$	-	-	-	-	-	-	-	-	-	-
	sd	-	-	-	-	-	-	-	-	-	-
 -10 dB	$\phi_m$	152	-17	-46	-93	163	-53	-104	82	-93	137
	$\psi_m$	-	-	-	-	-	-	-	-	-	-
	sd	-	-	-	-	-	-	-	-	-	-
 -20 dB	$\phi_m$	-160	65	-64	174	-16	43	-144	12	91	-85
	$\psi_m$	2%	1%	1%	2%	-	-	1%	-	-	-
	sd	2%	2%	1%	2%	-	-	5%	2%	-	-
											

Table 4-cxxiv. Subject SR, K, age 20, at 500 Hz.

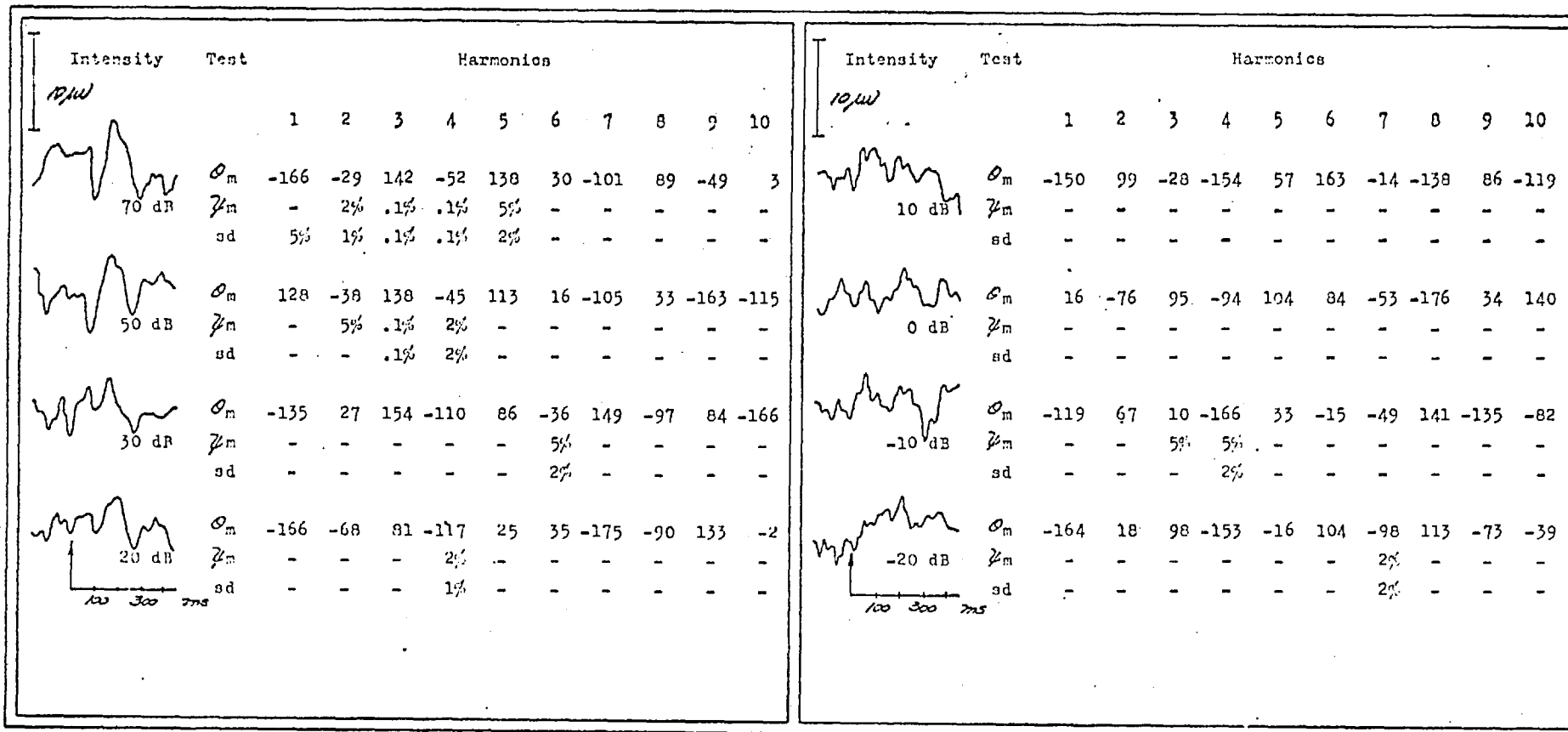


Table 4-cxxv. Subject PS, F, age 23, at 1 kHz.

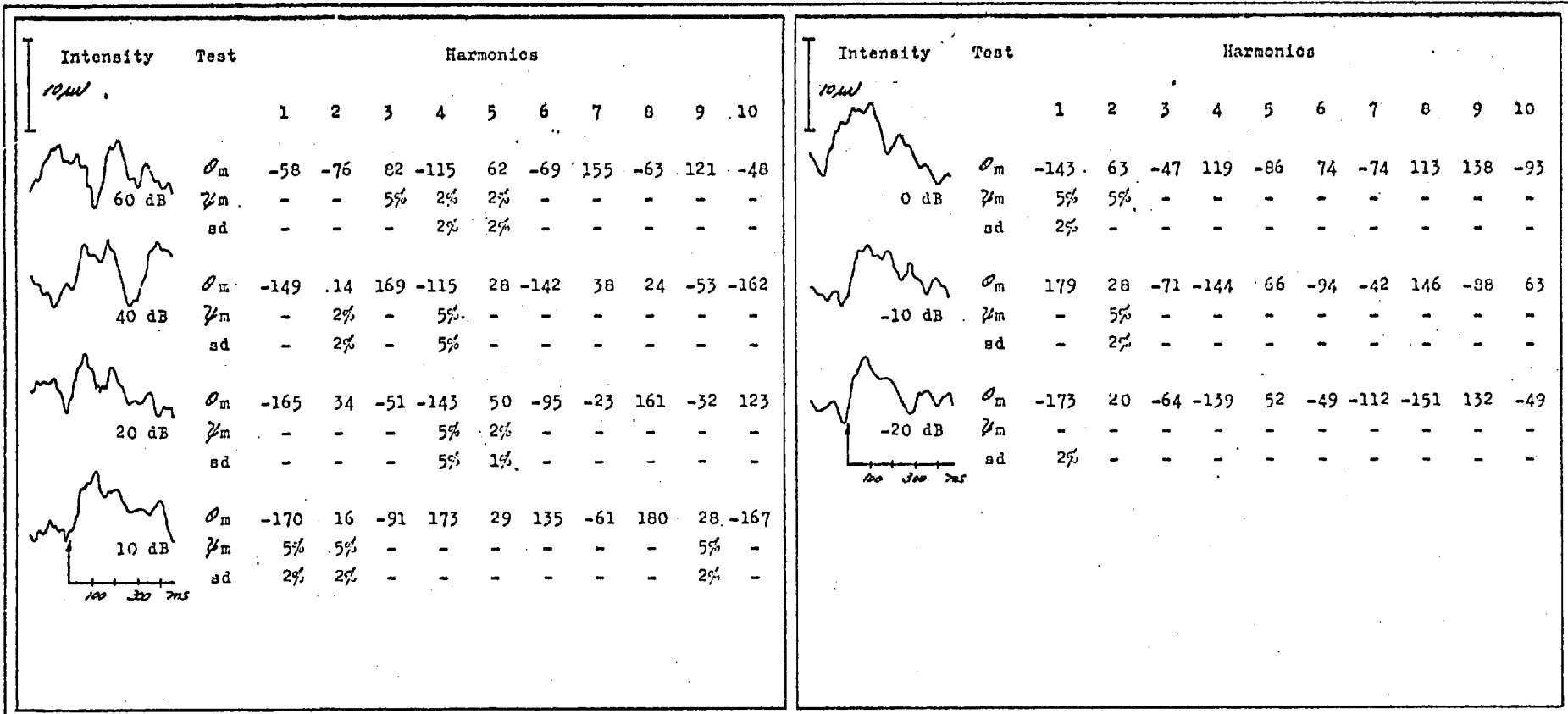


Table 4-cxxvi. Subject BS, F, age 23, at 4 kHz.

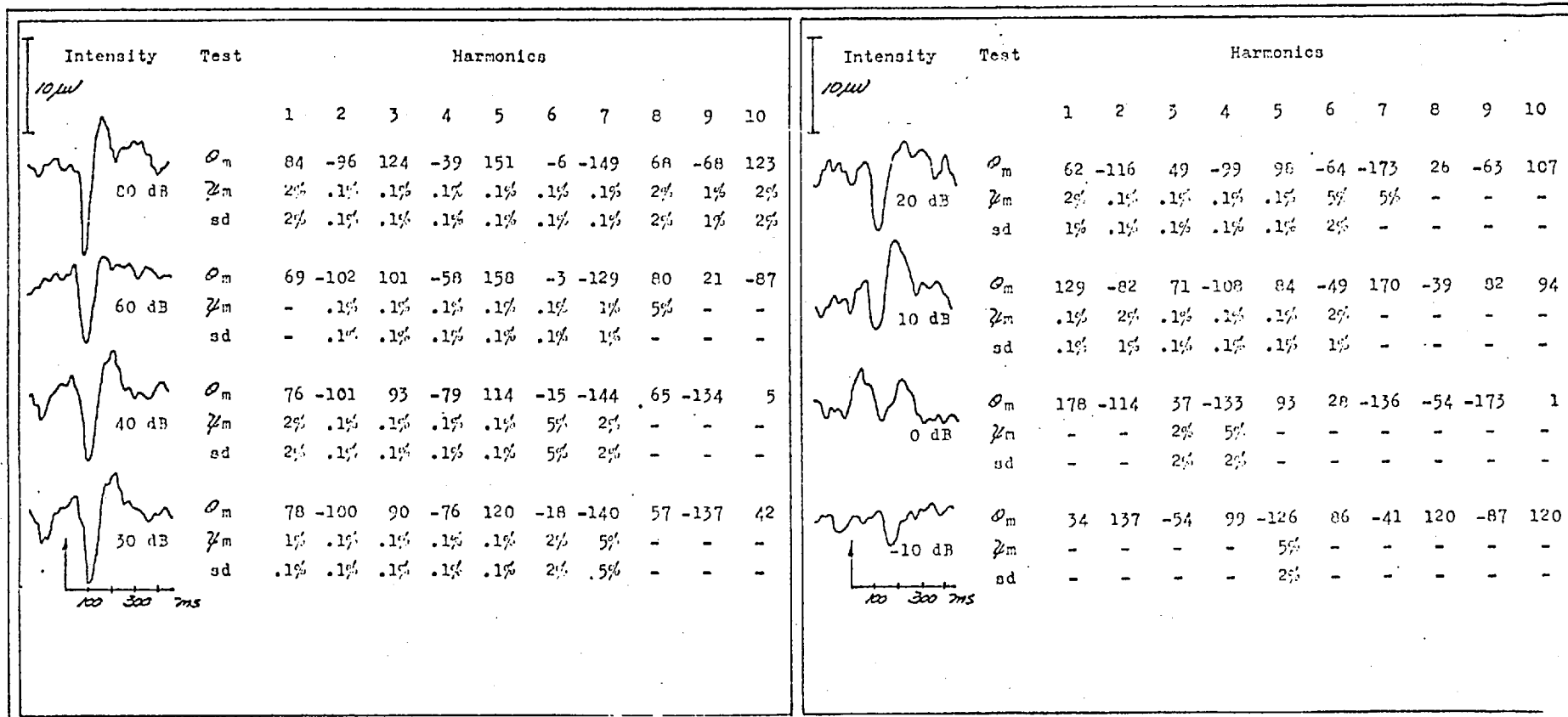


Table 4-cxxvii. Subject TR, M, age 31, at 1 kHz.

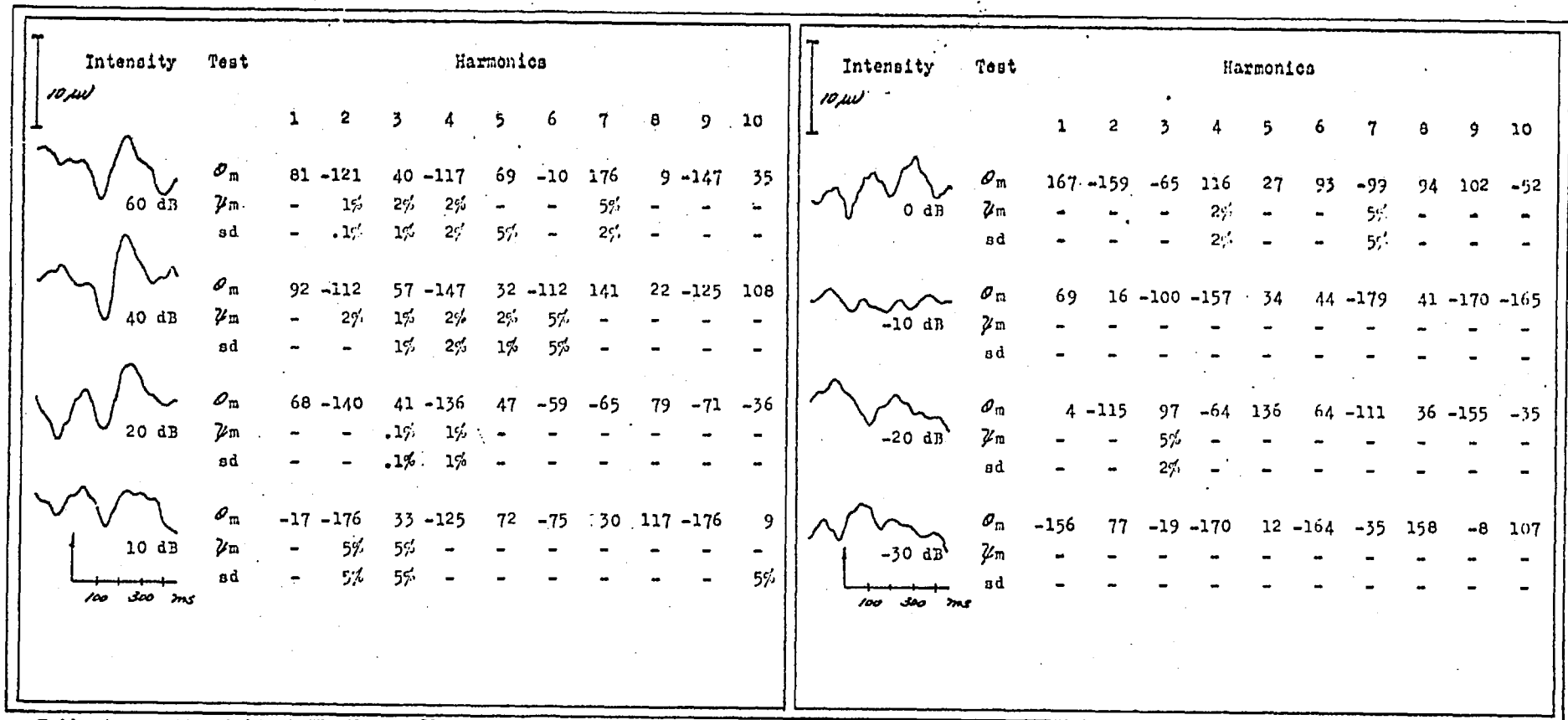


Table 4-cxxviii. Subject TR, M, age 31, at 1 kHz.

## CHAPTER FIVE

## TEMPLATE MATCHING BY CROSS-CORRELATION

## 5.1.i. Introduction

The phase analysis discussed in Chapter Four reveals how promising pattern recognition techniques can be in AEP detection and analysis. It is reasonable, then, to examine other pattern recognition methods in order to assess their effectiveness as response indicators. To this end, a simple template matching procedure is discussed in this chapter.

Template matching by cross-correlation makes use of specific information about the characteristic features of the pattern to be detected. Phase spectra, too, contain much of this information. Thus, they are related to the cross-correlation coefficient between a response template and an individual post-stimulus sweep. ( Beagley, Sayers, and Ross, 1978 ) The contribution of an individual harmonic to the correlation coefficient is dependent on its relative amplitude, and on its phase in relation to the response template. Clearly, only high amplitude spectral components can contribute substantially, and this contribution is determined by their relative phases.

## 5.1.ii. Template Matching

Template matching techniques assume a similar pattern is

present in the EEG following acoustic stimulation. Here, a reference waveform, or template, is compared with individual sweeps, usually by some means of cross-correlation. The simplest detection procedure involves the use of the cross-correlation coefficient which measures the degree of similarity between two waveforms, both referred to zero time.

In any template matching procedure, the choice of a suitable template is of considerable importance. Use of a template synthesized from second order differential equations has been examined and found to be reasonably effective in detecting the presence of individual AEP's. ( Derbyshire, Osenar, et al., 1971 ) Choice of this particular template, however, fails to account for either the inter- or intra-subject variability known to exist in ERA data. A high level averaged response taken from each subject tested would eliminate variability on an inter-subject basis, and possibly improve the sensitivity of the technique. Should this reference waveform prove inadequate in accommodating the intra-subject variability, it could then be adapted to account for certain known sources of variation, viz., the shift in latency at reduced stimulus intensities. The present study is only concerned with exploring the possibilities of this method in order to validate a pattern recognition approach to AEP analysis. Improving the sensitivity of the test procedures has not been attempted.

#### 5.1.iii. Cross-correlation Coefficients: the Null Hypothesis

To investigate the possibilities of template matching as a means of detecting the AEP, a simple comparison involving the cross-correlation coefficient was chosen for an exploratory study.



The cross-correlation coefficient,  $r_o$ , measures the degree of similarity between two waveforms, provided this dependence is linear in nature. If  $x_i$  are the sampled values of the template, and  $y_i$ , the samples from an individual post-stimulus sweep, then the cross-correlation coefficient is given by:

$$r_o = \frac{\sum_{i=1}^N (x_i - \bar{x})(y_i - \bar{y})}{s_x s_y}$$

where  $\bar{x}$  and  $\bar{y}$  are the sample means of  $x$  and  $y$  respectively, and  $s_x$  and  $s_y$  are their respective standard deviations.  $N = 64$  is the number of samples of  $x$  or  $y$  in a sweep.

$r_o$  can take on any value from  $-1$  to  $+1$ , the higher the value of  $r_o$ , the greater the similarity between  $x$  and  $y$ . If, on average,  $x$  and  $y$  bear no linear relationship to one another, as is the case for unstimulated EEG, the expected value of  $r_o$  will tend to zero. Should a pattern similar to the template be present in successive sweeps of an ensemble, as with supra-threshold records, the mean cross-correlation coefficient will then exceed some positive value,  $R$ . Mathematically, the null, and alternative, hypotheses can be stated simply as:

$$H_0: \langle r_o \rangle = 0$$

$$H_1: \langle r_o \rangle > R$$

Before these working hypotheses can be tested on stimulated data,  $R$  must be derived from the distribution of  $r_o$  taken from control EEG. To this end, nine records of spontaneous EEG, each 54 sweeps long, were subjected to cross-correlation analysis,

and the estimated probability density function shown in Fig. 5.1. derived.

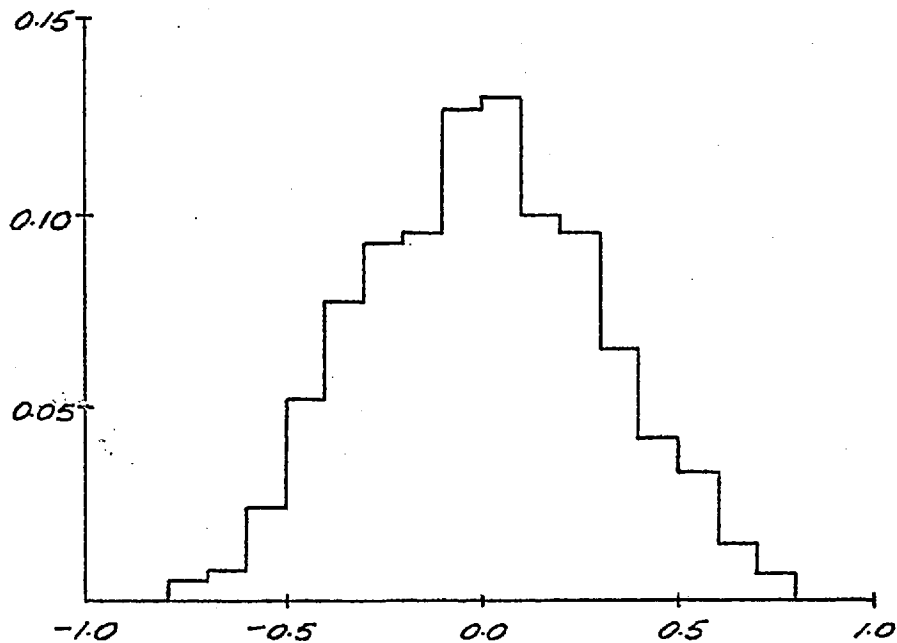


Fig. 5.1. Distribution of  $r_0$  from 1080 estimates on spontaneous EEG records.

As can be seen from Fig. 5.1., the distribution of  $r_0$  is essentially normal, with a population mean of zero and a standard deviation equal to 0.2391. In all but 5% of cases under the null hypothesis, the sample mean should lie within 1.96 standard errors of the population mean. Because we have devised a one-tailed test, the confidence interval for  $R$  must be defined in the following way:

$$R > \langle r_0 \rangle + t.se$$

or

$$R > t. \frac{0.2391}{\sqrt{M}}$$

where  $t$  is the value corresponding to a probability of  $P(r_0 > t)$  taken from a table of normal variables, and  $M = 54$ , the number of sweeps making up each ensemble.

The confidence intervals associated with probabilities of 5%, 2.5%, 1% and .1% are tabulated below.

$P(r_0 > t)$	R
5%	.054
2.5%	.064
1%	.076
.1%	.100

#### 5.2.i. An Exploratory Cross-correlation Study

Given the sampling statistics of  $r_0$  for control EEG, the null hypothesis was tested on the stimulated records from 17 normal hearing adults. Each subject was tested at two different tone burst frequencies and seven intensities of stimulation ranging from 80 dB to 0 dB HL. A trial consisted of 54 sweeps of post-stimulus EEG 640 ms ( 64 samples ) long. For each series of eight trials, the averaged response to an 80 dB HL tone burst was chosen as the reference waveform. Individual sweeps at lower intensities were then correlated with this template. Thus, for every trial, 54 estimates of  $r_0$  were available for analysis. The mean cross-correlation coefficient for the trial was determined and compared

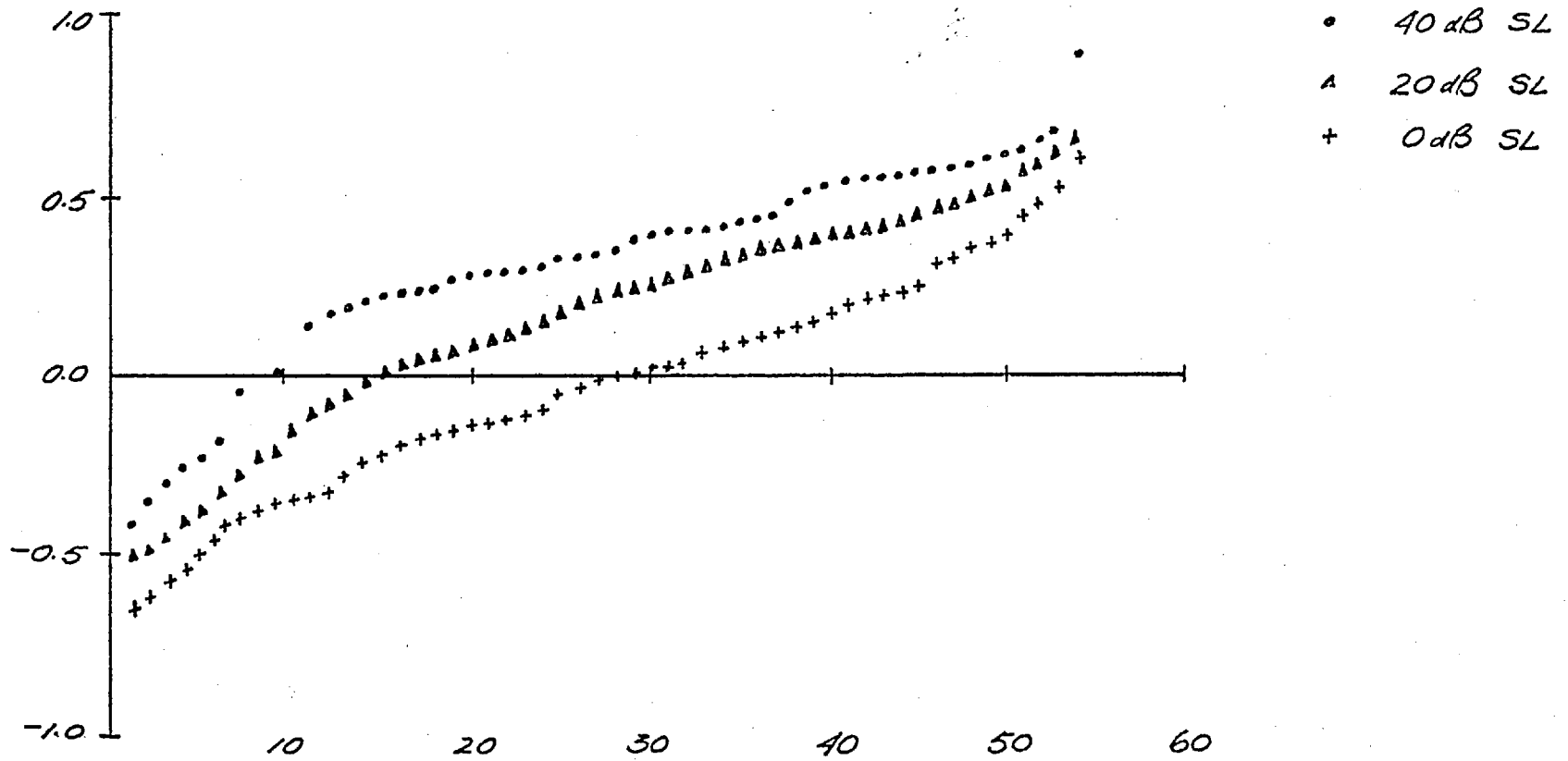


Fig. 5.2. Rank ordered curves for  $r_0$  at three different stimulus intensities. Note the way in which the curves shift to the right as the intensity is reduced, yet the slope remains essentially constant.

M

with the confidence intervals set up under  $H_0$ .

The results of this exploratory study can be found in Tables 5-i to 5-xvii. Every table is divided into two sections, one pertaining to each of the two tone burst frequencies used in testing the subjects. Here, intensities are quoted in dB SL for comparisons between cross-correlation and subjective estimates of threshold. For all eight trials, the averaged response is shown. The first entry is the template, below which are tabulated the mean cross-correlation coefficient,  $\bar{r}_0$ , and its associated probability levels for the 7 records at lower intensities. For simplicity of presentation, probabilities of 2.5% are recorded as 2%. Any  $\bar{r}_0$  value which is not significant at 5% is denoted by a dashed line.

#### 5.2.ii. Discussion

Whenever a recurring pattern similar to the template is present in successive post-stimulus sweeps, the mean cross-correlation coefficient should be significantly greater than zero. For most of the supra-threshold records in Tables 5-i to 5-xvii, this expectation is confirmed. At high intensities of acoustic stimulation, the mean cross-correlation coefficient is large, and usually remains so to about 20 or 30 dB SL, at which point it drops off rapidly, often becoming nonsignificant. See Subject FN at 2 kHz and 500 Hz. ( Table 5-v ) The decline in the magnitude of  $\bar{r}_0$  may be more gradual, as Subject GF at 1 kHz ( Table 5-ii ) illustrates.

A characteristic S-shaped curve results from ranking an ensemble of cross-correlation coefficients from the most negative to the most positive values. For ERA data, reductions in the

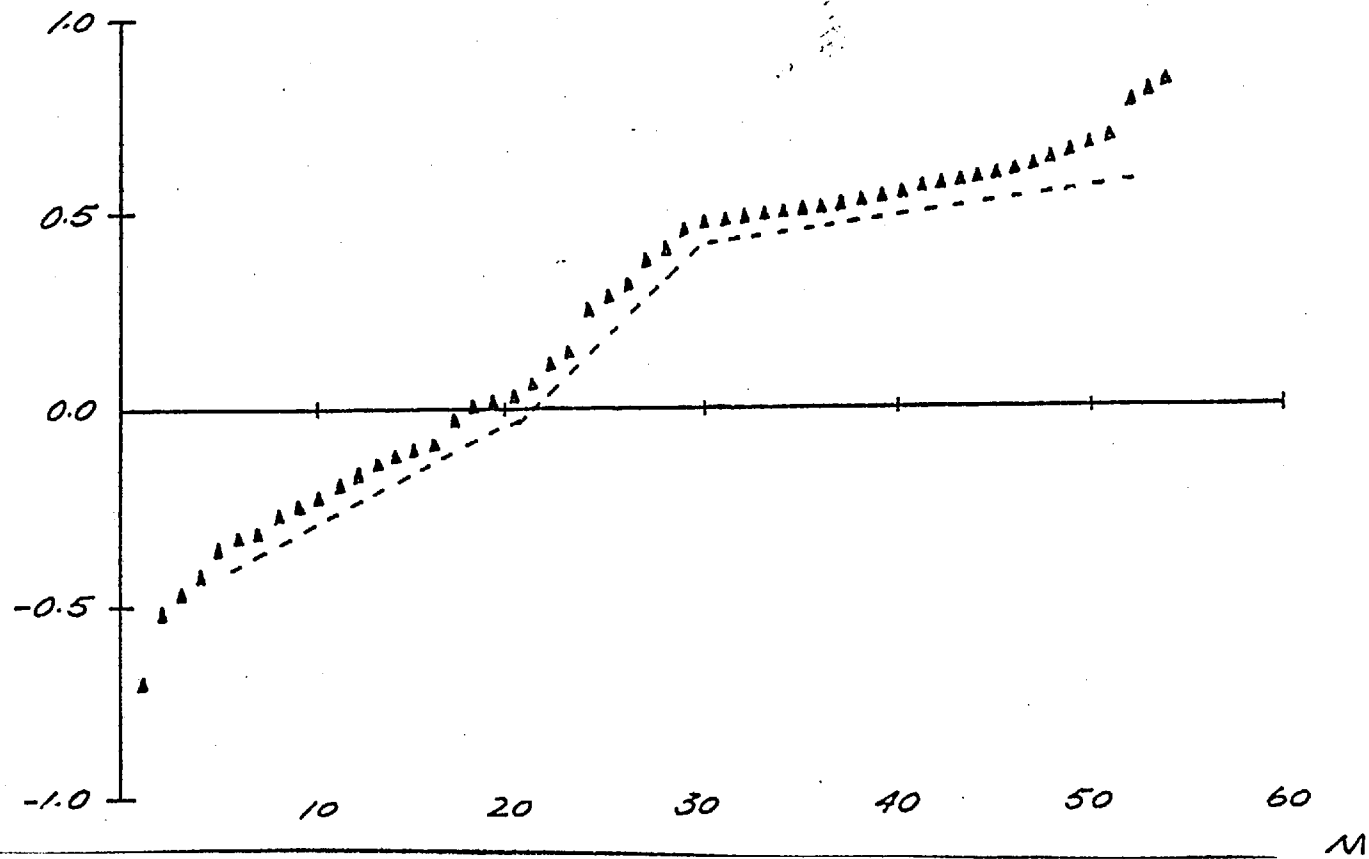


Fig. 5.3. A rank ordered curve where more than one slope is evident. This irregularity can indicate the presence of more than one population in the record.

stimulus intensity cause this curve to move downwards towards a larger percentage of negatively correlated sweeps. See Fig. 5.2. This downward shift suggests that, in addition to the mean correlation coefficient, either the median or the zero crossing of the rank ordered curve could be implemented as a response indicator.

Occasionally, more than one slope can be seen in a rank ordered curve, indicating the possible existence of two or more populations in that particular record. See Fig. 5.3. The overall slope of this line, as measured by a least squares best fit to all but the first and last 10% of values, is 0.023, not significantly different from the mean of 0.027 found for all records analysed. However, three distinct slopes, shown in dotted lines, may be seen in this curve. These have values of 0.02, 0.045, and 0.01 respectively. In this particular case, each of these slopes lies within two standard errors of the mean, suggesting that the data here is still within the 5% confidence intervals for the slope statistic.

Taken overall, this simple cross-correlation procedure usually detects the presence of the AEP to within +15 dB of subjective threshold. Admittedly, this is not as sensitive as the phase statistics discussed in the previous chapter, but no attempt has been made as yet to refine the procedure, thereby improving the sensitivity of the test. On this basis, a false negative score of 16% is not unreasonable or unacceptable. The false positive rating is well within the expected 5%. Such findings indicate that this particular pattern recognition approach does indeed hold promise as a means of AEP detection and analysis.

### 5.3.i. An On-line Study

The preliminary off-line study indicated that the cross-correlation procedure could well be implemented effectively in a clinical setting. To this end, an on-line investigation was undertaken to assess its merits and provide more data for further analysis off-line.

Fifteen normal hearing adults, aged 18 to 31, were chosen as subjects for the study. Each was tested at either one or two tone burst frequencies, and a range of intensity levels from 80 dB to -10 dB HL. Conventional ERA equipment was employed in presenting 64 stimuli for each intensity level. The marker pulse and the amplified EEG were then fed into the analog-to-digital interface of a small computer for immediate analysis of the data. At the same time, analog recordings of both signals were taken for future verification of the procedure. See Chapter Two for a detailed description of the experimental apparatus.

For a sampling rate of 100 Hz, 640 ms or 64 samples of post-stimulus record were considered. The subject's coherent average to 64 80 dB HL tone bursts was chosen as the template or reference waveform. For each lower intensity level, 64 individual sweeps were cross-correlated with the reference, yielding a sample of  $r_0$  values. These were rank ordered, and their mean,  $\bar{r}_0$ , and standard deviation,  $s$ , calculated.

Because 64 sweeps made up each ensemble of  $r_0$  values, the confidence intervals quoted in Section 5.1.iii. have to be modified slightly to the figures tabulated below.



$P(\bar{r}_0 > t)$	R
5%	.049
2%	.061
1%	.070
.1%	.093

The results of this study can be found in Tables 5-xviii to 5-xxviii. The confirming off-line study, for ensembles of length 54, are tabulated in Tables 5-xxix to 5-xxxix. Each table is divided into two sections, one pertaining to the eight trials on a given subject at a single tone burst frequency. Intensity levels are all quoted in dB SL and accompanied by their respective averages over the 640 ms interval considered for the analysis. To the right of each entry are tabulated the mean cross-correlation coefficient,  $\bar{r}_0$ , and its associated probability level. Any value of  $\bar{r}_0$  which is not significant at 5% is denoted by a dashed line.

### 5.3.ii. Discussion

On average, use of the cross-correlation technique matches subjective thresholds to within 15 dB. High intensity levels of stimulation usually correspond to very high values of  $\bar{r}_0$  and correspondingly low levels of significance. As the intensity is reduced, the mean correlation coefficient decreases in magnitude, then very sharply drops to values typical of continuous EEG. Consider Subject AR at 1 kHz as an example. ( Table 5-xxiii ) All records to +10 dB of threshold are significant. With slight

fluctuations, the value of  $\bar{r}_0$  decreases with intensity level, until it drops from 0.0953 at 10 dB to 0.0257 at 0 dB SL.

In certain cases, the disparities between subjective thresholds and those determined on the basis of cross-correlation are extremely large and occasionally erratic. Consider Subject AP at 4 kHz. ( Table 5-xx ) Although the averaged waveforms indicate a definite response in records to within 10 dB of subjective threshold, only two trials, those at 40 dB and 20 dB SL return values of  $\bar{r}_0$  which are significant at 5%. The rank ordered curves reveal no evidence of more than one population in any of the records, suggesting some other mechanism must be responsible for the anomalies observed. In part, these may be due to the choice of template, less typical for this subject than the 60 dB HL record because of the large negative deflection following the P<sub>200</sub> complex. In part, the disparities may reflect the presence of recording, or other, artifacts, because no provisions were made for their rejection in this on-line investigation. The off-line verification ( Table 5-xxxii ) shows a marked improvement in the test results, suggesting that saturation of the input amplifiers may well have been the cause of the anomalies observed.

Subject BS at 4 kHz ( Table 5-xxvii ) brings to light one problem encountered with this, and to some extent, the on-line phase study. For both investigations three subjects in 32, or approximately 10% of all tested, failed to display coherent averages even at high intensity levels. This has been known to happen in ERA testing ( Davis, 1976, Rose, Keating, et al., 1974 ) and reasons for its occurrence still remain uncertain. For these subjects, it may be that the conventional electrode placement is poorly situated to detect the dipole measured. The maximum of

this dipole does shift with maturation of the CNS ( Davis, 1976, Davis and Onishi, 1969 ), being most readily detected between vertex and mastoid in the adult subject. If surface mapping of the evoked potential were undertaken, it could well reveal whether a different spatial orientation of the dipole is responsible for the very poor responses recorded.

When the results of both the on-line study and its off-line verification are considered overall, the false positive rating is 3%, while the false negative score is approximately 14%. Both figures are comparable to those found for the exploratory study discussed in Section 5.2. Template matching procedures, then, hold considerable promise as a means of detecting the AEP, even if no allowance is made for the intra-subject variability of evoked potentials. Their decided effectiveness assures us that pattern recognition techniques are indeed the best means of studying the AEP.

#### 5.4. Concluding Remarks

Interesting features have come to light in the use of this simple template matching procedure. Certain subjects, for example, reveal little by way of a coherent response, even at high levels of acoustic stimulation. This raises important questions about the spatial sampling of the AEP which, to date, have not been adequately resolved. Contour mapping of the evoked potential over the surface of the scalp could provide us with much important information. As well as specifying the spatial sampling requirements for AEP recording, a study of this kind could help to explain some of the disparities observed. Through the use of

spatio-temporal methods of signal analysis, the temporal and three-dimensional spatial propagation of the AEP could be studied more thoroughly, and its origins more clearly defined.

Though simple in its application, template matching by cross-correlation is a reasonably effective and reliable response indicator. Its sensitivity could be improved by adapting the response template to accommodate the shift in latency of the AEP at reduced stimulus intensities. This could well make template matching comparable to the phase measures of Chapter Four in detecting the presence of the evoked potential. As it stands, though, the cross-correlation analysis is sufficiently sensitive to indicate that a pattern recognition approach to AEP data is indeed justified.

Tables 5-i to 5-xvii

Preliminary Cross-correlation Study

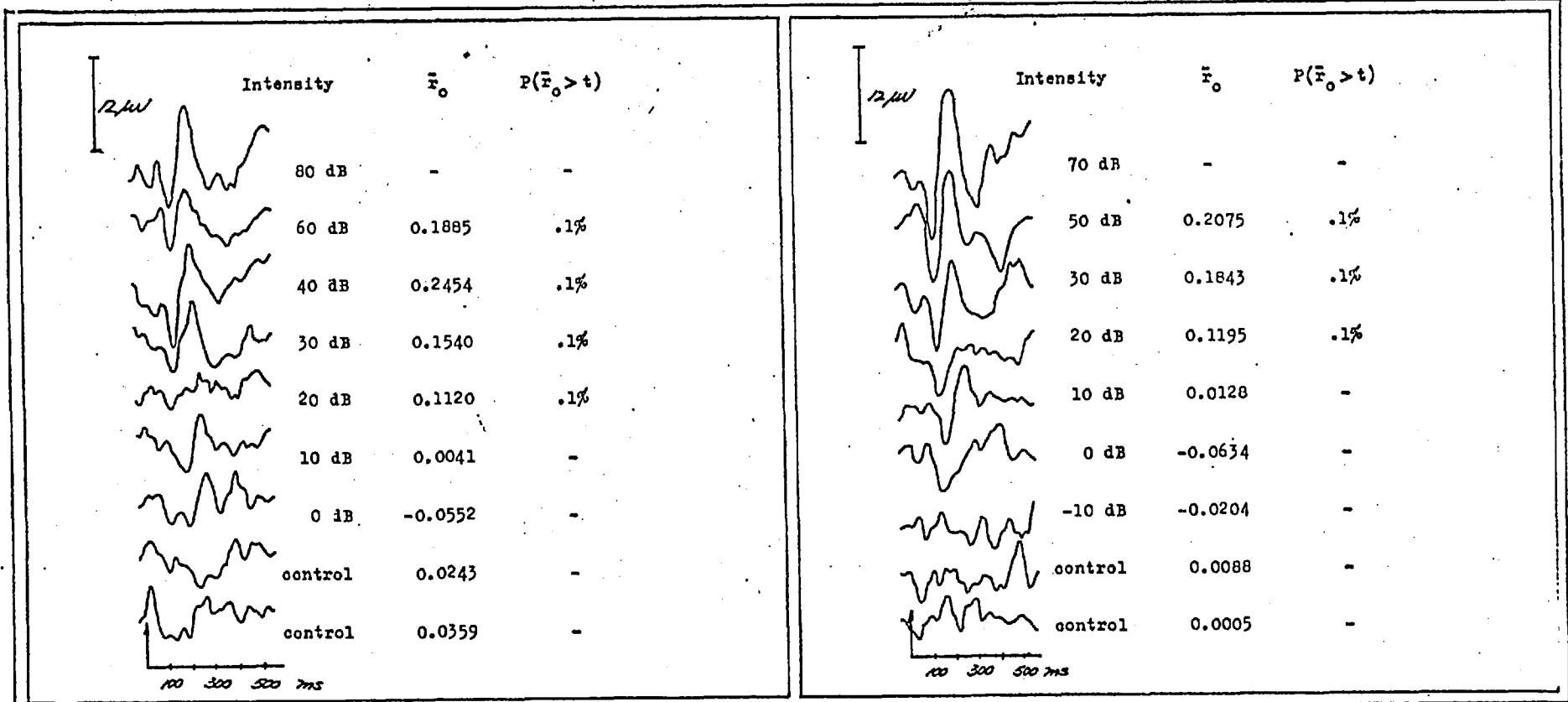


Table 5-1. Subject CH, F, age 23, at 2 kHz and 500 Hz.

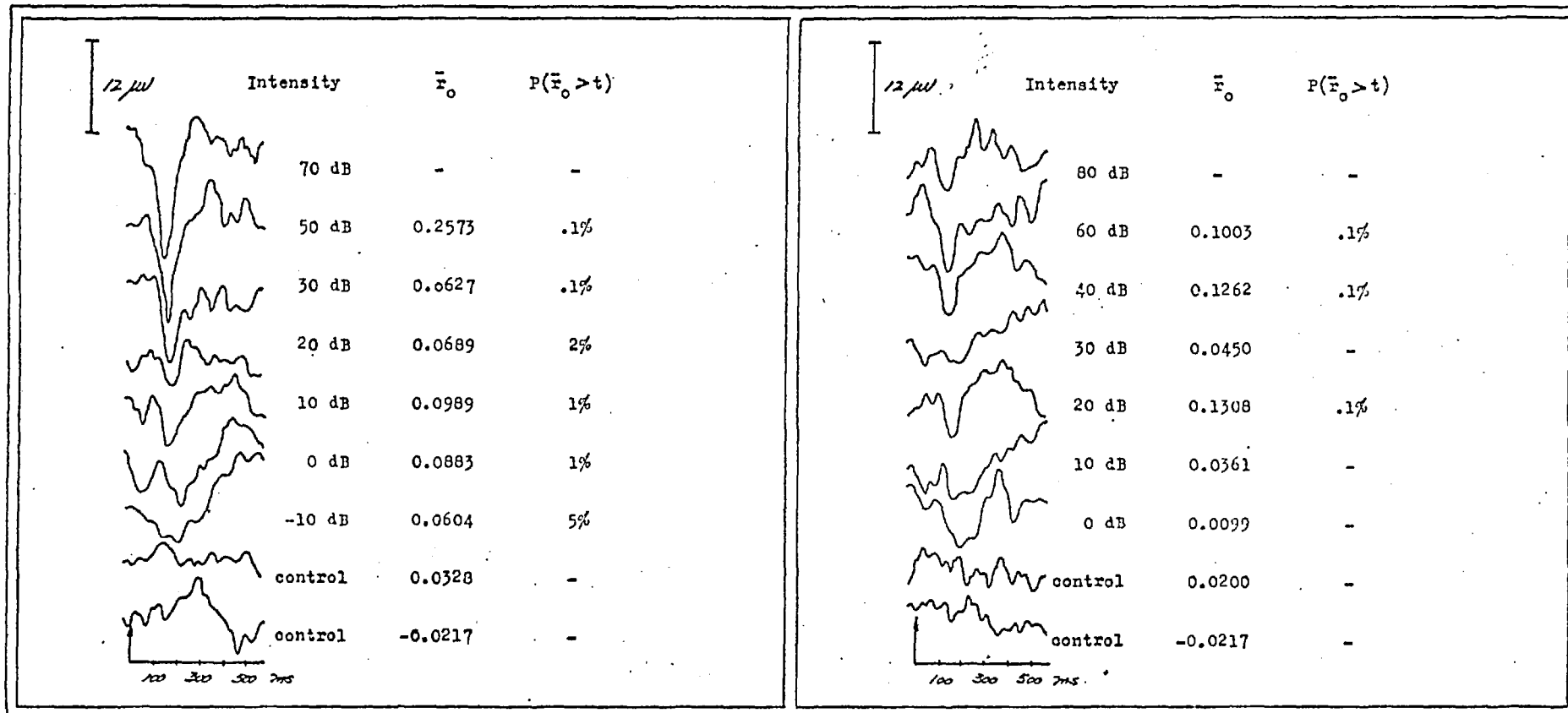


Table 5-ii. Subject GF, M, age 28, at 1 kHz and 4 kHz.

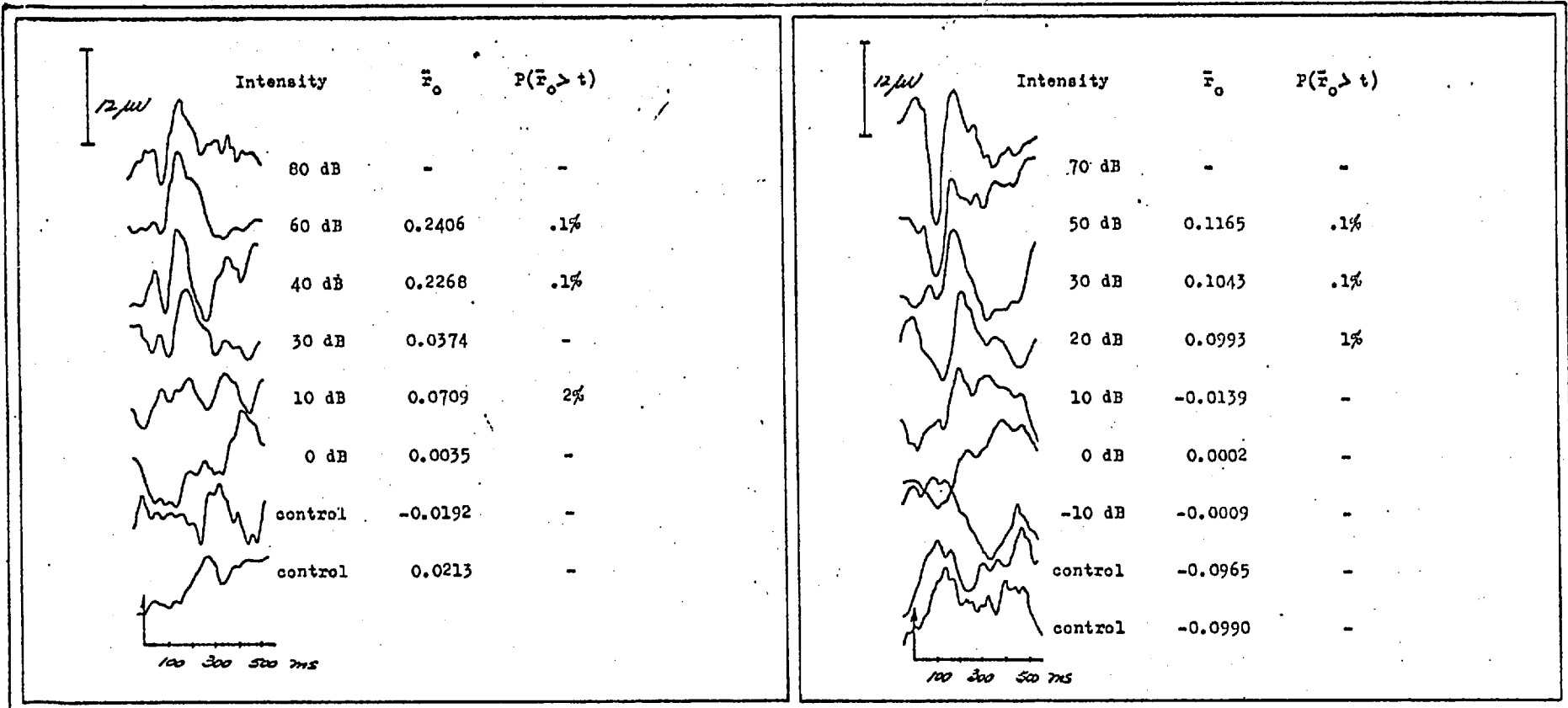


Table 5-iii. Subject JS, F, age 23, at 2 kHz and 500 Hz.



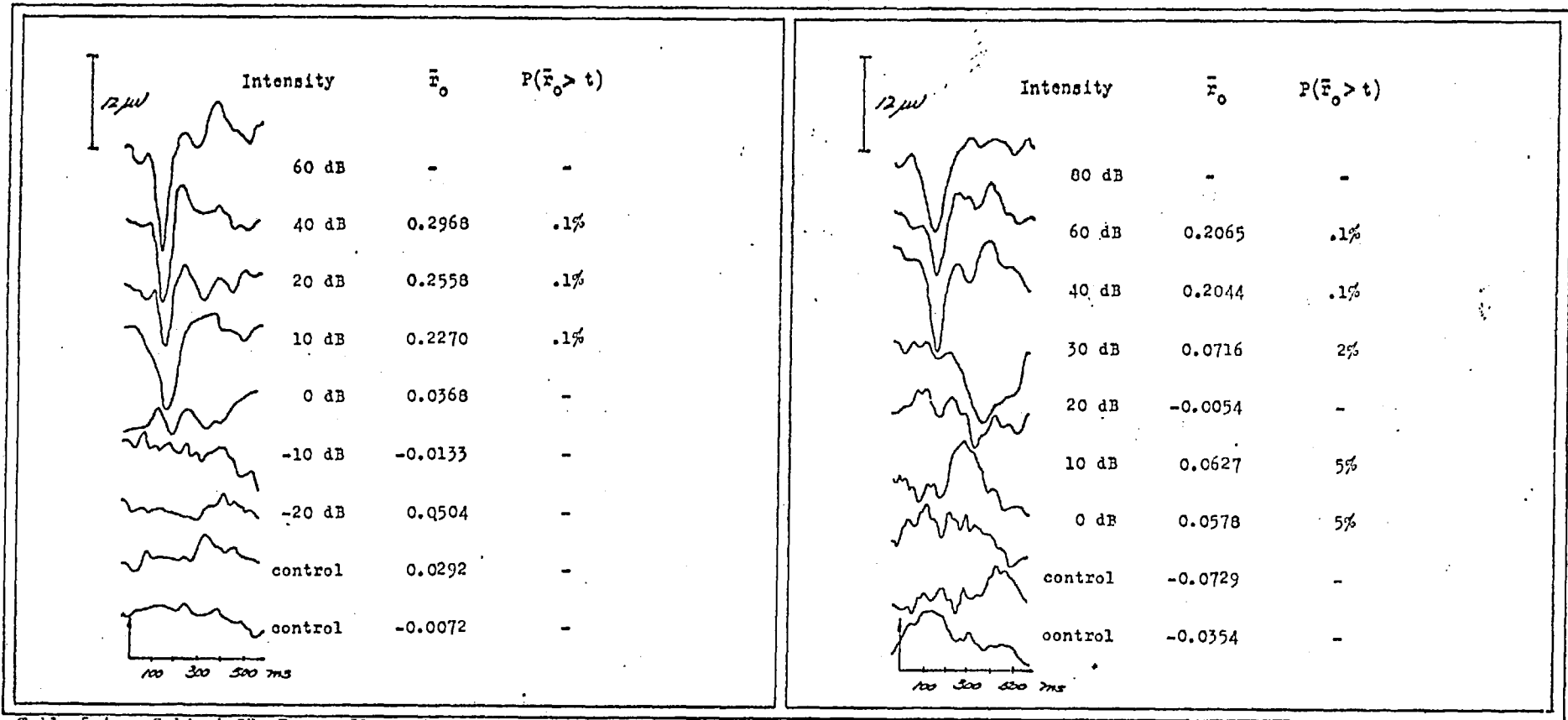


Table 5-iv. Subject GR, F, age 31, at 1 kHz and 4 kHz.

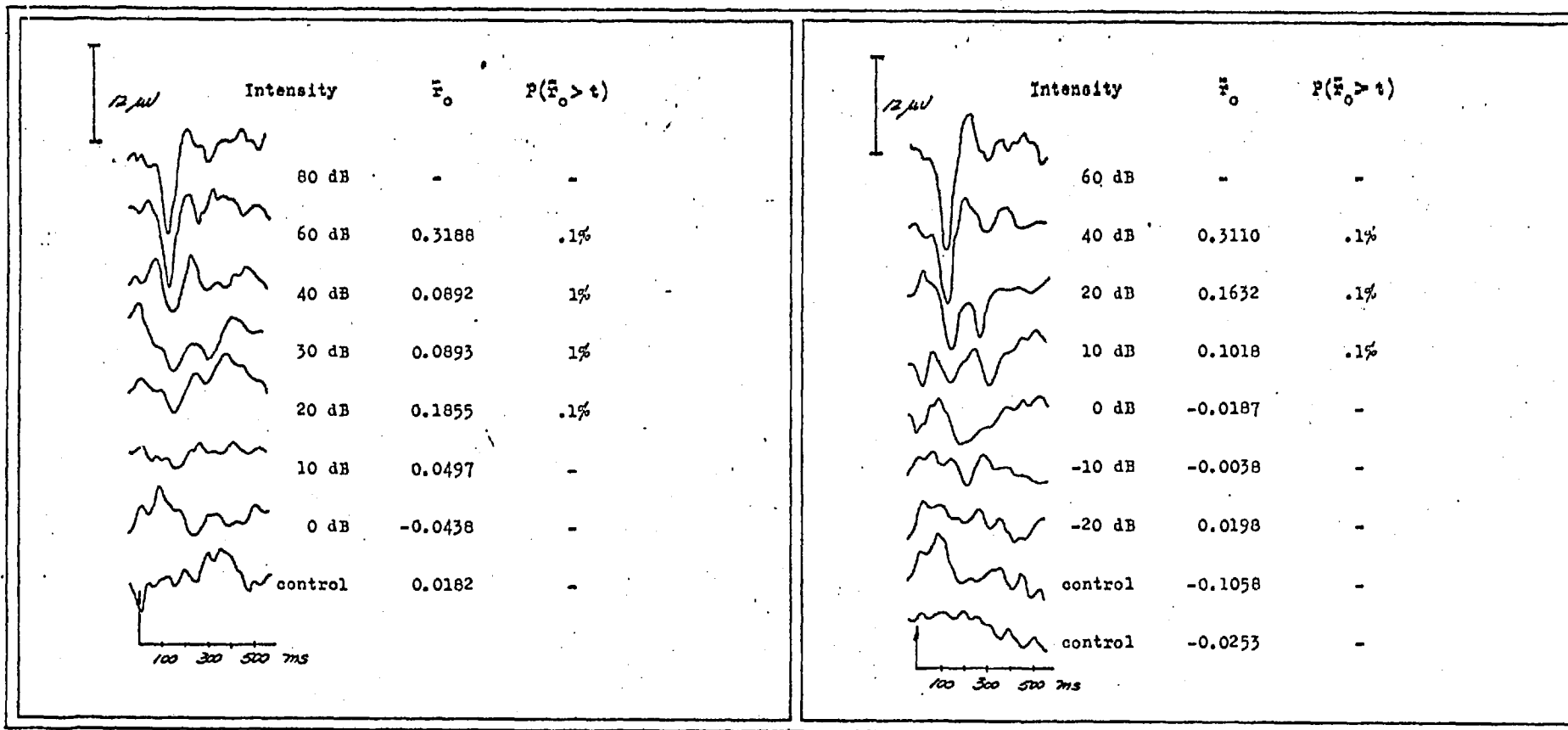


Table 5-v. Subject FN, M, age 28, at 2 kHz and 500 Hz.

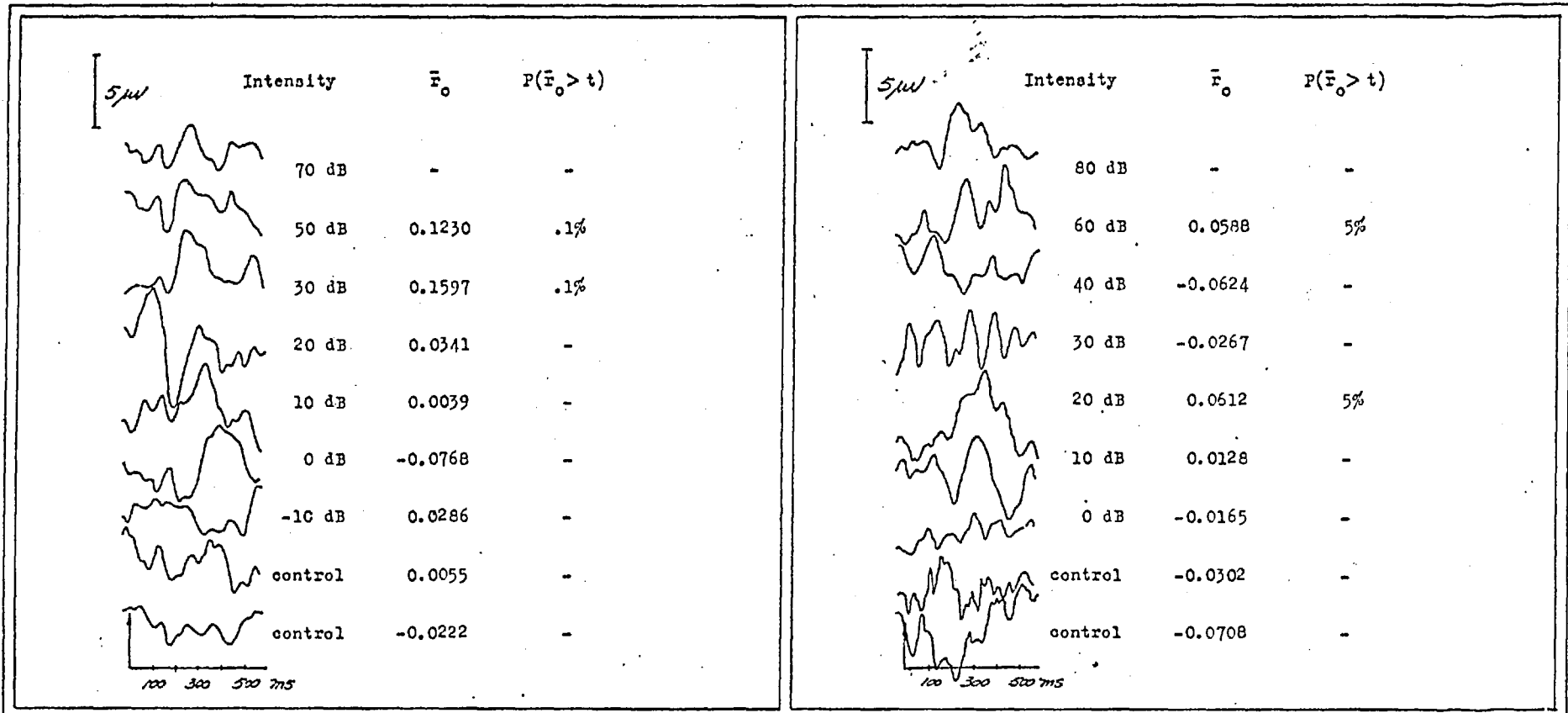


Table 5-vi. Subject TE, M., age 20, at 1 kHz and 4 kHz.

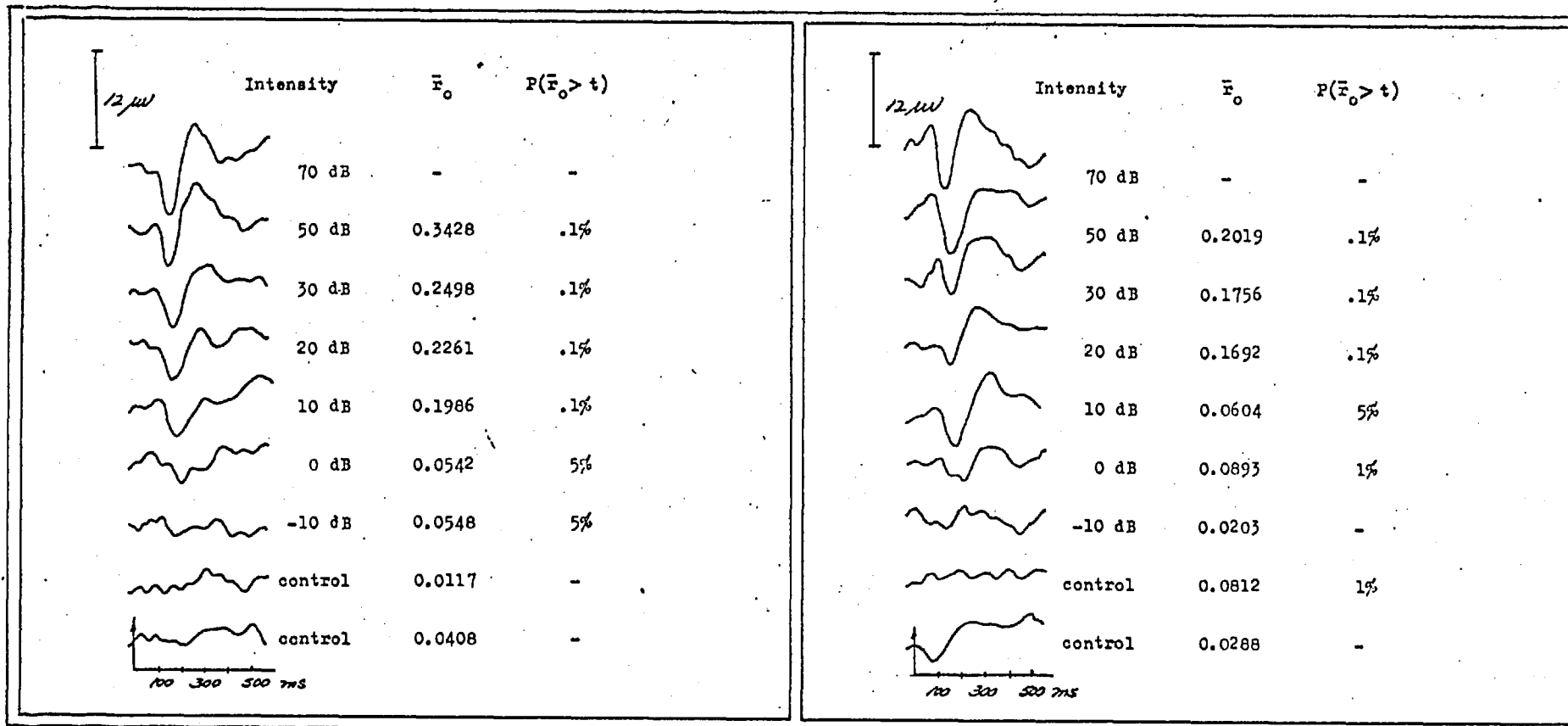


Table 5-vii. Subject BO, M, age 31, at 2 kHz and 500 Hz.

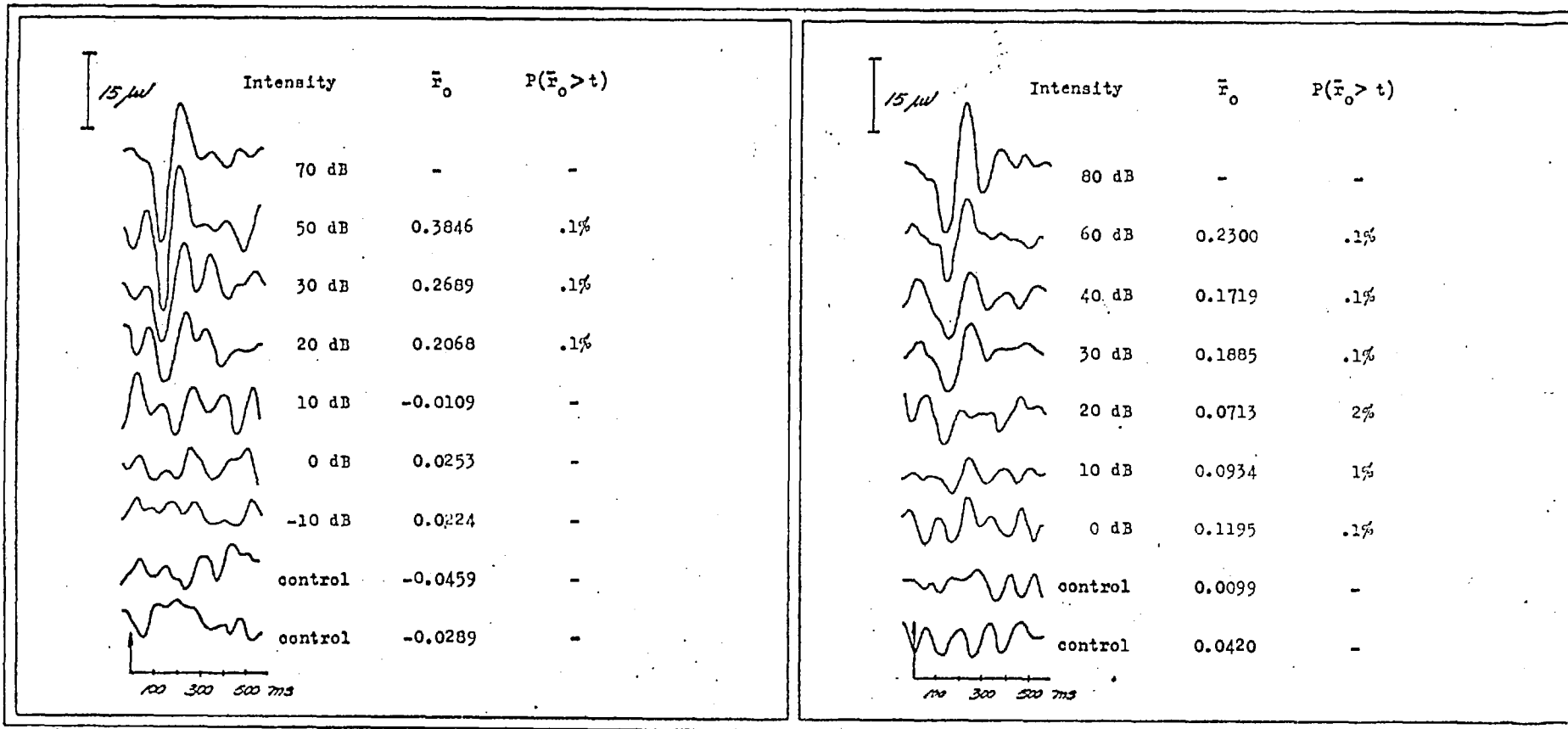


Table 5-viii. Subject JD, F, age 23, at 1 kHz and 4 kHz.

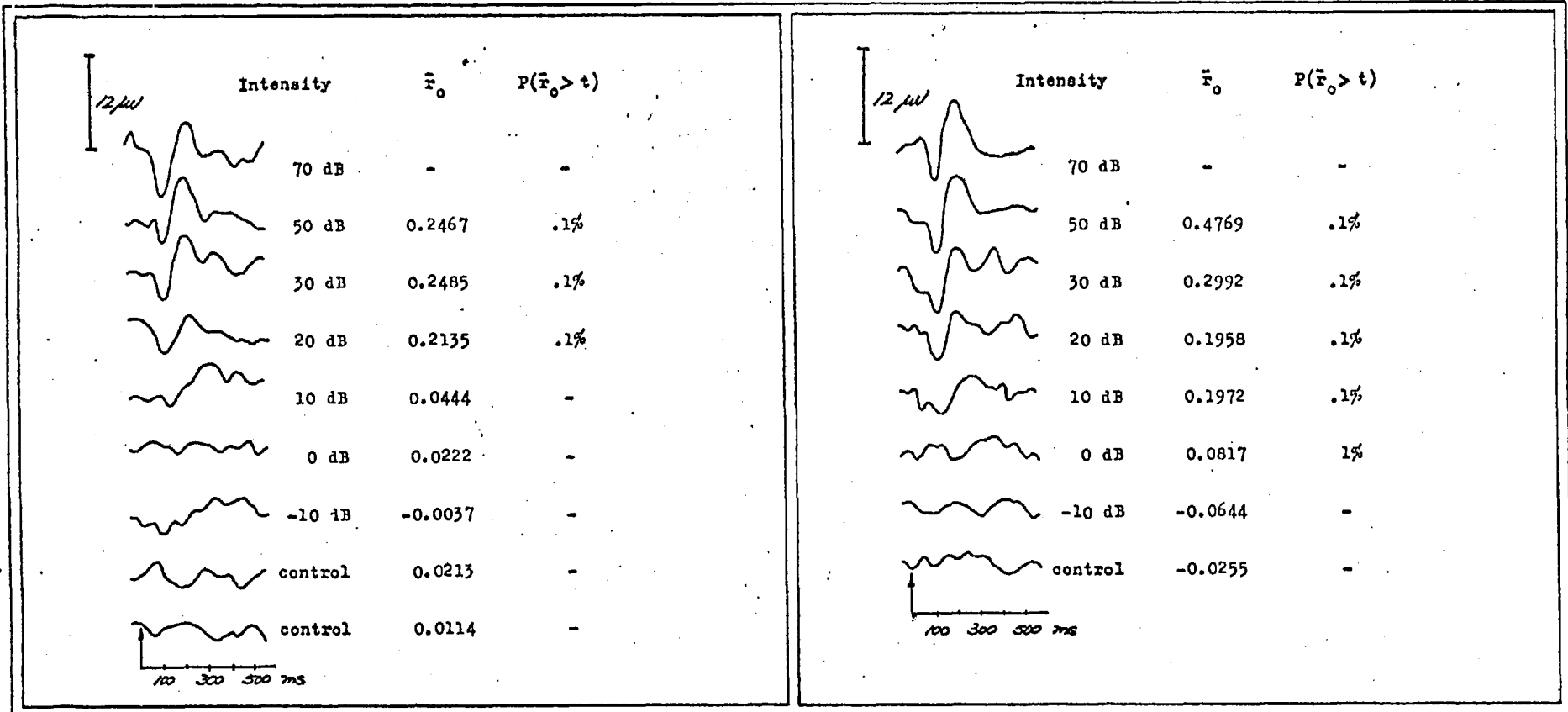


Table 5-ix. Subject DT, F, age 24, at 2 kHz and 500 Hz.

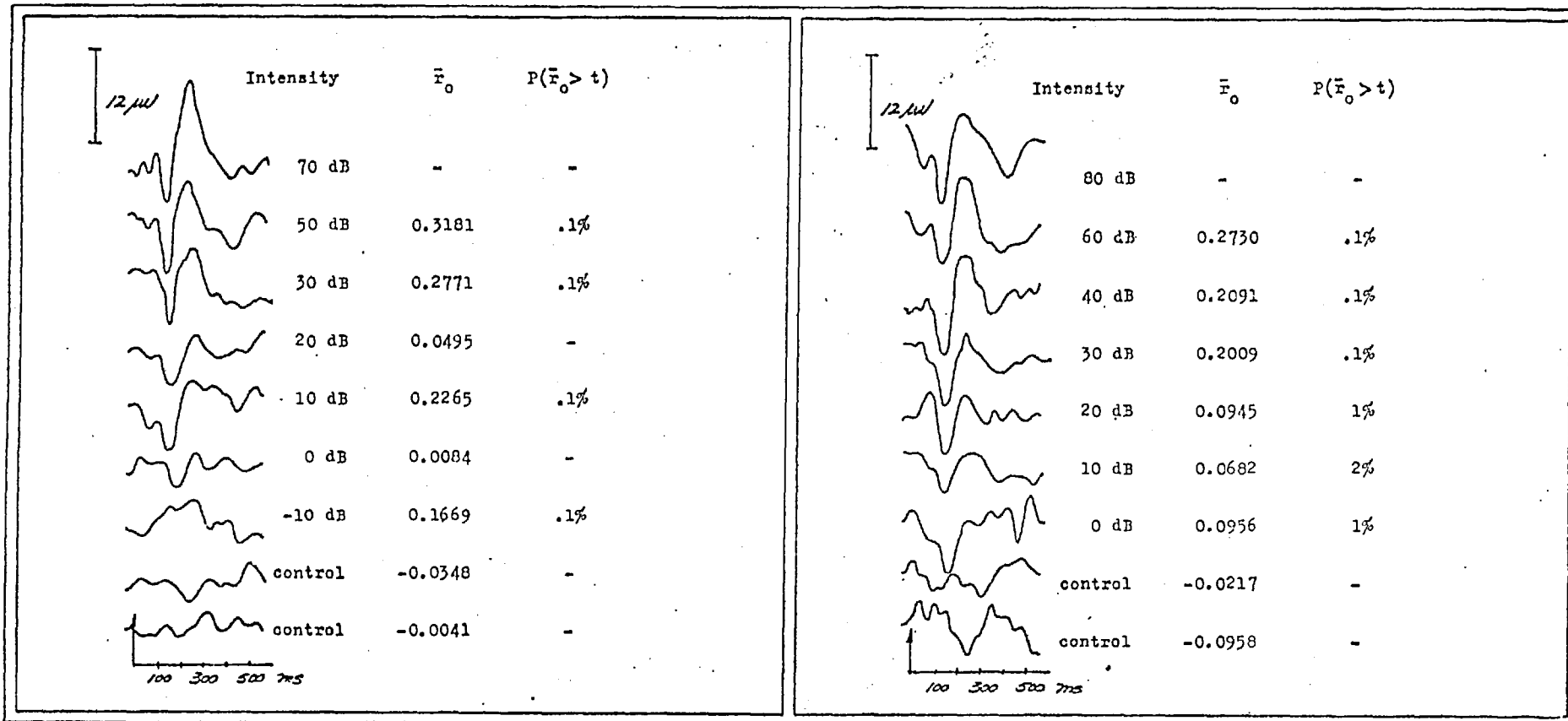


Table 5-x. Subject JN, M, age 30, at 1 kHz and 4 kHz.

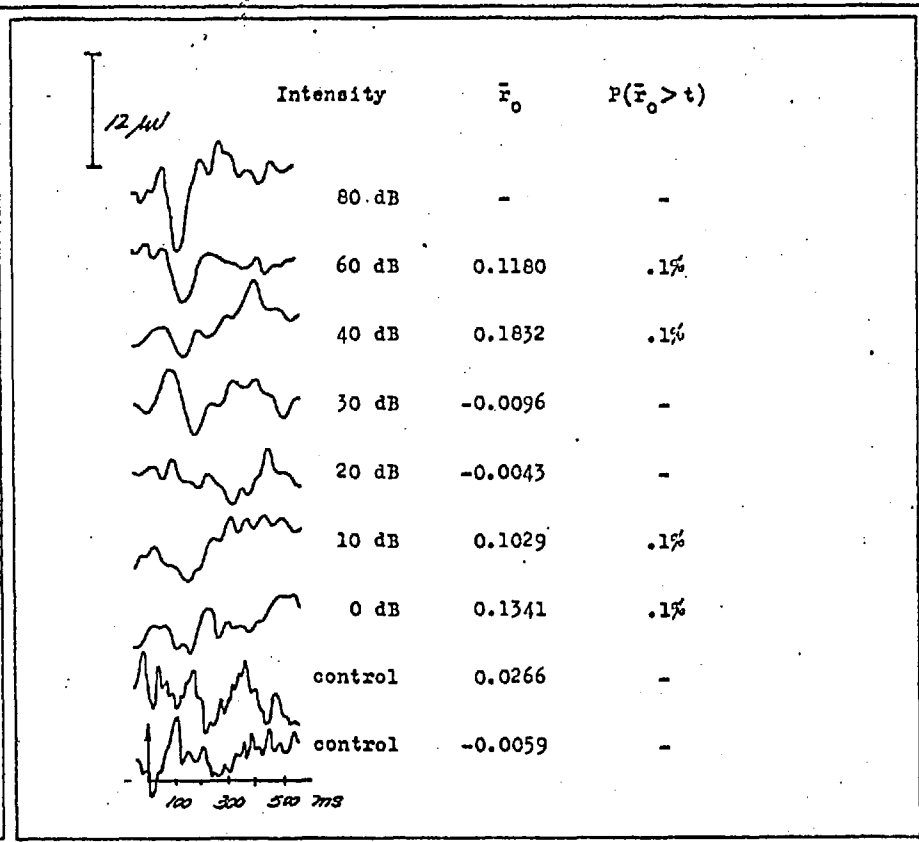
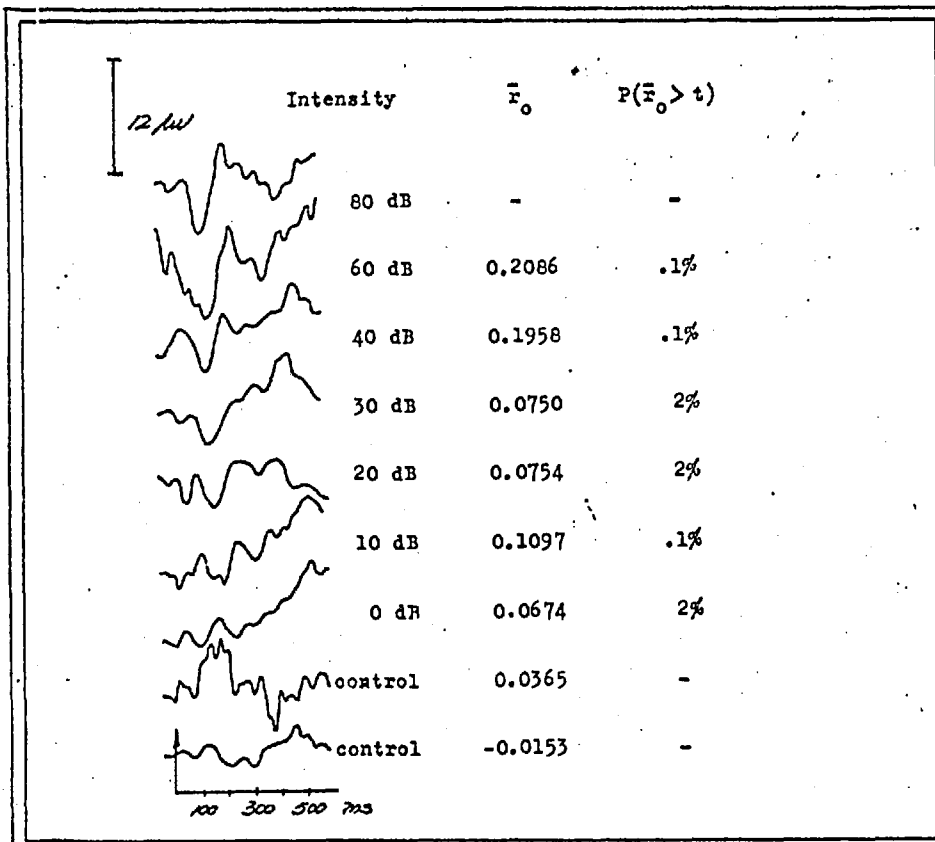


Table 5-xi. Subject SB, M, age 18, at 1 kHz and 4 kHz.



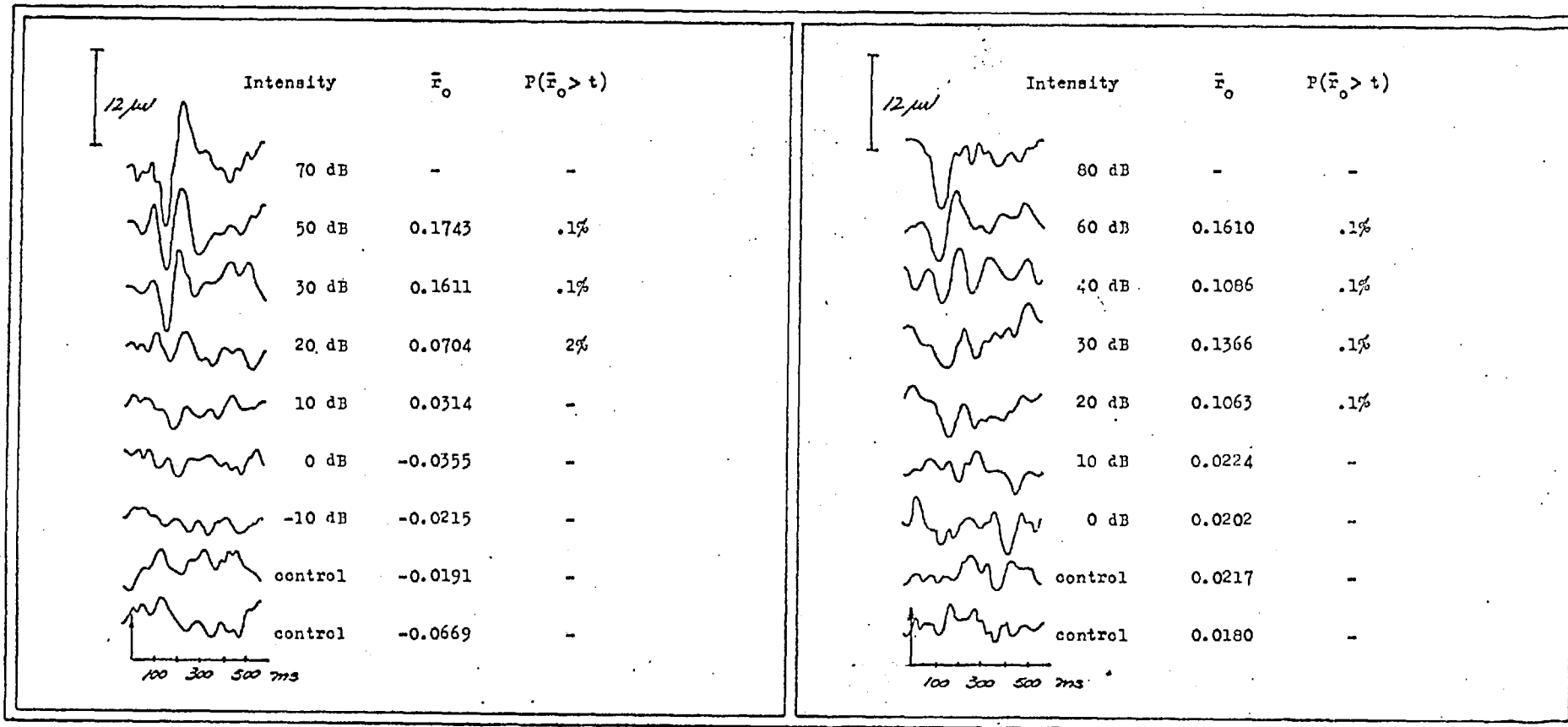


Table 5-xii. Subject VM, F, age 24, at 1 kHz and 4 kHz.

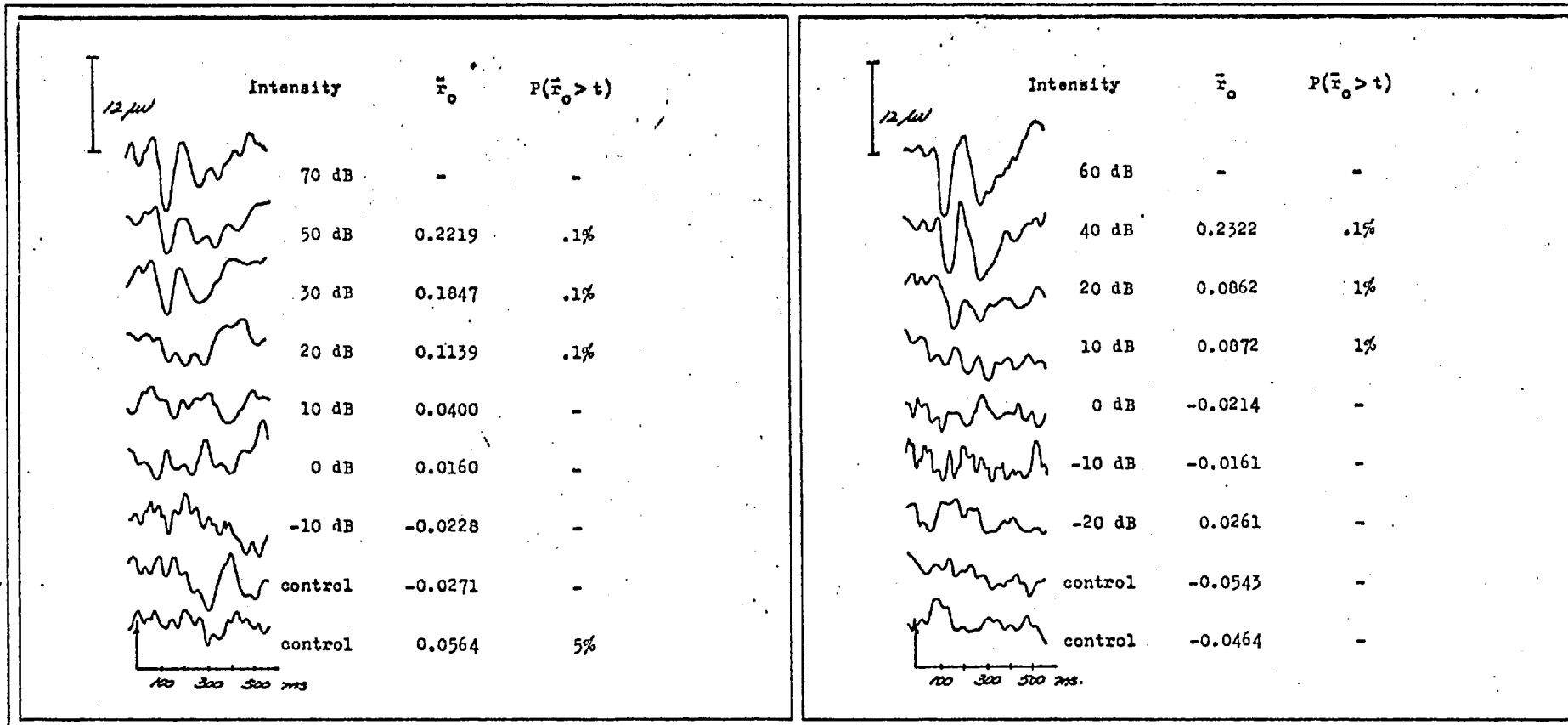


Table 5-xiii. Subject SBa, F, age 20, at 2 kHz and 500 Hz.

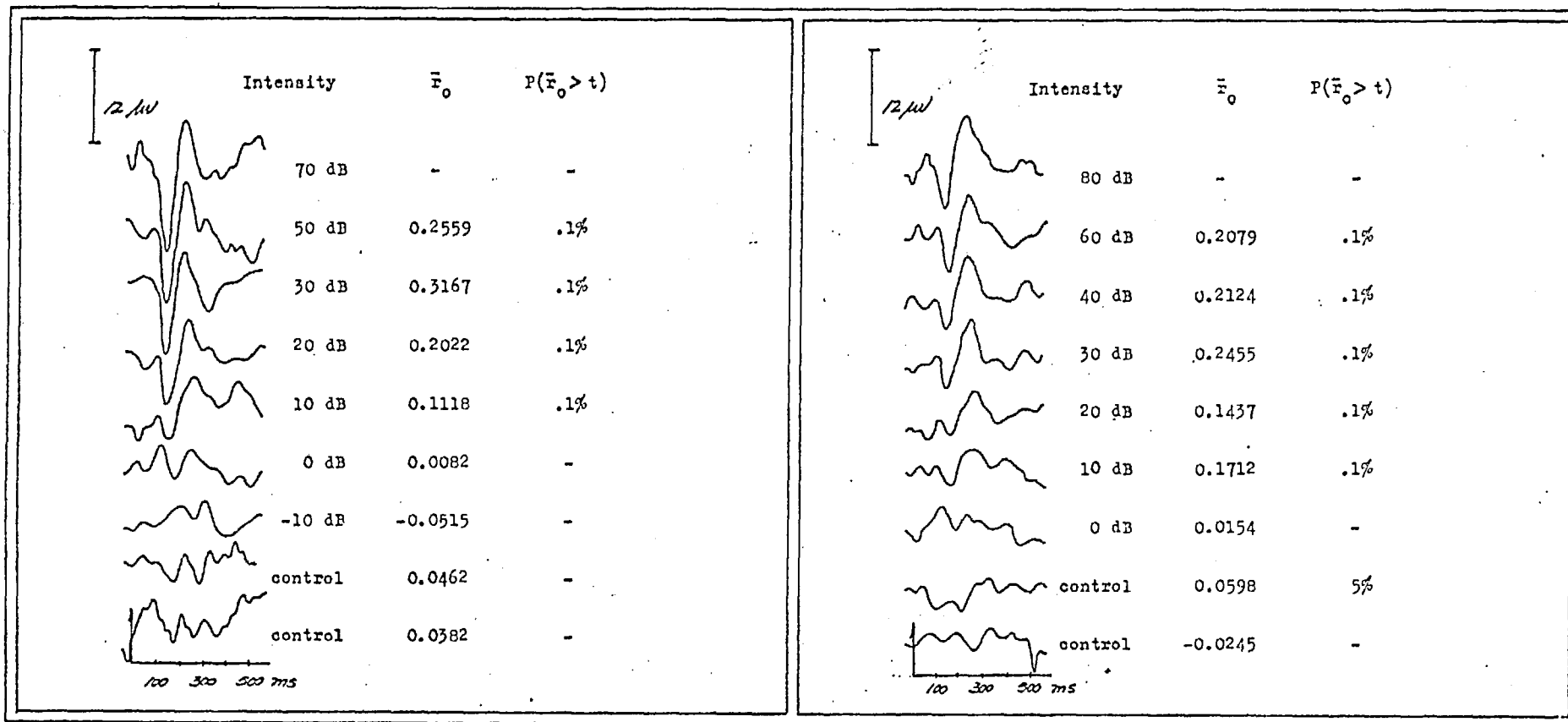


Table 5-xiv. Subject PC, M, age 24, at 2 kHz and 500 Hz.

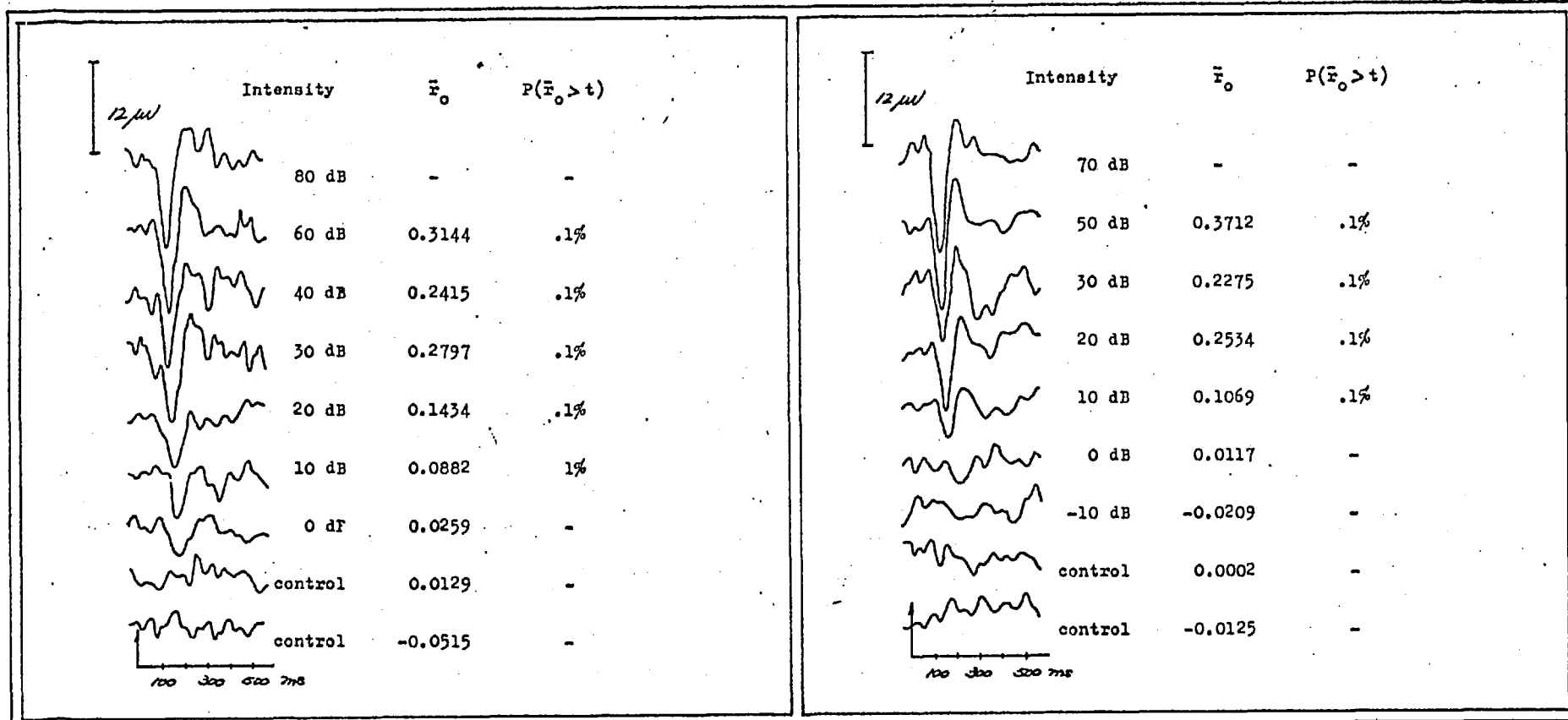


Table 5-xvi. Subject SA, M, age 28, at 2 kHz and 500 Hz.

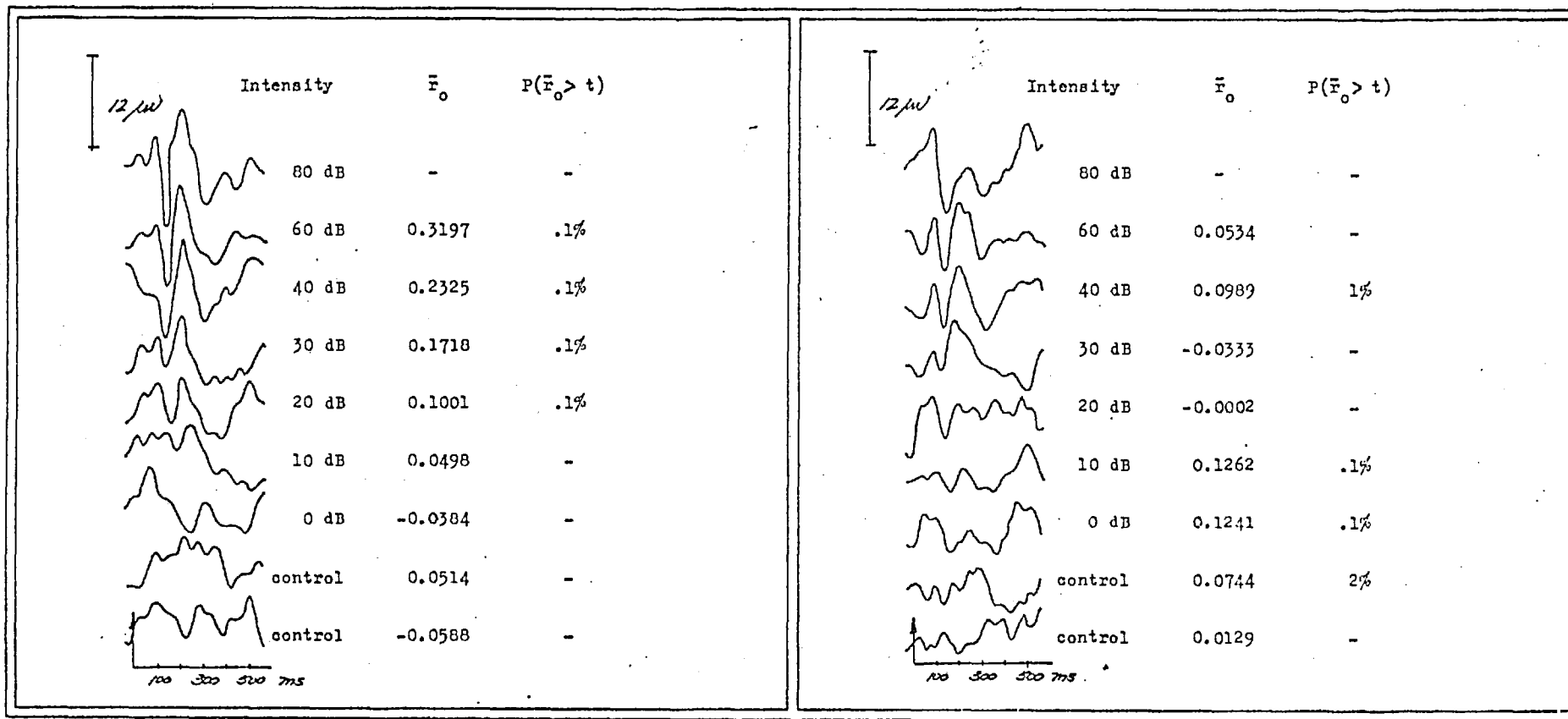


Table 5-xvi. Subject LS, F, age 20, at 1 kHz and 4 kHz.

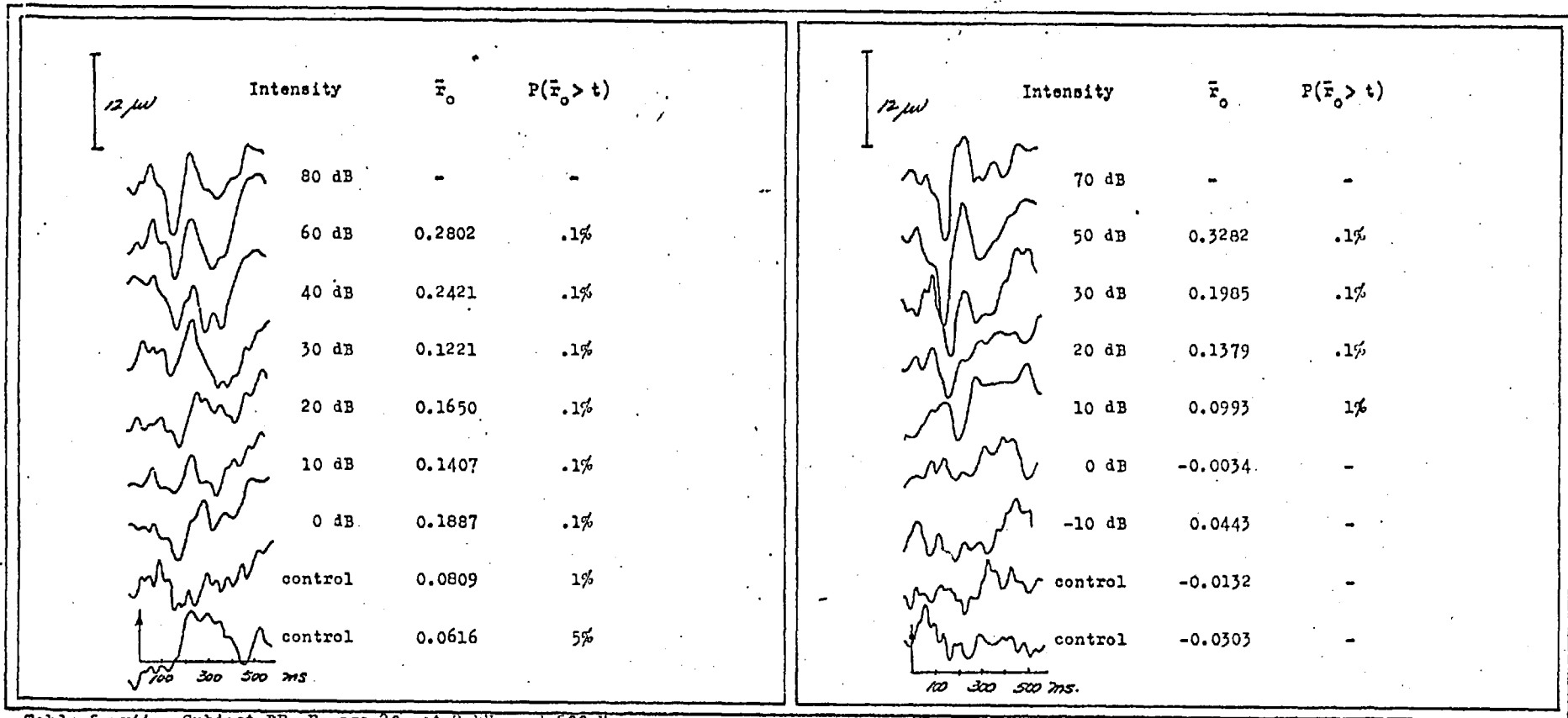


Table 5-xvii. Subject DF, F, age 20, at 2 kHz and 500 Hz.

Tables 5-xviii to 5-xxviii

The On-line Cross-correlation Study

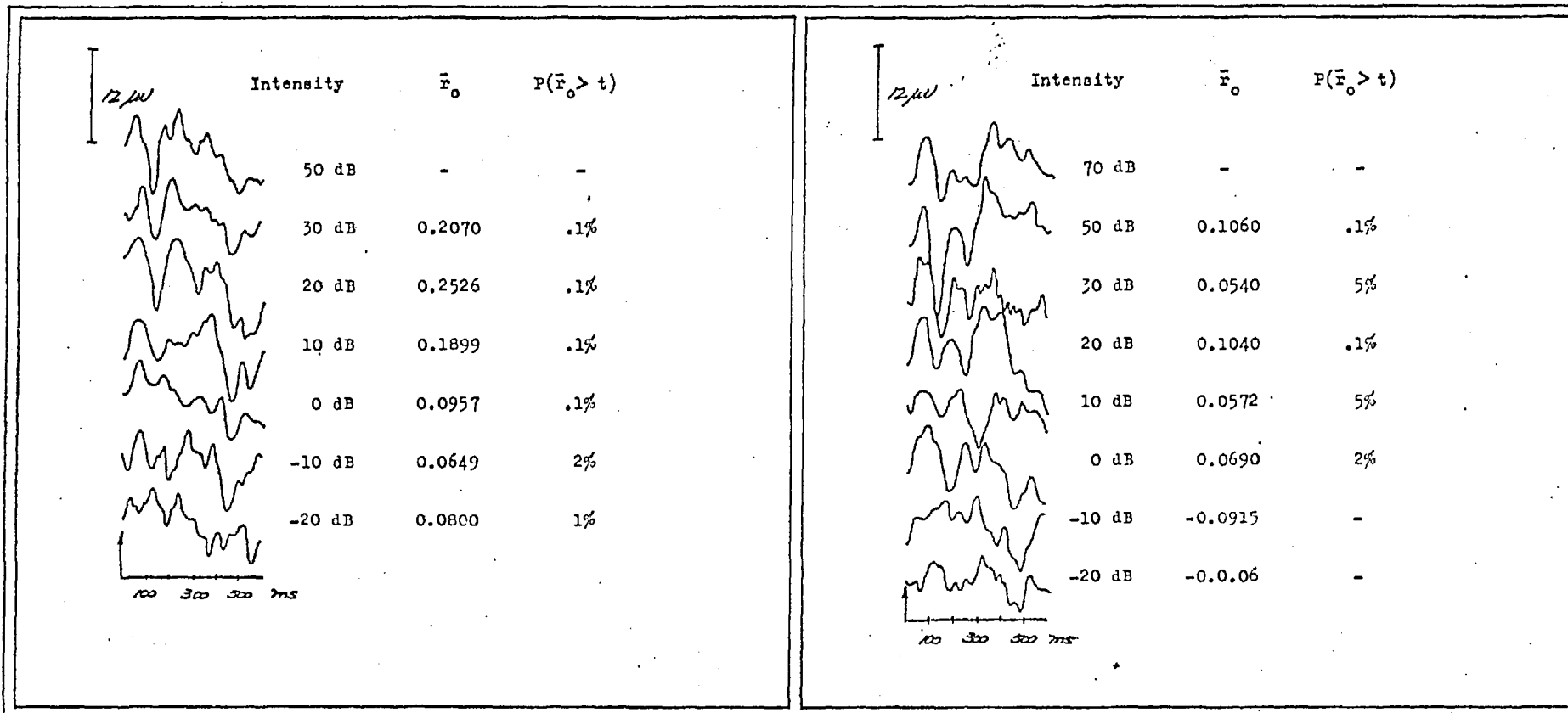


Table 5-xviii. Subjects GP, M, age 18, at 500 Hz, and EB, F, age 18, at 1 kHz.



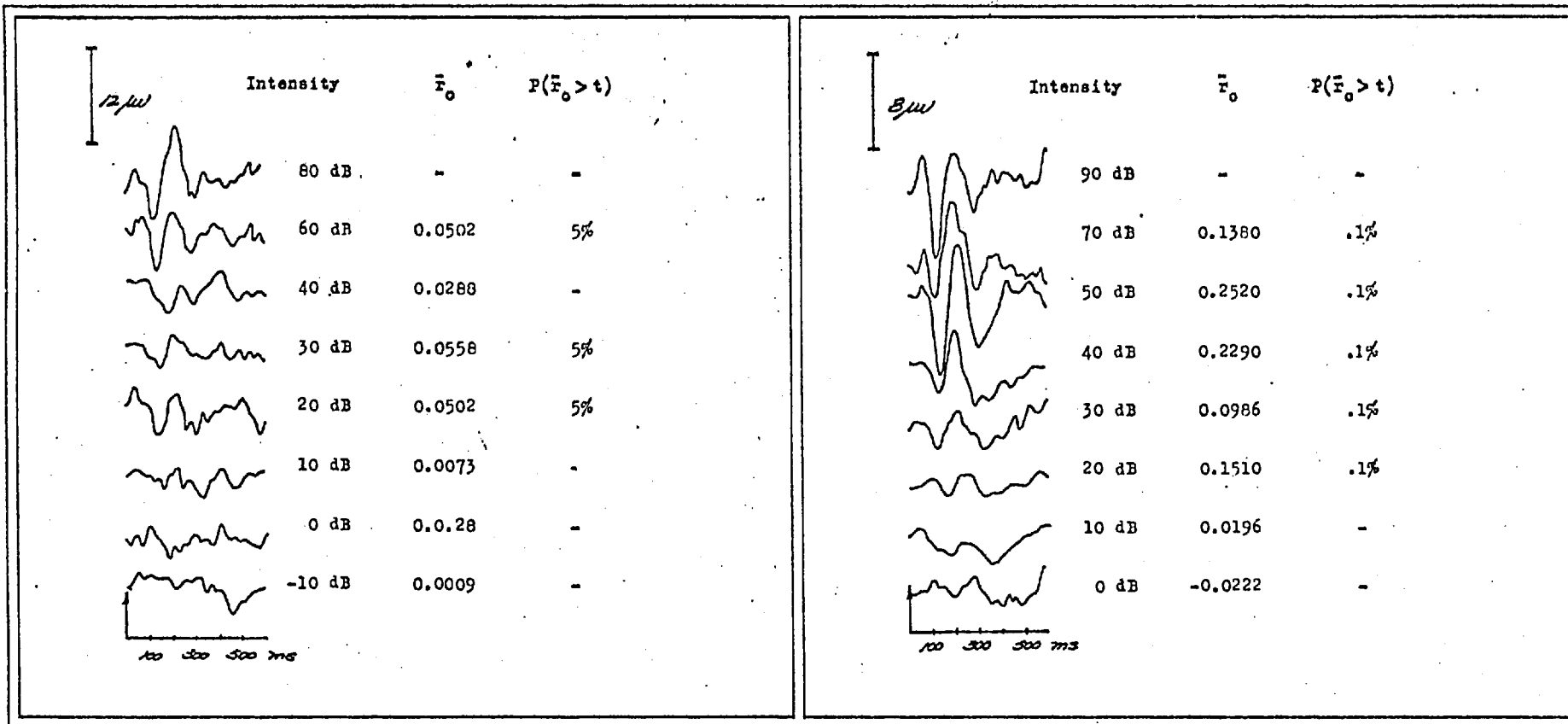


Table 5-xix. Subjects SH, F, age 20, at 2 kHz and RB, F, age 20, at 2 kHz.

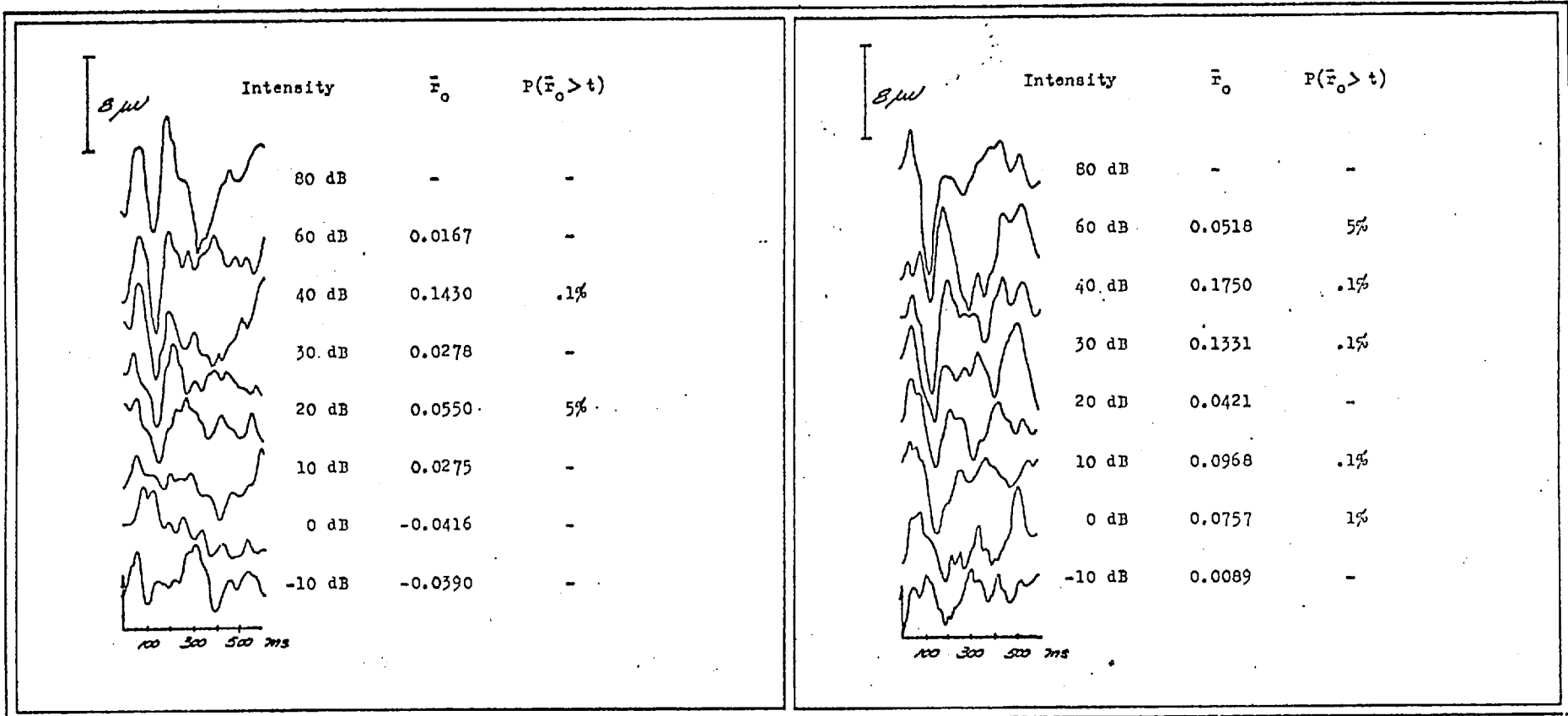


Table 5-xx. Subject AP, F, age 20, at 4 kHz and 1 kHz.

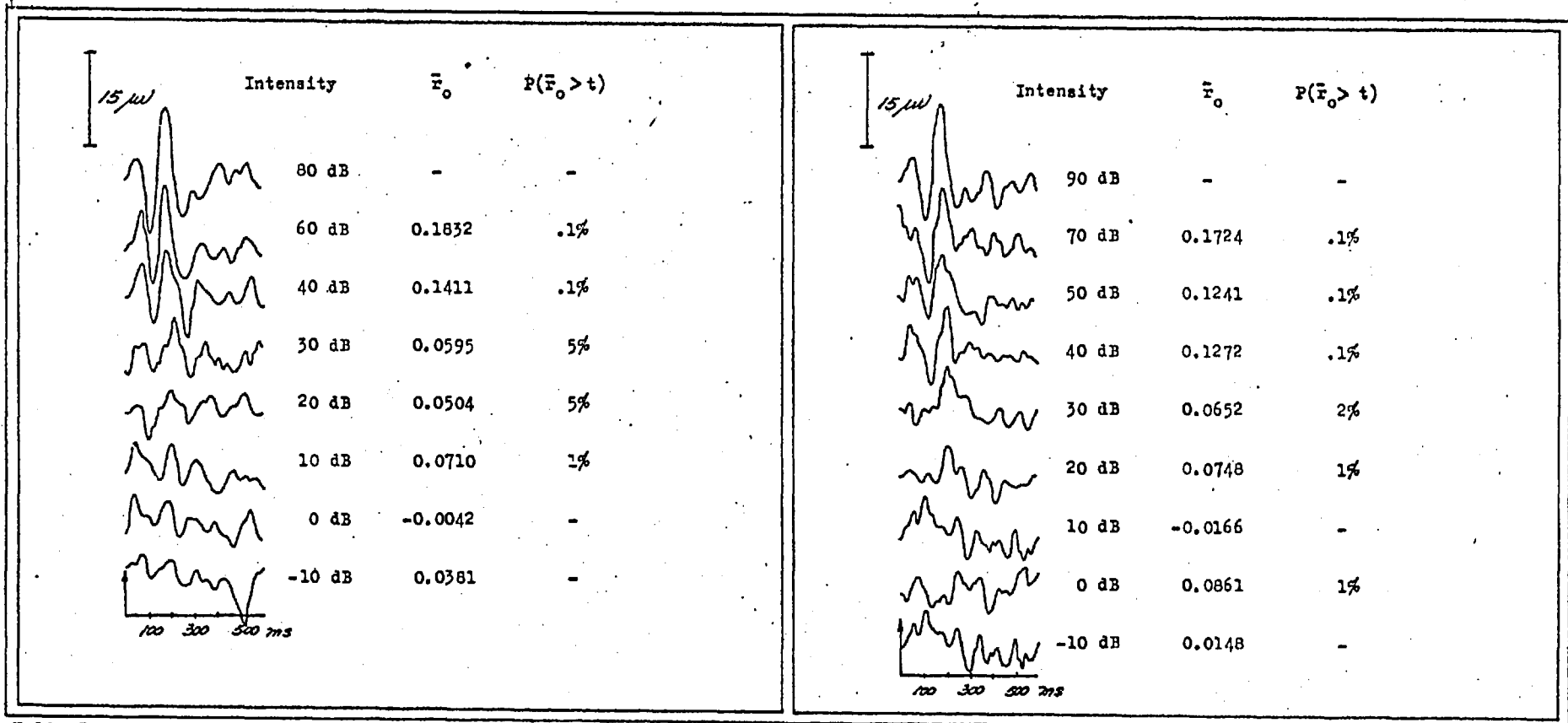


Table 5-xxi. Subject KC, F, age 20, at 1 kHz and 4 kHz.

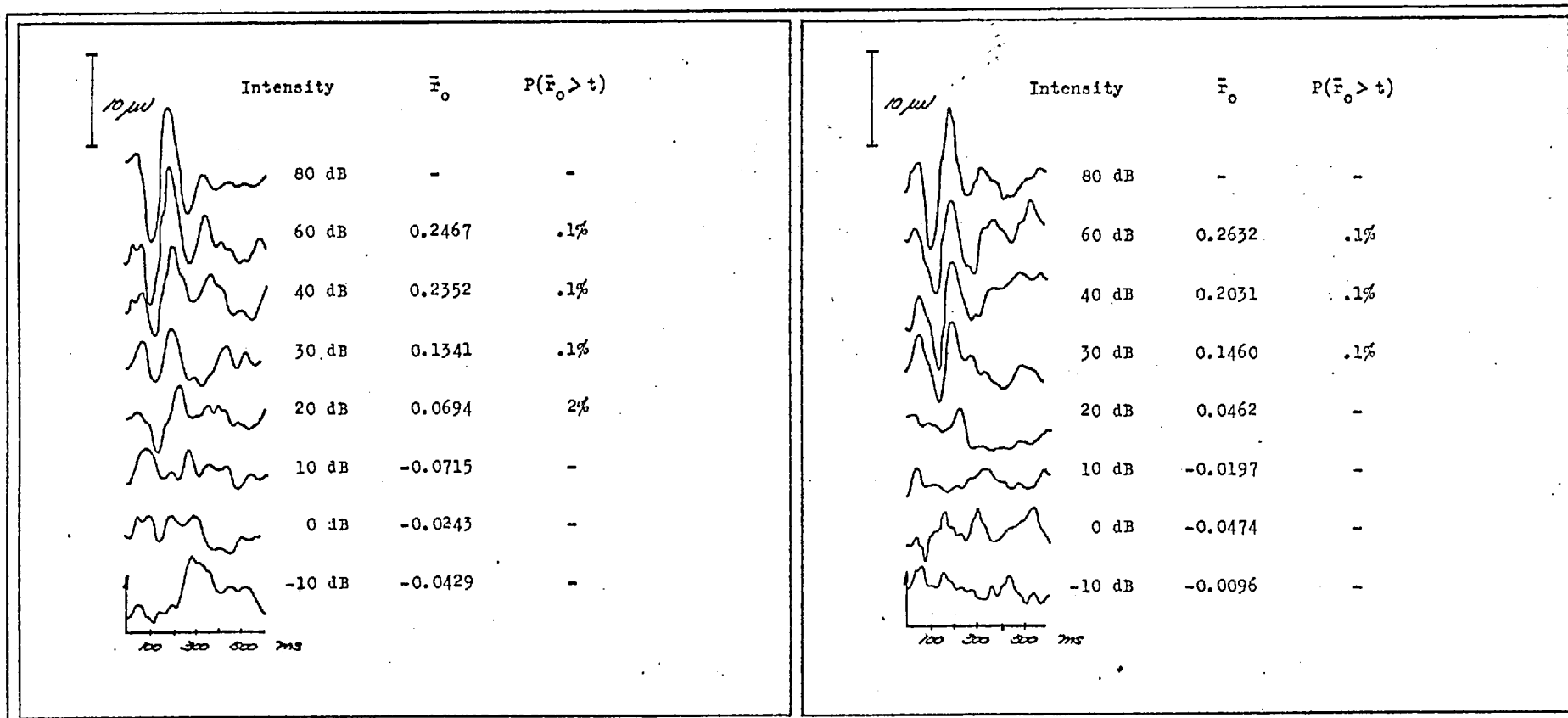


Table 5-xxii. Subject SC, F, age 22, at 2 kHz and 500 Hz.

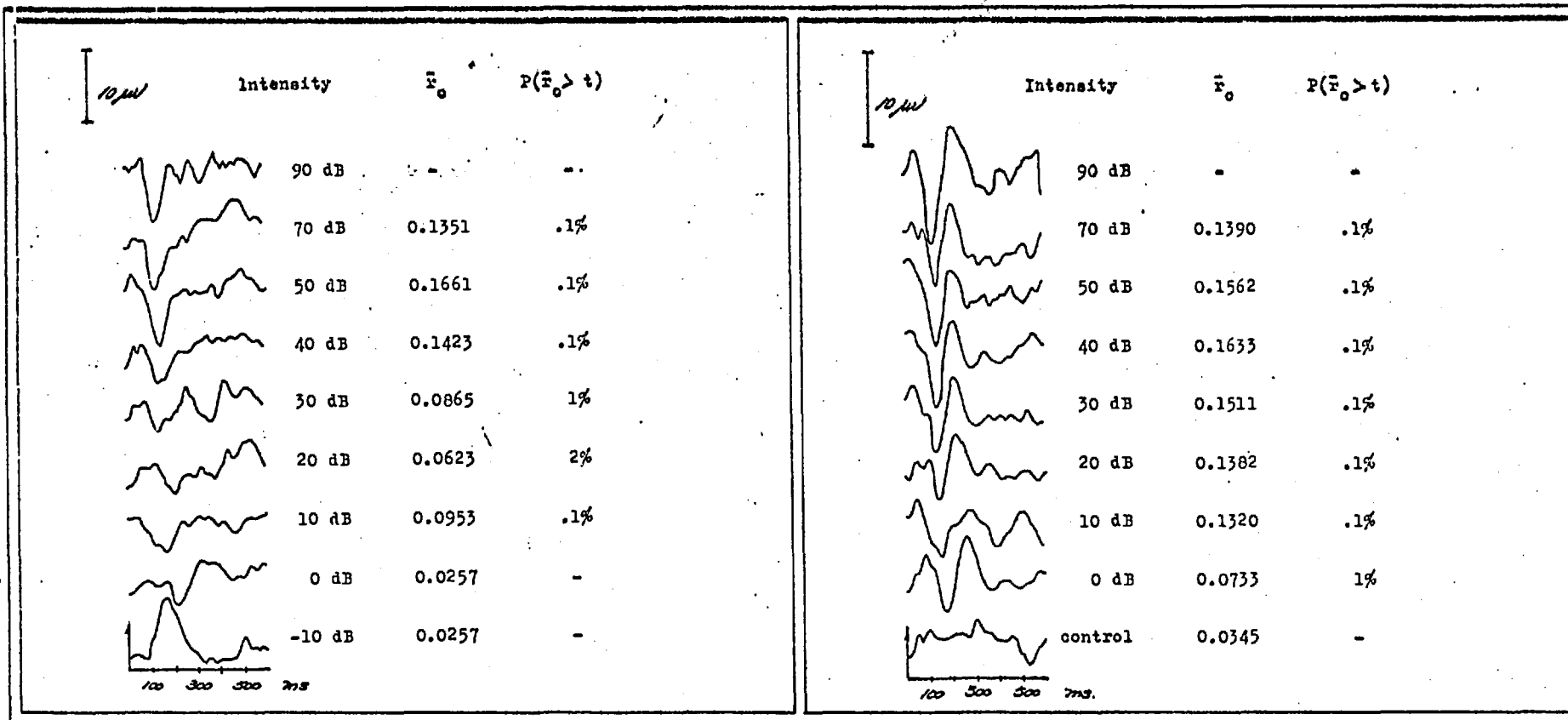


Table 5-xxiii. Subjects AR, M, age 19, at 1 kHz, and RW, M, age 19, at 4 kHz.

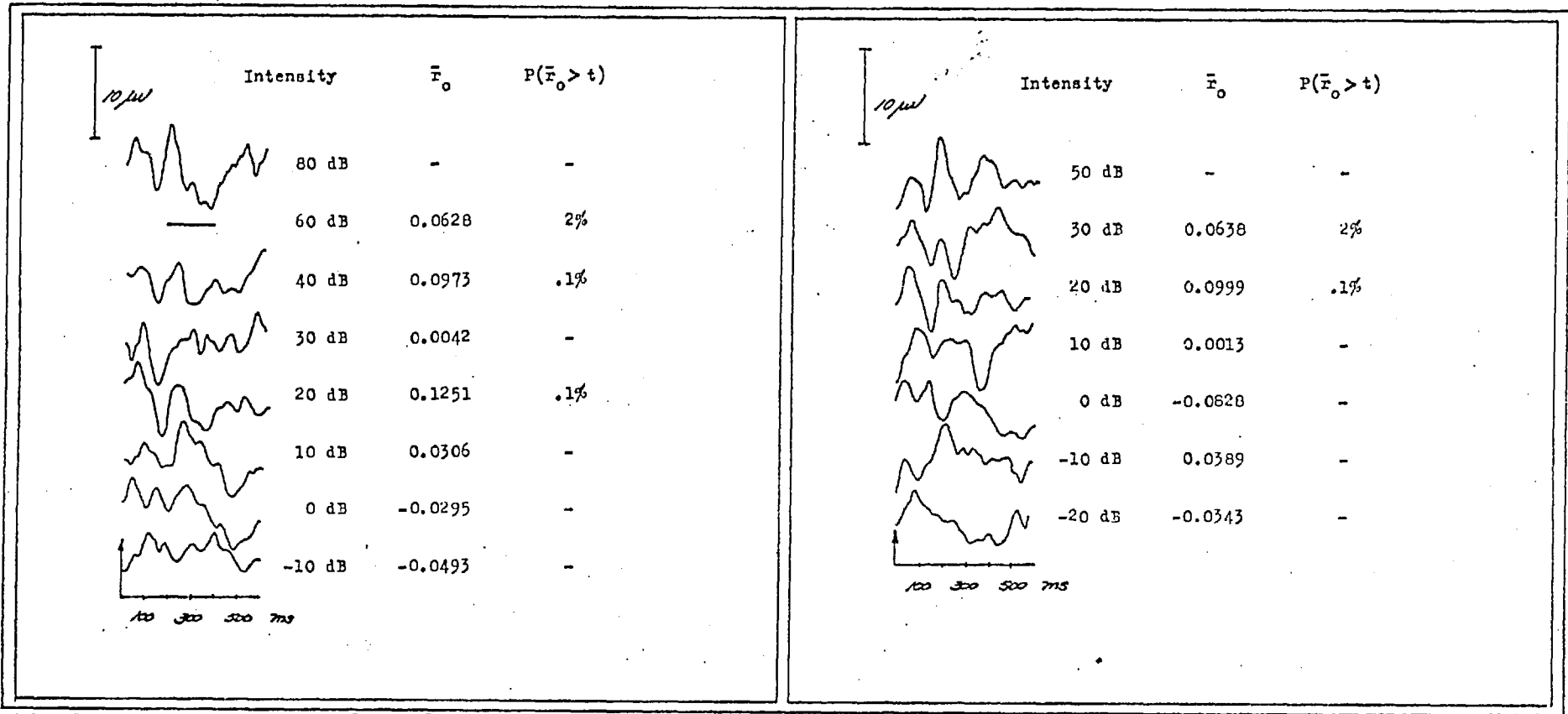


Table 5-xxiv. Subject CK, R, age 19, at 2 kHz and 500 Hz.

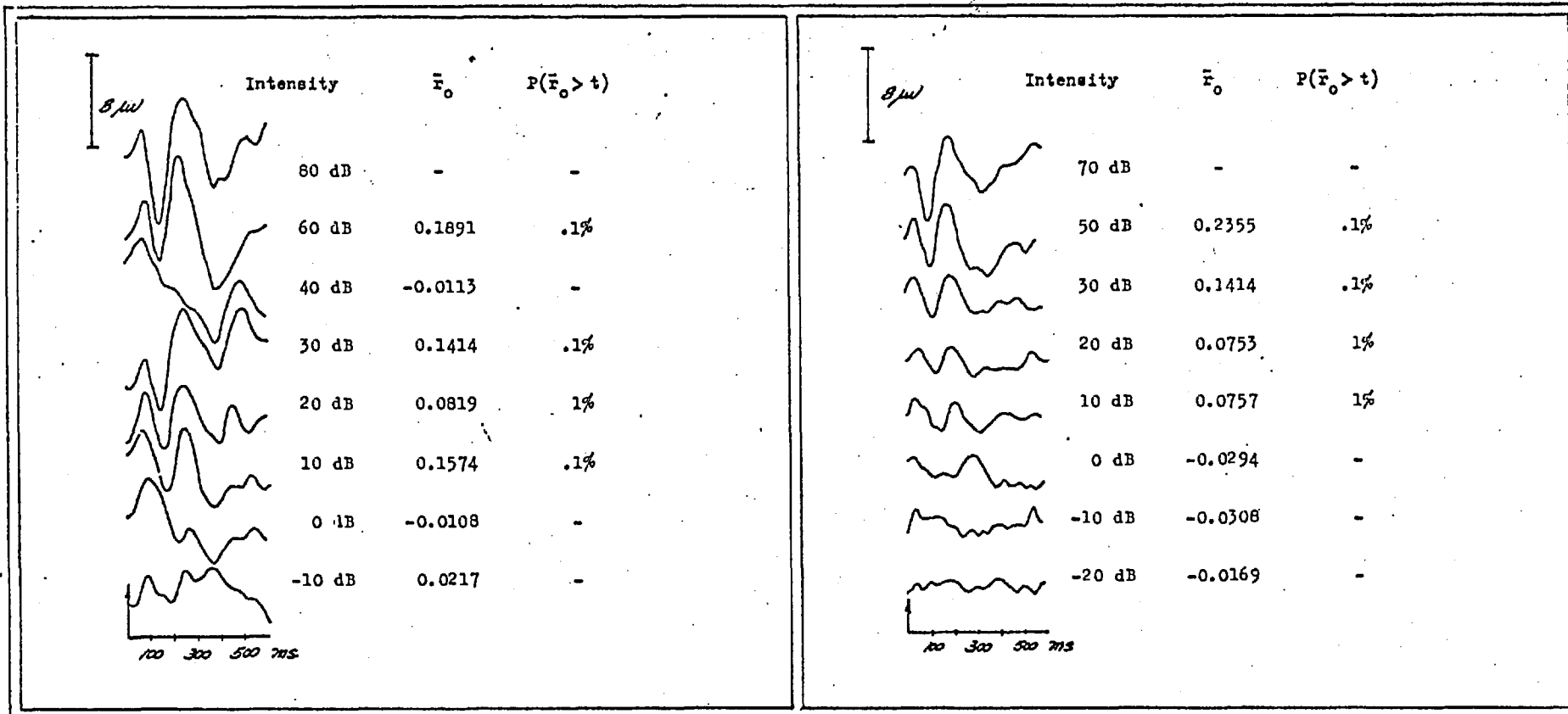


Table 5-xxv. Subject GD, F, age 19, at 2 kHz and 500 Hz.

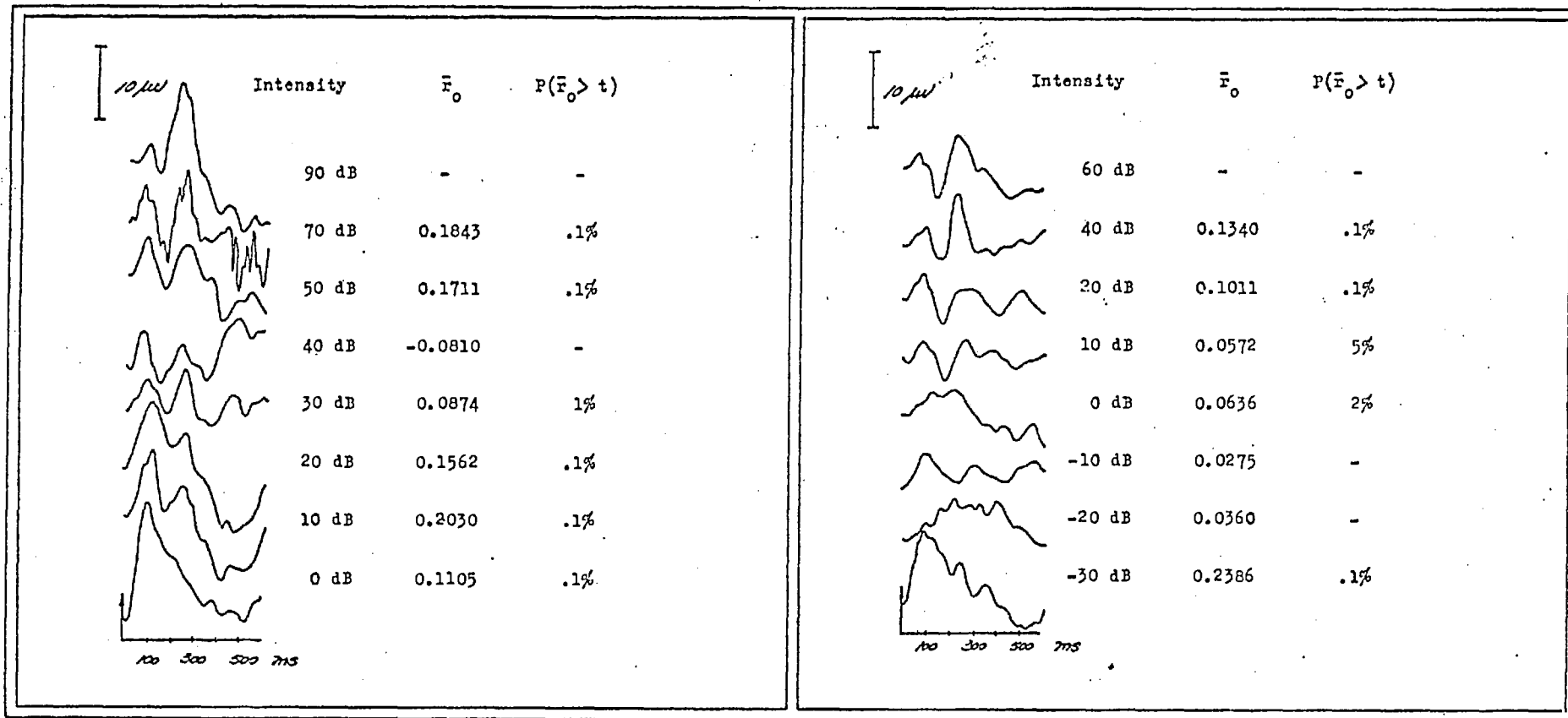


Table 5-xxvi. Subject SR, M, age 20, at 2 kHz and 500 Hz.



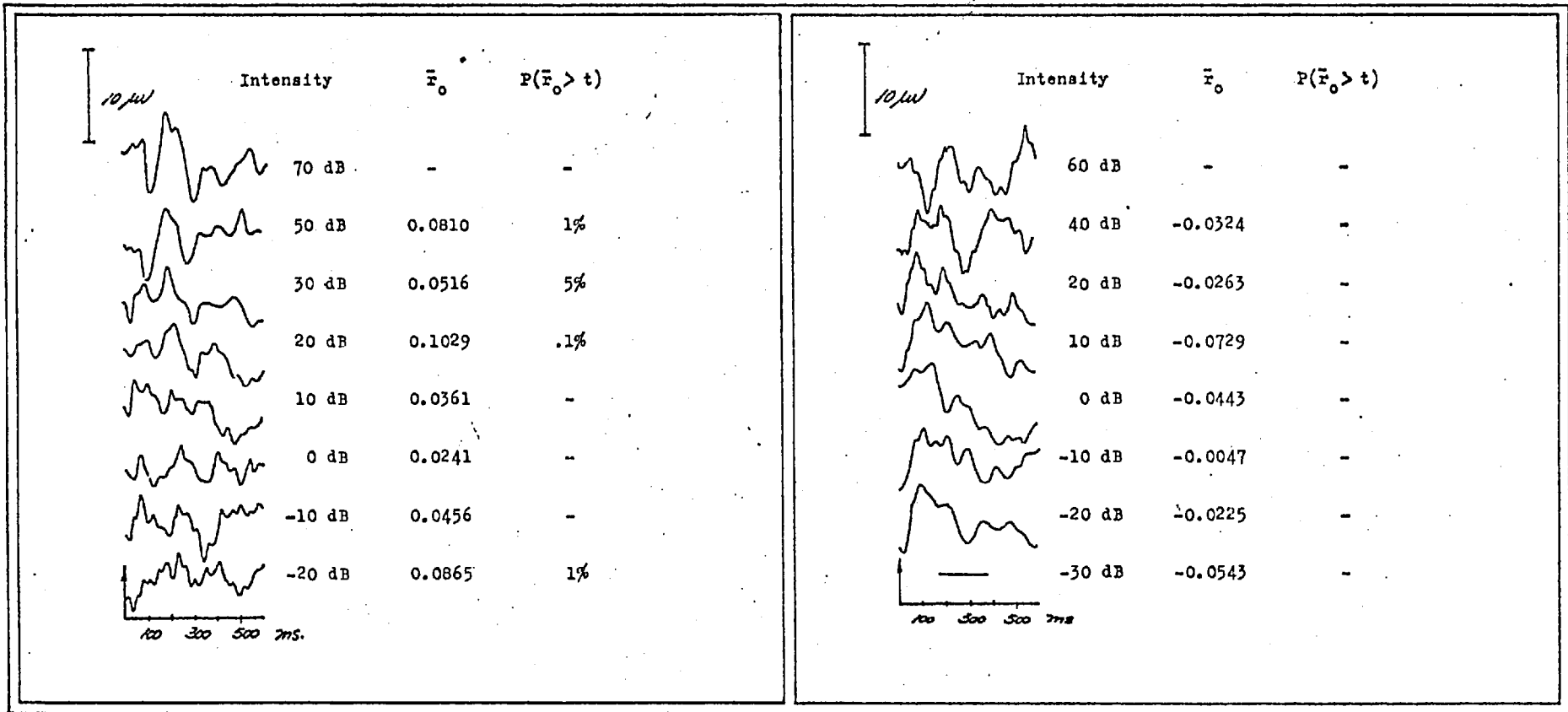


Table 5-xxvii. Subject BS, F, age 23, at 1 kHz and 4 kHz.

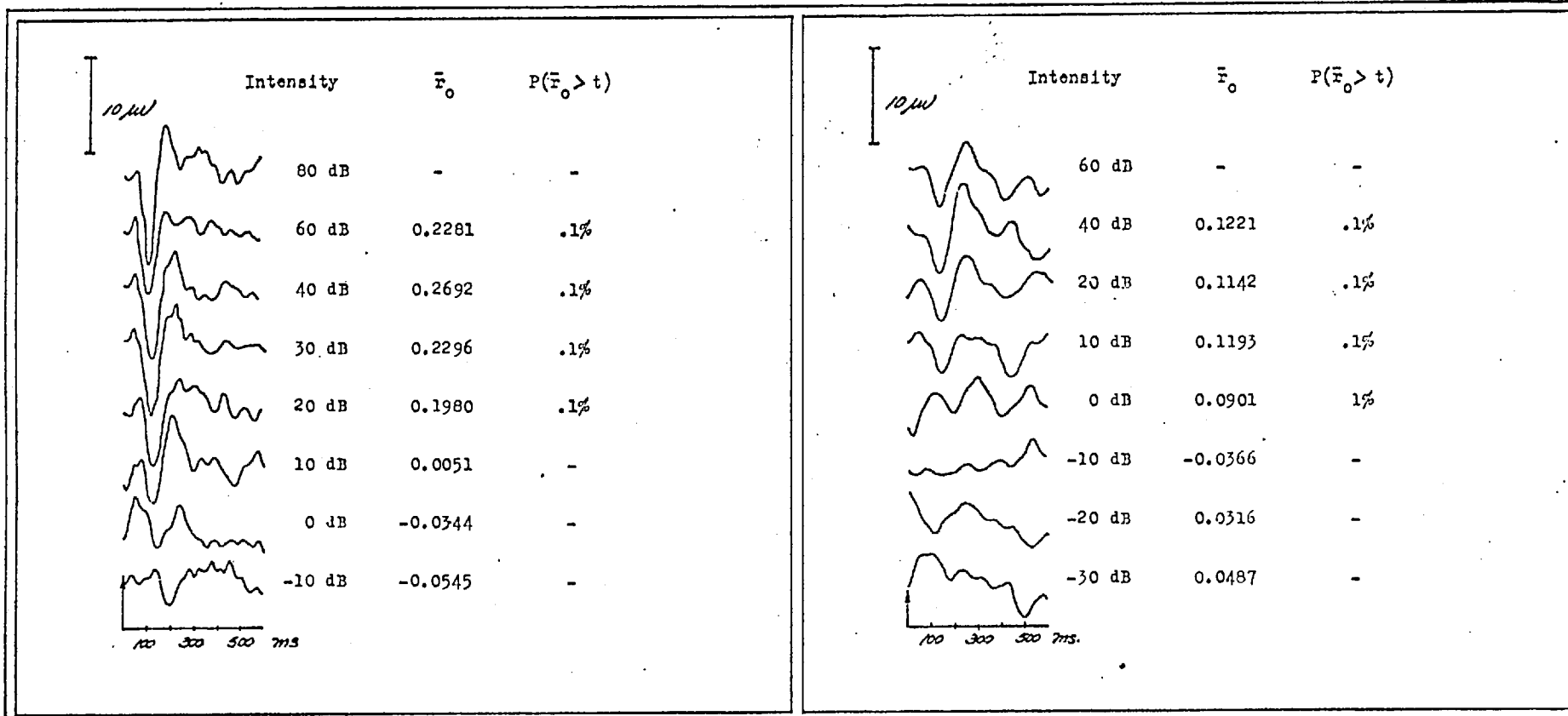


Table 5-xxviii. Subject TR, M, age 31, at 1 kHz and 4 kHz.

Tables 5-xxix to 5-xxxix

The Off-line Verification

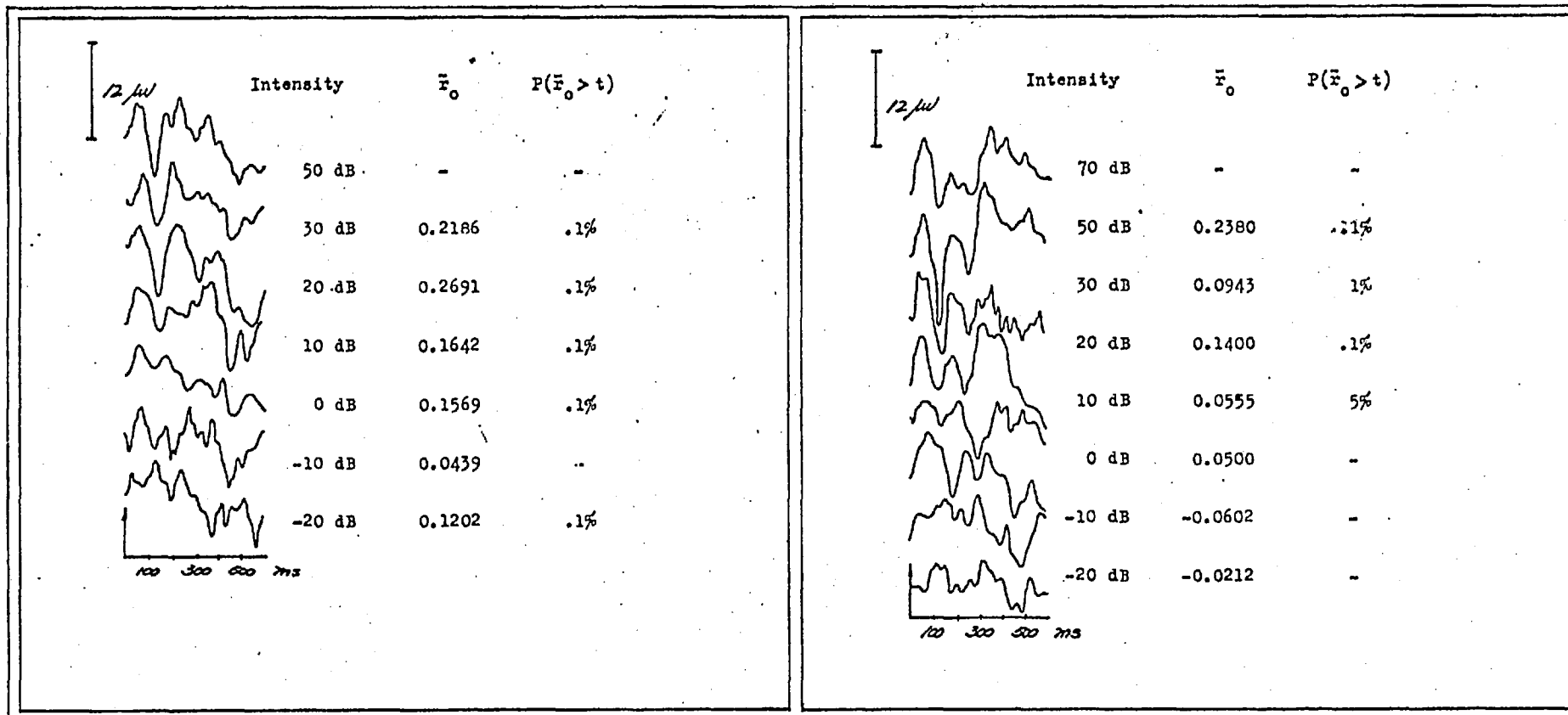


Table 5-xxix. Subjects GP, M, age 18, at 500 Hz and EB, F, age 18, at 1 kHz.

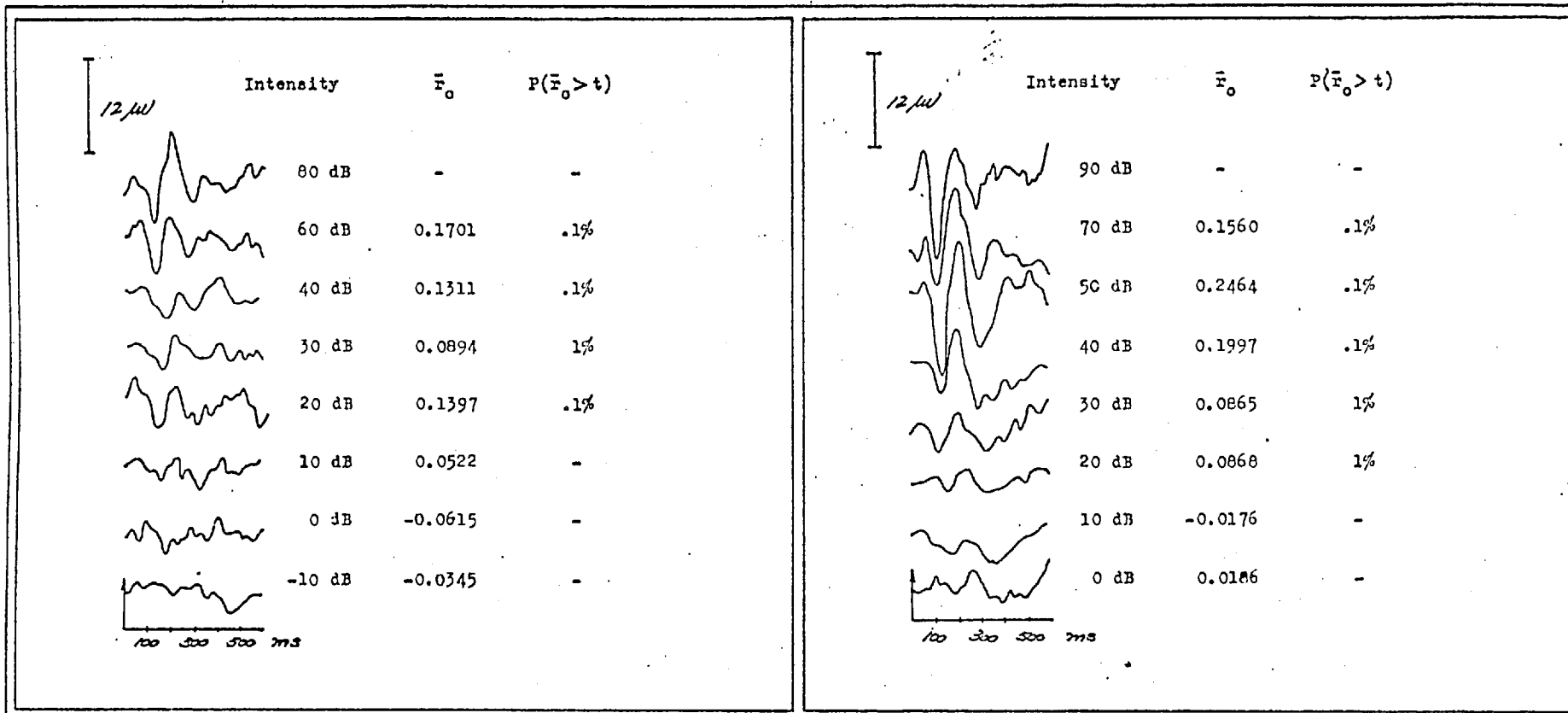


Table 5-xxx. Subjects SH, F, age 20, at 2 kHz and RB, F, age 20, at 2 kHz.

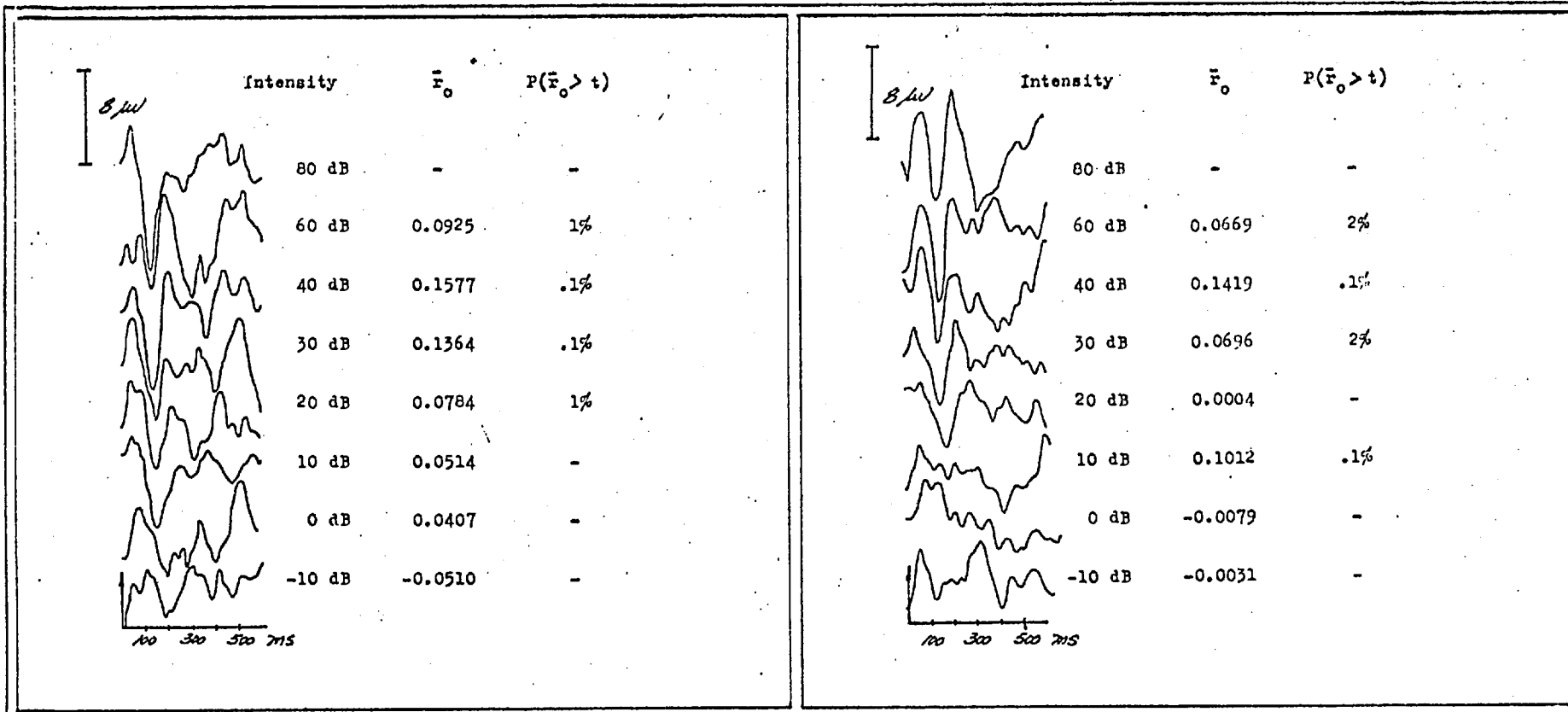


Table 5-xxxi. Subject AP, F, age 20, at 1 kHz and 4 kHz.

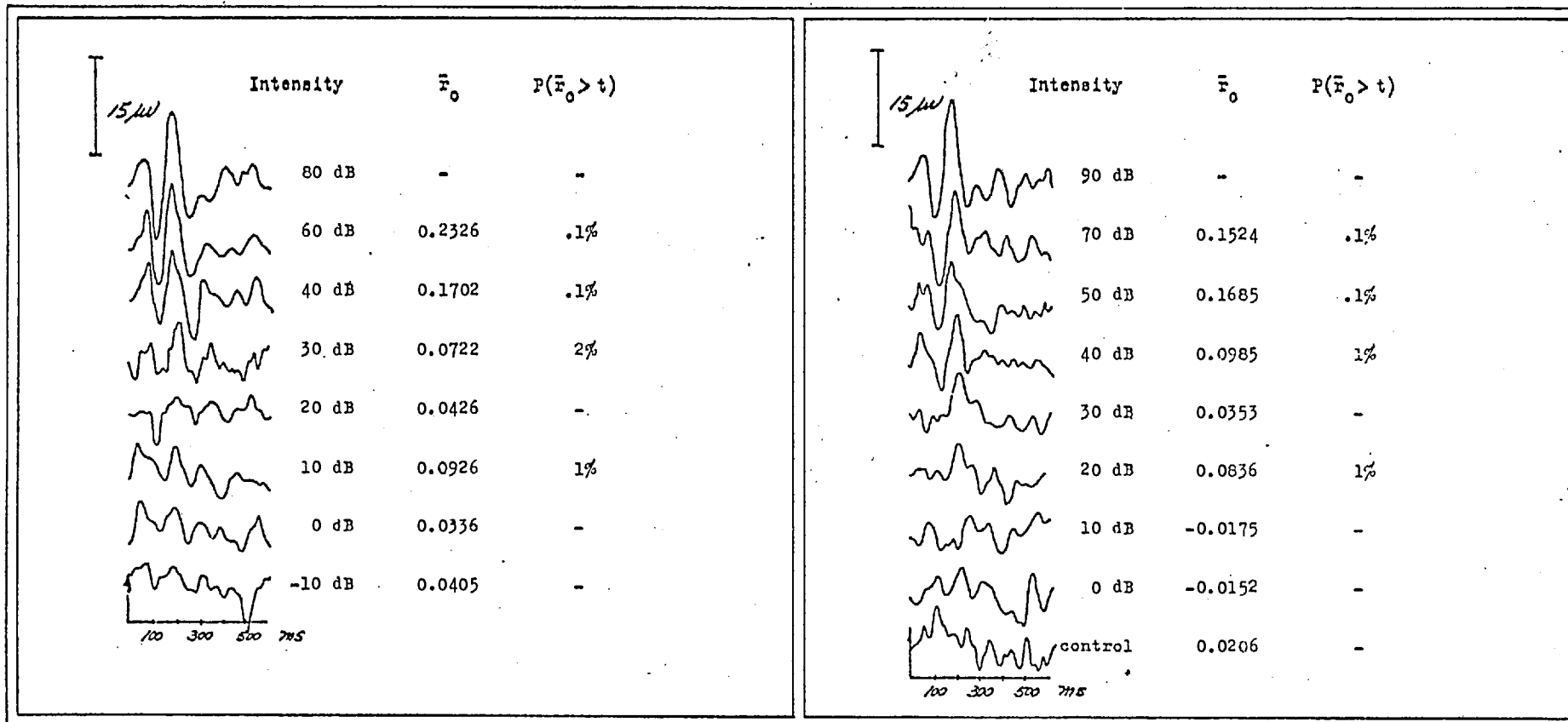


Table 5-xxxii. Subject KC, F, age 20, at 1 kHz and 4 kHz.

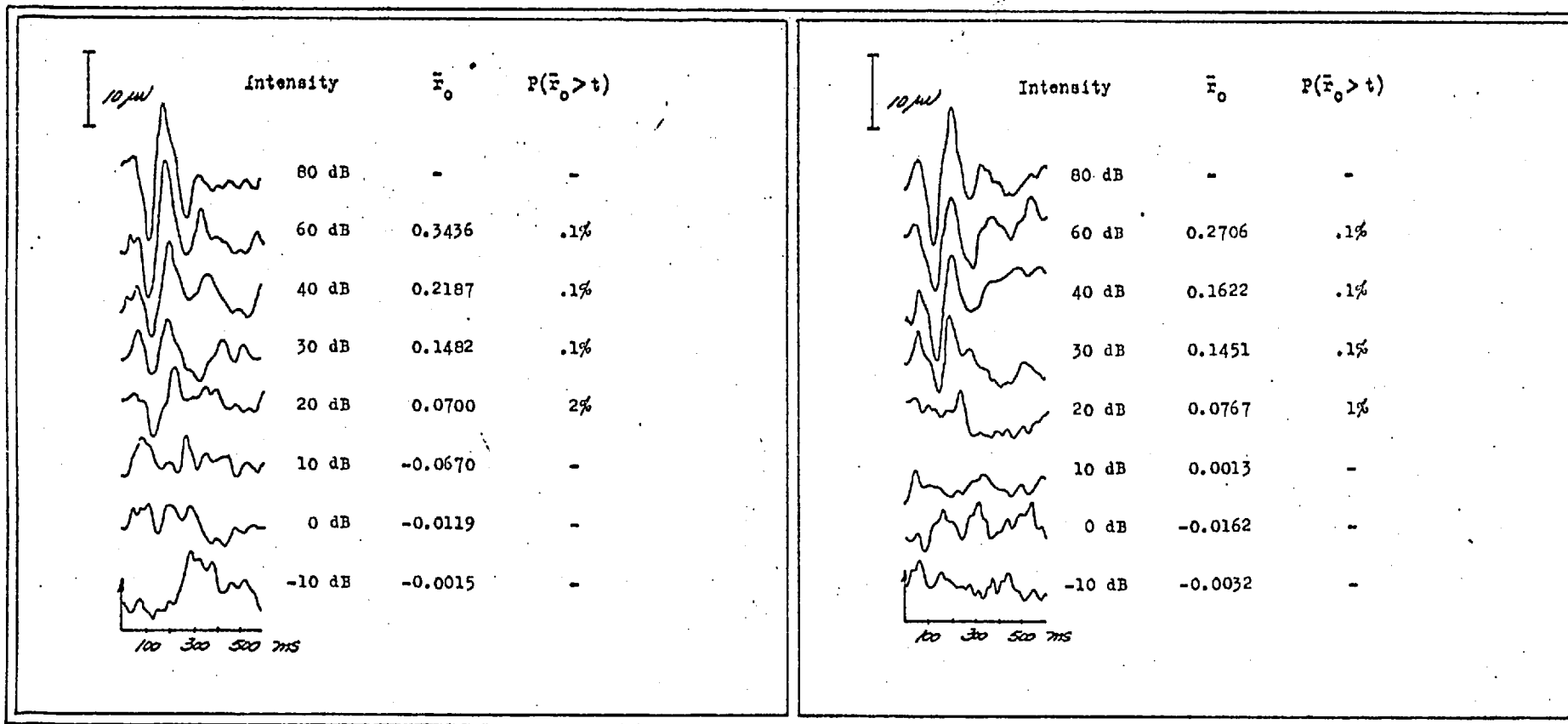


Table 5-xxxiii. Subject SC, F, age 22, at 2 kHz and 500 Hz.



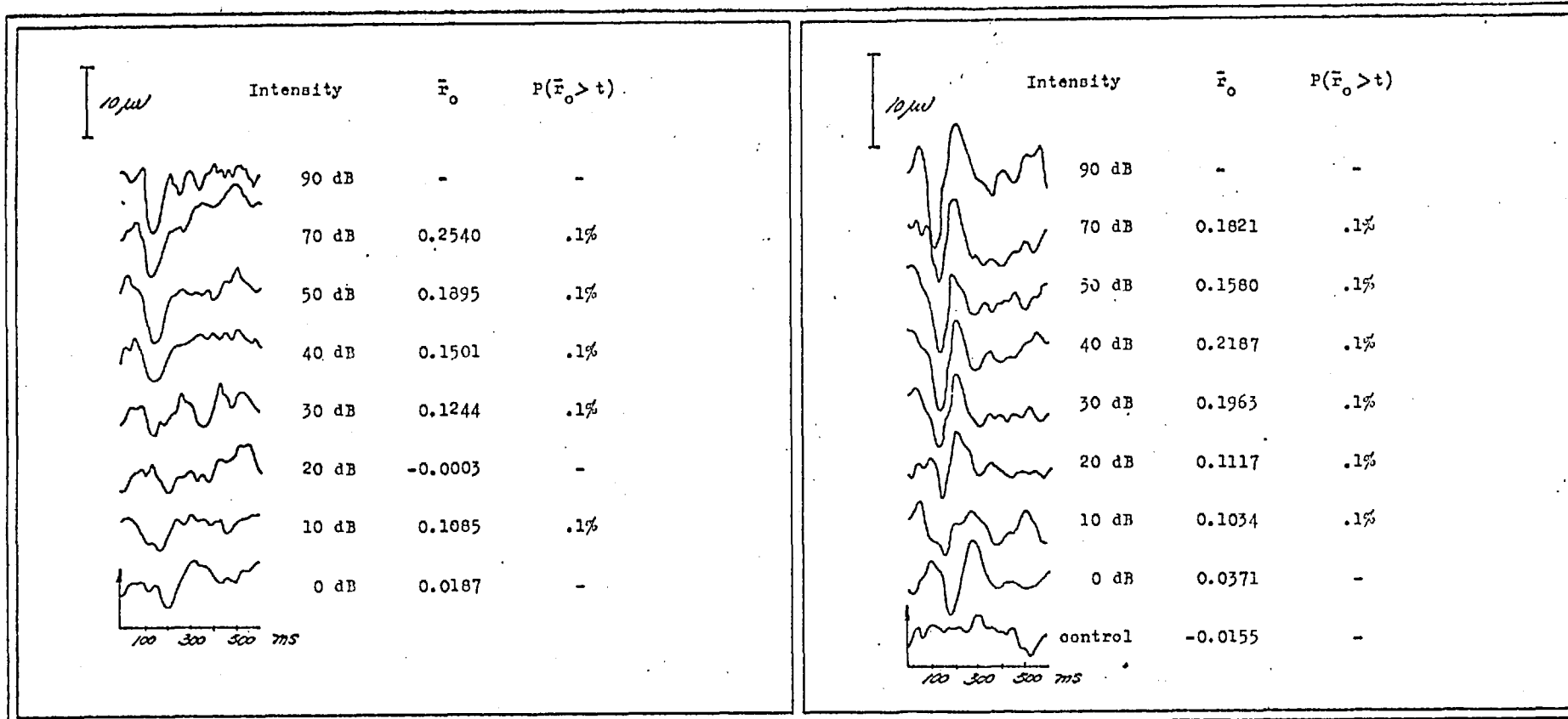


Table 5-xxxiv. Subjects AH, M, age 19, at 1 kHz and RW, M, age 19, at 4 kHz.

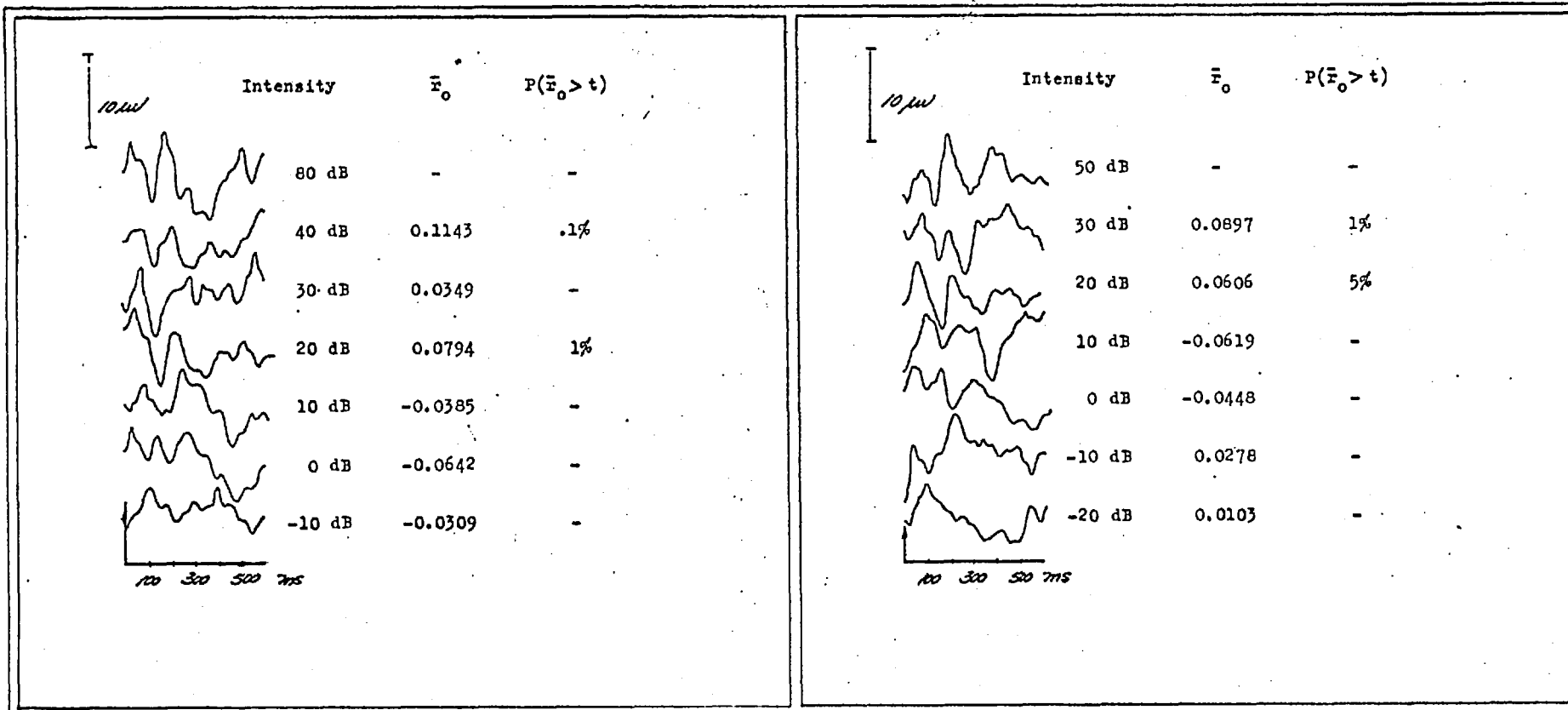


Table 5-xxxv. Subject CK, F, age 19, at 2 kHz and 500 Hz.

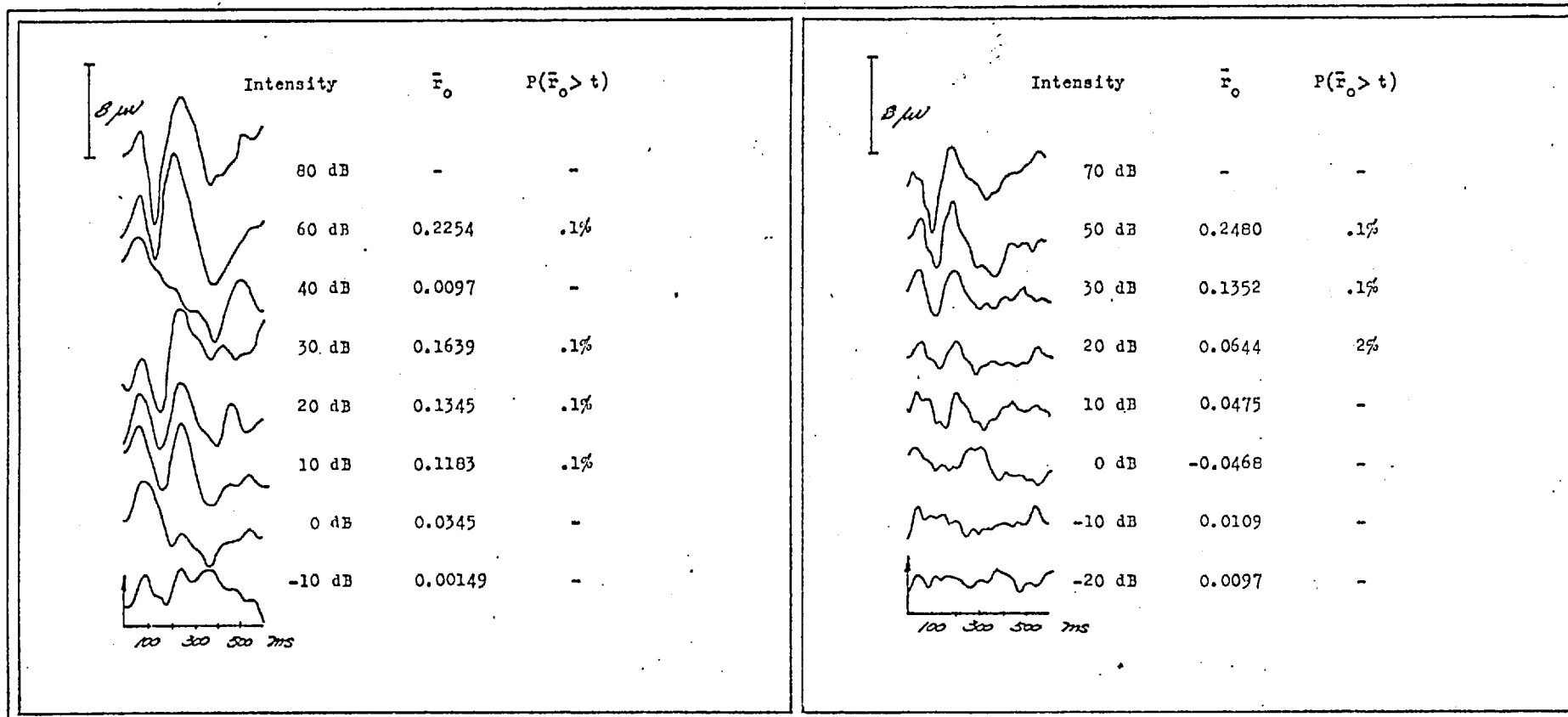


Table 5-xxxvi. Subject GD, F, age 19, at 2 kHz and 500 Hz.

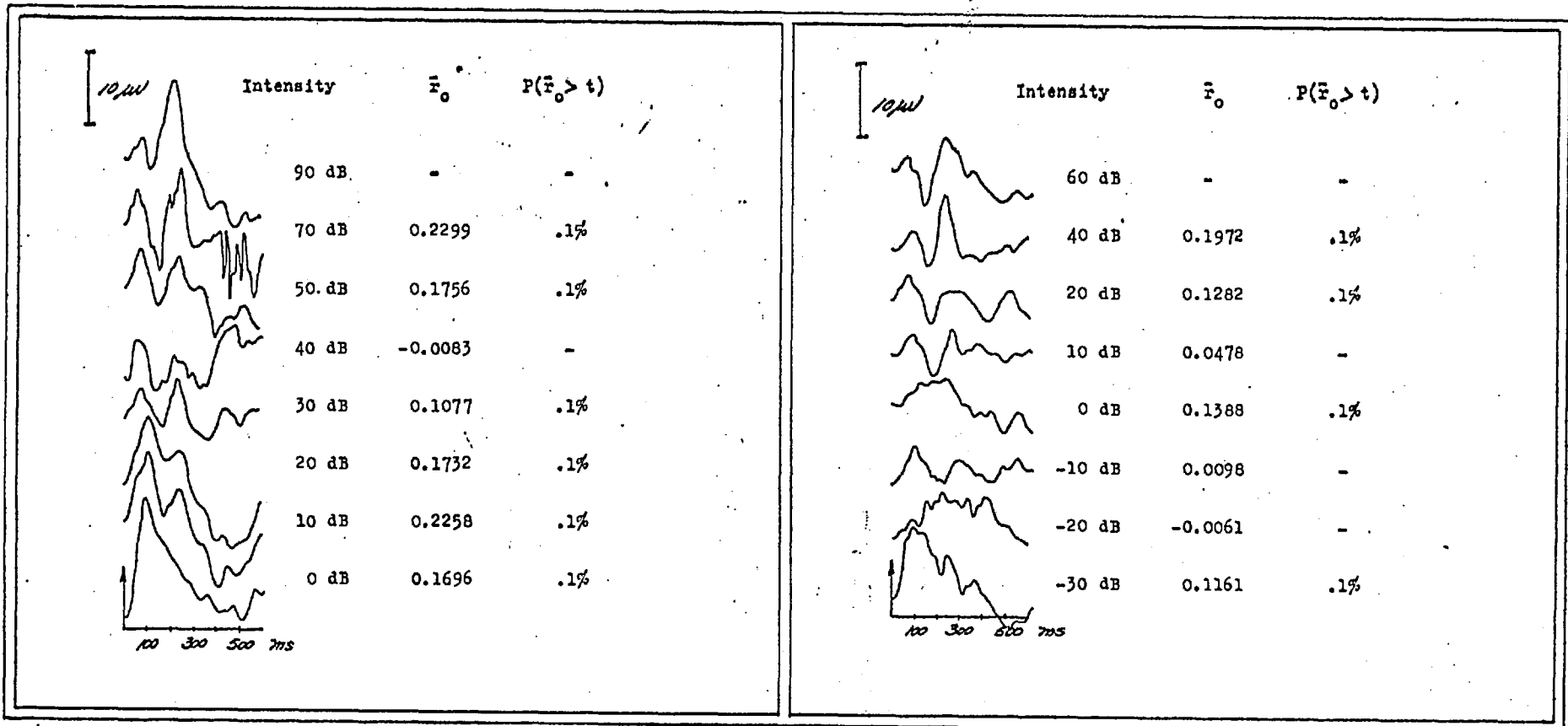


Table 5-xxxvii. Subject SR, M, age 20, at 2 kHz and 500 Hz.

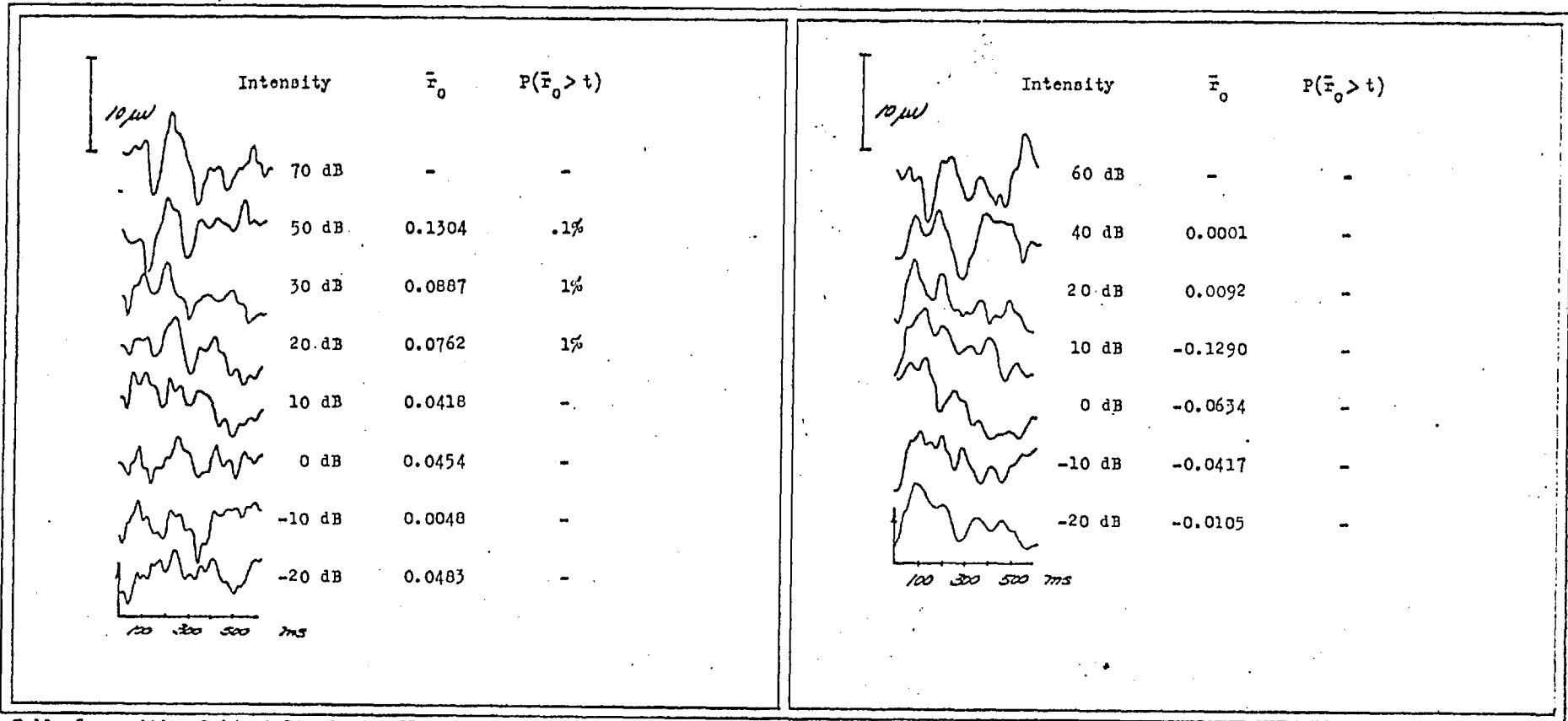


Table 5-xxxviii. Subject BS, F, age 23, at 1 kHz and 4 kHz.

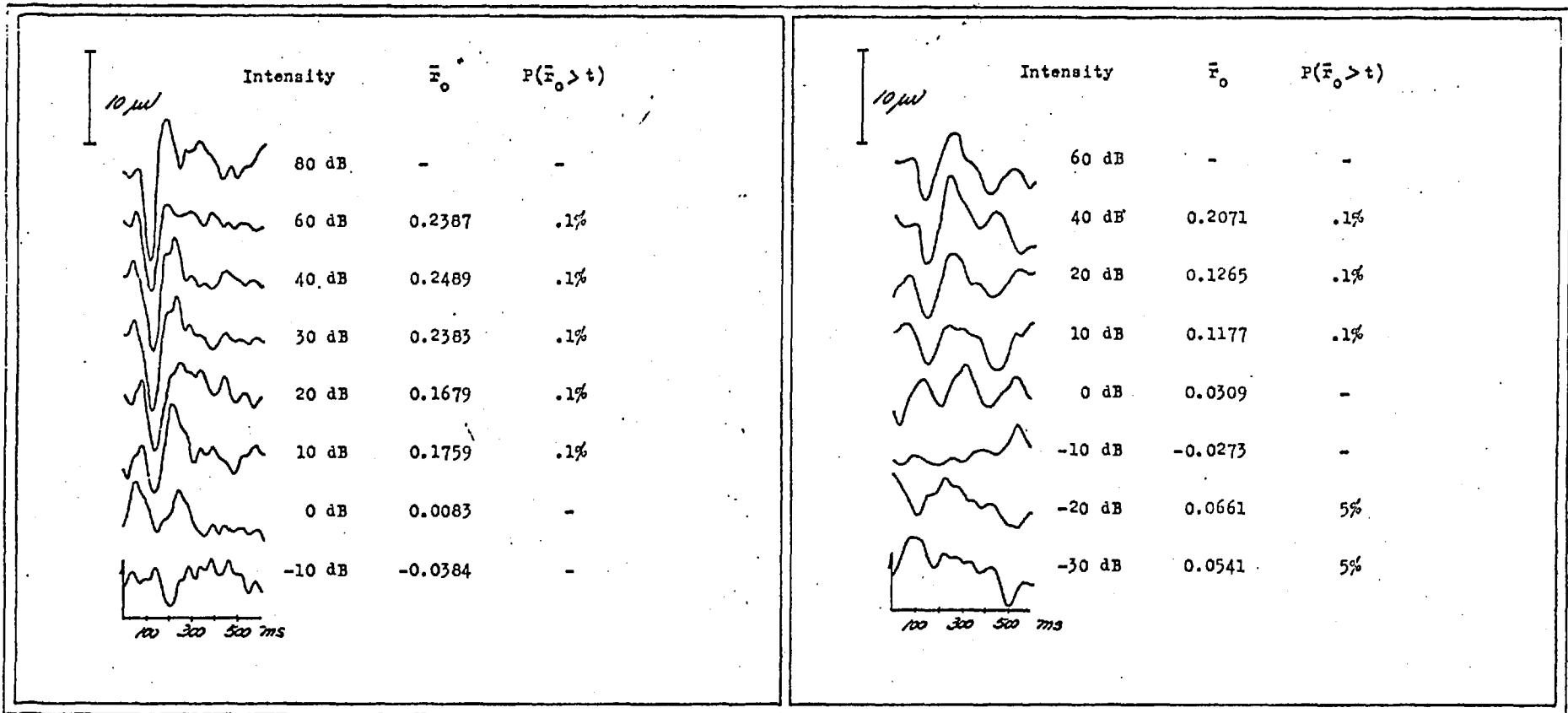


Table 5-xxxix. Subject TR, M, age 31, at 1 kHz and 4 kHz.

## CHAPTER SIX

## CONCLUSION

## 6.1. Introduction

The aim of the work reported in this thesis was to develop objective methods for detecting the auditory evoked potential present in the EEG. The statistical properties of the data were only vaguely understood at the outset of this study. It soon became clear that the data was frequently ill-behaved; its statistical properties, therefore, needed examination, delineation, and required understanding before any effective means of detection could be proposed and implemented. The signal analysis approach adopted here made possible a thorough examination of signal and noise sources, thereby defining their nature. These investigations led to the development of several reliable means of AEP detection.

## 6.2. Objective AEP Detection

In order to provide some effective means of detecting the AEP, three different signal approaches have been developed and assessed. Two important conclusions were drawn from the power analyses of Chapter Three. First, the typically low signal-to-noise ratio of ERA data does not allow power measures to be effective in discriminating the presence of a response. Second, the ensemble power or variance of EEG records is a nonstationary statistic.

Thus, it is an unsuitable means of AEP detection.

The use of phase phenomena suffers from no such disadvantages. This has been established by the detailed phase analyses of Chapter Four. Phase values are inherently cyclic ( exhibit 'wrap-around' ) and this invariably complicates measurements, statistical analyses and interpretation. Further, the large record-by-record variability of the phase values of individual harmonic components requires the use of substantial sample sizes, making the use of histograms or other statistical simplifications unavoidable. However, the sampling statistics of none of the obvious measures are known, and so need empirical determination. This has been carried out and it is interesting that a sample size bias has emerged very clearly. Nevertheless, subject to recognizing this feature and its implications, the distributions and the statistics derived from them were found to be stationary and well-behaved. This approach is effective in detecting the AEP objectively to within 10 dB of subjective threshold. In consequence, it is clear that a pattern recognition approach is fully justified. This finding was followed up and further supported by the cross-correlation studies carried out in Chapter Five.

No satisfactory and objective reference exists for estimating the effectiveness of the statistical procedures developed in this thesis. Both the pure tone audiogram (SL) or a visually scored average response, for example, are subjective on the part of the listener or of the tester. Yet, it is only on the basis of one or more of these subjective estimates that comparisons can be made and some relevant statistics derived, viz., the false positive or false negative scores for a particular test. The following table



indicates the similarities and disparities between the subjective measures of SL and a visually assessed coherent average on the one hand, and the objective procedures developed in this thesis on the other. For each entry, A represents the percentage agreement between the two scores, FP and FN, the percentage false positive or false negative ratings respectively on the basis of the subjective reference.

	Test	SL			Coherent Average		
		A	FP	FN	A	FP	FN
Power	F	58%	10%	32%	64%	11%	25%
	$\chi^2_3$	83%	5%	12%	88%	5%	7%
Phase	$\chi^2_r$	83%	3%	14%	90%	3%	7%
	sd	84%	5%	11%	88%	5%	7%
Template Matching	$\bar{r}_0$	81%	3%	16%	84%	4%	12%

Table 6-i. Comparison of subjective and objective procedures for estimating auditory threshold.

These tabulated comparisons reveal that the objective phase statistics are in good agreement with these two subjective methods routinely used in assessing auditory thresholds. Phase statistics, however, have the added advantage of objectivity. The criteria for response/no response conditions are statistically based, and thus, time and tester invariant. In addition, the phase statistics are unaffected by the presence of high variance EEG sweeps which often distort the ensemble average: each sweep contributes only  $1/N$  to

the test result.

The phase studies conducted in this thesis establish that the method could now be implemented clinically, either in the  $\chi^2$  or phase vector form, thus reducing the expense of ERA by eliminating the need for experienced clinicians to assess each record visually. A special-purpose minicomputer or microprocessor system could certainly be developed and programmed to perform the simple analyses required for extensive on-line trials of the technique. With the satisfactory completion of clinical trials, a device of this kind could then be considered for large-scale epidemiological studies, thereby achieving one of the further objectives of this research.

### 6.3. AEP Analysis

At the outset of this study, a few qualitative features about the averaged AEP were known and widely accepted. Its subject to subject variability, or its changes in shape and latency as a function of intensity level had been well documented. Other features of the data, such as the interaction of signal and noise sources, or the presence of nonstationarities, had been recognized sometimes, but largely overlooked. Thus, the assumption of a stationary EEG source was commonly implicit in most detection techniques. So, indeed, was the notion that the AEP could be modelled as a characteristic signal superimposed upon it.

As the present study progressed, it became increasingly evident that hypotheses could not be applied to the data without first testing their relevance. The simulation study of Chapter Three illustrates this point very clearly. Given the superposition model of AEP generation, its underlying assumption of stationarity for the EEG cannot be justified. Though the additive mechanism this model postulates may still be valid in describing the data, it fails to suggest procedures reliable enough for objective AEP detection. Thus, other models, with their correspondingly appropriate detection techniques, may provide a more satisfactory description of the data.

The phase statistics derived in Chapter Four reveal the presence of any consistent pattern present in an ensemble, regardless of the mechanism by which that pattern is produced. Thus, either superposition, or the synchronization model appropriate to phase analysis, could be responsible for the constraint seen in supra-threshold records. Recent unpublished work in this department

suggests that either model could be applicable to approximately 30 dB SL. Below this level, data simulated by superposition fails to reveal evidence of phase constraint. Phase aggregation, however, can still be seen in ERA data and in that simulated by constraining the phase values of bandlimited Gaussian random noise. Such findings suggest that the synchronization model presented in Chapter Four is more suitable in describing the AEP. Before any conclusions are drawn, however, a detailed study should be carried out on data simulated by these two means. With the results from that study, a thorough assessment of the two models can be made.

Details of the data, including its statistical properties, need to be assessed fully before instruments are developed for its measurement or guidelines set down for its interpretation. The work reported here has implemented this philosophy practically. As such, it marks the first systematic attempt to define the parameters of ERA data and determine their sampling statistics before testing their effectiveness as response indicators.

#### 6.4. Proposals for Future Study

As mentioned above, further validation of the phase procedures in a clinical setting is now warranted. So, too, is a simulation study to assess the basic tenets of the synchronization model. Comparisons between data simulated by synchronization and superposition could provide the information necessary to establish which of these models is more appropriate for AEP data.

The phase statistics developed in Chapter Four should be explored for further sampling effects. The phase vector statistics

are known to be biased estimators. The same may be true of the distribution of the maximum  $\chi^2_1$ , and this should be established.

The relationship between the phase and other pattern recognition techniques could be explored more thoroughly. For example, the contribution of each harmonic to the overall correlation coefficient could be coupled with its phase value, possibly providing further information about the behaviour of the data in relation to these statistics.

Some studies could be proposed to investigate the source of the AEP. Contour mapping of the evoked potential would provide spatial distributions of the signal. With the proper choice of signal analysis procedures, the information derived from a study of this kind could well enhance and quantify much existing knowledge of AEP and EEG behaviour.

## REFERENCES

1. Adrian, E.D., and Matthews, B.H.C. (1934)  
The interpretation of potential waves in the cortex  
J. Physiol., 81: 440-471.
2. Adrian, E.D., and Matthews, B.H.C. (1934)  
The Berger rhythm: potential changes from the occipital lobes in man  
Brain, 57(4): 355-385.
3. Beagley, H.A. (1971)  
Present day scope and limitations of evoked response audiometry  
Rev. Laryng. (Bordeaux) Suppl. 1971: 753-763.
4. Beagley, H.A., and Kellogg, S.E. (1969)  
A comparison of evoked response and subjective auditory thresholds  
Int. Aud., 8: 345-353.
5. Beagley, H.A., and Knight, J.J. (1967)  
Changes in auditory evoked response with intensity  
Rep. Inst. Laryng. Otol., 17: 263-275.
6. Beagley, H.A., Sayers, B.McA., and Ross, A.J. (1978)  
Fully objective ERA by phase spectral analysis  
Acta Otolaryng., in press
7. Bendat, J.S., and Piersol, A.G. (1971)  
Random Data: Analysis and Measurement Procedures  
Wiley-Interscience, New York
8. Berger, H. (1929)  
Hans Berger: On the electroencephalogram of man  
Gloor, P., ed.  
EEG Clin. Neurophysiol., Suppl. 28: 1969.

9. Blackman, R.B., and Tukey, J.W. (1959)  
The Measurement of Power Spectra  
Dover, New York
10. Borsanyi, S.J., and Blanchard, C.L. (1964)  
Auditory evoked brain responses in man  
Arch. Otol., 80: 149-154.
11. Brazier, M.A.B. (1966)  
Varieties of computer analysis in electrophysiological potentials  
EEG. Clin. Neurophysiol., Suppl. 26: 1-8.
12. Brigman, E. (1974)  
The Fast Fourier Transforms  
Prentice-Hall, Englewood Cliffs, N.J.
13. Butler, R.A. (1968)  
Effects of changes in stimulus frequency and intensity on habituation of the human vertex potential  
J. Acoust. Soc. Amer., 44: 945-950.
14. Caton, R. (1875)  
The electric currents of the brain  
Br. Med. J., 2: 278.
15. Celesia, G.G. (1968)  
Auditory evoked responses: intracranial and extracranial average evoked responses  
Arch. Neurol., 19: 430-437.
16. Celesia, G.G., and Puletti, F. (1969)  
Auditory cortical areas of man  
Neurology, 19(3): 211-220.
17. Clark, W.A. (1958)  
Average response computer (ARC-1)  
Quart. Rep. Electronics, MIT: 114-117.

18. Cochran, W.G. (1952)  
The  $\chi^2$  test of goodness of fit  
Ann. Math. Statist., 23: 315-345.
19. Cochran, W.G. (1954)  
Some methods for strengthening the common  $\chi^2$  tests  
Biometrics, 10: 417-451.
20. Cooper, R., Osselton, J.W., and Shaw, J.C. (1974)  
EEG Technology  
Butterworth, London
21. Davis, H. (1964a)  
Some properties of the slow cortical response in humans  
Science, 146: 434.
22. Davis, H. (1964b)  
Slow cortical responses evoked by acoustic stimuli  
Acta Otolaryng. Suppl. 206: 128-134.
23. Davis, H. (1973)  
Classes of auditory evoked responses  
Audiology, 12: 464-469.
24. Davis, H. (1976)  
Principles of Electric Response Audiometry  
Ann. Otol. Rhin. Laryng., Suppl. 28(85)
25. Davis, H., Davis, P.A., Loomis, A.L., Harvey, E.N., and  
Hobart, G. (1939)  
Electric reactions of the human brain to auditory stim-  
ulation during sleep  
J. Neurophysiol., 2: 500-514.
26. Davis, H., Hirsh, S.K., Shelmutt, J., and Bowers, C. (1967)  
Further validations of evoked response audiometry  
J. Speech Hear. Res., 10(4): 717-732.



27. Davis, H., and Onishi, S. (1969)  
Maturation of auditory evoked potentials  
Int. Aud., 8: 24-33.
28. Davis, H., and Zerlin, S. (1964)  
The variability of evoked responses  
Physiologist, 7: 114.
29. Davis, P.A. (1939)  
Effects of acoustic stimuli on the waking brain  
J. Neurophysiol. 2: 494-499.
30. Dawson, G.D. (1947)  
Cerebral responses to electrical stimulation of peripheral  
nerve in man  
J. Neurol. Neurosurgery Psych. 10: 134-140
31. Dawson, G.D. (1951)  
A summation technique for detecting small signals in a  
large irregular background  
J. Physiol. 115: 2P-3P
32. Dawson, G.D. (1954)  
A summation technique for the detection of small evoked  
potentials  
EEG. Clin. Neurophysiol., 6: 65-84.
33. Derbyshire, A.J., and McCandless, G.A. (1964)  
Template for the EEG response to sound  
J. Speech Hear. Res., 7: 96-98.
34. Derbyshire, A.J., Osenar, S.B., Hamilton, L.R., and Joseph,  
M.E. (1971)  
Problems in identifying an acoustically evoked potential  
to a single stimulus  
J. Speech Hear. Res., 14: 160-171.

35. Geddes, L.A., Baker, L.E., and Moore, A.G. (1969)  
Optimum electrolytic chloriding of silver electrodes  
Med. Biol. Eng., 7: 49-56.
36. Keating, L.W., and Rhum, H.B. (1971)  
Within average variability of the acoustically evoked  
response  
J. Speech Hear. Res., 14(1): 179-188.
37. Lynn, P.A. (1973)  
The Analysis and Processing of Signals  
MacMillan, London.
38. McCandless, G.A., and Lentz, W.E. (1968)  
Amplitude and latency characteristics of auditory evoked  
responses at low sensation levels  
J. Aud. Res., 8: 273-282.
39. Rapin, I. (1974)  
Testing for hearing loss with auditory evoked responses -  
successes and failures  
J. Comm. Dis., 7: 3-10.
40. Reneau, J.P., and Hnatiow, G.Z. (1975)  
Evoked Response Audiometry: a Topical and Historical  
Review  
Univ. Park Press, Baltimore.
41. Riha, J. (1975)  
A phase distribution method for detection of auditory  
evoked EEG responses  
DIC Thesis, Imperial College, U. London.
42. Roberts, J.R., and Watson, B.W. (1974)  
Evoked Response Audiometry, in  
D.W. Hill and B.W. Watson, eds,  
IEE Medical Electronics Monographs, 7-12  
Peter Peregrinus, London, 105-140.

43. Roeser, R.J., and Price, L.L. (1969)  
Effects of habituation on the auditory evoked response  
J. Aud. Res., 9(4): 306-313.
44. Rose, D.E., Keating, L.W., Hedgecock, L.D., Miller, K.E., and Schreurs, K.K. (1972)  
A comparison of evoked response audiometry and routine clinical audiometry  
Audiology, 11: 236-243.
45. Rose, D.E., Keating, L.W., Hedgecock, L.D., Schreurs, K.K., and Miller, K.E. (1971)  
Aspects of acoustically evoked responses - inter-judge and intra-judge reliability  
Arch. Otol., 94(4): 347-350.
46. Russ, F.M., and Simmons, F.B. (1974)  
Five years of experience with electric response audiometry  
J. Speech Hear. Res., 17: 184-193.
47. Saloman, G. (1970)  
Clinical electric response audiometry on a general purpose computer ( IBM 1800 )  
Acta Otolaryng. Suppl. 263: 238-241.
48. Saloman, G. (1974)  
Electric response audiometry (ERA) based on rank correlation  
Audiology, 13: 181-194.
49. Saloman, G., and Barford, J. (1977)  
A new concept of vertex ERA and EEG analysis applying inverse filtering  
Acta Otolaryng., 83: 200-210.

50. Sayers, B.McA. (1970)  
Inferring Significance from Biological Signals, in  
M. Clynes and J.H. Milsum, eds,  
Biomedical Engineering Systems  
McGraw-Hill, New York, 84-163.
51. Sayers, B.McA., and Beagley, H.A. (1974)  
Objective evaluation of auditory evoked EEG responses.  
Nature, 251: 608-609.
52. Sayers, B.McA., Beagley, H.A., and Henshall, W.R. (1974)  
The mechanisms of auditory evoked EEG responses  
Nature, 247: 481-483.
53. Schimmel, H., Rapin, I., and Cohen, M.M. (1974)  
Improving evoked response audiometry with special ref-  
erence to the use of machine scoring  
Audiology, 13: 33-65.
54. Shimizu, H., and Glackin, R.N. (1967)  
Comparison of graphic and computer averaging methods in  
EER  
J. Speech Hear. Res., 10: 373-376.
55. Siegel, S. (1956)  
Nonparametric Statistics  
McGraw-Hill, New York
56. Sutton, S., Braren, M., and Zubin, J. (1965)  
Evoked potential correlates of stimulus uncertainty  
Science, 150: 1187-1188.
57. Sutton, S., Teuting, P., and Zubin, J. (1967)  
Information delivery and the sensory evoked potential  
Science, 155: 1436-1439.
58. Taguchi, K., Picton, T.W., Orpin, J.A., and Goodman, W.S. (1969)  
Evoked response audiometry in newborn infants  
Acta Otolaryng., Suppl. 252: 5-17.

59. Teas, D.C. (1965)  
Analysis of evoked and ongoing electrical activity at the  
scalp of human subjects  
J. Speech Hear. Res., 8: 371-387.
60. Vaughan, H.G., and Ritter, W. (1970)  
The sources of auditory evoked responses recorded from the  
human scalp  
EEG. Clin. Neurophysiol., 28: 360-367.
61. Walter, W.G. (1964)  
The contingent negative variation: an electrocortical sign  
of significant association in the human brain  
Science, 146: 434.
62. Walter, W.G., Cooper, R., Aldridge, V.J., McCallum, W.C., and  
Winter, A.L. (1964)  
Contingent negative variation: an electric sign of sensor-  
imotor association and expectancy in the human brain  
Nature, 203: 380-384.
63. Wever, E.G. (1970)  
Theory of Hearing  
Dover, New York